

ENABLING TECHNOLOGIES TO
ACCESS NEW MATERIALS USING
FRUSTRATED LEWIS PAIRS



Jamie Carden

A thesis submitted to Cardiff University in
candidature for the degree of
Doctor of Philosophy

Department of Chemistry, Cardiff University

February 2021

I – Acknowledgements

First and foremost, I would like to thank my supervisor Dr Rebecca Melen for all of the support and guidance over the past three and a half years. Studying for this doctorate has been an adventure, and I am very thankful to her for letting me join her research group. I don't think I've ever worked so hard, but my publications, the conferences I got to attend, and my time in the laboratory were all absolutely worth every second of tears and broken dreams!

I would also like to thank my secondary supervisors Dr Duncan Browne and Prof. Duncan Wass for their friendly and helpful discussions throughout the years, and for welcoming me into their research groups. Thanks also to all the other academic staff that were great inspirations. Particularly Dr Newman, Dr Amoroso, Dr Ward, Dr Easun, and Prof. Pope for the wisdom and sarcastic humour! Also, a huge thanks to the technical staff that made working in the lab possible: Dr Jenkins, Simon, Tom, Robin, Steve, Evelyn, Shane, Jamie, Simon, Rich, and James. Finally, a big shout out to Dr Mason, Dr Willock, and Dr Thomas for giving me the opportunity to get into STEM outreach, and Owen, Alen, Al, and Rob for making all of the undergrad teaching labs more enjoyable.

It is also important to me to thank Prof. Morley. If it had not been for him, I would never have travelled to Finland for my Erasmus year. Without that I never would have gotten a taste for research or even considered continuing my studies at the postgraduate level. Kiitos Paljon to Prof. Laitinen who welcomed me into his group in Oulu, and to Minna, Esther, and Clara who gave up so much of their time to make me a better chemist. Honestly, 20 year old me couldn't have asked for better teachers!

I would also like to thank the EPSRC and the CDT in catalysis for funding my research and for giving me the opportunity to study for a second Masters degree. In extension I would also like to thank Helen and Michal for managing the programme and always being friendly faces around the chemistry department. Thanks also to the whole of my CDT cohort, but in particular to Stephen and Callum for their continued support after they left to study at the University of Bath. Also thank you to Rich and Ouardia for all their help, guidance and good humour during my Masters research sabbaticals.

My days in the lab were never dull, and for that reason I would like to say thanks to everybody that I worked with in lab 2.84. I was really lucky to get to work alongside most of the Melen group in one shape or another and I definitely learnt lots from every

single one of them. A huge shout out to Lukas for using his art to make the lab a brighter place and for always having a useful suggestion when things weren't working. To Yashar for kicking off my PhD research projects and being an inspirational column chromatography machine. To Darren Ould for his help in the alane project, for running all of my crystals and for teaching me everything I'll ever need to know about a glovebox. To Kate for teaching me how to make diazo compounds and for the impressive research that went into the 100-page FLP catalysis book chapter. To Theo and Mashaël for helping me write the nitrogen activation book chapter and for their help and optimism in the phosphinoborane project. To Ayan for his help with the *Chem Soc Rev*. To Darren Willcox and Ruddy for their help in the chiral hydroboration project, and finally to Darren, Yashar, Lewis, and Ruddy for welcoming me to the group back when I first started. I also need to thank Darren, Lukas, and Jack for teaching me about DFT, and also Alex, Corey, Luke, Dom and Vlad for making the lab a great environment to work in.

It's also really important to me to thank the undergraduate students that I worked with during my PhD. In particular: Lukas for his great help, positivity, and friendship during the microwave assisted hydroboration project; Rowan for his assistance in making the alanes, and for really helping to get the project off the ground following his weird crystal structures; Jessie for her help during the hydroamination project and for sharing my distaste in radio one; and finally to Sam and Luke for being my hands in the lab when I could only use one of mine, and for working on the superacid project I was never able to get round to. I was also lucky enough to get to know other undergraduate students that passed through the lab, so special mentions to Brandon, Laura and Barney for carrying on my MChem project; to Becky and Joe for introducing me to gin, and to Dale, Vlad, Emily and Adam for their friendship. Most of them are off doing their own PhDs now and if any of you ever read this then I wish you every success.

Of course, lab 2.84 was just a small part of the inorganic chemistry community at Cardiff University that made me feel at home. From day one it felt like I was coming into a big family of PhDs and postdocs and I'm really glad I got to share the drinks, lunch breaks and trips to Cathays' finest takeaways with them before COVID came along. There's too many of you to list every single one of you, but thanks to you all!

Some special shout outs: to Micol, Tobi, and Lukas who gave up their time to proofread this thesis; to Stokes and Alex who taught me how to fend off imposter syndrome; and to Ben, James, and the NHS for patching me up following a nasty laboratory accident. I would also like to thank the Dial-A-Molecule programme for

giving me the opportunity to attend a summer school on enabling technologies, and also to the Royal Society of Chemistry for granting me funds to present my research at international conferences.

On a personal note, I'd like to send my thanks to all of my non-chemist friends and my undergraduate chemistry friends, who were always there for moral support on the days when things had gone wrong and to celebrate with me on the days when things had gone right. I would like to thank my parents for constant support and for pushing me to be one of the first in the family to go to university, let alone become a doctor. I would also like to thank my brother for his own type of realism and positivity (e.g. "when are you going to finish your PhD and get a real job!") Finally, I'd like to thank my girlfriend for putting up with me for the past few years. There's nobody else I would have wanted to suffer through the COVID pandemic with!

And thank you if you're reading this – I hope you enjoy it! =)

II – Abstract

The work presented in this thesis concerns the use of Lewis acidic compounds based upon the main-group elements boron and aluminium, and their applications towards catalysis. Furthermore, the use of flow chemistry and microwave assisted heating, commonly described as ‘enabling technologies’, are investigated to augment existing reactions.

Chapter one provides a general introduction into the three central themes of this thesis: Lewis acidity, including an explanation of the generic use of a Lewis acid and also methods in which Lewis acidity can be determined; catalysis, in particular the use of boron and aluminium based catalysts for hydroboration and hydroamination transformations; and finally enabling technologies, with a description of flow chemistry and microwave assisted heating, along with their applications towards main-group chemistry. In chapter two, the synthesis of boron and aluminium based Lewis acids is explored, with an accompanying discussion of their Lewis acidities. Chapter three concerns the preparation of what is often described as the archetypal borane Lewis acid, tris(pentafluorophenyl)borane, using the enabling technology of flow chemistry. Whilst this project was ultimately unsuccessful, an analysis behind the reasons why this project did not go as planned is discussed. Chapter four focuses on the use of the Lewis acidic compound tris(3,4,5-trifluorophenyl)borane and its aluminium congener tris(3,4,5-trifluorophenyl)alane as catalysts for the hydroboration reaction using classical heating techniques. Chapter five expands upon chapter four by investigating tris(3,4,5-trifluorophenyl)borane-catalysed reactions with the use of microwave assisted heating. Finally, chapter six considers the use of tris(pentafluorophenyl)borane towards the hydroamination of alkenes, expanding upon the literature known alkyne hydroamination scope.

III – List of abbreviations

°C	degrees Celsius
9-BBN	9-borabicyclo[3.3.1]nonane
ϵ'	dielectric constant
ϵ''	dielectric loss
η	chemical hardness
μ	chemical potential
ρ	density
χ	Mulliken electronegativity
ω	electrophilicity
AN	acceptor number
ASAP	atmospheric solids analysis probe
BPR	back pressure regulator
BSSE	basis set superposition error
cat	catechol
CCSD	coupled cluster single-double
Cy	cyclohexyl
DABCO	1,4-diazabicyclo[2.2.2]octane
Da	Damköhler number
DCM	dichloromethane
DCE	dichloroethane
DFT	density functional theory
ECP	effective core potential
EI	electrospray ionisation
FIA	fluoride ion affinity
FLP	frustrated Lewis pair
GEI	global electrophilicity index

GHz	gigahertz
Ha	Hartree units
HIA	hydride ion affinity
HRMS	high resolution mass spectrometry
HSAB	hard soft acid base
IR	infra-red
IUPAC	International Union of Pure and Applied Chemistry
kJmol^{-1}	kilojoules per mole
LA	Lewis acid
M	molar
Mes	mesityl
MeV	megaelectronvolt
mm	millimetre
nacnac	β -diketiminato
NBO	natural bond order
NHC	N-heterocyclic carbene
NMR	nuclear magnetic resonance
OTf	triflate
Pin	pinacol
PMDETA	<i>N,N,N',N'',N''</i> -pentamethyldiethylenetriamine
ppm	parts per million
Re	Reynolds number
$\tan\delta$	loss factor
THF	tetrahydrofuran
THP	tetrahydropyran
TMS	trimethylsilyl

IV – List of publications

1. *Frustrated Lewis pairs in catalysis*, Katarina Stefkova, Jamie L. Carden and Rebecca L. Melen. Book chapter in *Comprehensive Organometallic Chemistry III*. Manuscript accepted. (Chapter one)
2. *Triarylboranes in the activation of azo containing compounds*, Theodore A. Gazis, Jamie L. Carden, Mashaal M. Alharbi and Rebecca L. Melen. Book chapter in *Encyclopedia of Inorganic and Bioinorganic Chemistry*, Wiley, 2021, pp. 1–19.
DOI: 10.1002/9781119951438.eibc2780 (Not included in this thesis)
3. *Synthesis and reactivity of fluorinated triaryl aluminum complexes*, Darren M. C. Ould[†], Jamie L. Carden[†], Rowan Page and Rebecca L. Melen. († Equal contribution) *Inorg. Chem.*, 2020, **59**, 14891–14898. (Front cover)
DOI: 10.1021/acs.inorgchem.0c01076 (Chapters two and four)
4. *Halogenated triarylboranes: synthesis, properties, and applications in catalysis*, Jamie L. Carden, Ayan Dasgupta and Rebecca L. Melen. *Chem. Soc. Rev.*, 2020, **49**, 1706–1725. (Back cover)
DOI: 10.1039/C9CS00769E (Chapters one and two)
5. *Asymmetric ketone hydroboration catalyzed by alkali metal complexes derived from BINOL ligands*, Darren Willcox, Jamie L. Carden, Adam J. Ruddy, Paul D. Newman and Rebecca L. Melen. *Dalton Trans.*, 2020, **49**, 2417–2420.
DOI: 10.1039/D0DT00232A (Not included in this thesis)
6. *Unlocking the catalytic potential of tris(3,4,5-trifluorophenyl)borane with microwave irradiation*, Jamie L. Carden, Lukas J. Gierlichs, Duncan. F. Wass, Duncan L. Browne and Rebecca L. Melen. *Chem. Commun.*, 2019, **55**, 318–321.
DOI: 10.1039/C8CC09459D (Chapters four and five)

Table of Contents

I – Acknowledgements.....	i
II – Abstract	iv
III – List of abbreviations	v
IV – List of publications	vii
Chapter one – Introduction	1
1.1 An introduction to Lewis acids	1
1.1.1 Definitions of Lewis acids and bases	1
1.1.2 Lewis acidity determination	2
1.1.3 Reactivity of Lewis acids	5
1.1.4 Frustrated Lewis pairs.....	6
1.1.5 An introduction to boron and aluminium Lewis acids.....	8
1.2 An introduction to catalysis.....	13
1.2.1 A brief introduction to catalysis.....	13
1.2.2 The importance of main-group catalysis.....	13
1.2.3 Catalytic hydroboration	14
1.2.4 Hydroboration catalysed by boron-based Lewis acids.....	15
1.2.5 Hydroboration catalysed by aluminium-based Lewis acids.....	23
1.2.6 Catalytic hydroamination.....	30
1.2.7 Hydroamination catalysed by boron-based Lewis acids	30
1.3 An introduction to enabling technologies	34
1.3.1 What is an enabling technology?	34
1.3.2 An introduction to microwave assisted synthesis	34
1.3.3 Application of microwave assisted synthesis towards hydroboration, triel Lewis acid catalysis, and frustrated Lewis pairs.....	38
1.3.4 An introduction to flow chemistry.....	40
1.3.5 Application of flow chemistry towards Lewis acid catalysis and frustrated Lewis pairs	45
1.4 Conclusions.....	48
1.5 Aims of this thesis	49
Chapter two – Synthesis of boron- and aluminium-based Lewis acids in batch.....	50
2.1 Aims of this chapter.....	50
2.2 Boron- and aluminium-based Lewis acid synthesis in the literature	50
2.2.1 Borane synthesis in the literature	50
2.2.2 Alane synthesis in the literature	52
2.3 Borane synthesis.....	54

2.3.1 Tris(pentafluorophenyl)borane	54
2.3.2 Tris(3,4,5-trifluorophenyl)borane	56
2.3.3 Tris(2,3,4-trifluorophenyl)borane	56
2.3.4 Tris(2,4,6-trifluorophenyl)borane	57
2.4 Alane synthesis	58
2.4.1 Tris(3,4,5-trifluorophenyl)alane	59
2.4.2 μ_2 -dimethyl-bis[(3,4,5-trifluorophenyl)methyl-alane]	61
2.4.3 Tris(2,3,4-trifluorophenyl)alane	62
2.5 Comparisons of Lewis acidity	65
2.5.1 The Gutmann-Beckett method	66
2.5.2 The Childs method	68
2.5.3 The fluoride ion affinity method	70
2.6 Conclusions and outlook	71
Chapter three – Synthesis of tris(pentafluorophenyl) borane using continuous flow technologies	73
3.1 Aims of this chapter	73
3.2 Initial reactor design	74
3.3 Optimisation of lithiation procedure	75
3.4 Optimisation of the borylation procedure	79
3.5 Reinvestigation of lithiation procedure	82
3.6 Conclusions and outlook	87
Chapter four – Hydroboration catalysis using conventional heating techniques	89
4.1 Aims of this chapter	89
4.2 Hydroboration using tris(3,4,5-trifluorophenyl)borane as a catalyst	89
4.2.1 Optimisation	90
4.2.2 Scope of reaction	91
4.2.3 Mechanism of hydroboration at room temperature	95
4.2.4 Mechanism of hydroboration at 70 °C	98
4.3 Hydroboration using tris(3,4,5-trifluorophenyl)alane etherate as a catalyst	102
4.3.1 Optimisation	102
4.3.2 Scope	104
4.3.3 Mechanism of hydroboration	106
4.4 Conclusions and outlook	111
Chapter five – Hydroboration catalysis using microwave irradiation	113
5.1 Aims of this chapter	113
5.2 Investigation of B(3,4,5-F ₃ C ₆ H ₂) ₃ as a hydroboration catalyst for substrates with homonuclear unsaturated bonds using microwave irradiation	114

5.2.1 Optimisation.....	114
5.2.2 Scope	115
5.3 Investigation of B(3,4,5-F ₃ C ₆ H ₂) ₃ as a hydroboration catalyst for substrates with heteronuclear unsaturated bonds using microwave irradiation	117
5.3.1 Optimisation.....	117
5.3.2 Scope	118
5.4 Mechanism of hydroboration under microwave irradiation	121
5.4.1 Mechanism of hydroboration in the microwave for substrates containing heteronuclear unsaturated bonds	121
5.4.2 Mechanism of hydroboration in the microwave for substrates containing homonuclear unsaturated bonds.....	123
5.5 Conclusions and outlook	125
Chapter six – Hydroamination catalysis with B(C ₆ F ₅) ₃	126
6.1 Aims of this chapter	126
6.2 Optimisation	126
6.3 Scope.....	128
6.4 Mechanism.....	130
6.5 Conclusions and outlook	133
Chapter seven – Conclusions and outlook	135
Chapter eight – Experimental	138
8.1 General experimental	138
8.2 Synthesis and characterisation of boranes	140
8.3 Synthesis and characterisation of alanes	146
8.4 Lewis acidity determination	155
8.4.1 The Gutmann-Beckett method of Lewis acidity determination.....	155
8.4.2 The Childs method of Lewis acidity determination	156
8.4.3 FIA calculations for Lewis acidity determination	157
8.5 B(3,4,5-F ₃ C ₆ H ₂) ₃ -catalysed hydroboration	158
8.5.1 Synthesis of starting materials	160
8.5.2 Synthesis of reduction products	163
8.6 Al(3,4,5-F ₃ C ₆ H ₂) ₃ ·Et ₂ O-catalysed hydroboration	182
8.6.1 Synthesis of starting materials	182
8.6.2 Synthesis of reduction products	184
8.7 B(C ₆ F ₅) ₃ -catalysed hydroamination	192
8.7.1 Synthesis of reduction products	192
V – References.....	196

Chapter one – Introduction

1.1 An introduction to Lewis acids

1.1.1 Definitions of Lewis acids and bases

In 1923, Lewis coined a theory of acids and bases based upon the movement of electrons. Herein, a Lewis base was a molecule capable of donating electrons, whilst a Lewis acid was a molecule which could accept them. Furthermore, upon a Lewis base sharing its electrons to an acid it would form a Lewis adduct. In his book 'Valence and the Structure of Atoms and Molecules', Lewis described:¹

“a basic substance is one which has a lone pair of electrons which may be used to complete the stable group of another atom, and that an acidic substance is one which can employ a lone pair from another molecule in completing the stable group of one of its own atoms.”

In the same year, the other major theory of acids and bases was postulated independently by Brønsted and Lowry.^{2,3} This theory instead relied upon the transfer of protons, thus upon the reaction of an acid and base, the acid formed its conjugate base, whilst the base formed its conjugate acid. These theories are summarised in Figure 1.

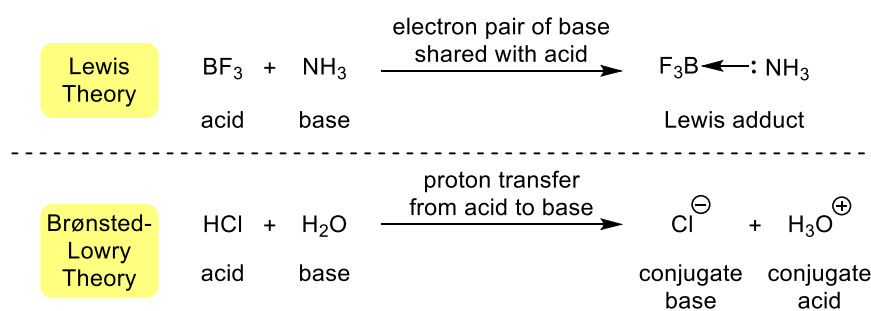


Figure 1 – Comparison of Lewis and Brønsted-Lowry theories of acidity and basicity.¹⁻³

The concept of Lewis acids and bases were improved upon by Pearson with the hard and soft acid and base (HSAB) principle.⁴ Here, small chemical species with high oxidation states were described as hard acids, whilst large chemical species with low oxidation states were described as soft acids. Furthermore, hard acids were shown to have an affinity for hard bases, with the same relationship between soft acids and

soft bases. Hard and soft mixtures between acids and bases were generally found to be less stable.⁵

The current description of a Lewis acid described by IUPAC (the International Union of Pure and Applied Chemistry) does not substantially differ from that of Lewis a century ago:⁶

“A Lewis acid is a molecular entity that is an electron pair acceptor and therefore able to react with a Lewis base to form a Lewis adduct by sharing the electron pair furnished by the Lewis base.”

1.1.2 Lewis acidity determination

Unlike the quantitative pKa scale for Brønsted-Lowry acids, a universal method of scaling Lewis acidity has yet to be established; however, there are many experimental and theoretical methods that have been used to rank Lewis acids for the purpose of catalyst design (Figure 2).

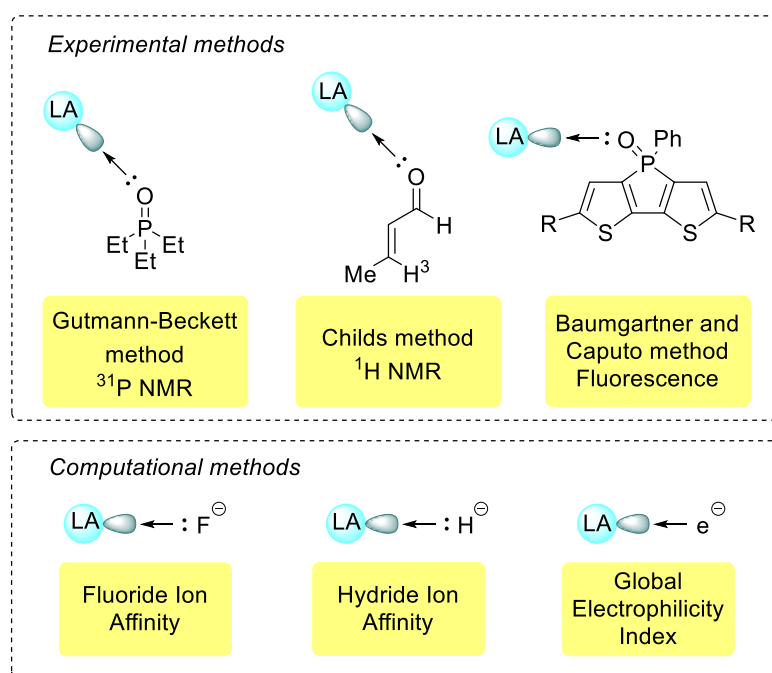


Figure 2 – Experimental methods of determining Lewis acidity.⁷⁻¹³

One of the most well-established techniques of Lewis acidity determination is the Gutmann-Beckett method. In 1975, Gutmann proposed an acceptor number (AN) protocol to scale the acidity of a range of solvents.⁷ Beckett later adopted the AN scale and applied it towards the calculation of Lewis acidity in boron-containing

complexes.⁸ The popularity of the Gutmann-Beckett method can be attributed to its simplicity. Herein, a Lewis acid is combined with an excess of triethylphosphine oxide (Et₃PO) to form a Lewis adduct. By comparing the shift of the phosphorus signal in the ³¹P NMR (nuclear magnetic resonance) spectrum of the adduct against free Et₃PO (δ /ppm: 41.0), the strength of the Lewis acid can be derived through Equation 1. Demchuck recently refined this method with the introduction of an inert triphenylphosphine standard (δ /ppm: -5.21).¹⁴

$$AN = 2.21 \times (\delta_{\text{sample}} - 41.0)$$

Equation 1 – Calculation of Lewis acidity through the Gutmann-Beckett method.^{7,8}

Stronger Lewis acids form adducts that produce more downfield shifts in the ³¹P NMR spectrum, therefore they correspond to higher ANs. On Beckett's scale, the non-acidic hexane was found to possess an AN of 0 (³¹P NMR shift of 41.0 ppm, a difference of 0 ppm to free Et₃PO), whilst the highly Lewis acidic antimony pentafluoride (SbF₅) was found to possess an AN of 100 (³¹P NMR shift of 86.4 ppm, a difference of 45.4 ppm to free Et₃PO).⁸

Another well-established experimental technique of determining Lewis acidity is the Childs method.⁹ Herein, a Lewis acid is combined with an excess of crotonaldehyde, and the Lewis acidity can be derived from the perturbation of the H³ signal of crotonaldehyde in the ¹H NMR spectrum upon the formation of an adduct using Equation 2. This crotonaldehyde probe is smaller than Et₃PO, thus steric factors are less pertinent for the Childs method compared to the Gutmann-Beckett method. In the Childs method, Lewis acids are ranked by 'relative acidity' and are measured against 0.3 M solutions of boron tribromide and hexane in dichloromethane at -20 °C. Here, boron tribromide is assigned a relative acidity of 1.00 ($\delta^1\text{H}$ of H³ = 8.47 ppm), whilst hexane is assigned a relative acidity of 0.00 ($\delta^1\text{H}$ of H³ = 6.89 ppm).⁹

$$\text{Relative acidity} = \frac{\Delta^1\text{H LA crotonaldehyde adduct}}{\Delta^1\text{H BBr}_3 \text{ crotonaldehyde adduct}}$$

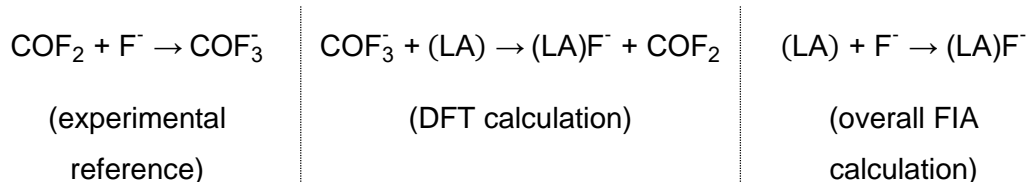
Equation 2 – Calculation of Lewis acidity through the Childs method.⁹

Other experimental methods of Lewis acidity determination have also been reported with alternative bases to the Gutmann-Beckett and Childs methods. These include Nödling's use of pyridine-*d*₅ as a Lewis base, in combination with ²H NMR spectroscopy following the *para*-deuterium shift,¹⁵ Zheng's use of *tert*-butyl phosphine as a Lewis base, with a shift in the ³¹P NMR spectrum determining Lewis acidity,¹⁶ and Baumgartner and Caputo's use of dithienophospholes, with shifts in the visible

spectrum detectable by the naked eye depending on the strength of the Lewis acid.^{10,17}

Despite the simplicity of these experimental probes, there are inconsistencies between the scales and inherent drawbacks of all methods. Argued causes of these differences include: solvent effects, as discussed by Gutmann in the initial use of Et₃PO as a Lewis acidity probe; steric factors, as acids containing bulky groups situated close to the empty *p*-orbital prevent the coordination of large probes, or the hardness of the base used for the probe, for example the oxygen atom of Et₃PO is harder than that the oxygen atom of crotonaldehyde.^{7,18} There is also the consideration of human or mechanical error in measurements. Thus, there are many methods to determine the Lewis acidity of compounds *via* computational means.

One popular method of determining Lewis acidity is fluoride ion affinity (FIA), in which the reaction enthalpy of the complexation of a simulated free gaseous Lewis acid to a fluoride ion is calculated. FIA was first introduced by Bartlett,¹⁹ but due to difficulties in calculations the method did not become widespread until Christie simplified the procedure with the introduction of an experimental value for the ionisation of carbonyl fluoride (COF₂) as a reference, thus making the addition of COF₃⁻ to the Lewis acid the only DFT (density functional theory) calculation required (Equation 3).¹¹



Equation 3 – Calculations required for FIA.^{11,19}

Other ion affinities have also been investigated, with the most common being the hydride ion affinity (HIA). This can be calculated through the isodesmic reaction between a Lewis acid and HBEt₃⁻ (Equation 4).¹²



Equation 4 – Calculation required for HIA.¹²

The most recent method of ranking Lewis acidity is Stephan's global electrophilicity index (GEI), wherein the affinity of a Lewis acid towards a single electron is calculated (Equation 5).¹³ Here, the measure of the ability of an acid to accept electrons, or electrophilicity (ω), is related to μ (chemical potential), η (chemical hardness), and χ (Mulliken electronegativity). Furthermore, μ can be derived from the difference

between the HOMO and LUMO energies (E_{HOMO} and E_{LUMO}) of a Lewis acid.^{13,20} Other ion affinities found in the literature include the addition of NH_3 , PH_3 , CH_3^- , and Cl^- , to rank their acidities, but these are more seldom used.^{21–24}

$$\omega = \mu^2 / 2\eta = \chi^2 / 2\eta$$

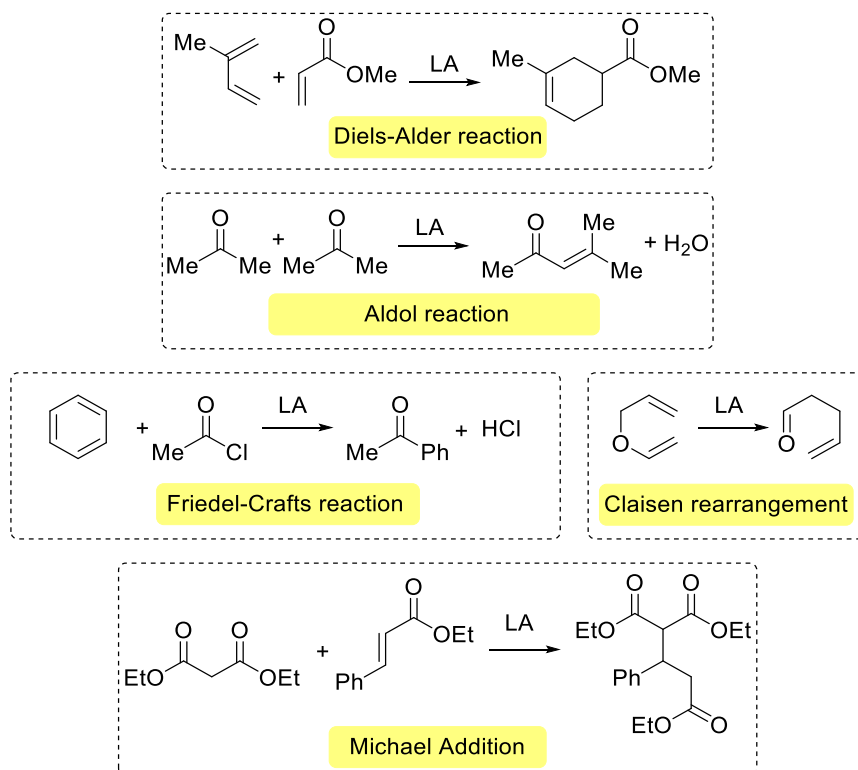
$$\eta = E_{\text{LUMO}} - E_{\text{HOMO}}$$

Equation 5 – Calculations required for the GEI.¹³

As with experimental methods, variations in computational methodologies can result in different accuracies in the values produced.²⁵ As with all DFT, the level of accuracy is dependent upon the exchange correlation functional chosen. Full details of these functionals are beyond the scope of this thesis, but in brief: hybrid-DFT functionals such as B3LYP are excellent compromises between accuracy and speed. Complex post Hartree-Fock functionals such as CCSD (coupled cluster single-double) will give more accurate values but will take significantly more computational time and power to calculate. Therefore, different computational methods will result in different calculated values for ion affinity, and thus analysing the trends in Lewis acidity by each individual method is more reliable than the analysis of the exact values calculated.

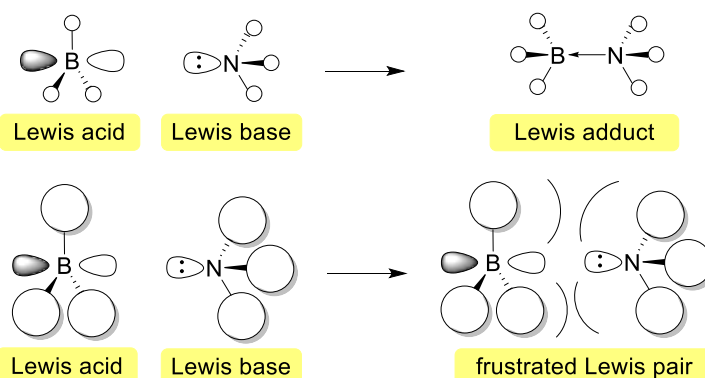
1.1.3 Reactivity of Lewis acids

The reactivity of a Lewis acid lies in its vacant p -orbital and its ability to accept electron density from a Lewis base. There is an extensive library of reactions that can be catalysed by Lewis acids, including but not limited to: the Friedel-Crafts reaction; the Claisen rearrangement; the Diels-Alder reaction; the Michael addition; and the Aldol condensation reaction (Scheme 1).^{26,27} In these examples, the Lewis acid acts through aiding heterolytic bond cleavage, by lowering the LUMO of an electrophile and making it more susceptible to nucleophilic attack from an external agent, or in the case of Diels-Alder reactions, by reducing electron repulsion between the diene and dienophile. Furthermore, Lewis acids can be used in both heterogeneous and homogeneous catalytic systems.^{26–28}

Scheme 1 – Examples of Lewis acid (LA) catalysed reactions.^{26,27}

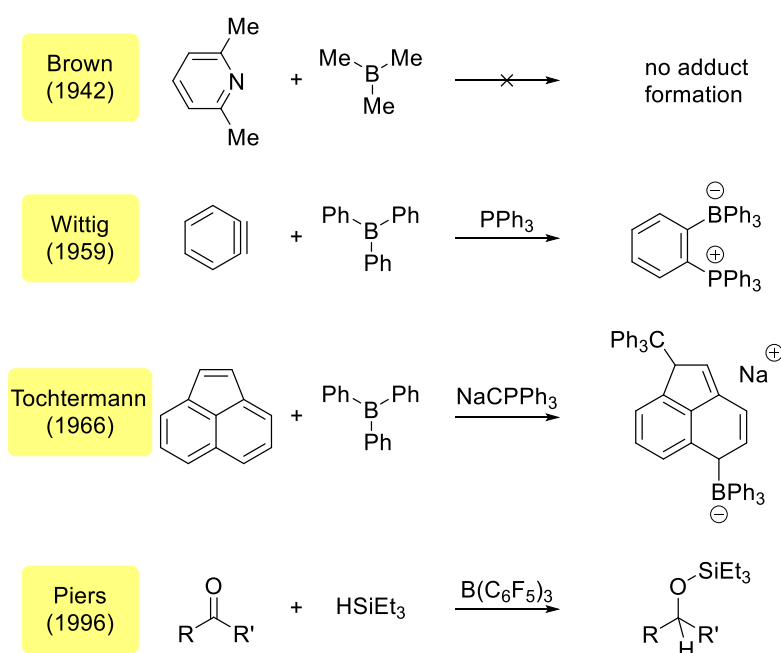
1.1.4 Frustrated Lewis pairs

Frustrated Lewis pairs (FLPs) are systems in which a Lewis acid and a Lewis base attempt to form a classical Lewis adduct, but due to segregation between the acidic and basic sites are unable to combine (Figure 3). This results in both the Lewis acidic and basic centres retaining their reactivity and the resultant frustrated Lewis pair being able to partake in reactions that classical Lewis adducts are inactive towards.^{29–31}

Figure 3 – Frustrated Lewis pair compared to a classical Lewis adduct.²⁹

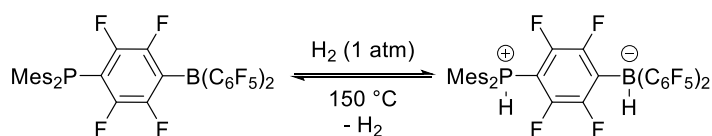
Examples of Lewis acids and bases not conforming to the expected reactivity of the time can be seen as antecedent towards FLPs (Scheme 2). As early as 1942, Brown

noted that 2,6-lutidine and trimethylborane would not combine to form a classical Lewis adduct.³² Wittig and Tochtermann both reported unexpected addition of sterically hindered Lewis bases over unsaturated C=C bonds rather than the expected polymerisation reactions. Indeed, Tochtermann described the resultant compound as an ‘antagonistic pair’, but neither Tochtermann nor Wittig explored this reactivity further.^{33,34} More recently, Piers investigated the reactivity of tris(pentafluorophenyl)borane [B(C₆F₅)₃] as a catalyst towards the hydrosilylation of carbonyls by triphenylsilane, noting that the acid and base ‘unusually’ acted simultaneously upon the Si–H cleavage, in a process which is now described as FLP catalysis.³⁵



Scheme 2 – Examples of FLP-type reactivity before the term FLP was coined.^{32–35}

The term frustrated Lewis pair was coined by Stephan in 2006, upon the discovery of a phosphinoborane which was capable of reversible dihydrogen activation (Scheme 3).³⁶ This phosphinoborane displayed high steric demand around the Lewis acidic boron centre and the Lewis basic phosphorus centre, which prevented any dimerisation or oligomerisation that could have quenched reactivity towards small molecule activation. Activation of dihydrogen was observed at one atmosphere of hydrogen, and this equivalent of dihydrogen could be relinquished under thermal conditions.³⁶



Scheme 3 – Reversible activation of dihydrogen by Stephan's first FLP.³⁶

The facile nature of this metal-free hydrogenation led to a plethora of interest in the field. Both intermolecular and intramolecular FLPs have been extensively covered to fully explore the capabilities of these novel systems. Thus the scope of small molecule activation by FLPs has widened to include CO₂, NO₂, SO₂, and alkenes.^{31,37–39} Following on from Piers' report of B(C₆F₅)₃-catalysed hydrosilylation, many other examples of FLP-catalysed reactions have surfaced. Catalysis by FLPs now includes reduction of a wide range of substrates including: carbonyls; alkenes; imines; N-heterocycles; and polyaromatics.^{30,40,41}

In recent years, the field of FLP chemistry has transcended the area of main-group chemistry, with examples of transition metals acting as either the Lewis acidic or Lewis basic component. Selected examples in the literature include investigations into group four metallocene Lewis acids in FLPs for homogeneous catalysis,^{42–44} and solid-state FLPs based upon zeolites, polymers and nanoparticles for heterogeneous catalysis.^{45–48}

1.1.5 An introduction to boron and aluminium Lewis acids

Pertinent to the subject matter of this thesis are triel (group 13) Lewis acids. The triels are characterised as containing three electrons in their valence shell, with a vacant *p_z* orbital, and thus the chemistry of these elements is largely dictated by their ability to fill this electron deficient shell. Consequentially boron and aluminium compounds are centrepiece in the fields of Lewis acid catalysis and FLP chemistry.

Upon examination of the Lewis acidity of the boron halides, the trend is unexpected when the electronegativity of the halide is considered. Electronegativity decreases down the periodic table, and thus one would expect fluorine to withdraw the most electron density from boron. This should cause the boron atom of BF₃ to be the most electron deficient and thus most Lewis acidic out of the boron halides; however, Lewis acidity increases upon descending the triels (Figure 4).⁴⁹

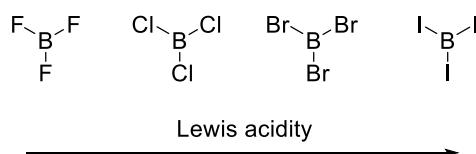


Figure 4 – Lewis acidity of the boron halides.⁴⁹

This trend is often attributed to the efficiency of electron density back-donation from the halogen into the boron's empty p_z orbital, effectively increasing the Lewis acidity of the boron centre; such back-donation is more efficient with smaller halogens causing the observed trend.⁴⁹ The trend of boron trihalide Lewis acidity is also determined by their ability to form adducts. DFT calculations have shown that charge transfer in boron trihalide adducts is less efficient when the halide is smaller, resulting in the larger halides being more acidic. Moreover, the aforementioned electron density back-donation in boron trihalides effectively forms π -bonds between the halogen and the boron atom. As the presence of π -bonds causes the un-coordinated Lewis acid to favour a planar structure, when larger halides are attached to the boron the π -bonds are weaker, causing the BX_3 unit to be more able to take the form of a pyramidal structure and consequentially making it more acidic.⁵⁰

Under the rich umbrella of organoboron complexes are triarylboranes. The BC_3 core of a triarylborane is trigonal planar, with the vacant p_z orbital lying perpendicular to this plane. The aryl groups often arrange into a paddlewheel type structure, protecting the vacant p_z orbital somewhat and making triarylboranes ideal candidates for FLP chemistry. $B(C_6F_5)_3$ has been described as the perfect triarylborane due to its strong Lewis acidity and large steric bulk. Compared to other fluorinated boron-based Lewis acids, it is relatively stable towards oxygen, and forms water adducts upon hydration instead of decomposing through the elimination of BF_3 .^{51,52} Before the surge in popularity of FLPs, $B(C_6F_5)_3$ was thoroughly investigated for its capability as a polymerisation catalyst initiator due to its alkyl abstraction abilities.⁵¹

$B(C_6F_5)_3$ is not ubiquitously the perfect triarylborane, as triarylboranes with different Lewis acidities display different reactivity to $B(C_6F_5)_3$ in a variety of situations.⁵³ The Lewis acidity of a triarylborane can be attenuated through modifications of the substituents on the aryl rings. A thorough theoretical study on fluorinated triarylboranes by Gilbert found that the position of fluorine atoms around the aryl ring imparted a strong influence towards Lewis acidity, with an increased number of fluorines resulting in an increased Lewis acidity. An exception was found when substitution in both *ortho* positions was present, which had the effect of lowering Lewis acidity rather than increasing it.⁵⁴

Further methods of altering the Lewis acidity of borane compounds include increasing the number of fluorine atoms through replacement of aryl rings with perfluoronaphthyl or perfluorobiphenyl moieties,^{55,56} through replacement of fluorine with heavier halogens,⁵⁷ and through the preparation of heteroleptic triarylboranes.^{57–59} Another factor that can influence the Lewis acidity of boron is the reorganisation energy between the un-coordinated trigonal planar state and the adduct pyramidal state. Thus, forcing the boron into a pyramidal geometry has also been shown to increase Lewis acidity.^{60–62} General trends for Lewis acidity of organoborane complexes are shown in Figure 5.⁶³

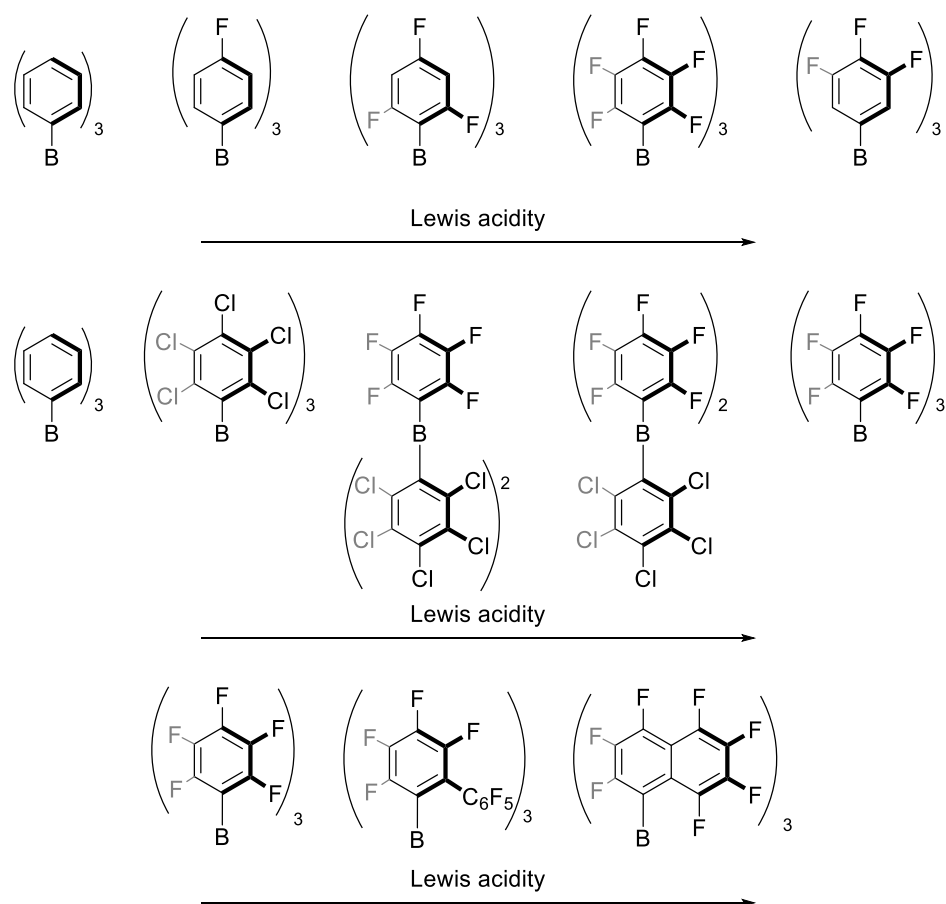


Figure 5 – Trends in Lewis acidity of boron complexes.⁶³

Lewis acidic borocation compounds also reside in the (+III) oxidation state. Figure 6 shows the structure of borinium (2-coordinate), borenium (3-coordinate), and boronium (4-coordinate) ions.⁶⁴ As the coordination number decreases, the reactivity increases as a result of increased Lewis acidity. Therefore, borinium ions are seldom utilised as their high reactivity results in low stability, conversely, boronium ions are often too stable to participate in many reactions. Borenium ions offer a compromise of stability and reactivity that can be exploited in catalytic reactions.⁶⁴

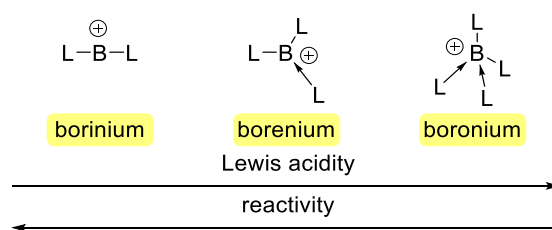


Figure 6 – Lewis acidity trends of cationic boron compounds.⁶⁴

Aluminium is more electropositive than boron, thus unsurprisingly organoaluminium compounds are more Lewis acidic than their organoboron congeners. Table 1 displays the FIA values of many common Lewis acids.⁶⁵ Here the higher acidity of aluminium compared to boron can be seen clearly, with the trend of Lewis acidity increasing upon heavier halogens attached to aluminium mirroring that observed for boron. As previously discussed, variations in computational methodologies can result in different accuracies in the values produced, leading to the slight discrepancy in Lewis acidity trend between AlF_3 and AlCl_3 . Indeed, in more recent FIA calculations, AlF_3 is calculated correctly to be less Lewis acidic than AlCl_3 .²⁵

A recent extension to the field of Lewis acids are Lewis superacids. These have been defined by Krossing as molecular Lewis acids which are more Lewis acidic than monomeric SbF_5 in the gas phase; an arbitrary milestone that stems from SbF_5 historically being regarded as the strongest Lewis acid.⁶⁵ Here, the FIA of SbF_5 is calculated as 489 kJ mol^{-1} , thus the aluminium compounds with a higher FIA than this value are defined as Lewis superacids.⁶⁵

Table 1 – FIAs of common Lewis acids in the gas phase.⁶⁵

Lewis Acid/Anion	FIA (kJ mol^{-1})	Lewis Acid	FIA (kJ mol^{-1})
$\text{BF}_3 / [\text{BF}_4]^-$	338	$\text{AlF}_3 / [\text{AlF}_4]^-$	467
$\text{BCl}_3 / [\text{FBCl}_3]^-$	405	$\text{AlCl}_3 / [\text{FAlCl}_3]^-$	457
$\text{BBr}_3 / [\text{FBBr}_3]^-$	433	$\text{AlBr}_3 / [\text{FAlBr}_3]^-$	494
$\text{BI}_3 / [\text{FBI}_3]^-$	448	$\text{AlI}_3 / [\text{FAlI}_3]^-$	499
$\text{B}(\text{C}_6\text{F}_5)_3 / [\text{FB}(\text{C}_6\text{F}_5)_3]^-$	471	$\text{Al}(\text{C}_6\text{F}_5)_3 / [\text{FAl}(\text{C}_6\text{F}_5)_3]^-$	530
$\text{SbF}_5 / [\text{SbF}_6]^-$	489		

Experimental probes into the Lewis acidic properties of tris(pentafluorophenyl)alane $[\text{Al}(\text{C}_6\text{F}_5)_3]$ in comparison to $\text{B}(\text{C}_6\text{F}_5)_3$ have led to conflicting results. Parks and Mark independently suggested that $\text{B}(\text{C}_6\text{F}_5)_3$ was more Lewis acidic than $\text{Al}(\text{C}_6\text{F}_5)_3$ through

probes into benzonitrile adduct stretching frequencies and methide abstraction/formation in metallocene complexes respectively.^{66,67} Conversely, comparisons between the acids in adduct formation with arenes, double activation of metallocene catalysts for olefin polymerisation, and silane activation have found the alane to be more acidic.⁶⁸⁻⁷¹ A possible explanation for the discrepancy is solvent coordination. $\text{Al}(\text{C}_6\text{F}_5)_3$ is generally isolated as a solvent adduct for safer handling, and thus solvent donation into the empty p_z -orbital of aluminium partially quenches its Lewis acidity. Theoretical probes through FIA calculations and DFT on the unsolvated acids have found the alane to be more Lewis acidic than its borane congener.^{21,65,72}

Few halogenated triarylalanes exist further to $\text{Al}(\text{C}_6\text{F}_5)_3$. Examples include Miyata's $\text{Al}(\text{4-FC}_6\text{H}_4)_3$ in the optimisation of sequential retro-ene arylation and [3,3]-sigmatropic rearrangement/nucleophilic arylation reactions,^{73,74} and $\text{Al}(\text{2,3,5,6-F}_4\text{C}_6\text{H})_3$ as the Lewis acidic component of FLPs for H_2 and olefin activation.⁷⁵

1.2 An introduction to catalysis

1.2.1 A brief introduction to catalysis

Whilst the idea of catalysis was proposed in the early 18th century by leading scientists such as Priestley, Davy, and Faraday, it was not until 1835 that the term catalysis was coined by the Swedish chemist Berzelius.⁷⁶ Berzelius stated in his seminal paper:⁷⁷

“It is, then, proved that several simple or compound bodies, soluble and insoluble, have the property of exercising on other bodies an action very different from chemical affinity. By means of this action they produce, in these bodies, decompositions of their elements and different recombinations of these same elements to which they remain indifferent.”

The current definition of a catalyst by IUPAC carries the same ideology:⁶

“A catalyst is a substance that increases the rate of a reaction without modifying the overall standard Gibbs energy change in the reaction without being consumed.”

Essentially, a catalyst acts by allowing an alternate pathway for a reaction to occur with a lower energy barrier, thus making said reaction more energy efficient. As a result, catalysis has earned a place as one of the twelve principles of green chemistry and remains a focus for chemists worldwide.⁷⁸

1.2.2 The importance of main-group catalysis

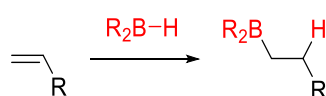
Currently, it is commonplace for large industrial processes to use catalysts based upon *d*-block elements. Whilst some catalytic processes are readily catalysed by first-row transition metals (e.g. the Haber Bosch and Fischer Tropps processes), many more are catalysed by the platinum group metals (ruthenium, rhodium, palladium, osmium, iridium, and platinum). Whilst these metals are extremely efficient catalysts due to high activity and tunability, they come with significant disadvantages: they have a limited supply within the Earth's crust; they are often mined in places with geopolitical issues, making supply unreliable; and they are often toxic, causing potential issues downstream in the agricultural and pharmaceutical industries.⁷⁹

An alternative to the platinum group metals are the main-group elements, which consists of elements within the *s*- and *p*-blocks of the periodic table. These elements

are generally less toxic and more abundant than those in the *d*-block, making them attractive substitutes to chemists focusing on phasing out the use of platinum group metals as catalysts. Whilst not as chemically versatile as the platinum group metals, the properties of main-group elements have recently been exploited so that they can begin to replicate those of the *d*-block, with examples in 1,2-functionalisation, hydrogenation, and cross-coupling reactions.^{80–83} Therefore, the use of benign main-group elements such as boron or aluminium to replicate and improve upon the chemistry of platinum group metals is of high importance.

1.2.3 Catalytic hydroboration

Hydroboration is a well-known method used to functionalise unsaturated substrates into materials with wide applicability in the pharmaceutical, agricultural, and fine chemical markets (Scheme 4). This 1,2-functionalisation was first reported by Brown, who used catecholborane (HBCat) as the borane source in a range of uncatalysed reactions, research which was awarded the 1979 Nobel prize in chemistry.^{84–87} Unfortunately, the catecholboronate esters formed through Brown's efforts were unstable towards water and air, which limited applicability somewhat. The hydroboration methodology was improved by Knochel with the introduction of pinacolborane (HBPin).⁸⁸ The pinacolboronate esters formed after hydroboration by HBPin were found to be more resistant to hydrolysis and decomposition than their catechol counterparts.⁸⁸ Currently, boronate esters formed by hydroboration are valued for their application in C–C bond forming reactions, particularly the Suzuki-Miyaura cross-coupling transformation.⁸⁹



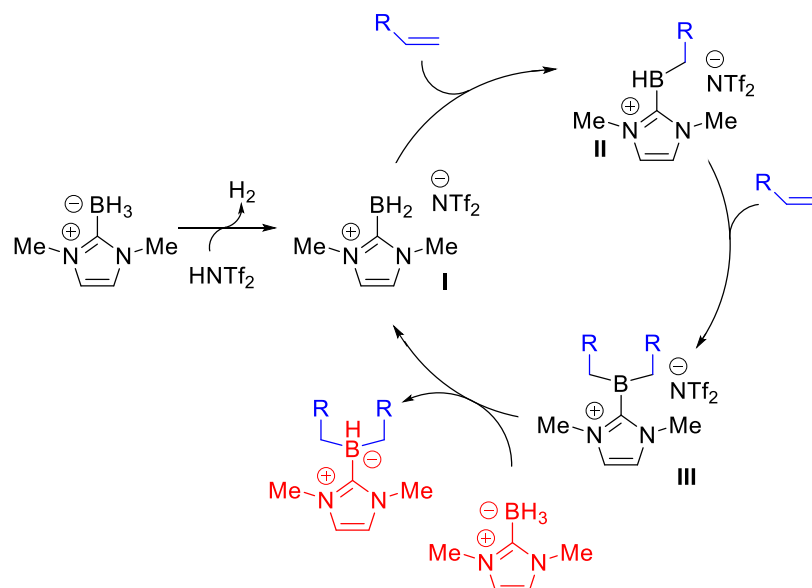
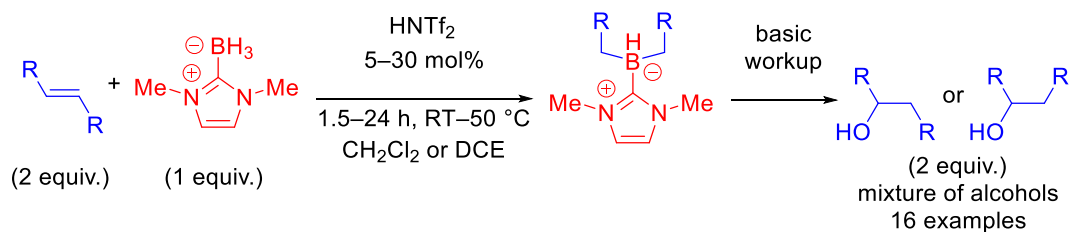
Scheme 4 – Hydroboration of an alkene.⁸⁹

For many years the catalysts used for the hydroboration reaction were based upon the platinum group metals.⁹⁰ There is ongoing investigation into the use of precious metal catalysts for the hydroboration transformation; however, focus is now on very specific regioselectivity, chemoselectivity and stereoselectivity.⁹⁰ Meanwhile, a drive towards sustainable chemistry has led to many research groups exploring catalysts from the main-group and the first-row of transition metals to replicate and improve upon their transition metal forebearers, the results of which have been summarised

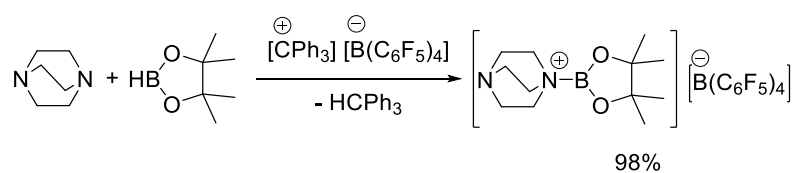
in recent reviews.^{91,92} In sections 1.2.4 and 1.2.5, recent literature on boron- and aluminium-catalysed hydroboration reactions will be discussed.

1.2.4 Hydroboration catalysed by boron-based Lewis acids

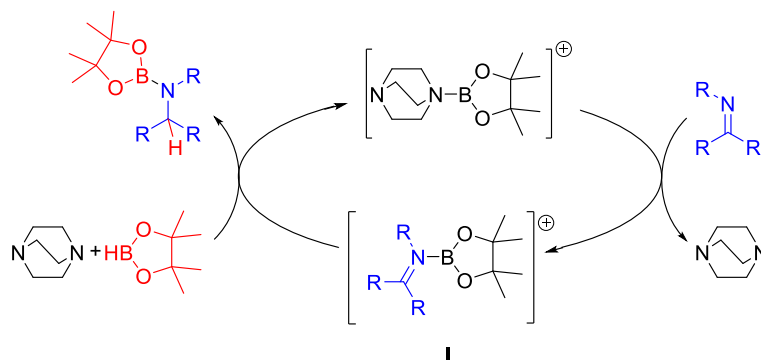
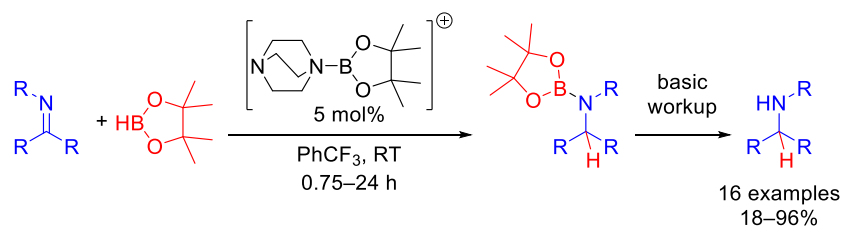
Whilst borane-catalysed hydroboration was first explored by Periasamy in the early 1990s,^{93,94} Interest in boron-catalysed hydroboration was piqued for many as a result of Vedejs' and Crudden's simultaneous publications on borenium-ion-catalysed hydroboration in 2012.^{95,96} Vedejs' study investigated the use of an *in situ* generated NHC (N-heterocyclic carbene)-borenium ion for the addition of NHC-boranes across alkenes (Scheme 5).⁹⁵ Here, the NHC-borenium ion was found to hydroborate two equivalents of alkene per turnover, and upon an oxidative workup was found to liberate alcohols; however, a mixture of Markovnikov and *anti*-Markovnikov products, along with some migration products were often observed (8 examples of internal and terminal olefins, probed with 16 sets of conditions).⁹⁵ Mechanistically, the NHC-borenium ion catalyst was generated through addition of triflimide to the NHC-borane used as the boron source (**I**). Two equivalents of alkene were then able to sequentially react with this NHC-borenium ion (**II**; **III**), before hydride transfer with NHC-borane liberated the dihydroboration product and regenerated the catalyst. Unfortunately, migration of the borenium ion across the olefin resulted in a mixture of alcohol products upon workup, highlighting the limitations of this procedure.⁹⁵

Scheme 5 – Proposed catalytic hydroboration of alkenes by Vedejs' NHC-borenum ion catalyst.⁹⁵

Crudden's borenium ions were prepared through hydride abstraction by trityl salts of [B(C₆F₅)₄][−] in the presence of DABCO (1,4-diazabicyclo[2.2.2]octane). This resulted in a borenium ion catalyst, a catalytically innocent [B(C₆F₅)₄][−] counterion, and the liberation of triphenylmethane (Scheme 6).⁹⁶

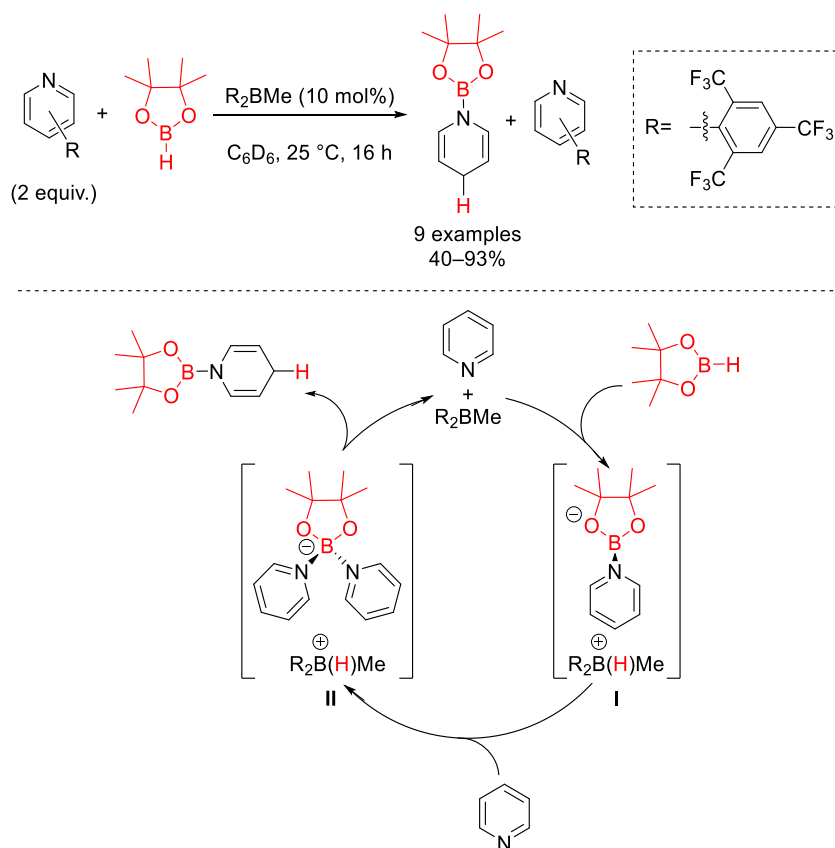
Scheme 6 – Preparation of Crudden's borenium ion hydroboration catalyst.⁹⁶

Upon application towards catalysis, Crudden's borenium ion was shown to be capable of reducing sixteen imine substrates at room temperature. Following a basic workup, the resultant amines could be isolated in up to 96% yield. Mechanistic studies suggested that the reaction was initiated by the transfer of the borenium part of the catalyst to the imine, thereby liberating the DABCO (I). The resultant boron-activated iminium ion could then be reduced by HBPi to form the hydroborated product, whilst simultaneous recombination with the liberated DABCO reformed the catalyst (Scheme 7).⁹⁶

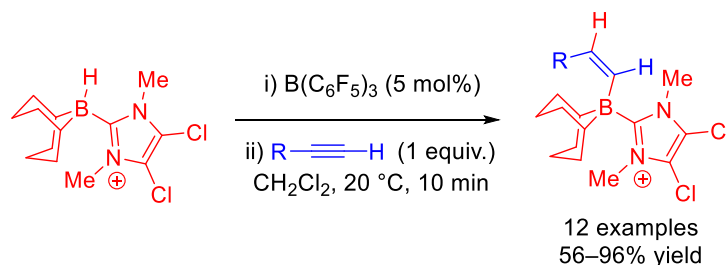


Scheme 7 – Proposed catalytic hydroboration of imines by Cruden's borenium ion catalyst.⁹⁶

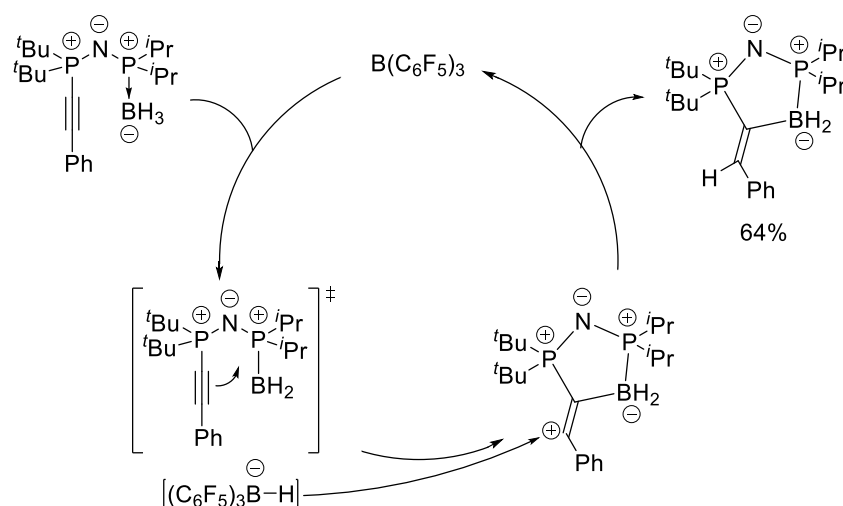
There have been many further investigations into the use of borenium ions in hydroboration catalysis; however, they are less pertinent to this thesis. Further examples can be found in recent reviews by Cruden and Melen.^{97,98} In 2015, Wang investigated the 1,4-hydroboration of pyridines by a diarylmethylborane catalyst (Scheme 8).⁹⁹ Herein, two equivalents of pyridine were required: the first equivalent formed a borenium ion with pinacolborane, whilst the borane catalyst abstracted the hydride from pinacolborane (**I**); the second equivalent of pyridine then coordinated to the borenium ion, forming a four-coordinate boronium ion (**II**) and allowing it to undergo facile hydride transfer from the generated borohydride to liberate the catalyst, an equivalent of pyridine, and the 1,4-hydroboration product. The exclusive formation of the 1,4-hydroboration product over the 1,2-hydroboration product was attributed to the large steric repulsion between the BPin and the borohydride immediately before the hydride transfer step (**II**) of the mechanism. Albeit with some substrate limitations (disubstituted and *para*-substituted pyridines), this system allowed for the hydroboration of nine pyridine derivatives in up to 93% yield.⁹⁹

Scheme 8 – Hydroboration of pyridines by Wang's borane catalyst.⁹⁹

In 2016, Ingleson recorded the first use of $B(C_6F_5)_3$ as a hydroboration catalyst (Scheme 9).¹⁰⁰ Herein $B(C_6F_5)_3$ acted as a catalyst to *trans*-hydroborate alkynes selectively with an NHC-borenium ion (NHC-9-BBN) as the boron source. These hydroborations exclusively formed the *anti*-Markovnikov products, with 12 examples of terminal alkyne substrates forming vinylboranes in up to 96% yield. Furthermore, these vinylboranes were subjected to Suzuki-Miyaura couplings to form alkenes, demonstrating the industrial applicability of the reaction.¹⁰⁰

Scheme 9 – Ingleson's use of $B(C_6F_5)_3$ as a hydroboration catalyst.¹⁰⁰

Stephan later reported the use of $B(C_6F_5)_3$ as a hydroboration catalyst in the intramolecular formation of a novel PNPCB heterocycle from an alkynyl P–N–P complex in 64% yield (Scheme 10).¹⁰¹



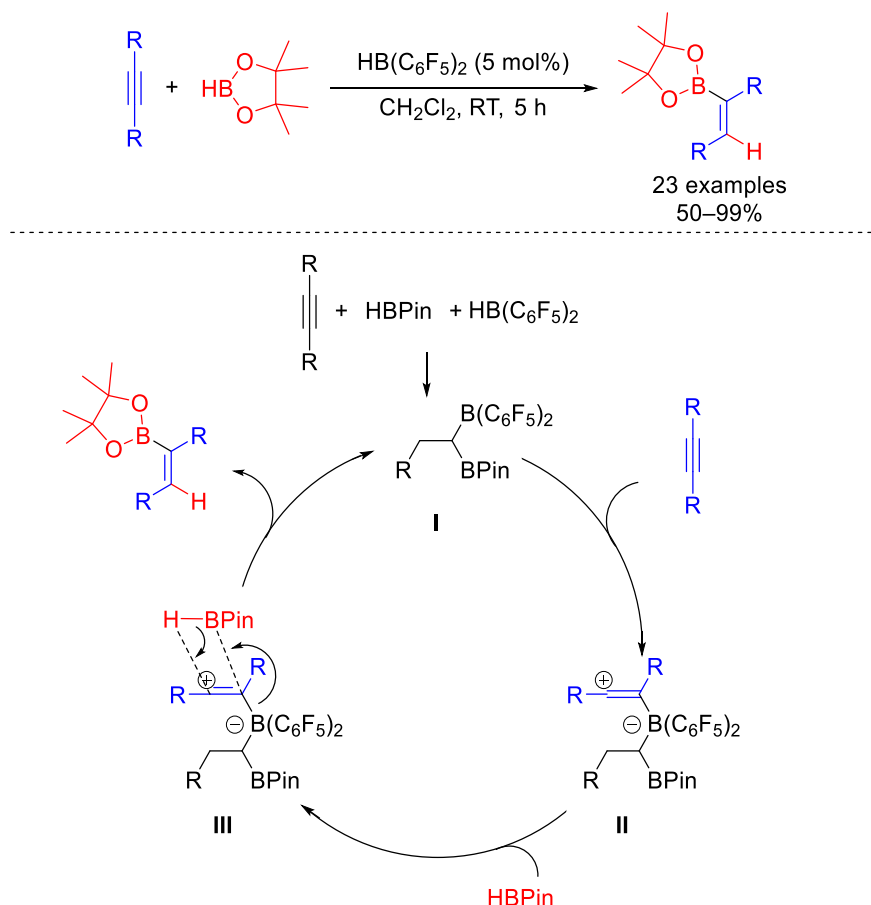
Scheme 10 – Catalytic formation of a PNPCB heterocycle using intramolecular hydroboration.¹⁰¹

In these reports, the catalyst required the presence of a Lewis base, such as an amine, NHC, or phosphine to allow the catalytic hydroboration to occur.^{95,96,99–101} This was important for two reasons: first, the presence of the base energetically favoured B–H heterolysis in the catalytic cycles; and second, it stabilised the borocations present in solution. Furthermore this meant that in the cases where B(C₆F₅)₃ or diarylmethylboranes were employed as a catalyst, their corresponding borohydrides functioned as the reducing agent instead of the borane source (e.g. pinacolborane).^{96,100,102}

Diarylboranes have also been reported to act as efficient hydroboration catalysts. Hoshi reported the hydroboration of terminal alkynes with pinacolborane using a catalytic amount of dicyclohexylborane (HBCy₂) (8 examples, 67–95% yield).¹⁰³ HBCy₂ was later used by Ellis to hydroborate alkynyl pinacolboronates before subjecting them to a proto-deboronation reaction, essentially converting alkynyl pinacolboronates into alkenyl pinacolboronates (10 examples, 57–93% yield).¹⁰⁴

More recently, Stephan and Glorius reported that Piers borane [HB(C₆F₅)₂] could be used for the hydroboration of internal and terminal alkynes.¹⁰⁵ Unlike HBCy₂, Piers borane was proposed to act as a pre-catalyst, forming a catalytically active 1,1-diborylated alkane species upon addition to the alkyne substrate and pinacolborane (**I**). In the proposed mechanism (Scheme 11), the alkyne substrate could coordinate to the bisborylated catalyst (**II**), allowing for a concerted hydroboration with pinacolborane (**III**) and subsequent release of product. This methodology was used to hydroborate 23 alkynes, to form boronate esters in up to 99% yield.¹⁰⁵

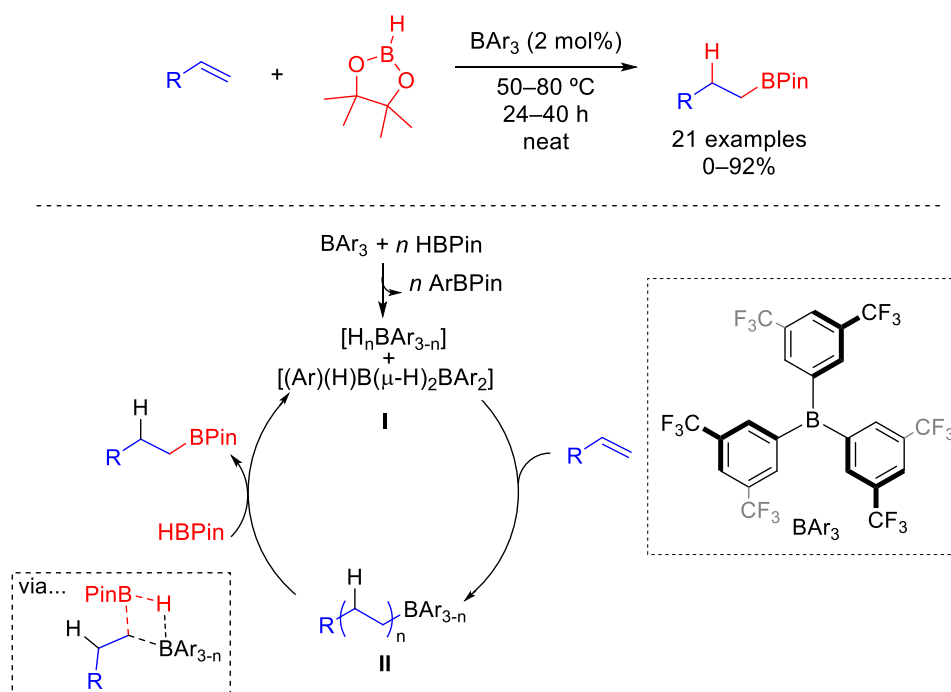
Notably, recent in-depth isotopic mechanistic studies by Lloyd-Jones and Thomas have contested the validity of this mechanism. It was shown that the proposed addition then dehydroboration was unlikely to occur due to the fact that the *cis*-hydrogen installed onto the product originated from the diarylborane catalyst rather than the HBPIn. The true mechanism was instead suggested to be a stepwise 1,2-addition involving metathesis, similar to that later proposed by Oestreich.^{102,106}



Scheme 11 – Proposed mechanism of hydroboration of alkynes using Piers borane as a pre-catalyst.¹⁰⁵

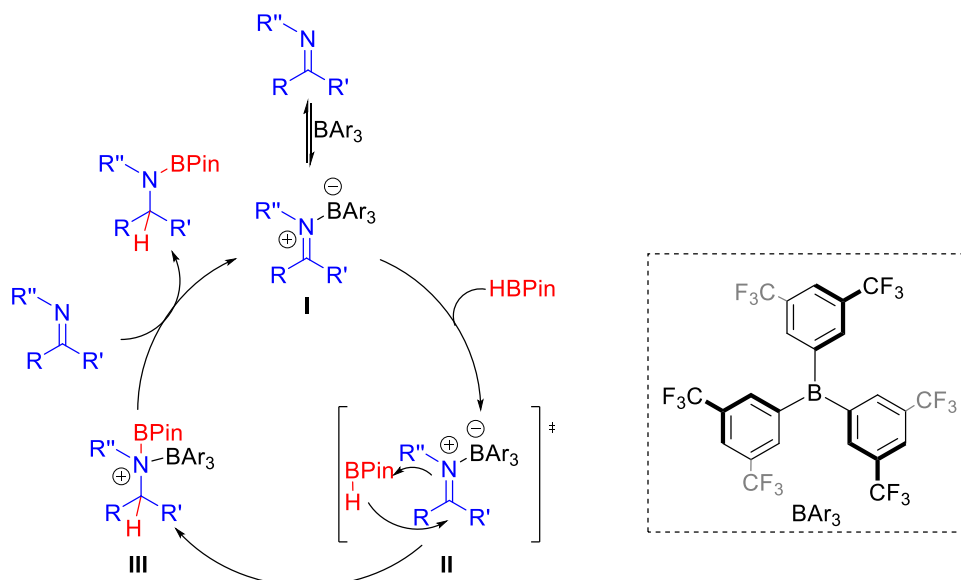
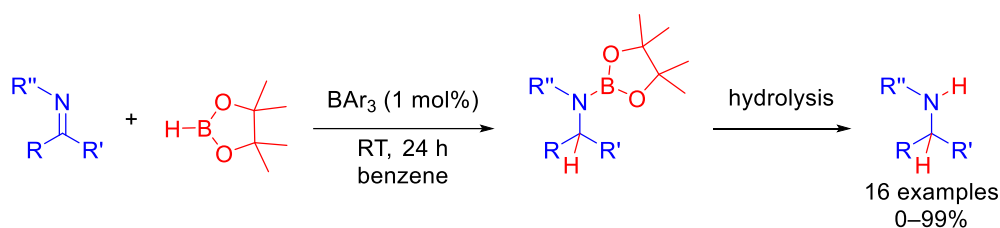
In 2016, Oestreich reported the first triarylborane-catalysed hydroboration without the presence of a Lewis base.¹⁰² In a particularly noteworthy example, tris(3,5-bis(trifluoromethyl)phenyl)borane [B(3,5-(CF₃)₂C₆H₃)₃] was observed to be active towards the transformation where the archetypal triarylborane B(C₆F₅)₃ was not. Stoichiometric control experiments between B(C₆F₅)₃ and HBPIn found that the borane simply cleaved the 1,3,2-dioxaborolane ring of HBPIn, resulting in the formation of B₂Pin₃ amongst other decomposition products instead of catalytically active borohydride species. Meanwhile, the addition of HBPIn to B(3,5-(CF₃)₂C₆H₃)₃ resulted in a mixture of diboranes that were active towards hydroboration.¹⁰²

A mechanism for this hydroboration is shown in Scheme 12. Initially, catalytically active hydroborane species were formed through reaction of $B(3,5-(CF_3)_2C_6H_3)_3$ with HBPIn (I). The alkene substrates were then able to coordinate to the catalyst to form a range of hydroboration adducts (II). Subsequent substituent exchange with HBPIn allowed for the formation of the desired boronate ester and regeneration of the active catalyst. The catalytic system using a $B(3,5-(CF_3)_2C_6H_3)_3$ pre-catalyst was shown to be efficient for the hydroboration of 21 aliphatic and aromatic alkenes, to form boronate esters in up to 92% yield.¹⁰² This mechanism was later confirmed through in-depth isotropic and computational studies by Lloyd-Jones and Thomas.¹⁰⁶ Here, it was discovered that the metathesis step occurred through a μ -B-H-B bridged, 2-electron-3-centre bonded B-C-B intermediate.



Scheme 12 – Alkene hydroboration with a $B(3,5-(CF_3)_2C_6H_3)_3$ pre-catalyst.^{102,106}

Shortly afterwards, Oestreich reported that $B(3,5-(CF_3)_2C_6H_3)_3$ could also be used in the hydroboration of ketimines; however, mechanistic probes revealed that the catalyst did not dissociate into a mixture of hydroboranes in the presence of HBPIn at room temperature.¹⁰⁷ A proposed mechanism suggested that the borane catalyst initially coordinated to the nitrogen atom of the imine (I), thereby lowering its LUMO and making it more susceptible to reduction by pinacolborane (II). The resultant amine-borane adduct could then be exchanged with a more basic imine (III) to close the catalytic cycle and generate the desired amine. Through this, the hydroboration of 16 imines was observed in up to 99% yield (Scheme 13).¹⁰⁷

Scheme 13 – Imine hydroboration with a $B(3,5-(CF_3)_2C_6H_3)_3$ catalyst.¹⁰⁷

A further justification to the high activity of $B(3,5-(CF_3)_2C_6H_3)_3$ in comparison to $B(C_6F_5)_3$ was that its aryl rings were devoid of *ortho*-fluorine atoms. This was theorised because $B(3,5-(CF_3)_2C_6H_3)_3$ and $B(C_6F_5)_3$ have similar Lewis acidities as determined by the Gutmann-Beckett method, leading to differences in steric hindrance becoming their primary differentiating factor. As a result, the novel borane tris(3,4,5-trifluorophenyl)borane [$B(3,4,5-F_3C_6H_2)_3$] was synthesised to justify further this hypothesis. $B(3,4,5-F_3C_6H_2)_3$ was applied in a stoichiometric amount towards the hydroboration of *N*,1-diphenylethan-1-imine and was shown to result in full conversion to the corresponding boronate ester in four hours at room temperature. This was compared to the same reaction with $B(C_6F_5)_3$ which resulted in an imine-borane adduct only.¹⁰⁷

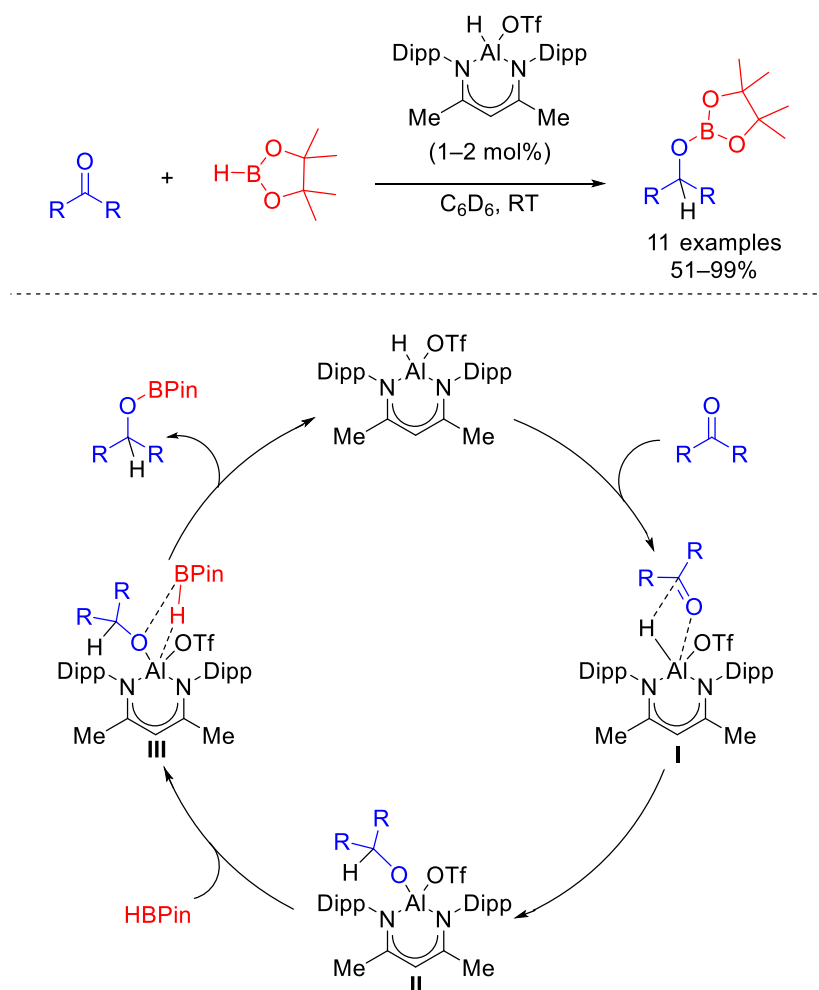
The Melen group later investigated the use of the weakly acidic borane tris(2,4,6-trifluorophenyl)borane [$B(2,4,6-F_3C_6H_2)_3$] as a hydroboration catalyst, and found it efficient in the reduction of aldehydes, imines and alkynes. 52 examples were given, with product yields ranging from 55–99%.¹⁰⁸ Thomas reported the use of the simple commercially available borane adducts $BH_3 \cdot THF$ and $BH_3 \cdot SMe_2$ for alkyne and alkene hydroborations with HBPin in neat conditions. Here, 18 substrates were

explored with isolated yields between 26 and 94%.¹⁰⁹ A recent study by Thomas found that many *s*-block based hydroboration catalysts such as ⁿBuLi and NaO^tBu were in fact pre-catalysts, forming BH₃ through nucleophilic decomposition of HBPIn.¹¹⁰

1.2.5 Hydroboration catalysed by aluminium-based Lewis acids

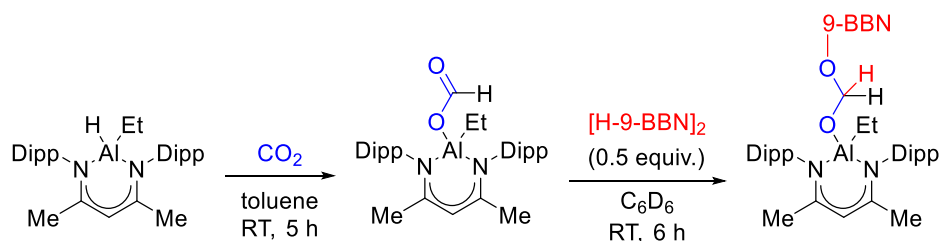
Triarylalanes have not previously been reported to act as hydroboration catalysts, with focus instead directed towards their applications in FLP chemistry and polymerisation catalysis.^{67,71,111–115} Aluminium based compounds for hydroboration catalysts from the literature are categorised as either aluminium hydrides or anionic aluminate species.

The first report of an organoaluminium-hydride-catalysed hydroboration process was developed in 2015 by Yang, Parameswaran, and Roesky.¹¹⁶ Here, an aluminium nacnac (β -diketiminate) hydride was shown to hydroborate aldehydes and ketones under ambient conditions with catalyst loadings at 1% for aldehydes and 2% for ketones. A combination of computational and experimental probes suggested a mechanism (Scheme 14). Upon exposure to the carbonyl, a four-membered transition state was formed with the catalyst, with weak coordination between the carbonyl oxygen and the Lewis acidic aluminium centre, and the aluminium's hydride with the electrophilic carbonyl carbon atom (**I**). Subsequent hydride shift from the aluminium to the carbonyl carbon resulted in the formation of a coordinated complex (**II**). Addition of HBPIn and σ -bond metathesis between the Al–O bond of the coordinated complex and the B–H bond of HBPIn (**III**) ensued in the release of the hydroborated product and regeneration of the catalyst. Notably, the hydrogen atom which was added onto the carbonyl originated from the hydride catalyst and not the HBPIn, with the HBPIn replenishing the hydride on the catalyst through each turnover.¹¹⁶



Scheme 14 – Hydroboration by Yang, Parameswaran, and Roesky's aluminium nacnac hydride catalyst.¹¹⁶

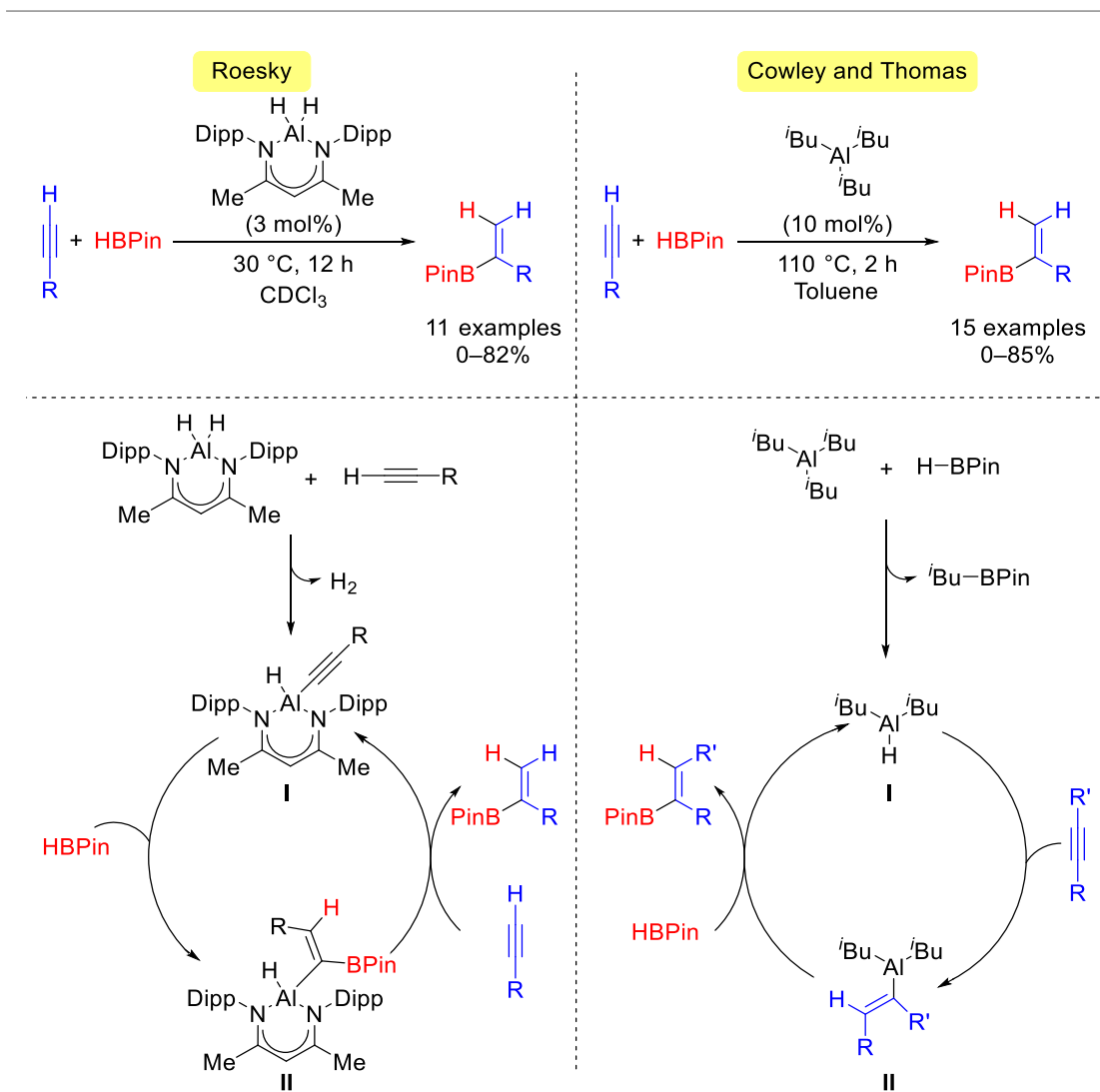
Related aluminium nacnac hydride catalysts have also been prepared by Goicoechea and Aldridge to probe their reactivity with CO₂ and commercially available boranes.¹¹⁷ Whilst no reactivity was observed with HBPIn, the successful hydroboration of CO₂ was observed with 9-BBN (9-borabicyclo[3.3.1]nonane) to form an aluma-bora-acetal. Notably, no σ -bond metathesis between the Al–O bond and the B–H bond of 9-BBN was observed, highlighting a difference in mechanism compared to the hydroboration of carbonyls by Yang, Parameswaran, and Roesky.¹¹⁷



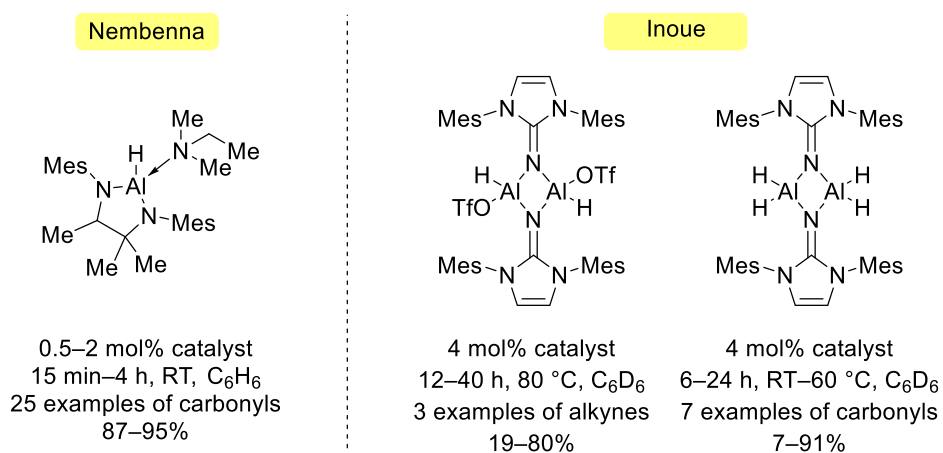
Scheme 15 – Hydroboration of CO₂ by an aluminium nacnac hydride catalyst.¹¹⁷

Yang, Parameswaran, and Roesky later investigated the use of an aluminium dihydride species in the catalytic hydroboration of alkynes.¹¹⁸ This proceeded through a slightly different mechanism to its monohydride predecessor, as the active catalyst was not the dihydride, rather an alkynyl aluminium species formed through deprotonation of the dihydride by an alkyne and resultant loss of dihydrogen (I) (Scheme 16, left). The catalytic cycle was calculated to be initiated by hydroboration of the alkynyl aluminium complex with HBPIn (II), followed by a σ -bond metathesis with this alkenyl boronate ester and an alkyne. The aluminium-based catalyst was found to catalyse the hydroboration of nine alkynes to boronate esters in up to 82% yield.¹¹⁸

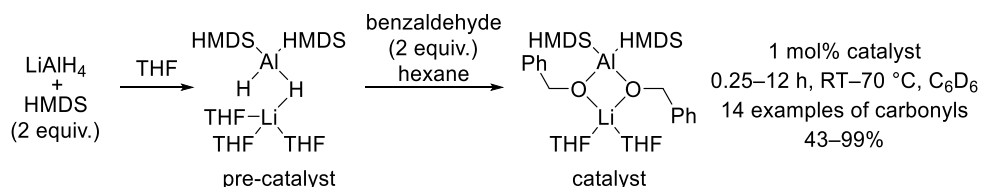
In the same year, Cowley and Thomas reported that two commercially available aluminium species, *triisobutyl* aluminium and DABCO stabilised triethyl aluminium, could also catalyse the hydroboration of alkynes, with 15 examples given for each, and yields up to 89% for *triisobutyl* aluminium and 84% for DABCO·AlEt₃.¹¹⁹ Both species were found to be pre-catalysts, which generated active aluminium hydride species through ligand exchange with HBPIn. Mechanistic studies for the *triisobutyl* aluminium pre-catalyst displayed a notable contrast to those proposed by Roesky (Scheme 16, right). Here the active catalyst was generated through reaction with HBPIn to form an aluminium hydride (I). This aluminium hydride could then act as an hydroalumination agent towards an alkyne (II), which in turn underwent σ -bond metathesis with HBPIn to form the alkenyl boronate ester and regenerate the active catalyst.¹¹⁹

Scheme 16 – Alkyne hydroboration with aluminium based catalysts.^{118,119}

Inoue and Nembenna have also reported aluminium hydride catalysts that are active towards the hydroboration of carbonyls and alkynes (Figure 7).^{120,121}

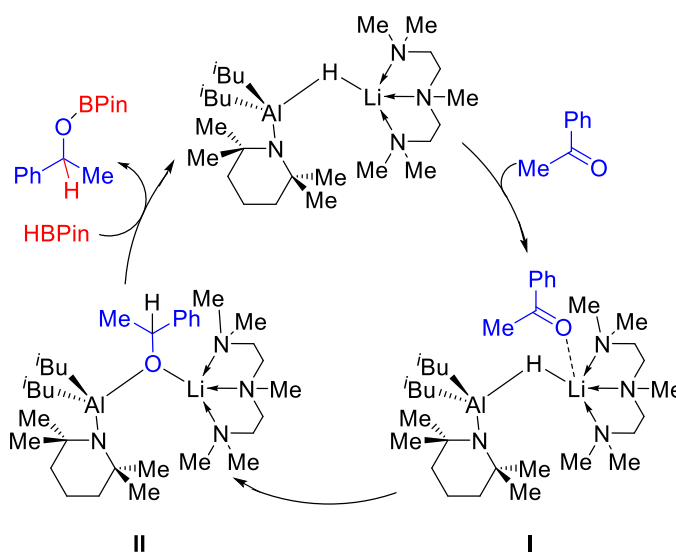
Figure 7 – Further aluminium hydride catalysts for hydroboration.^{120,121}

Anionic aluminate species which incorporate lithium have also been shown to be efficient hydroboration catalysts. In 2018, Mulvey investigated the use of lithium diamidodihydridoaluminate in the hydroboration of carbonyls. This complex was actually a pre-catalyst, which formed a hydrometallated bis-benzyloxy catalyst upon exposure to two equivalents of a carbonyl (Scheme 17).¹²² Through a synergistic bimetallic process, these catalysts were found to hydroborate 14 carbonyls into their corresponding boronate esters.¹²²

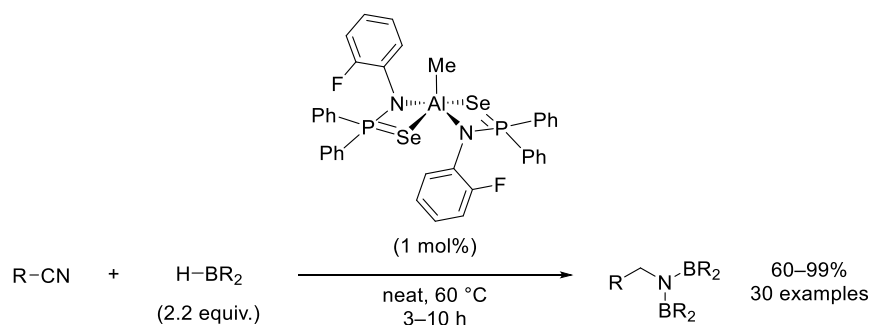


Scheme 17 – Synthesis of a lithium diamidodihydridoaluminate pre-catalyst and resultant hydroboration catalyst.¹²²

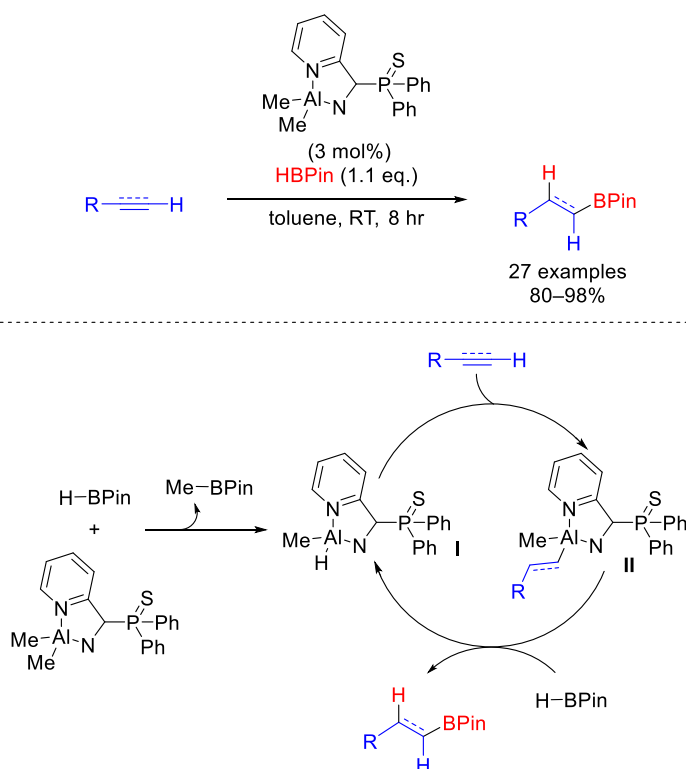
Mulvey later investigated the use of heteroleptic dialkyl-monoamido-monohydrido lithium aluminates, and investigated the effect of donating solvents (Scheme 18).¹²³ Here, pentamethyldiethylenetriamine (PMDETA) was found to bind too strongly to the lithium atom of the catalyst, thereby reducing the rate of hydroboration; however, the donation of DABCO and THF towards the lithium counterion was observed to increase the rate of catalysis.¹²³ Mechanistic investigations were performed using the PMDETA ligand (Scheme 18). This found that the carbonyl would first coordinate with the lithium centre (**I**), which allowed for substrate insertion into the Al–H bond to form an Al-hydroxide intermediate (**II**). Addition of HBPIn and a resulting σ -bond metathesis allowed for the formation of the boronate ester and regeneration of the catalyst.¹²³



Scheme 18 – Proposed mechanism of hydroboration of carbonyls by solvated heteroleptic dialkyl-monoamido-monohydrido lithium aluminates.¹²³

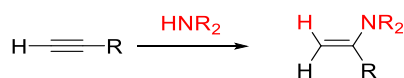
Scheme 20 – Hydroboration of nitriles by an aluminium alkyl pre-catalyst.¹²⁶

A subsequent study by Panda revealed that a related aluminium bis-alkyl complex was capable of acting as a pre-catalyst for the hydroboration of a wide scope of alkenes and alkynes.¹²⁷ It was proposed that, following metathesis with HBPIn, the aluminium bis-alkyl complex formed a highly active aluminium hydride catalyst (I). It was then suggested that this aluminium hydride would initially hydroaluminate the substrate (II) before undergoing metathesis with HBPIn to release the hydroborated product (Scheme 21). Sixteen alkenes and eleven alkynes were efficiently reduced and isolated as exclusively the *anti*-Markovnikov product.¹²⁷

Scheme 21 – Hydroboration of alkenes and alkynes by an aluminium bis-alkyl pre-catalyst.¹²⁷

1.2.6 Catalytic hydroamination

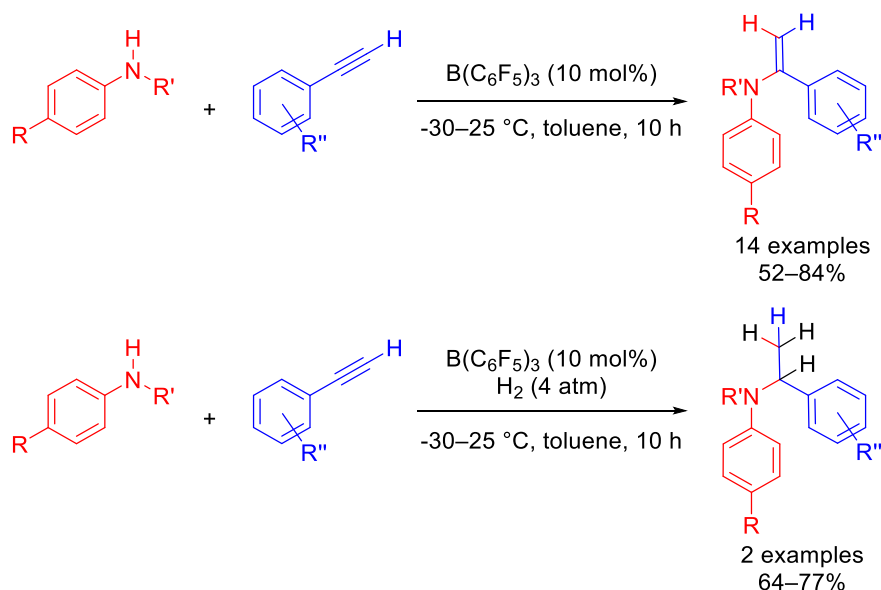
Hydroamination is another well-known type of 1,2-functionalisation reaction that has a myriad of applications within the pharmaceutical, agricultural, and fine chemical markets (Scheme 22).¹²⁸ The vast majority of hydroamination catalysts are based upon transition metals, usually with a lanthanide or a group four metallocene centre; however, a focus on sustainable chemistry has led towards more abundant and environmentally friendly catalysts being applied to the hydroamination transformation. Mostly these catalysts are based upon the alkaline metals,⁸³ but there are infrequent examples of boron based Lewis acid catalysts that can also be used to promote this reaction using FLP-type reactivity.¹²⁹



Scheme 22 – Hydroamination of an alkyne.¹²⁸

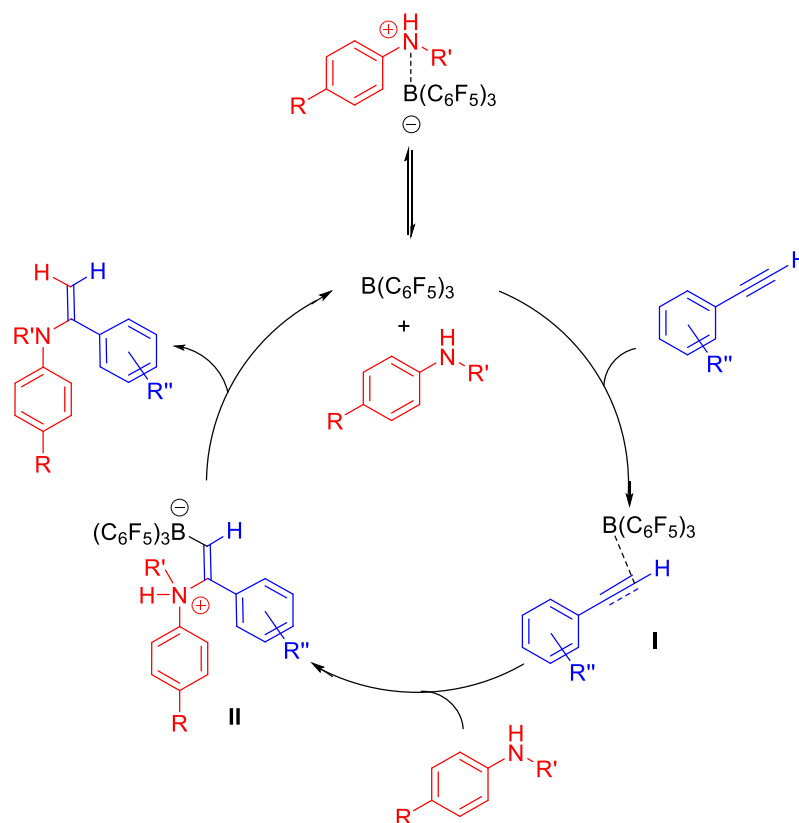
1.2.7 Hydroamination catalysed by boron-based Lewis acids

The first example of $\text{B}(\text{C}_6\text{F}_5)_3$ -catalysed hydroamination was reported by Stephan in 2013, who used the catalyst to promote the hydroamination of 14 amines and alkynes into their respective enamines. Notably, only the Markovnikov addition product was generated in all cases. A one-pot hydroamination/reduction reaction was subsequently investigated by performing the reaction under a hydrogen atmosphere. Whilst only two examples were reported, two tertiary amines were generated in good yield from an enamine intermediate (Scheme 23).¹³⁰

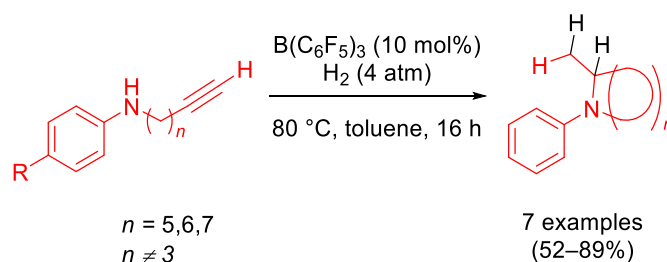


Scheme 23 – B(C₆F₅)₃ mediated hydroamination of terminal alkynes and B(C₆F₅)₃ mediated tandem hydroamination/reduction of alkynes.¹³⁰

The observed enamine products from Markovnikov addition suggested the reaction to be FLP-like in nature, whereupon the amine acted as both the substrate and as the FLP's Lewis basic component. A proposed mechanism suggested that the alkyne initially coordinated to B(C₆F₅)₃ to generate an adduct between the terminal alkyne carbon and the Lewis acidic boron atom (I). A subsequent nucleophilic attack by the amine resulted in the generation of a zwitterionic intermediate whereupon the Lewis acidic and basic centres activated the alkyne moiety (II). This zwitterionic intermediate resembled an FLP-activated complex and promoted the generation of the exclusively Markovnikov product. A final 1,3-hydride shift in this intermediate formed the desired enamine. Notably, due to the basic nature of the amine, it existed in equilibrium as the free amine and an adduct with the borane catalyst in solution before the reaction (Scheme 24).¹³⁰

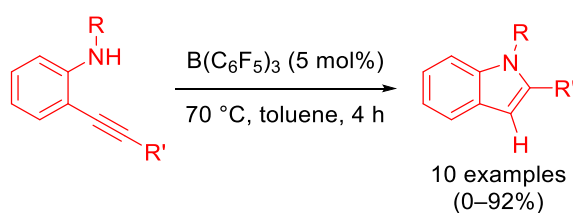
Scheme 24 – Mechanism of $B(C_6F_5)_3$ mediated hydroamination of terminal alkynes.¹³⁰

Stephan later expanded this protocol towards tandem intramolecular hydroamination/reduction reactions to form cyclic amines.¹³¹ The preparation of five, six, and seven-membered heterocycles was observed to be possible over seven examples; however, the attempted cyclisation of *N*-propynyl-substituted anilines into their respective three-membered aziridines could not be achieved (Scheme 25).¹³¹

Scheme 25 – $B(C_6F_5)_3$ mediated tandem hydroamination/reduction of alkynes.¹³¹

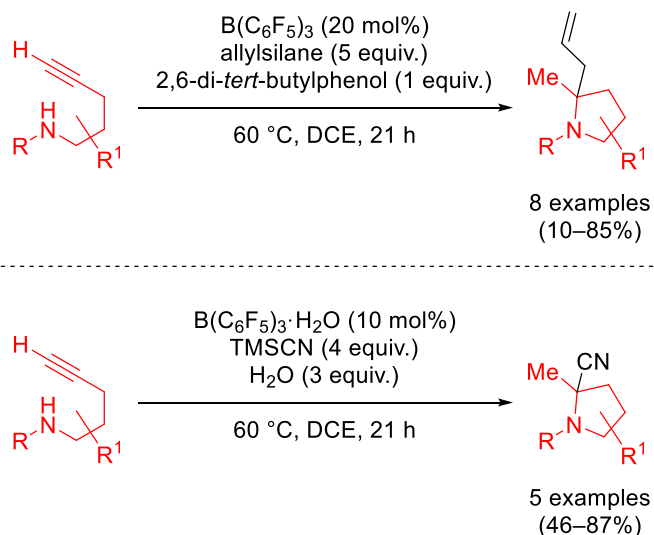
The synthesis of indoles was later observed *via* borane-catalysed intramolecular hydroamination. Whilst a range of Lewis acidic boranes were applied towards the transformation, only $B(C_6F_5)_3$ was observed to promote the reaction, with the less Lewis acidic boranes $B(2,6-F_2C_6H_3)_3$ and $B(2,4,6-F_3C_6H_2)_3$ recalcitrant towards the reaction. Six indoles were successfully prepared through 5-*endo*-dig cyclisations;

however, four amines were unreactive due to the low nucleophilicity of the nitrogen atom (Scheme 26).¹³²



Scheme 26 – $\text{B(C}_6\text{F}_5)_3$ -catalysed indole synthesis through intramolecular hydroamination.¹³²

The most recent foray into the field of borane-catalysed hydroamination was Yamamoto's investigation into intramolecular tandem hydroamination/hydroallylation and hydroamination/hydrocyanation procedures to form polysubstituted pyrrolidines from secondary amines installed with an alkyne functionality. In each of these cases, hydroamination was first performed, followed by the hydroallylation or hydrocyanation. Notably in this case the $\text{B(C}_6\text{F}_5)_3$ catalyst was used in its hydrated form for the tandem hydroamination/hydrocyanation reaction; however, the anhydrous borane was required for efficient reactivity in the tandem hydroamination/hydroallylation reaction (Scheme 27).¹³³



Scheme 27 – $\text{B(C}_6\text{F}_5)_3$ mediated tandem hydroamination/hydroallylation (top) and tandem hydroamination/hydrocyanation (bottom).¹³³

1.3 An introduction to enabling technologies

1.3.1 What is an enabling technology?

An enabling technology is defined as a tool which can assist a user to improve their performance and capabilities, by speeding up or facilitating processes and tasks.¹³⁴ The concept of enabling technologies expands further than the chemical sciences. For example, tools such as the printing press and the internet have served as enabling technologies for communication, whilst the invention of the steam engine was a key enabling technology behind the industrial revolution. The latest enabling technology seen by many to revolutionise the way we work is the 3D printer. This modern technology has also found many applications in the chemical world, from 3D printed reactors to catalysts which are amenable to 3D printing onto surfaces. Indeed, drug molecules have even been observed to be 3D printable on demand.^{135,136}

To focus on chemistry, much of the equipment that the modern chemist uses on a day to day basis does not differ much from that of the scientists and alchemists of the 18th and 19th centuries.¹³⁷ Even intricate pieces of equipment that are required to handle air sensitive or dangerous compounds, such as the Schlenk line or nitrogen filled glove boxes, have been used for decades.^{138,139} With this in mind it is unsurprising that there is a wide scope of enabling technologies for chemists to exploit. Whilst there are still many benefits from the use of classical equipment such as beakers, Erlenmeyer flasks and Büchner funnels, a vast selection of recent technologies can be used to aid chemists by exploring novel reactivities and increasing outputs. In this chapter the benefits of two types of enabling technologies, microwave assisted synthesis and flow chemistry, will be discussed.

1.3.2 An introduction to microwave assisted synthesis

Microwave energy exists in the electromagnetic spectrum between 0.3 to 300 GHz. The most common scenario in which one would find microwave energy is in the kitchen, wherein domestic microwave ovens emit frequencies of 2.45 GHz. The energy of microwave photons at 2.45 GHz is 1.6 MeV, which is too small to make or break chemical bonds, but is strong enough to exert rapid molecular rotation upon polar molecules and thus accelerate heating within reaction mixtures through molecular friction.¹⁴⁰

To understand how this occurs, the underlying physics must be considered. Electromagnetic radiation is composed of perpendicular, synchronised oscillating electric and magnetic waves, which fluctuate at a given frequency (Figure 9). The magnetic component is generally non-functional towards molecules. Contrarily, the electronic component can interact with molecules with a dipole. As microwave radiation oscillates, molecules with a strong dipole also oscillate to keep in alignment with the bulk electric field. Due to the high frequency of the microwave radiation, this causes rapid rotation within the molecules and a resultant generation of heat due to friction. Depending on the reaction mixture, this heat can then be dissipated through the medium as a whole, resulting in rapid heating of the bulk sample.¹⁴⁰

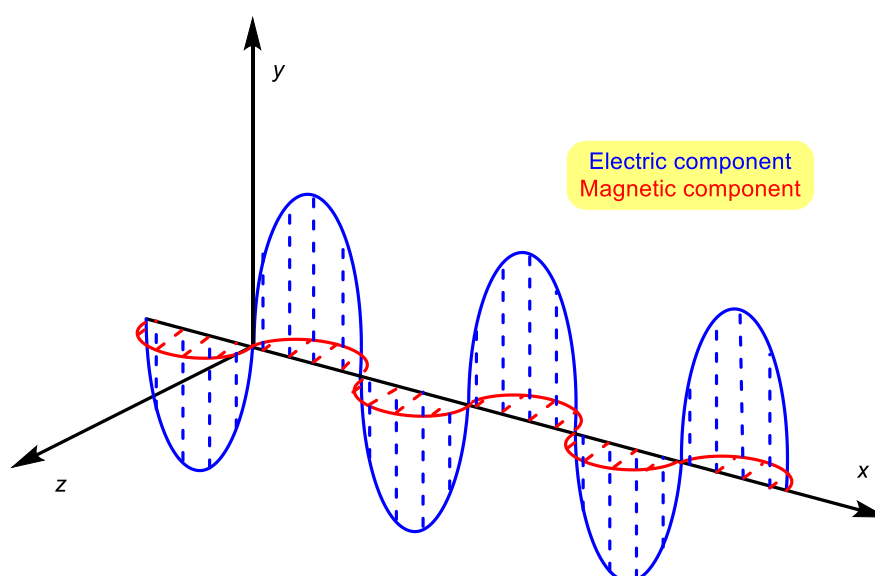


Figure 9 – Components of microwave radiation.¹⁴⁰

At this juncture, a comparison of microwave assisted heating compared with conventional heating reveals the power of the technique. Microwaves work by heating a sample internally through molecular friction, which results in uniform heat dissipation throughout the bulk sample. In contrast, during conventional heating there is a gradient between the boundary of the solvent (where it is in contact with the surface of the heating vessel) and its centre. This uneven temperature gradient can result in inefficient heating throughout the reaction medium.

Only solvents or compounds with a dipole are compatible with microwave radiation. The efficiency of microwave energy upon a compound can be determined by its loss factor ($\tan\delta$), or its ability to convert the energy into heat. The loss factor of a compound can be derived from two values: its dielectric constant (ϵ'), its ability to be polarised by an external electric field; and its dielectric loss (ϵ''), its efficiency at converting microwave energy to heat (Equation 6).¹⁴⁰

$$\tan\delta = \frac{\epsilon''}{\epsilon'}$$

Equation 6 – Calculation of loss factor ($\tan\delta$).¹⁴⁰

Consideration of loss factor is paramount when optimising microwave assisted protocols, as some solvents such as benzene are microwave transparent, and thus ineffective when employed within a microwave reactor. Loss factors of typical organic solvents are displayed in Table 2, with high absorbing solvents possessing a loss factor above 0.5, medium absorbing solvents between 0.1–0.5, and low absorbing solvents below 0.1. Solvents with low loss factors can still be used in the microwave with the addition of highly polar ionic liquids as sensitising agents, or if the reaction takes place within a strongly microwave absorbing silicon carbide heating vessel.¹⁴⁰

Table 2 – Loss factor of common solvents.¹⁴⁰

Solvent	$\tan\delta$	Solvent	$\tan\delta$
Ethylene glycol	1.350	Acetonitrile	0.062
Ethanol	0.941	Ethyl acetate	0.059
Nitrobenzene	0.589	THF	0.047
1,2-Dichlorobenzene	0.280	Dichloromethane	0.042
Dimethylformamide	0.161	Toluene	0.040
Water	0.123	Hexane	0.020
Chloroform	0.091	Benzene	0.000

A contentious question in this field is the existence of non-thermal and specific microwave effects.^{141,142} The nonthermal microwave effects concern the possibility that the electromagnetic field could interact with molecules in a way which does not affect the reaction temperature, such as by stabilising intermediates or transition states. The specific microwave effect suggests that the method in which microwaves heat a sample can alter the chemistry as opposed to conventional heating, such as by heating polar molecules selectively over a non-polar solvent. In these scenarios an increased field strength would have an intensified non-thermal or specific microwave effect.^{141,142}

The existence of these non-thermal or specific microwave effects has been disputed by many.^{142–145} An experiment to disprove these effects was reported by Kappe in 2009, who did a control reaction through the comparison of heating vessels. Typical microwave vessels are composed of Pyrex® for their microwave transparency and their ability to withstand high temperatures. Kappe compared this to a silicon carbide vessel, a material that had already been shown to withstand high temperatures but is a strong microwave absorber and can be used to heat microwave transparent solvents at the same rate as solvents with a high loss factor.^{146,147} In control experiments between the two vessels, for a range of reactions including Heck

coupling, the Claisen rearrangement, and alkylation of triphenylphosphine with benzyl chloride, the same yield of product was obtained regardless of the heating vessel after the same reaction length. Through these control experiments, Kappe determined that the magnetic field did not have an effect on the reaction and that the increased reaction rate was caused by temperature effects alone.¹⁴⁶

Whilst the existence of specific or non-thermal microwave effects have not been ruled out completely, they have generally been described as being of marginal synthetic importance. It has further been stated that most results that suggest the presence of these effects can be rationalised by bulk temperature phenomena.^{144,148}

To summarise key advantages of microwave assisted heating over conventional heating:^{140,149}

- *Automation* – Many modern microwave reactors (for example the Biotage® Initiator+ Robot 60 reactor in Figure 10) can be equipped with autosamplers, allowing for many reactions to be run in series without external intervention.
- *Reaction temperature* – The temperature of microwave assisted reactions are no longer limited by a solvent's boiling point. Thus, temperatures far higher than would ordinarily be conceivable for a given solvent are safely attainable.
- *Reaction speed* – Due to the higher temperatures that are obtainable through microwave assisted synthesis, dramatic increases in reaction rates can be achieved. Application of the Arrhenius law [$k = A \exp(-E_a/RT)$] suggests that an increase of 10 °C results in a twofold rate enhancement, turning reactions from hour or day timeframes to seconds or minutes.
- *Safety* – Microwave vessels are designed to withstand high pressures that are safely attainable whereas otherwise specially designed reactors (e.g. Parr reactors) would be required.
- *Efficiency* – The heating method of microwave irradiation is more uniform, resulting in more efficient heating. Furthermore, microwave energy is a more power-efficient heating method compared to classical oil-bath heating.
- *In line monitoring* – The ability to monitor reaction parameters is a common feature in modern microwaves, resulting in better temperature and pressure control and thus increased reproducibility between reactions.



Figure 10 – The Biotage® Initiator+ Robot 60 Microwave Synthesizer

Use of microwave irradiation for organic synthesis was first reported in 1986 by Giguere and Gedye.^{150,151} These reactions took place in modified domestic microwave ovens, but it was not long before specialised microwave reactors were commercialised and allowed the field to blossom. The most common use of microwave irradiation as an enabling technology is for rapid cross-coupling reactions;^{152,153} however, there has also been extensive investigations in other areas, evident by comprehensive reviews into applications of microwaves in the valorisation of waste feedstocks to biomass,^{154,155} drug discovery,^{156,157} metal organic framework (MOF) synthesis,^{158,159} and heterogeneous catalysis.^{160,161}

1.3.3 Application of microwave assisted synthesis towards hydroboration, triel Lewis acid catalysis, and frustrated Lewis pairs

Despite the high interest in microwave assisted organic reactions, reports of its application towards hydroboration is relatively scarce. These generally use transition metal catalysts, such as nickel,¹⁶² rhodium,^{163–165} platinum,¹⁶⁶ and zirconium.¹⁶⁷ Some groups have gone further to exploit the benefits of microwave irradiation in both the formation of boronate esters and further transformations upon them. Nelson used a zirconium catalyst for the microwave assisted hydroboration of allyl propargyl esters, then used microwave irradiation again to promote an iridium-catalysed Claisen rearrangement to convert them into heterocycles.¹⁶⁷ Meanwhile Kappe used microwave irradiation to promote the hydroboration of alkynes with a platinum catalyst, before the addition of a palladium catalyst to perform a Suzuki cross-coupling reaction.¹⁶⁶

Rocheblave reported the use of 4-(dimethylamino)benzoic acid as a catalyst in the microwave-assisted hydroboration of alkynes. These reactions took place unsolvated, in as little as 15 minutes with 18 examples in 28–92% yield.¹⁶⁸

The application of microwaves in the context of triel Lewis acid catalysis or frustrated Lewis pair chemistry was limited to a single example before the publication of the material discussed in chapter five. Here, Paradies reported how microwave irradiation could be used to assist FLP-catalysed hydrogenation of a range of substrates including imines, alkenes and quinolines (15 examples), comparing the conversion rates between microwave assisted reactions and conventionally heated reactions taking place at the same temperature.¹⁶⁹ Herein, Paradies noted that a rate acceleration of up to 2.5 times was registered when microwave irradiation was used, which was attributed to an increased heating efficiency.

It is noteworthy that in some literature examples, the full potential of microwave irradiation is not exploited. For example, in Robinson's investigation into the use of Wilkinson's catalyst in the hydroboration of octene, the temperature of the reaction under microwave irradiation is merely 25 °C.¹⁶³ Furthermore, this was compared to a reaction completed under ambient conditions which surprisingly proceeded faster.¹⁶³

In Rocheblave's report on 4-(dimethylamino)benzoic acid as a hydroboration catalyst, the reactions took place unsolvated.¹⁶⁸ This was deduced from a short optimisation against octane, dioxane and acetonitrile. Octane is a poor microwave solvent due to its low loss factor and thus it is unsurprising that an unsolvated reaction may work better. Whilst solvents with better loss factors were also investigated (dioxane and acetonitrile) they did not return better results, suggesting that this reaction could have been optimised further.¹⁶⁸

Finally, in Paradies' research into FLP-catalysed hydrogenation, the rate of microwave assisted heated and conventionally heated reactions are compared at the same temperature. This can be rationalised as Paradies used hydrogen gas in these reactions, and applying high temperatures to gaseous hydrogen, even with a safe method such as microwave irradiation, carries significant safety risks. Nevertheless, the full capability of the microwave was not taken advantage of as the reaction temperature did not exceed the boiling point of the solvent under ambient conditions.¹⁶⁹

1.3.4 An introduction to flow chemistry

Continuous flow chemistry is an alternative to conventional batch processes that has gained significant attention in recent years.¹⁷⁰ In flow chemistry, reagents are pushed through tubes with small internal diameters (typically <1 mm) by pumps. An example of a flow chemistry assembly is shown in Figure 11. Here syringe pumps (green) push reagents through tubing at extremely accurate flow rates to ensure correct stoichiometries between reagents. The reagents meet at 'T-pieces' (blue), before entering reactor coils (red) whereupon mixing and reaction can occur. Following reaction, the solution is collected (purple). Although not depicted in Figure 11, common additions to this assembly include the installation of a back pressure regulator (BPR) to allow the system to operate at higher pressures,¹⁷¹ and in/online devices that can provide *in situ* monitoring for real-time analysis.¹⁷² Flow chemistry can also be performed within packed bed reactors when heterogeneous reagents or catalysts are required,^{173,174} or upon dedicated microchips with well-defined microchannels and mixing sections.¹⁷⁵ Advances in 3D printing has led to 3D printed microchips used as reactors in flow chemistry.^{176–178}

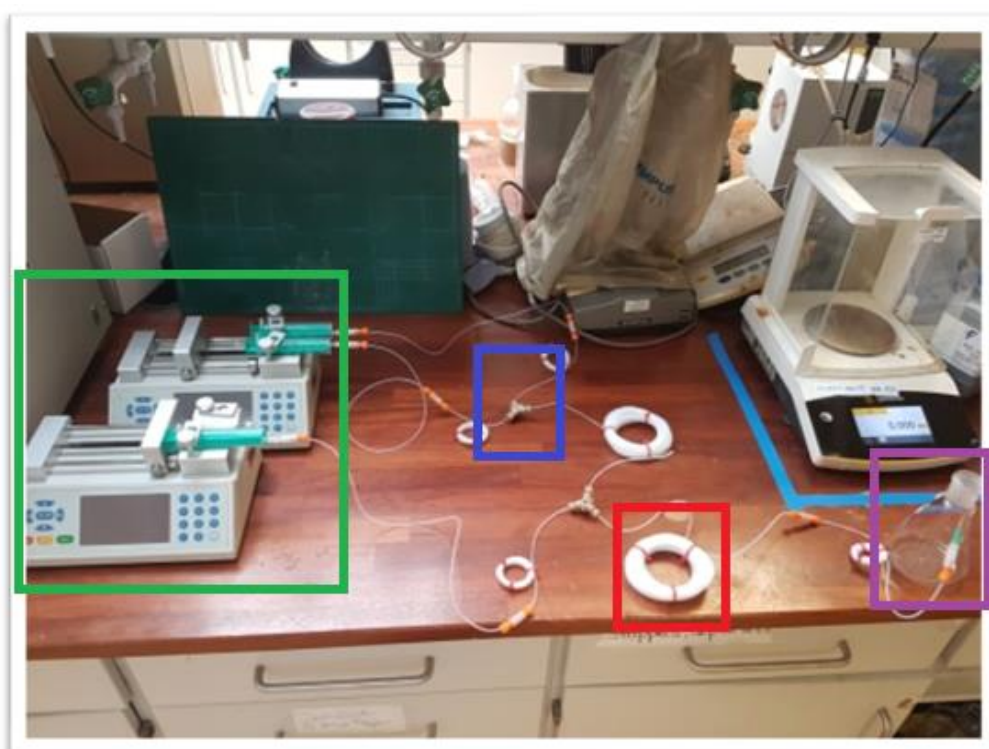


Figure 11 – A basic flow chemistry assembly.

The apparatus in Figure 11 can be transcribed into a scheme using a graphical representation (Figure 12).

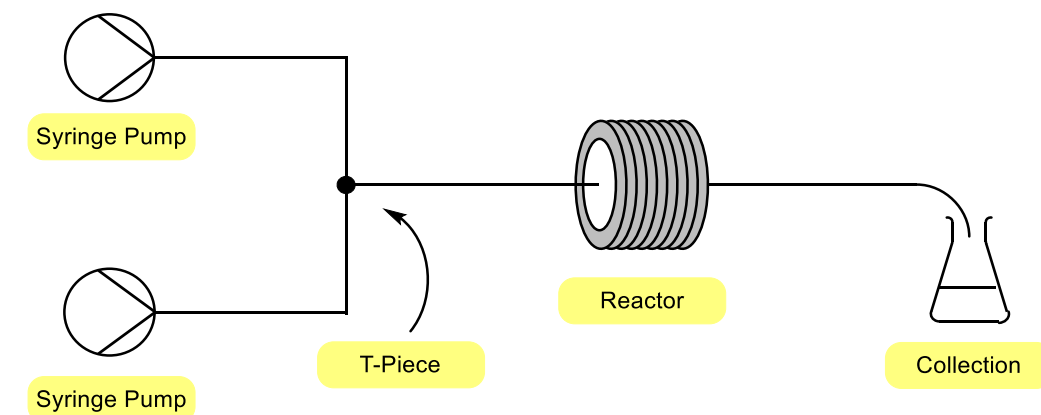


Figure 12 – Typical flow chemistry scheme.

Due to the continuous nature of flow chemistry, reaction time is no longer the determining factor in the progression of a reaction, as is the case in conventional batch chemistry. Instead, the reaction progression is dependent upon residence time (Equation 7).¹⁷⁰

$$\text{residence time} = \frac{\text{volume of the system}}{\text{flow rate of the system}}$$

Equation 7 – Calculation of residence time.¹⁷⁰

Thus, longer residence times (hence longer reaction times) can be achieved through slower flow rates of a reagent, or through increasing the length of the reactor, and the progression of the reaction depends on the point at which the reagents are located along the reactor coil (Figure 13).¹⁷⁰

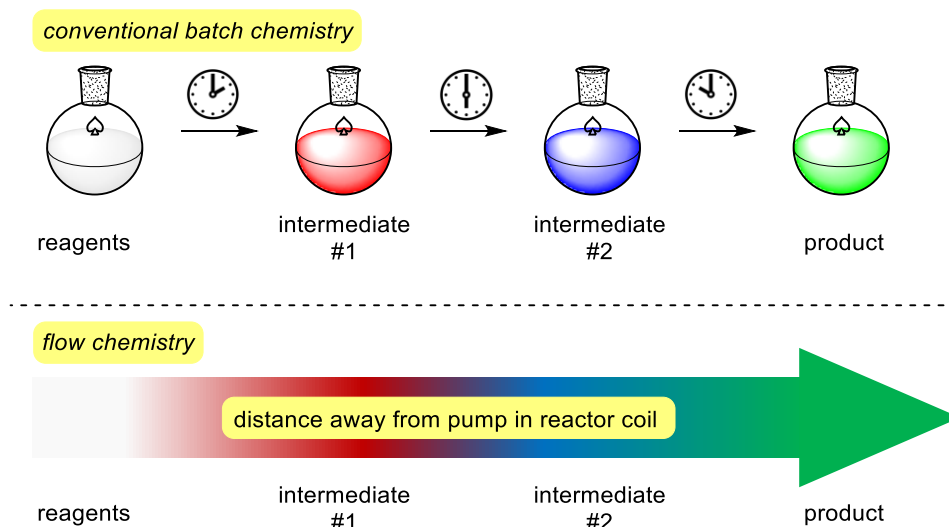


Figure 13 – Progression of a reaction in batch chemistry compared to flow chemistry.¹⁷⁰

The small internal diameter of the reactor in which the reaction occurs is responsible for the increased mass transfer and heat transfer which places flow chemistry at an advantage over traditional batch chemistry. To understand why mass transfer and heat transfer is increased, a brief discussion of the underlying physics is necessary.

The mass transfer, or mixing efficiency is determined by the Reynolds number of a fluid. The Reynolds number (Re) is a dimensionless ratio between inertial and viscous forces within a fluid, and can be derived from the fluid's density (ρ) and viscosity (μ) and from the flow speed (v) and diameter of the vessel (D) in which the fluid is situated (Equation 8).¹⁷⁹

$$\text{Re} = \frac{\text{inertial forces}}{\text{viscous forces}} = \frac{\rho D v}{\mu}$$

Equation 8 – Calculation of Reynolds number.¹⁷⁹

Therefore, at high Reynolds numbers, flow is turbulent, with differences in the fluid speed and direction, sometimes resulting in flow in the reverse direction. Turbulent flow is found on the macroscale, such as in rivers or the atmosphere. At low Reynolds numbers, typically below 250, flow is laminar. This means there is no turbulence or back mixing and fluids are able to travel in parallel. Liquids with high viscosity such as honey or tar have laminar flow.¹⁷⁹ Between these extremes exists a transitional flow, which is often found in small-scale vessels such as a magnetically stirred solution in a round bottomed flask. Here there is turbulent mixing in the vicinity of the stirrer bar, but a laminar environment at the extremities of the flask. During transitional flow, mixing generally relies on diffusion.¹⁸⁰

In the context of flow chemistry, the small diameter of the reactor results in small Reynolds numbers ($\text{Re} < 250$), therefore the fluids have a laminar flow (Figure 14, left). Under laminar flow there is a large longitudinal interface between the fluids and thus a large surface area for diffusion.¹⁷⁹ Slug-flow regimes are often seen when solutions are introduced at a T-piece (Figure 14, right). The slugs are produced when addition of the secondary phase plugs the channel, causing a pressure build-up. Once this pressure reaches a certain threshold, a droplet is formed, and the initial phase continues. This process occurs repeatedly to form the slug flow, which results in a large surface area between the two phases (a transverse interface), and thus efficient diffusion.¹⁷⁰ In both of these scenarios the diffusion between the two phases is far more rapid than would be at the meso-scale, thus resulting in better mixing than in a round bottomed flask.

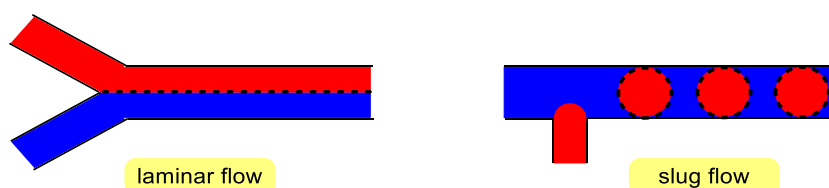


Figure 14 – Flow types at the microscale.¹⁷⁰

A further factor to note is the Damköhler number (Da), another dimensionless value which relates the reaction rate to the diffusion rate (Equation 9). Where Da is much smaller than one, the diffusion is more rapid than the reaction, thus there is efficient mixing before the reaction reaches equilibrium. This means that the two phases are homogeneous before the reaction occurs. Conversely, where Da is much larger than one, the reaction rate is faster than diffusion, resulting in concentration gradients and a greater probability of side reactions or incomplete reaction. In flow chemistry, the Da is much larger than one due to the high surface area between the phases, and this can allow the possibility of flash chemistry, where reactions can occur on the milli- or micro-second scale.¹⁸¹

$$Da = \frac{\text{reaction rate}}{\text{diffusion rate}} = \frac{\text{diffusion time}}{\text{reaction time}}$$

Equation 9 – Calculation of the Damköhler number.¹⁸¹

A further advantage of reactors with small diameters is precise temperature control. Due to the small surface area to volume ratio, temperature can be controlled to a much finer degree than in a conventional batch reaction. This can be understood through Newton's law of cooling (Equation 10).¹⁷⁰ Here, the rate of heat loss of a body (q) is proportional to the logarithmic mean temperature difference between the body and its surroundings (ΔT_{LM}). It is also related to the heat transfer coefficient (U), and the heat transfer area (A). Simply put, heat transfer is proportional to surface area, thus as flow tubing has a much larger surface area than conventional flasks, heat transfer is significantly more efficient. This allows for rapid dissipation of generated heat in highly exothermic reactions, and reduces the risk of run-away reactions.¹⁸²

$$q = UA(\Delta T_{LM})$$

Equation 10 – Calculation of heat removal, through Newton's law of cooling.¹⁷⁰

To summarise key advantages of continuous flow over conventional batch chemistry:^{170,179}

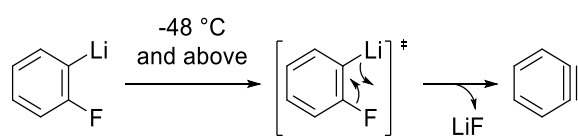
- *Safety* – Completing reactions in flow carries many safety benefits over traditional batch reactions. Firstly, due to efficient heat transfer, highly exothermic reactions dissipate their heat faster, making reaction runaway less likely. Multi-step reactions performed in flow mean that highly toxic or hazardous intermediates can be produced and further reacted upon without external interaction. Furthermore, due to the nature of flow chemistry, only small amounts of hazardous intermediates are present at any one time.
- *Selectivity* – In some reactions, a desired product may only be formed within a small temperature range, with side-products or degradation occurring at high temperature. Due to the homogeneity of conditions with a flow reactor and resulting precise temperature control, the selectivity of a reaction can be tuned.
- *Reproducibility* – Due to the automated nature of flow chemistry, reproducibility is increased as a result of no external interaction.
- *Speed* – As flow reactions can be performed at high pressures, temperature restrictions of solvents at ambient conditions are no longer a problem. Thus, reaction kinetics can be increased. Furthermore, due to the high Damköhler number found in flow chemistry reactors, flash chemistry can be achieved whereas it cannot in batch.
- *Scalability* – Due to the continuous nature of flow chemistry, scale up is far simpler than traditional batch reactions, as associated problems in mass and heat transfer changes are not applicable. The easiest method of scaling up a reaction is to simply leave it running for a longer period of time; however, this may not be practical for the synthesis of chemicals on a multikilogram scale. An alternative is to run many flow reactors in parallel, but this does have associated costs due to the high price of pumps.
- *In situ monitoring* – There have been many techniques that have been adapted for use in flow. This allows for rapid optimisation and analysis. Examples of techniques that have been applied towards flow chemistry include: NMR spectroscopy; IR spectroscopy; UV/Vis spectroscopy; mass spectrometry; HPLC analysis; and gas chromatography.
- *Integration* – The modular nature of flow chemistry means that it can easily be adapted to be run with other types of enabling technologies, such as photochemistry, electrochemistry, and microwave heating.

1.3.5 Application of flow chemistry towards Lewis acid catalysis and frustrated Lewis pairs

The scope of reactions that can be completed using flow chemistry is expansive. Due to the benefits of enhanced safety, selectivity and scale up, there is high interest in its application for the synthesis of natural products and pharmaceuticals.^{183,184}

Flow chemistry is also used prominently in organic synthesis when hazardous materials are required. The safety benefits explained in section 1.3.4 are exemplary of why many research groups have turned to flow chemistry as a reliable alternative to batch chemistry. Examples of hazardous gases that have been used in flow are hydrogen, fluorine, ozone, phosgene, and carbon monoxide.¹⁷⁰ Furthermore, examples of reagents that have been used in flow due to the possibility of dangerous intermediates include diazo compounds, hydrazines, and organometallic compounds.¹⁷⁰

Noteworthy is the use of flow chemistry to make lithiation procedures safer by limiting the possibility of intermediate decomposition. Lithiation is particularly hazardous when the lithium atom is based on an aryl ring and *ortho* to a halide, due to the propensity of the lithium to eliminate, thereby forming a lithium halide and benzyne (Scheme 28). Benzyne is particularly dangerous due to its instability: it is explosive because it releases a large exotherm upon reaction. Flow chemistry allows one to form organolithium compounds safely due to the precise temperature control. This methodology has been exploited by many to decrease the hazard of using organolithium compounds in synthetic procedures.^{185–187}

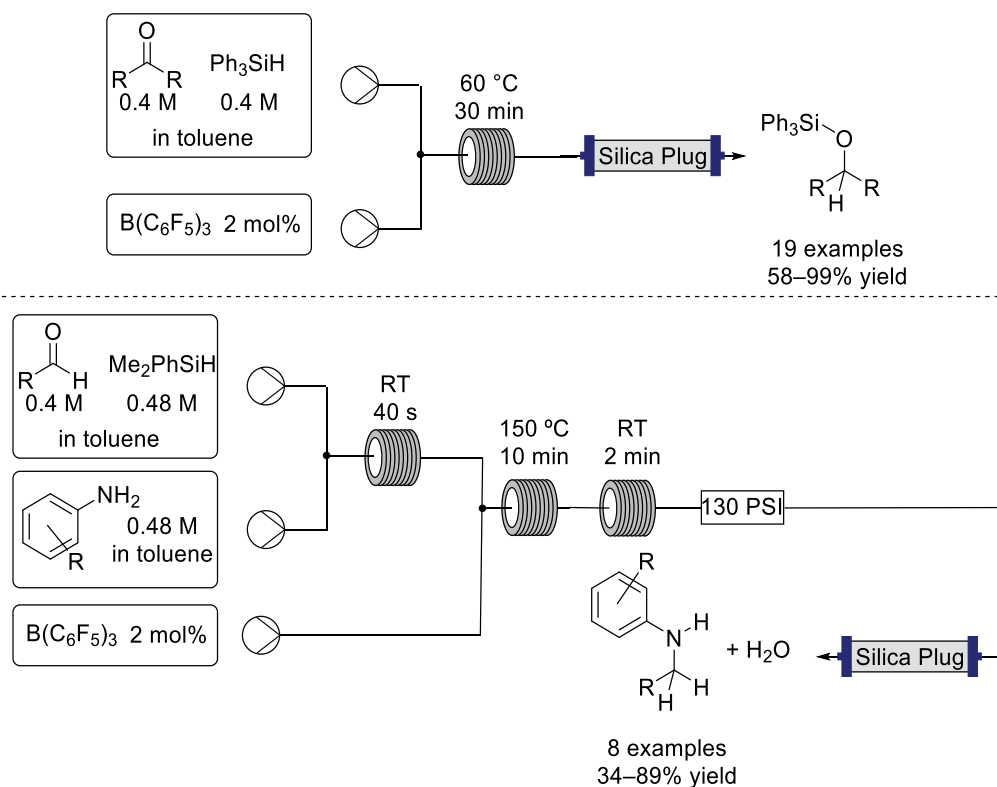


Scheme 28 – Decomposition of (2-fluorophenyl)lithium into benzyne.¹⁸⁶

In particular, Ley investigated the potential formation of benzyne whilst using organolithium intermediates for phenyl boronic acid synthesis.^{186,187} Here benzyne formation was monitored through *in situ* IR measurements, and exothermic degradation was found to start when temperature exceeded -48 °C.¹⁸⁶ Furthermore, the decomposition of the organolithium species was found to have a reaction enthalpy of -226 kJmol⁻¹ under an inert atmosphere, exemplifying the benefit of using flow chemistry.

Flow chemistry can also be used to enhance Lewis-acid-catalysed reactions. It is possible to embed a Lewis acid onto a solid support within a packed bed reactor, so that when a continuous flow system runs through it, catalysis can occur on a heterogeneous Lewis acid catalyst. Selected examples in the recent literature which use this technique include: the use of Lewis acidic MOFs embedded on silica for Diels-Alder reactions, Friedel-Crafts acylation, and alkene hydroalkylations;¹⁸⁸ and silica monoliths doped with Lewis acidic metal catalysts for the reduction of carbonyls.¹⁸⁹ Flow systems wherein a homogeneous Lewis acid catalyst is injected along with reagents have also been reported. Selected examples in the recent literature include the use of a tropylium cation catalyst for the prenylation of phenols,¹⁹⁰ and the preparation of morpholines from aldehydes and aminoethers through a combination of 2,4,6-triphenylpyrylium tetrafluoroborate promoted photocatalysis and TMSOTf promoted Lewis acid catalysis.¹⁹¹

A collaboration between the Melen and Browne groups in 2017 found that the borane Lewis acid $B(C_6F_5)_3$ could be used as an efficient hydrosilylation catalyst under continuous flow conditions (Scheme 29).¹⁹² Not only were a series of carbonyl compounds able to undergo hydrosilylation in excellent yield within 30 minutes (20 examples, 58–99%), the use of flow chemistry allowed for the synthesis of secondary amines from primary amines through a hydrosilylated intermediate (8 examples, 34–89%). Here an imine was synthesised through a forty-second-long condensation reaction and was telescoped towards a $B(C_6F_5)_3$ -catalysed hydrosilylation at 150 °C. The use of high temperature was permitted through a back-pressure regulator, and this allowed for decreased reaction times and increased yields compared to the batch reaction.¹⁹²

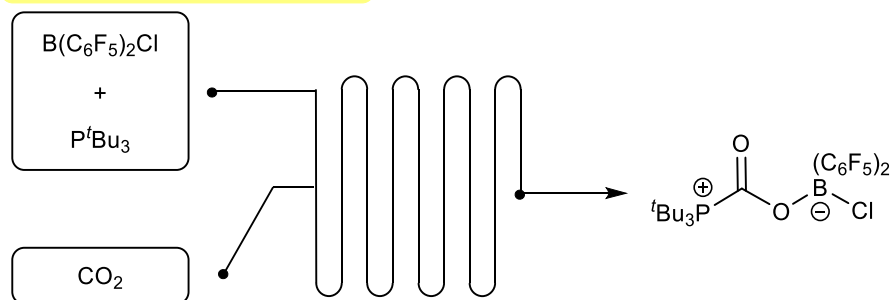


Scheme 29 – $\text{B}(\text{C}_6\text{F}_5)_3$ -catalysed hydrosilylation and tandem imine formation/hydrosilylation in flow.¹⁹²

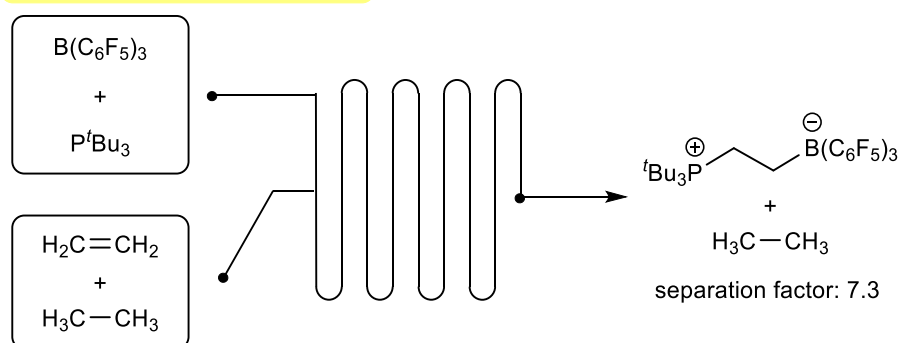
Stephan and Kumacheva have reported the only other examples of frustrated Lewis pairs being utilised as catalysts in continuous flow, with three joint-publications.^{193–195} Their first collaboration investigated the capture of CO_2 by a $\text{P}^t\text{Bu}_3/\text{ClB}(\text{C}_6\text{F}_5)_2$ FLP in a microfluidic system based on a chip, to determine various thermodynamic constants that could be used to further the understanding of other FLP reactions in flow (Scheme 30, top).¹⁹³ Flow chemistry was beneficial due to *in situ* monitoring and the removal of risk of atmospheric exchange products forming, which were previously a problem in determining the thermodynamic constants of this reaction in batch.¹⁹³ A recent publication quantified the efficiency of this CO_2 capture by a range of common FLPs, using thermodynamics to determine that the $\text{P}^t\text{Bu}_3/\text{B}(\text{C}_6\text{F}_5)_3$ FLP was the most efficient at ambient temperature.¹⁹⁴

The most recent collaboration found that a $\text{P}^t\text{Bu}_3/\text{B}(\text{C}_6\text{F}_5)_3$ FLP could separate ethane from ethylene under continuous flow conditions, by using the FLPs capability of binding with ethylene and its inactivity towards ethane. The high activity of the FLP towards ethylene resulted in a separation factor of 7.3 from a 1:1 mixture of the olefin and the alkane, as measured by IR spectroscopy. Moreover, 88% ethylene purity was reported, following calculations between the expected ethylene uptake and its recorded uptake (Scheme 30, bottom).¹⁹⁵

Kumacheva and Stephan, 2014



Kumacheva and Stephan, 2015

Scheme 30 – Examples of FLPs used for small molecule activation in flow.^{193,195}

1.4 Conclusions

In this chapter the main themes of this thesis have been introduced. The first subsection deals with the overarching topic of Lewis acids, examining how the strength of a Lewis acid can be measured, discussing the field of frustrated Lewis pairs, and finally introducing the boron and aluminium-based Lewis acids that are used within this thesis. The second subsection considers the recent interest towards main-group catalysis, with a literature review examining relevant boron and aluminium-catalysed hydroboration reactions and boron-catalysed hydroamination reactions. Finally, the topic of enabling technologies is introduced, with a discussion behind the basic principles of microwave assisted synthesis and flow chemistry along with the applications of these enabling technologies towards Lewis acid and frustrated Lewis pair-catalysed systems.

1.5 Aims of this thesis

Inspiration behind the aims of this thesis came from Melen and Browne's 2017 publication regarding the $B(C_6F_5)_3$ -catalysed hydrosilylation of carbonyls using continuous flow technologies.¹⁹² With interest piqued by the successful combination of frustrated Lewis pair chemistry and enabling technologies, this thesis aims to explore further avenues which combine the two areas. Moreover, this thesis will discuss the benefits and drawbacks of using such enabling technologies in comparison to conventional experimental techniques.

Chapter two will aim to discuss the synthesis of Lewis acidic boranes and alanes using conventional experimental techniques. Meanwhile, chapter three aims to explore the potential synthesis of $B(C_6F_5)_3$ using continuous flow technologies, with an emphasis upon safer synthesis, decreased reaction time, and improved yield compared to its batch counterpart.

Chapter four will aim to discuss hydroboration catalysis performed under conventional experimental techniques using select borane and alane catalysts. Chapter five will then discuss how this hydroboration procedure can be augmented using microwave assisted heating to expand the scope of reactivity and decrease reaction timescales.

Finally, chapter six aims to discuss the use of $B(C_6F_5)_3$ as a catalyst for the hydroamination of alkenes using conventional experimental techniques. Whilst ultimately time restraints precluded the use of enabling technologies to further explore this reactivity, this chapter acts as a solid foundation for further work in the area.

This thesis therefore aims to investigate further the fields of frustrated Lewis pairs and Lewis acid catalysis, but with a slant towards using enabling technologies to improve existing reaction protocols.

Chapter two – Synthesis of boron- and aluminium-based Lewis acids in batch

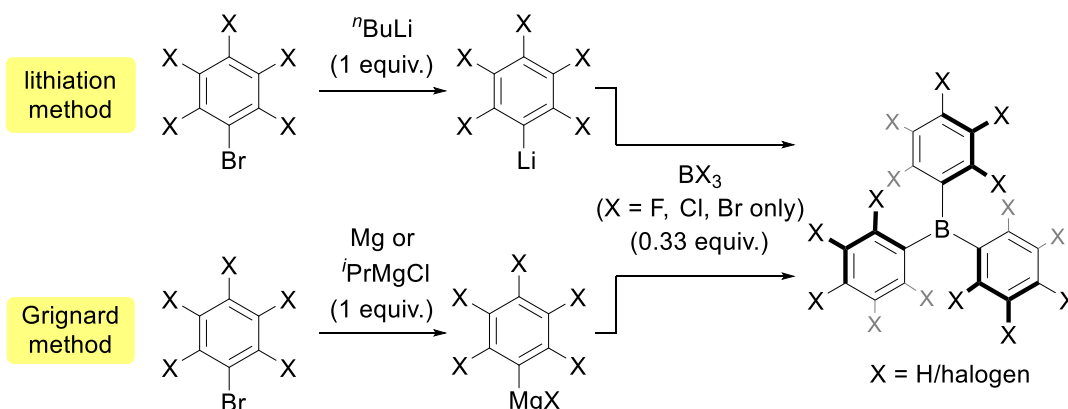
2.1 Aims of this chapter

This chapter aims to introduce the Lewis acidic boranes and alanes that have been synthesised and used in this thesis. First, a brief discussion of synthetic procedures for the literature known boranes and alanes will be described. This will be followed by descriptions of synthetic modifications to these procedures, which led to the preparation of the compounds used within this thesis. Finally, a comparison of Lewis acidity of these boranes and alanes will be discussed to understand trends in fluorine substitution pattern and triel centre upon Lewis acidity strength and subsequent reactivity.

2.2 Boron- and aluminium-based Lewis acid synthesis in the literature

2.2.1 Borane synthesis in the literature

The preparation of Lewis acidic triarylboranes is well documented in the chemical literature. The two common methods require an aryl bromide and a third of an equivalent of boron trihalide, but they differ in that one proceeds through a Grignard reagent and the other an organolithium species (Scheme 31). These procedures are ubiquitous through the synthesis of triarylboranes, with small modifications and purification methods to improve yields.⁵³ Notably, the preparation of heteroleptic triarylboranes is more complex, and often requires the use of organotin, organocopper or organozinc aryl transfer reagents alongside the Grignard or lithiation methods.^{57,58,196,197} Extensive research has gone into the preparation of halogenated triarylboranes other than the archetypal $B(C_6F_5)_3$. This chapter will highlight select examples used within this thesis, although there are many examples of homoleptic boranes that include alternate halogen substitution patterns and heteroleptic boranes which contain further variations.⁵³

Scheme 31 – General synthesis of homoleptic triaryl boranes.⁵³

The archetypal halogenated triarylborane $\text{B}(\text{C}_6\text{F}_5)_3$ was first reported in 1963 by Massey and Park, who prepared (pentafluorophenyl)lithium and subsequently reacted this with BCl_3 to form the desired borane.¹⁹⁸ Typical yields between 30% and 50% were reported after purification through sublimation.¹⁹⁹ Pohlmann and Brinckman introduced the Grignard method in 1965, which was found to form $\text{B}(\text{C}_6\text{F}_5)_3 \cdot \text{Et}_2\text{O}$ in up to 80% yield.²⁰⁰ Most recently, Lancaster improved upon the Grignard method with an additional purification step, using a hot hexane extraction followed by a twofold sublimation to form $\text{B}(\text{C}_6\text{F}_5)_3$ in an isolated yield of 70%.²⁰¹

Another borane that has been used in this thesis is tris(3,4,5-trifluorophenyl)borane [$\text{B}(3,4,5\text{-F}_3\text{C}_6\text{H}_2)_3$]. This borane was first prepared by Melen and Oestreich in investigations into borane-catalysed hydroboration; however, only a single stoichiometric example of hydroboration was reported with no further catalysis attempted. The lithiation procedure was employed, using 3,4,5-trifluorobromobenzene and $\text{BF}_3 \cdot \text{OEt}_2$ as starting materials, and following a sublimation purification a 16% yield was recorded.¹⁰⁷

The final literature known borane explored in this thesis is tris(2,4,6-trifluorophenyl)borane [$\text{B}(2,4,6\text{-F}_3\text{C}_6\text{H}_2)_3$]. This borane has been widely studied, with applications in hydroboration,¹⁰⁸ carboboration,²⁰² and polymerisation.²⁰³ Due to the *ortho*-fluorine atoms on the borane's aryl rings, this borane carries significant risks if the lithiation method is performed and thus the Grignard method is generally employed for its synthesis.^{108,202,203}

In these syntheses, sublimation is employed as the crude product is a solvent adduct of the borane. Typically, these reactions are run in ethereal solvents to accommodate for the Grignard or organolithium formation, and thus the weakly basic solvent has a propensity to coordinate to the Lewis acidic boron centre. These adducts are easily

detected through ^{11}B NMR spectroscopy, where ethereal adducts resonate around 40 ppm, whilst the unsolvated boranes correspond to signals around 60–80 ppm.

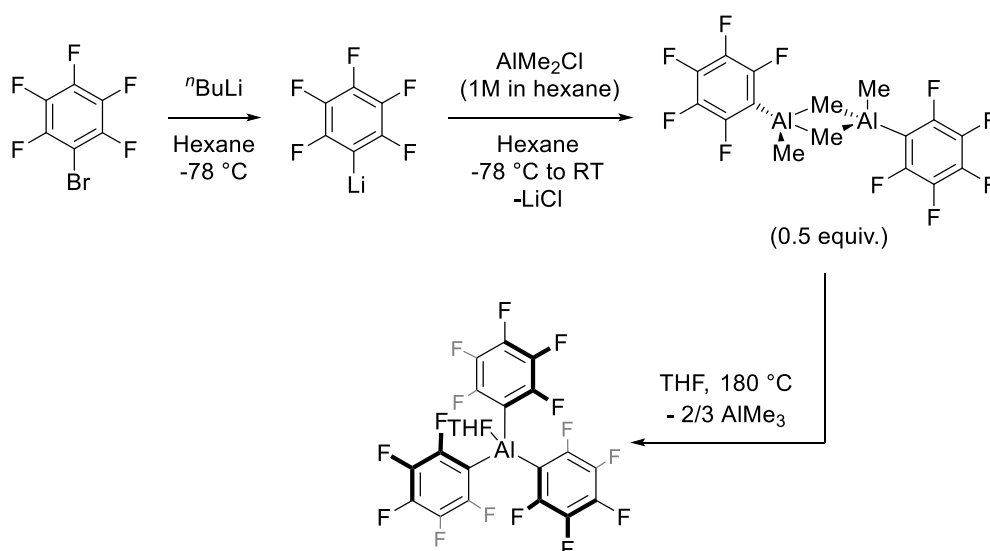
As explained in chapter one, if *ortho*-fluorine atoms are present on the aryl rings, the lithiation procedure can result in the unwanted formation of benzyne derivatives through the instability of the (fluoroaryl)lithium intermediates at ambient temperature. Consequentially the explosion risk of these benzyne derivatives carries a significant hazard. Thus in batch, the Grignard method is widely regarded as the safer method.^{51,53}

2.2.2 Alane synthesis in the literature

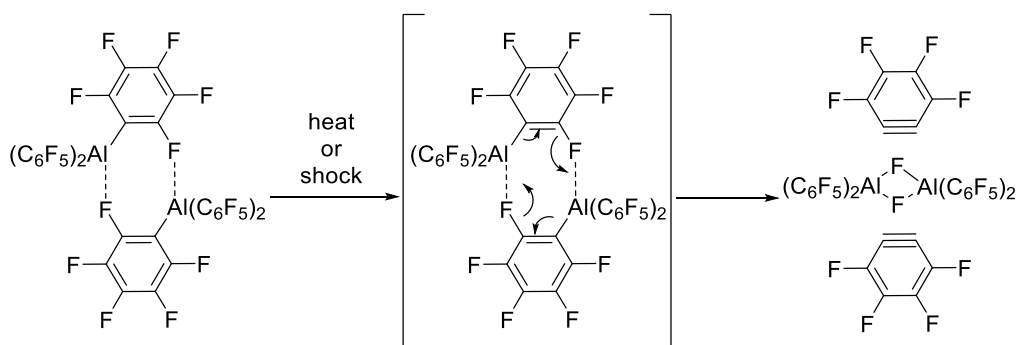
Fluorinated triarylalanes are more acidic than their borane congeners, but they are far less studied and thus there are few synthetic procedures for their preparation. Most of the literature focuses on the preparation of tris(pentafluorophenyl)alane $[\text{Al}(\text{C}_6\text{F}_5)_3]$; however, due to its instability this Lewis superacid is often isolated as a solvent adduct, which quenches its Lewis acidity partially.

The first preparation of $\text{Al}(\text{C}_6\text{F}_5)_3$ was attempted in 1965, in a similar vein to the Grignard method of $\text{B}(\text{C}_6\text{F}_5)_3$ synthesis.²⁰⁰ Here, (pentafluorophenyl)magnesium bromide was generated and reacted with aluminium trichloride in an ether solvent; however, only the ether adduct of the alane could be formed. Attempts to remove the ether through pyrolysis or sublimation led to an explosion, although the crude alane etherate could be isolated in 67% yield.²⁰⁰

$\text{Al}(\text{C}_6\text{F}_5)_3$ was not investigated again until 1995, when Roesky isolated its THF adduct.²⁰⁴ Here, pentafluorophenyl bromide was generated and reacted slowly with dimethylaluminium chloride to generate the dimeric species $[\text{Al}(\text{C}_6\text{F}_5)\text{Me}_2]_2$. Pyrolysis of this intermediate and concomitant loss of trimethylaluminium, formed the solvated $\text{Al}(\text{C}_6\text{F}_5)_3$ adduct in 64% yield (Scheme 32).²⁰⁴

Scheme 32 – Roesky's preparation of $\text{Al}(\text{C}_6\text{F}_5)_3 \cdot \text{THF}$.²⁰⁴

Subsequent preparations of $\text{Al}(\text{C}_6\text{F}_5)_3$ involved a transmetallation, wherein $\text{B}(\text{C}_6\text{F}_5)_3$ was combined with an equivalent of trimethylaluminium in toluene at room temperature.^{67,71} The trimethylborane by-product could be removed *in vacuo*, resulting in near quantitative amounts of the alane. The alane was isolated as a toluene adduct, as the unsolvated variant was found to be extremely thermally and shock sensitive.^{67,71} The preparation of unsolvated $\text{Al}(\text{C}_6\text{F}_5)_3$ was achieved by Chen, who performed a transmetallation of $\text{B}(\text{C}_6\text{F}_5)_3$ with trimethylaluminium in hexane.²⁰⁵ Analysis of the solid-state structure found that there were intramolecular interactions between the aluminium centre of one $\text{Al}(\text{C}_6\text{F}_5)_3$ and the *ortho*-fluorine of one aryl group on a second $\text{Al}(\text{C}_6\text{F}_5)_3$. The sensitivity of the molecule was thus proposed to be due to an entropically favourable rearrangement between two molecules of $\text{Al}(\text{C}_6\text{F}_5)_3$, with the formation of strong Al–F bonds acting as the driving force. This formed an aluminium fluoride dimer, and two equivalents of explosive perfluorobenzene (Scheme 33).²⁰⁵

Scheme 33 – Proposed decomposition pathway of $\text{Al}(\text{C}_6\text{F}_5)_3$.²⁰⁵

Other literature known alanes are scarce. $\text{Al}(\text{4-FC}_6\text{H}_4)_3$ has been generated through the Grignard method.^{73,74} Meanwhile, the $\text{Al}(\text{2,3,5,6-F}_4\text{C}_6\text{H})_3$ ·toluene adduct has also been prepared in the same manner as the $\text{Al}(\text{C}_6\text{F}_5)_3$ ·toluene adduct, through the transmetallation of trimethylaluminium with the corresponding parent borane.⁷⁵

2.3 Borane synthesis

In this thesis, the following boranes were prepared: $\text{B}(\text{C}_6\text{F}_5)_3$; $\text{B}(\text{3,4,5-F}_3\text{C}_6\text{H}_2)_3$; $\text{B}(\text{2,3,4-F}_3\text{C}_6\text{H}_2)_3$, and $\text{B}(\text{2,4,6-F}_3\text{C}_6\text{H}_2)_3$ (Figure 15). Both the Grignard and lithiation procedures were employed, adapted from literature methods.

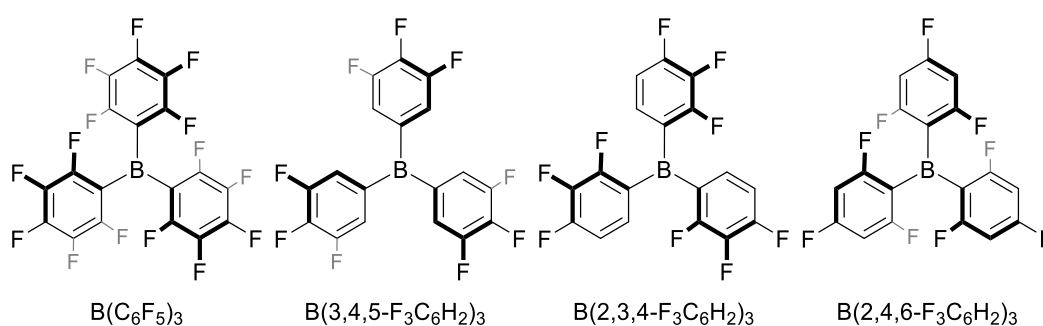
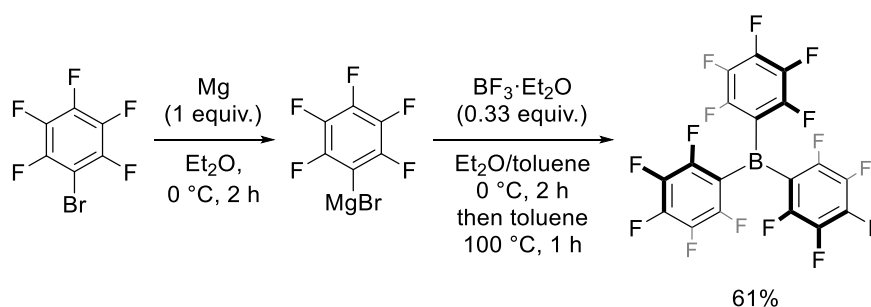


Figure 15 – Boranes prepared in this thesis.

2.3.1 Tris(pentafluorophenyl)borane

Tris(pentafluorophenyl)borane was synthesised by following Lancaster's synthesis.²⁰¹ The Grignard method was used (Scheme 34), which involved adding a stoichiometric amount of pentafluorophenyl bromide to magnesium turnings at 0 °C. Formation of the Grignard reagent was evident through darkening of the solution and consumption of the magnesium turnings. To this solution, a third of an equivalent of $\text{BF}_3 \cdot \text{Et}_2\text{O}$ in toluene was added slowly at 0 °C. After two hours, the ether was removed *in vacuo* and the toluene solution was heated to 100 °C to promote further the reaction of the Grignard reagent with the electrophile. At this juncture, crystals of crude $\text{B}(\text{C}_6\text{F}_5)_3$ etherate could be seen nucleating on the side of the flask.



Scheme 34 – Preparation of $B(C_6F_5)_3$ through the Grignard procedure.

To isolate the crude etherate, the toluene was removed *in vacuo*, and warm hexane (~45 °C) was added. This dissolved the crude etherate somewhat, leaving the magnesium salt impurities behind. A filter canula was used to isolate the warm hexane solution; however, multiple washings were required to ensure reasonable yields. The crude borane etherate was isolated by removing the hexane *in vacuo*.

Next, a sublimation was performed. The borane etherate was transferred into a sublimation apparatus (Figure 16) and heated to 80 °C for two hours under vacuum to drive off any residual solvent. After sufficient drying, the temperature was raised to 120 °C, and compressed air was applied to the cold finger to allow the borane to condense. The first sublimation generally produced oily pale-yellow crystals. These were washed with pentane and then sublimed again to yield $B(C_6F_5)_3$ as an amorphous powder. Typical yields were around 40–60% depending on the efficiency of the purification step, with a maximum yield observed of 61%.

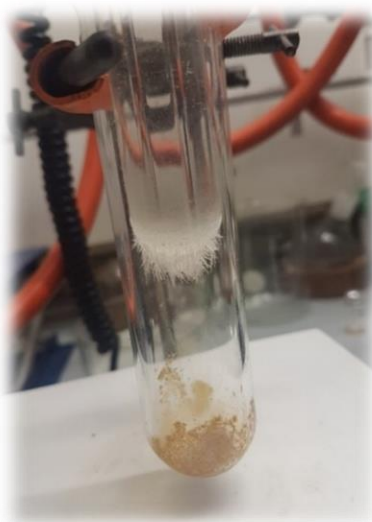
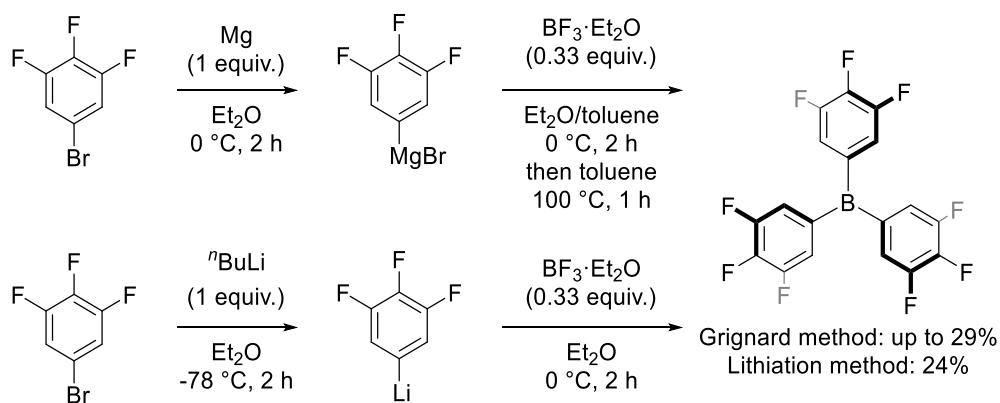


Figure 16 – Sublimation apparatus for borane purification.

2.3.2 Tris(3,4,5-trifluorophenyl)borane

$B(3,4,5-F_3C_6H_2)_3$ is a highly Lewis acidic borane which is devoid of *ortho*-fluorine atoms around its aryl rings. The lack of these *ortho*-fluorine atoms indicated that the organolithium intermediate from the lithiation procedure would be more stable than that from the analogous $B(C_6F_5)_3$ synthesis. Thus, both the Grignard method and the lithiation method were employed (Scheme 35).

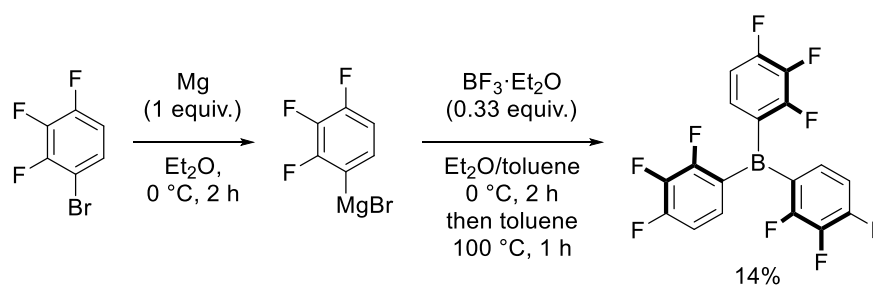
The Grignard method for $B(3,4,5-F_3C_6H_2)_3$ synthesis was performed using an adapted Lancaster procedure.²⁰¹ Yields were less impressive than the $B(C_6F_5)_3$ synthesis, ranging from 6–29%. Meanwhile, the lithiation procedure resulted in a maximum yield of 24%. The lithiation procedure involved the addition of nBuLi to a stoichiometric amount of 3,4,5-trifluorobromobenzene at $-78\text{ }^\circ\text{C}$. The reaction mixture was slowly warmed to $0\text{ }^\circ\text{C}$ over a period of two hours, at which point $BF_3 \cdot Et_2O$ was added and the reaction mixture was warmed to room temperature slowly overnight. Unlike the Grignard method, a reflux and subsequent warm hexane extraction was not employed, rather a simple dichloromethane extraction was used to isolate the borane etherate. A two-fold sublimation was then performed in a similar fashion to the Grignard method.



Scheme 35 – Synthesis procedures for $B(3,4,5-F_3C_6H_2)_3$.

2.3.3 Tris(2,3,4-trifluorophenyl)borane

Tris(2,3,4-trifluorophenyl)borane was a novel borane prepared *via* the Grignard method (Scheme 36). Due to the presence of a single *ortho*-fluorine atom on each aryl ring, the lithiation procedure was deemed unsafe. Procedurally this was prepared in an analogous fashion to $B(C_6F_5)_3$ and $B(3,4,5-F_3C_6H_2)_3$, with the only difference in the parent aryl bromide. Following purification by two-fold sublimation, colourless crystals of $B(2,3,4-F_3C_6H_2)_3$ were formed, with a yield of 14%.

Scheme 36 – Synthesis of $B(2,3,4-F_3C_6H_2)_3$.

The crystals of $B(2,3,4-F_3C_6H_2)_3$ were analysed by X-ray diffraction (XRD), and the resultant structure is shown in Figure 17.ⁱ As with other triarylboranes, the boron adopts a trigonal planar geometry, with C–B–C bond angles of $119.5(3)^\circ$, $123.1(3)^\circ$, and $117.4(3)^\circ$. The aryl rings of $B(2,3,4-F_3C_6H_2)_3$ arrange in a paddlewheel fashion to reduce their steric interaction in the solid state.

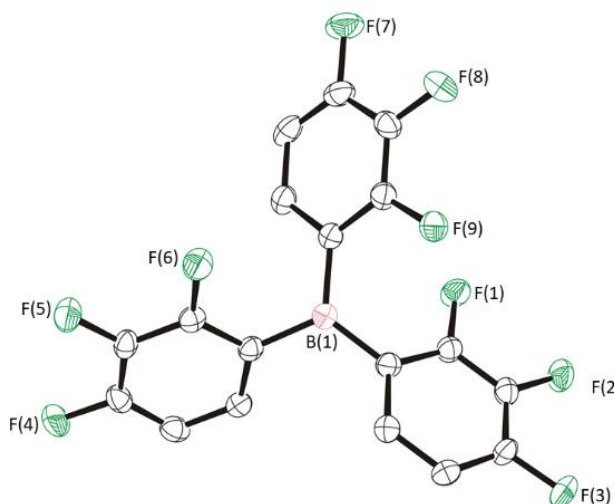
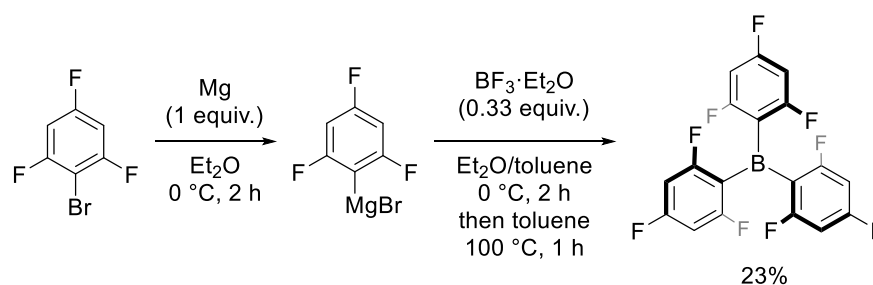


Figure 17 – X-ray crystal structure of tris(2,3,4-trifluorophenyl)borane. H-atoms omitted for clarity and thermal ellipsoids drawn at 50% probability.

2.3.4 Tris(2,4,6-trifluorophenyl)borane

Tris(2,4,6-trifluorophenyl)borane is a relatively weak Lewis acidic triarylborane that has been well studied in the literature.^{108,206–209} Due to its *ortho*-fluorine atoms, it was prepared using the standard Grignard method and purified *via* twofold sublimation (Scheme 37). The borane was isolated as colourless crystals in 23% yield.

ⁱ XRD analysis of $B(2,3,4-F_3C_6H_2)_3$ was performed by Dr Darren Ould.

Scheme 37 – Preparation of $B(2,4,6-F_3C_6H_2)_3$ through the Grignard procedure.

2.4 Alane synthesis

Due to the knowledge that halogenated triarylboranes with different halogen substitution patterns to $B(C_6F_5)_3$ could outperform $B(C_6F_5)_3$ in certain reactions, it was theorised that the congeners of $Al(C_6F_5)_3$ could also lead to interesting avenues of chemistry. The primary limitation of $Al(C_6F_5)_3$ is its stability; the presence of *ortho*-fluorine atoms on its aryl rings lead to the possibility of irreversible catalyst decomposition *via* the generation of explosive perfluorobenzynes.²⁰⁵ In response, the synthesis of $Al(3,4,5-F_3C_6H_2)_3$, which was devoid of these *ortho*-fluorine atoms, was initially targeted to explore the reactivity of more stable alanes. This venture led to the preparation of $Al(3,4,5-F_3C_6H_2)_3$, $Al(2,3,4-F_3C_6H_2)_3$, $\mu_2-[Al(3,4,5-F_3C_6H_2)Me]_2$, and corresponding solvent adducts (Figure 18). Both the Grignard procedure and a transmetalation procedure were used for alane syntheses. A lithiation procedure was also used for the preparation of $Al(3,4,5-F_3C_6H_2)_3$, to mixed success.

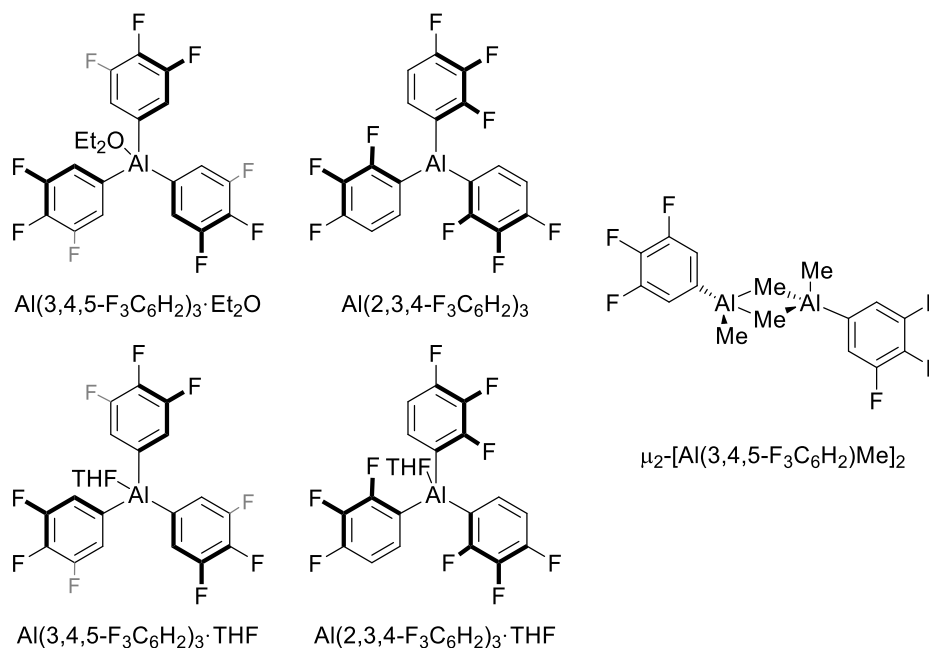


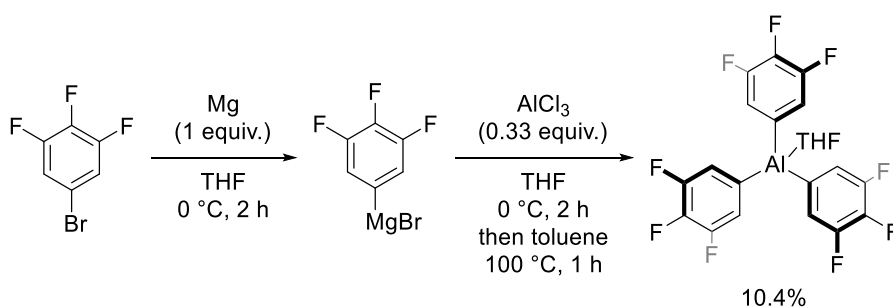
Figure 18 – Alanes prepared in this thesis.

2.4.1 Tris(3,4,5-trifluorophenyl)alane

Tris(3,4,5-trifluorophenyl)alane was initially targeted due to the lack of *ortho*-fluorine atoms on its aryl rings. As discussed by Chen, the *ortho*-fluorine atoms of $\text{Al}(\text{C}_6\text{F}_5)_3$ promoted its decomposition when subjected to shock or high temperatures.²⁰⁵ Thus, it was theorised that the lack of *ortho*-fluorines on $\text{Al}(\text{3,4,5-F}_3\text{C}_6\text{H}_2)_3$ would allow for the exploitation of the high Lewis acidity of aluminium, whilst also existing as a safer compound to handle.

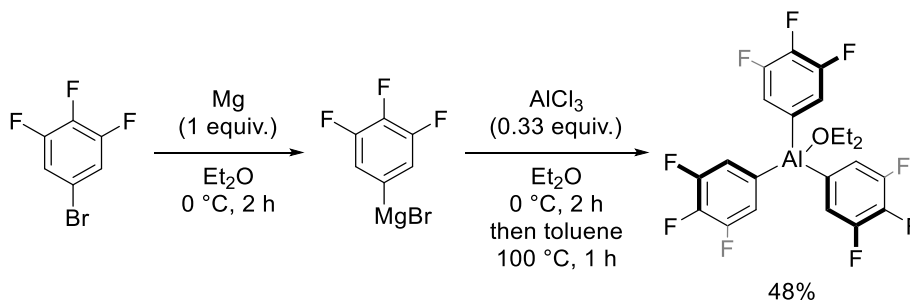
The initial attempted synthesis to produce $\text{Al}(\text{3,4,5-F}_3\text{C}_6\text{H}_2)_3$ used an adapted lithiation procedure typically used for triarylboranes. The differentiating factor was the electrophile: AlCl_3 was employed instead of $\text{BF}_3 \cdot \text{Et}_2\text{O}$. This synthetic procedure did not go according to plan and led to a mixture of products, as determined by multinuclear NMR spectroscopy. Surprisingly, crystals of $\text{Al}(\text{2,3,4-F}_3\text{C}_6\text{H}_2)_3 \cdot \text{THF}$ were isolated from the crude mixture and characterised. This is discussed further in section 2.4.3.

In response to the unreliability of the lithiation procedure, attention was turned to the Grignard method. This procedure mirrored that of Lancaster, with AlCl_3 used as the electrophile instead of $\text{BF}_3 \cdot \text{Et}_2\text{O}$. Initially this reaction was performed in THF. *In-situ* ^1H NMR spectroscopy noted the stoichiometric presence of THF, suggesting a strong Lewis acid/base adduct had been formed. Upon isolation this gave a 10.4% yield of the alane adduct (Scheme 38). Due to the safety risk of subliming the alane (in the event that fluorine atoms on adjacent alane molecules could partake in elimination reactions to form benzyne derivatives), the unsolvated alane was not isolated.



Scheme 38 – Synthesis of $\text{Al}(\text{3,4,5-F}_3\text{C}_6\text{H}_2)_3 \cdot \text{THF}$.

In response, Et₂O was employed as the ethereal solvent in the hope it would be easier to remove (Scheme 39).ⁱⁱ This was chosen due to a comparison of boiling points (THF = 66 °C; Et₂O = 35 °C). Sublimation was still not performed due to the risk of explosion. Gentle heating was applied in an attempt to break the adduct apart, but the unsolvated alane could not be isolated. The yield of the alane etherate was reported as 48%, a remarkable improvement over the THF route.



Scheme 39 – Synthesis of Al(3,4,5-F₃C₆H₂)₃·Et₂O.

Single crystals of Al(3,4,5-F₃C₆H₂)₃·Et₂O suitable for X-ray diffraction were grown from a concentrated toluene/pentane mixture (Figure 19). The crystal structure found that coordination of the ether caused the alane to adopt a near tetrahedral geometry, with O–Al–C bond angles of 104.11(16)°, 104.45(16)°, and 107.11(15)°.

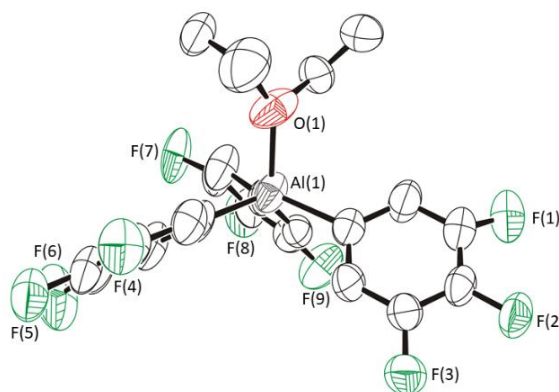


Figure 19 – Crystal structure of Al(3,4,5-F₃C₆H₂)₃·Et₂O.

FLP type reactivity was probed with Al(3,4,5-F₃C₆H₂)₃·Et₂O. A combination of the alane etherate with one of a range of bases (PMe₃, P^tBu₃, DABCO, and TMP) were dissolved in deuterated chloroform in a J-Youngs NMR tube. The combination of acid

ⁱⁱ The initial preparation and XRD analysis of Al(3,4,5-F₃C₆H₂)₃·Et₂O was performed by Dr Darren Ould.

and base was then degassed by freeze-thawing and was then subjected to an atmosphere of gaseous hydrogen (5 bar) at room temperature. Unfortunately, no small molecule activation was observed by multinuclear NMR spectroscopy. In response, combinations of the alane etherate with the same bases were dissolved in chloroform and then placed in a Parr reactor. Atmospheres of hydrogen (60 bar) or carbon dioxide (60 bar) were then applied to the mixtures at room temperature; however, still no reactivity was observed by multinuclear NMR spectroscopy suggesting that the ether did not willingly dissociate to allow the alane to partake in FLP-style chemistry.

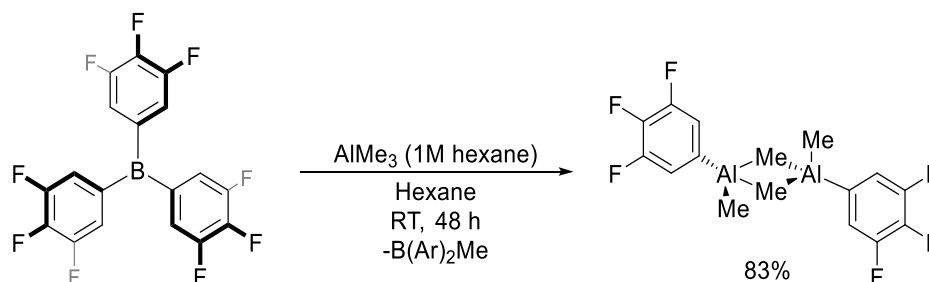
2.4.2 μ_2 -dimethyl-bis[(3,4,5-trifluorophenyl)methyl-alane]

The second common synthetic route for $\text{Al}(\text{C}_6\text{F}_5)_3$ is transmetallation, and thus this was employed for the preparation of unsolvated $\text{Al}(3,4,5\text{-F}_3\text{C}_6\text{H}_2)_3$. Literature precedent for the transmetallation reaction suggested that a mixture of the parent borane with AlEt_3 would yield the alane after two days; however, this proved unsuccessful for the preparation of $\text{Al}(3,4,5\text{-F}_3\text{C}_6\text{H}_2)_3$. A range of conditions were employed to promote reactivity, including increased reaction times, increased stoichiometries of AlEt_3 compared to the borane, higher temperatures (65 °C instead of room temperature), and even a change of aluminium source from AlEt_3 to AlMe_3 in case BMe_3 would be more easily generated than BEt_3 . Unfortunately, these reactions were all unsuccessful, with multinuclear *in situ* NMR spectra suggesting the formation of multiple products in all cases. These were suggested to be the result of partial transmetallation, where only a limited number of aryl groups from the parent borane were transferred to the corresponding alane. Despite repeated attempts, full transmetallation was not observed.

In one instance, X-ray quality crystals were obtained after 48 hours in 83% yield (Scheme 40).ⁱⁱⁱ Analysis of these crystals, and supporting analysis by multinuclear NMR found that a dimeric species was formed as a result of partial transmetallation: $\mu_2\text{-[Al}(3,4,5\text{-F}_3\text{C}_6\text{H}_2)\text{Me}]_2$. This suggested that the preparation of a dimer through loss of $\text{B}(3,4,5\text{-F}_3\text{C}_6\text{H}_2)_2\text{Me}$ was more favourable than the formation of monomeric alane through the loss of BMe_3 . The dimer had bridging methyl atoms, indicating the

ⁱⁱⁱ XRD analysis of the dimer $\mu_2\text{-[Al}(3,4,5\text{-F}_3\text{C}_6\text{H}_2)\text{Me}]_2$ was performed by Dr Darren Ould.

presence of Al–C–Al units with 3 centre 2 electron bonds, similar to those observed in Al_2Me_6 .²¹⁰ As shown in Scheme 32, a similar methyl bridged dimer was isolated as an intermediate in the preparation of $\text{Al}(\text{C}_6\text{F}_5)_3 \cdot \text{THF}$.²⁰⁴



Scheme 40 – Synthesis of $\mu_2\text{-[Al(3,4,5-F}_3\text{C}_6\text{H}_2)\text{Me}]_2$ through partial transmetalation.

Inspection of the solid-state structure of $\mu_2\text{-[Al(3,4,5-F}_3\text{C}_6\text{H}_2)\text{Me}]_2$ found an $\text{Al(1)} \cdots \text{Al(1')}$ distance of 2.5987(19) Å. The bridging $\text{Al(1)}\text{-C(1)}$ bond (2.096(3) Å) was found to be longer than the terminal $\text{Al(1)}\text{-C(2)}$ bond (1.940(5) Å), suggesting that the bridging methyl groups were more weakly bound than the neighbouring terminal methyl groups. Furthermore, asymmetry was present within the dimer, as the $\text{Al(1)}\text{-C(1')}$ bond was found to be 0.038 Å longer than the $\text{Al(1)}\text{-C(1)}$ bond. This asymmetry was further evident from C–Al–C bond angles of $116.7(2)^\circ$ and $106.4(9)^\circ$, which highlighted the distortion within the molecule compared to the symmetric Al_2Me_6 , which has a C–Al–C bond angle of 104.52° .²¹⁰

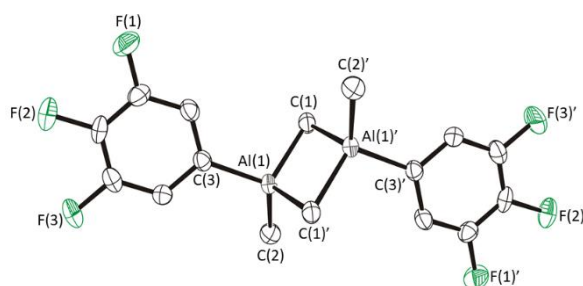
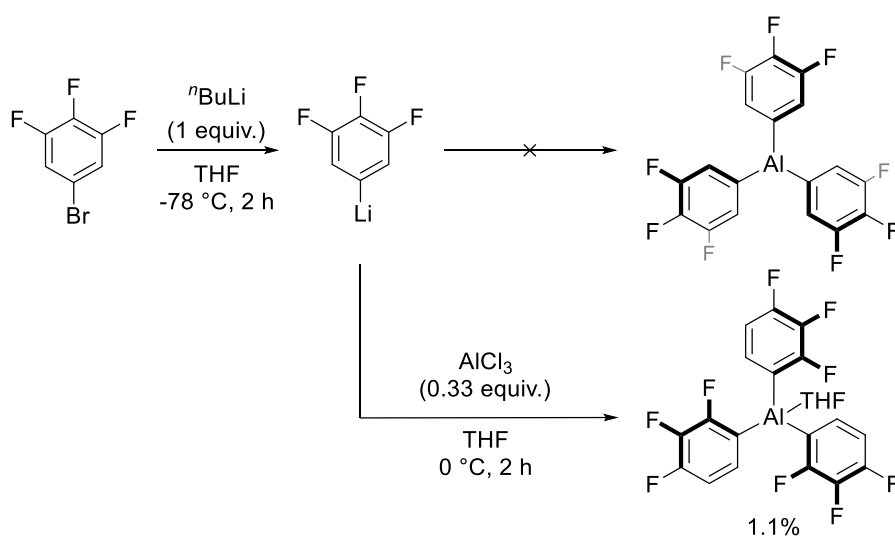


Figure 20 – X-ray crystal structure of $\mu_2\text{-Al(3,4,5-F}_3\text{C}_6\text{H}_2)\text{Me}_2$. H-atoms omitted for clarity and thermal ellipsoids drawn at 50% probability.

2.4.3 Tris(2,3,4-trifluorophenyl)alane

As discussed in section 2.4.1, the first attempted synthesis of $\text{Al(3,4,5-F}_3\text{C}_6\text{H}_2)_3$ employed an adapted lithiation procedure for borane synthesis, using AlCl_3 instead of $\text{BF}_3 \cdot \text{Et}_2\text{O}$. The lithiation procedure was eventually discarded in favour of the more reliable Grignard method. Upon addition of AlCl_3 to the organolithium species, a

mixture of products could be seen *via in situ* multinuclear NMR spectroscopy, making the isolation of $\text{Al}(\text{3,4,5-F}_3\text{C}_6\text{H}_2)_3$ problematic. The number of impurities was indicative of benzyne formation and subsequent decomposition, which was unexpected as the starting bromobenzene was devoid of *ortho*-fluorine atoms. In one instance, 78 mg of crystals were obtained from a DCM/pentane solution at $-40\text{ }^\circ\text{C}$. Whilst the isolation of $\text{Al}(\text{3,4,5-F}_3\text{C}_6\text{H}_2)_3$ or its solvated adduct was expected, XRD analysis identified that $\text{Al}(\text{2,3,4-F}_3\text{C}_6\text{H}_2)_3\cdot\text{THF}$ had instead been formed (Scheme 41).^{iv} The intermediate for this new adduct could have eliminated lithium fluoride to form benzyne, accounting for the number of impurities observed within the multinuclear NMR spectra and the chemical structure of the crystals formed.



Scheme 41 – Synthesis of $\text{Al}(\text{2,3,4-F}_3\text{C}_6\text{H}_2)_3\cdot\text{THF}$.

A plausible explanation to this result is credited to halogen dancing.^{211,212} Halogen dancing is a base induced reaction wherein the position of a halogen atom ‘dances’ around a haloaromatic compound, resulting in a different halogen substitution pattern in the product compared to the reagent. A summary of factors which can promote halogen dancing is displayed in Table 3.²¹¹ In the aforementioned reaction many of these factors were present: THF was employed as the solvent and the addition of stoichiometric $n\text{BuLi}$ to the bromobenzene occurred at $-78\text{ }^\circ\text{C}$. Notably, the $\text{Al}(\text{2,3,4-F}_3\text{C}_6\text{H}_2)_3\cdot\text{THF}$ adduct was isolated in a very small quantity, and thus it is possible that further products of halogen dancing were formed but not isolated.

^{iv} The reaction from which crystals of $\text{Al}(\text{2,3,4-F}_3\text{C}_6\text{H}_2)_3\cdot\text{THF}$ resulted was performed by Masters student Rowan Page. XRD analysis of these crystals was performed by Dr Darren Ould.

Table 3 – Conditions for promotion or prevention of halogen dancing.²¹¹

Halogen dance promotion	Halogen dance prevention
Low temperature	High temperature
No excess of base	Excess of base
Addition of base to halide	Addition of halide to base
Slow reacting electrophile	Fast reacting electrophile
THF solvent	THP (tetrahydropyran) solvent

The crystal structure of $\text{Al}(\text{2,3,4-}\text{F}_3\text{C}_6\text{H}_2)_3 \cdot \text{THF}$ is shown in Figure 21. Here the aluminium centre adapted a near tetrahedral geometry, with O–Al–C bond angles of $103.80(8)^\circ$, $109.54(8)^\circ$, and $102.47(8)^\circ$, revealing a more strained structure than $\text{Al}(\text{3,4,5-}\text{F}_3\text{C}_6\text{H}_2)_3 \cdot \text{Et}_2\text{O}$. The increased strain in the structure is likely to be due to the *ortho*-fluorine atoms on $\text{Al}(\text{2,3,4-}\text{F}_3\text{C}_6\text{H}_2)_3$ arranging themselves away from each other rather than the different coordinating base, as THF is more sterically compact than Et_2O .

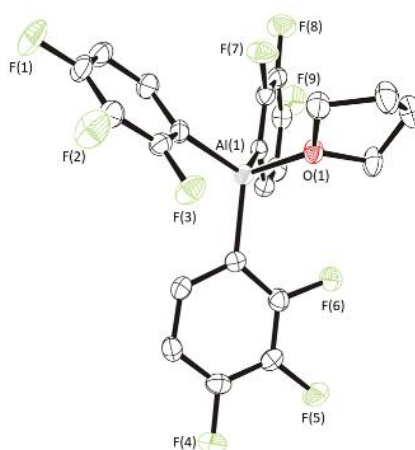
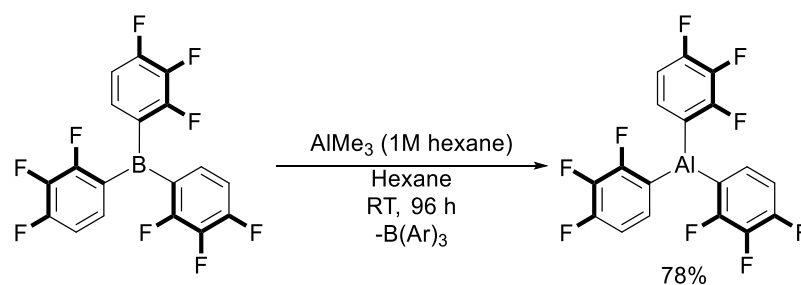


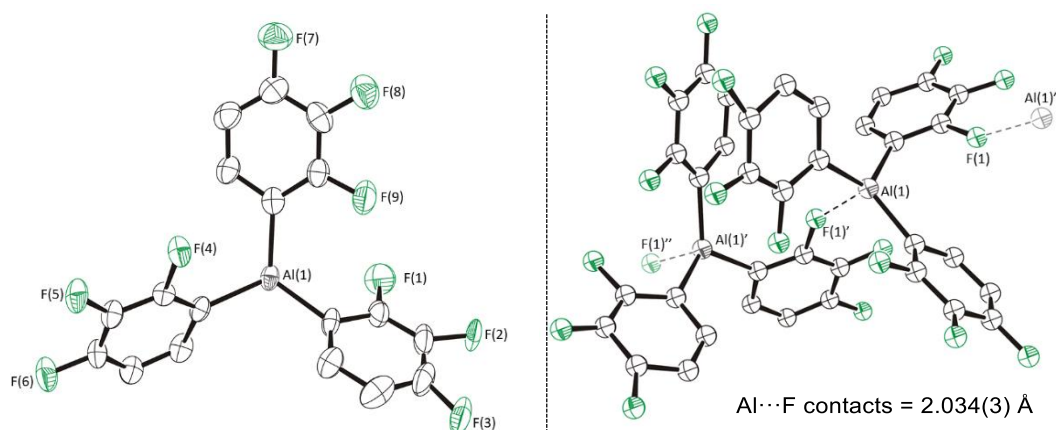
Figure 21 – X-ray crystal structure of $\text{Al}(\text{2,3,4-}\text{F}_3\text{C}_6\text{H}_2)_3 \cdot \text{THF}$. H-atoms omitted for clarity and thermal ellipsoids drawn at 50% probability.

In response to the surprising formation of $\text{Al}(\text{2,3,4-}\text{F}_3\text{C}_6\text{H}_2)_3 \cdot \text{THF}$, the preparation of the unsolvated species was targeted. Here, the transmetalation procedure of the parent borane with AlMe_3 was found to form crystals of the desired alane in 78% yield after four days of being left undisturbed at room temperature (Scheme 42).^v

^v XRD analysis of $\text{Al}(\text{2,3,4-}\text{F}_3\text{C}_6\text{H}_2)_3$ was performed by Dr Darren Ould.

Scheme 42 – Synthesis of $\text{Al}(2,3,4\text{-F}_3\text{C}_6\text{H}_2)_3$.

The structure of unsolvated $\text{Al}(2,3,4\text{-F}_3\text{C}_6\text{H}_2)_3$ is shown in Figure 22. Here, the alane displays similar features to its parent borane, with a paddlewheel structure and C–Al–C bond angles of $115.0(2)^\circ$, $121.5(2)^\circ$, and $115.9(2)^\circ$. Further investigation of the unit cell of $\text{Al}(2,3,4\text{-F}_3\text{C}_6\text{H}_2)_3$ finds Al \cdots F contacts of $2.034(3)$ Å between the *ortho*-fluorine of one alane's aryl group and another alane's aluminium centre. These contacts are repeated throughout the overall packing structure to form a long chain. This packing arrangement can be compared to that of unsolvated $\text{Al}(\text{C}_6\text{F}_5)_3$, where dimeric packing is observed in the bulk structure.²⁰⁵ Due to this packing structure, there was an inherent risk of benzyne formation, thus significant care was taken in its characterisation.

Figure 22 – X-ray crystal structure of $\text{Al}(2,3,4\text{-F}_3\text{C}_6\text{H}_2)_3$ (left). Al \cdots F contacts between adjacent molecules in the bulk crystal structure (right). H-atoms omitted for clarity and thermal ellipsoids drawn at 50% probability.

2.5 Comparisons of Lewis acidity

As discussed in chapter one, the calculation of Lewis acidity is paramount in the design of Lewis acid catalysts. Notably in the case of fluorinated triarylboranes, slight modifications to the fluorine substitution pattern on the aryl rings can impart significant

changes to Lewis acidity and consequentially reactivity. Both experimental and computational probes were employed to fully understand the trends of fluorine position in the Lewis acidity of borane and alane compounds discussed within this thesis.

2.5.1 The Gutmann-Beckett method

The Gutmann-Beckett method is widely used to compare the Lewis acidity of triarylboranes,⁶³ and thus was the first method used to compare the acidity of the boranes and alanes prepared in this thesis. The resultant acceptor numbers upon the complexation of the Lewis acids to Et₃PO are summarised in Figure 23 and are compared to commercially available boron Lewis acids: the bulky but weakly Lewis acidic triphenylborane,²¹³ the non-sterically demanding but strong Lewis acid BF₃,²¹⁴ and the triarylborane B(3,5-(CF₃)₂C₆H₃)₃.²¹⁵ Solvent effects are known to slightly alter Lewis acidity measurements,⁷ hence all measurements were recorded in CDCl₃. Notably, the novel unsolvated alanes were observed to decompose in CDCl₃ and thus the fluoride ion affinity was used to compare their Lewis acidity to their parent boranes (section 2.5.3). Gutmann-Beckett Lewis acidity calculations could be calculated for these unsolvated alanes with non-coordinating solvents such as toluene or benzene; however, these values would not be comparable to those calculated measured in CDCl₃. Moreover, even though the Al(3,4,5-F₃C₆H₂)₃·Et₂O adduct was stable in CDCl₃, the Et₃PO was unable to displace the ether and thus an acceptor number could not be calculated.

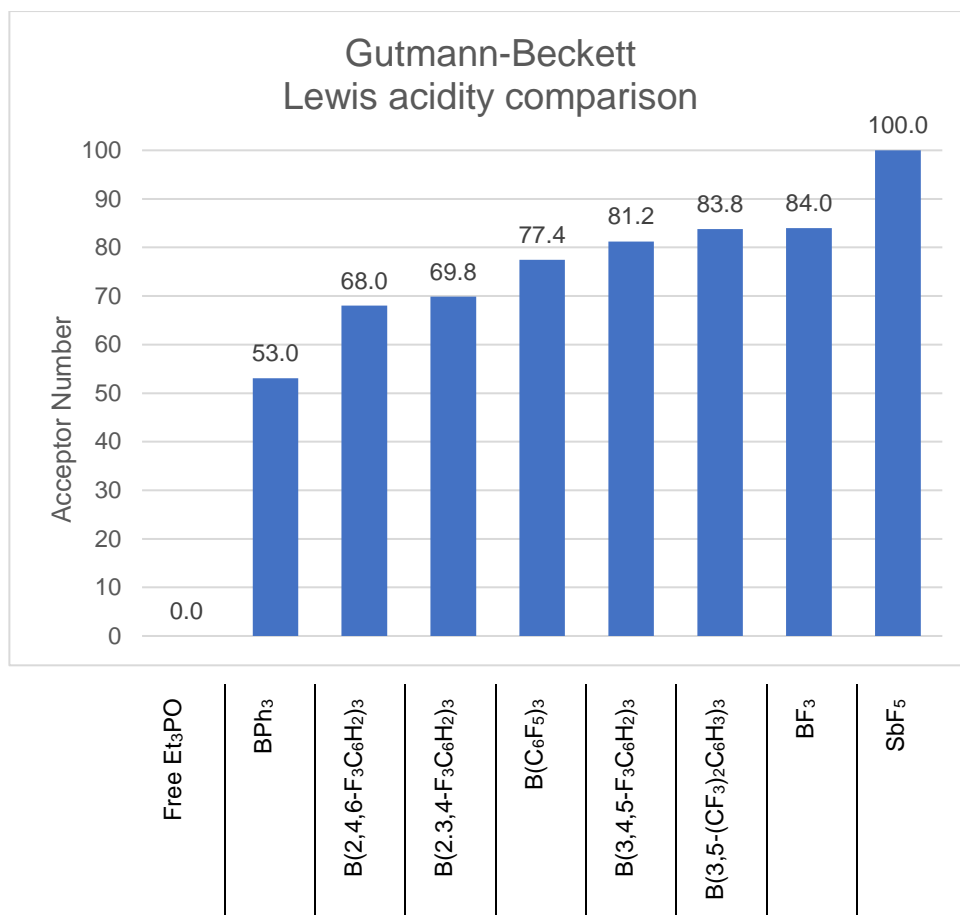


Figure 23 – Comparison of Lewis acidity through the Gutmann-Beckett method. Values for SbF₅, BF₃, BPh₃, and B(3,5-(CF₃)₂C₆H₃)₃ taken from literature sources.^{8,213–215}

Initial comparisons of the AN values reveal that all of the synthesised triarylboranes have a Lewis acidity between that of BPh₃ (AN = 53.0) and BF₃ (AN = 84.0), confirming their identity as strongly Lewis acidic catalysts. Towards the lower end of the AN scale are B(2,4,6-F₃C₆H₂)₃ (AN = 68.0) and B(2,3,4-F₃C₆H₂)₃ (AN = 69.8). Each of these boranes contain nine fluorine atoms and the discrepancy between the two can be attributed to the different positions of the fluorine atoms around the aryl ring imparting slightly different inductive effects upon the Lewis acidity of the borane. Rather surprisingly, the archetypal triarylborane B(C₆F₅)₃ (AN = 77.6) is shown to not be the strongest Lewis acid out of the triarylboranes probed, with B(3,4,5-F₃C₆H₂)₃ (AN = 81.2) recorded as stronger. Whilst one would expect the replacement of six protons in B(3,4,5-F₃C₆H₂)₃ with six fluorine atoms would generate a greater negative inductive effect upon the central boron atom, this result suggests they in fact decrease the Lewis acidity of the borane. It is possible that the negative steric influence of the *ortho*-fluorine atoms is more significant than their extra inductive effect, or that the electron rich *ortho*-fluorine atoms can donate some electron density into the boron's vacant *p*-orbital, thus reducing its Lewis acidity. The absence of *ortho*-fluorines in

$B(3,4,5-F_3C_6H_2)_3$ could also reduce the energy barrier required for pyramidalisation upon complexation to a Lewis base compared to $B(C_6F_5)_3$, which must also account for the steric hinderance of its *ortho*-fluorine atoms.

Such observations can be explained by a report by Gilbert, who calculated the binding energy of fluorinated triarylboranes to trimethylamine and trimethylphosphine to probe the effects that fluorine substitution patterns would have upon Lewis acidity.⁵⁴ In brief, it was discovered that the Lewis acidity of the borane was predominantly determined by electronics, and increased as fluorine atoms were positioned closer to the boron atom (*para*-position > *meta*-position > *ortho*-position). An exception to this rule was noted if both *ortho*-positions were simultaneously substituted by fluorine atoms, whereupon steric factors became more important and reduced the Lewis acidity of the borane.⁵⁴ Another example of steric repulsion decreasing the Lewis acidity of boranes was discussed by Ashley and O'Hare, who observed that triarylboranes with aryl rings furnished with chlorine atoms were less acidic than those furnished with fluorine atoms.⁵⁷ This steric argument explains why the Gutmann-Beckett method records $B(2,4,6-F_3C_6H_2)_3$ as less acidic than $B(2,3,4-F_3C_6H_2)_3$, and $B(C_6F_5)_3$ as less acidic than $B(3,4,5-F_3C_6H_2)_3$.

2.5.2 The Childs method

The Childs method of Lewis acidity determination relies on the complexation of a Lewis acid with crotonaldehyde and is calculated through the change in chemical shift of a proton which is relatively distant from said Lewis acid. Therefore, steric effects are significantly less pronounced than when compared to the Gutmann-Beckett method. One disadvantage of the Childs method is that the 1H NMR spectrum can become convoluted if the Lewis acid in question contains many proton environments which resonate at similar chemical shifts to crotonaldehyde, leading to the risk of incorrectly calculated relative acidity; however, this issue does not affect the Lewis acidity measurement of triarylboranes. The Childs method was also performed on the triarylboranes to ensure that the trends observed through the Gutmann-Beckett method were reliable (Figure 24). To avoid any discrepancy from solvent effects, all measurements were recorded in $CDCl_3$. As with the Gutmann-Beckett method, the $Al(3,4,5-F_3C_6H_2)_3 \cdot Et_2O$ adduct was unreactive towards crotonaldehyde and thus its relative acidity could not be calculated.

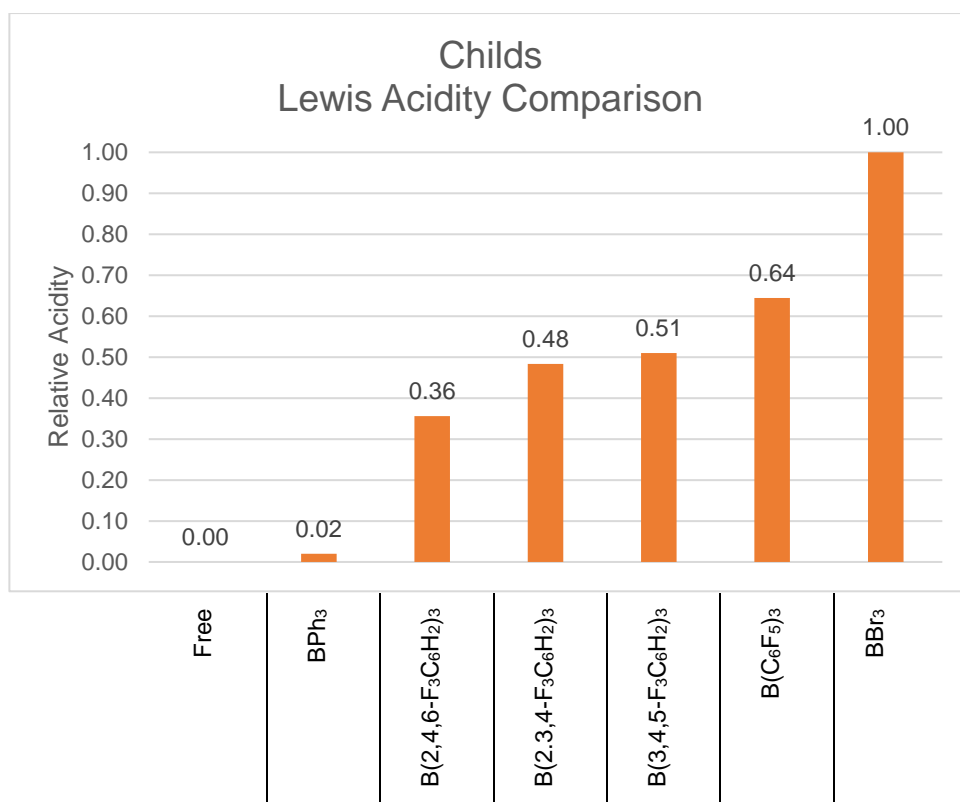


Figure 24 – Comparison of Lewis acidity through the Childs method. Value for BBr₃ taken from the literature.⁹

Through comparison of relative acidity, the trends observed through comparison of acceptor numbers generally appear to remain the same. BPh₃ appears to be very weakly acidic, imparting a very slight shift in the ¹H NMR between crotonaldehyde and its corresponding adduct. As expected, B(2,4,6-F₃C₆H₂)₃ is the weakest Lewis acid out of the fluorinated triarylboranes probed. B(2,3,4-F₃C₆H₂)₃ and B(3,4,5-F₃C₆H₂)₃ record similar relative acidities, attributable to both containing nine fluorine atoms and neither having the steric barrier of two *ortho*-fluorine atoms. As B(3,4,5-F₃C₆H₂)₃ is more Lewis acidic than B(2,3,4-F₃C₆H₂)₃, this suggests that the mesomeric effects of the *meta*-fluorine atoms contribute significantly towards overall Lewis acidity. Furthermore, this also suggests that there is still some influence of the *ortho*-fluorine atoms of B(2,3,4-F₃C₆H₂)₃ donating electron density into the central boron centre and decreasing acidity.

The largest discrepancy between the two methods is the observation that B(C₆F₅)₃ appears as more Lewis acidic than B(3,4,5-F₃C₆H₂)₃ through the Childs method. It thus appears that the steric hinderance imparted by the *ortho*-fluorines becomes more pronounced when the base is larger and thus confirms that the Gutmann-Beckett method cannot be used universally. This also suggests that the negative inductive

effect from the fifteen fluorine atoms is more important than the deleterious steric effects imparted by the *ortho*-fluorine atoms.

2.5.3 The fluoride ion affinity method

Fluoride ion affinity (FIA) was also calculated for select boranes and alanes.^{vi} As explained in chapter one, FIA calculates the energy required for the coordination of a single fluoride ion to the Lewis acidic centre in the gaseous phase.¹¹ Therefore, the trends recorded by FIA can be seen as more reliable than experimental probes as variables such as steric factors, solvent effects, and probe hardness are no longer applicable.^{7,18} The calculated FIA values and their relative value to $\text{Al}(\text{C}_6\text{F}_5)_3$ are shown in Table 4.

Table 4 – FIA values for boranes and alanes.

Lewis Acid	FIA (KJ mol ⁻¹)	Relative FIA to $\text{Al}(\text{C}_6\text{F}_5)_3$ (%)
$\text{B}(\text{C}_6\text{F}_5)_3$	459	85
$\text{B}(3,4,5\text{-F}_3\text{C}_6\text{H}_2)_3$	427	79
$\text{B}(2,3,4\text{-F}_3\text{C}_6\text{H}_2)_3$	404	75
$\text{Al}(\text{C}_6\text{F}_5)_3$	541	100
$\text{Al}(3,4,5\text{-F}_3\text{C}_6\text{H}_2)_3$	511	95
$\text{Al}(2,3,4\text{-F}_3\text{C}_6\text{H}_2)_3$	501	93

One further calculation for SbF_5 was also run, with a recorded FIA of 546 kJmol⁻¹, a value significantly larger than expected. This was a consequence of the basis set used for the calculations seen in Table 4. These values were calculated using a cc-PVDZ basis set; however, this basis set is not defined for antimony and thus an effective core potential (ECP) had to be used. To calculate the FIA of SbF_5 , the functional Def2-TZVP was used for the antimony atoms, whilst the functional cc-PVDZ was used for the F atoms. A full discussion of the details behind the basis sets is beyond the scope of this thesis, but a simple description is that because of the different basis sets used to calculate SbF_5 and the rest of the Lewis acids, a strong comparison between them cannot be made. Importantly, if one takes the most accurate calculation of SbF_5 as 501 kJmol⁻¹,²¹⁶ then both novel alanes $\text{Al}(2,3,4\text{-F}_3\text{C}_6\text{H}_2)_3$ and $\text{Al}(3,4,5\text{-F}_3\text{C}_6\text{H}_2)_3$ can be defined as Lewis superacids.

^{vi} FIA calculations were performed by Dr Darren Ould. Further details can be found in Chapter 8.1.

The trend in Lewis acidity strength between the boranes calculated by FIA is different to the acceptor numbers calculated in the Gutmann-Beckett method and agrees with the relative acidities determined by the Childs method. The FIA method suggests that $B(3,4,5-F_3C_6H_2)_3$ is in fact a weaker Lewis acid than $B(C_6F_5)_3$. As FIA is calculated in the gaseous phase with a single fluoride ion, steric effects are significantly less relevant in the formation of the resultant adduct than they are with larger probes such as Et_3PO and crotonaldehyde. Thus, this suggests that the steric influence of the *ortho*-fluorine atoms of $B(C_6F_5)_3$ have a more pronounced influence on reducing Lewis acidity when the corresponding probe is larger, agreeing with the hypothesis from the Childs method.

The most discernable comment from the calculated FIA values is that the aluminium complexes are typically 15% more Lewis acidic than their borane congeners. This increase in acidity is attributed to an increased electronegativity at the central triel atom. The trend in Lewis acidity strength of alanes mirrors that observed for boranes, suggesting that the effects of fluorine substitution pattern are not discriminate towards the size of the triel centre.

2.6 Conclusions and outlook

In conclusion, a range of boron and aluminium based Lewis acids were prepared. The boranes were synthesised using well-established methodologies, either using a Grignard reagent or an organolithium intermediate and were purified through sublimation. The alanes were either prepared through transmetallation of the parent borane or synthesised from the appropriate bromobenzene through a Grignard reagent intermediate.

The Lewis acidities of these boron and aluminium based compounds were then compared using a range of experimental and computational probes. Whilst the Gutmann-Beckett and Childs experimental methods offered conflicting results regarding the relative strengths of $B(3,4,5-F_3C_6H_2)_3$ and $B(C_6F_5)_3$, comparison with the FIA method suggested that the steric effects imposed by the *ortho*-fluorine atoms of $B(C_6F_5)_3$'s aryl rings resulted in decreased acidity readings when larger probes were used and that it was indeed the stronger Lewis acid. Figure 25 displays the recorded trends of Lewis acidity for the boranes used in this thesis, measured by the Gutmann-Beckett method, the Childs method and fluoride ion affinity.

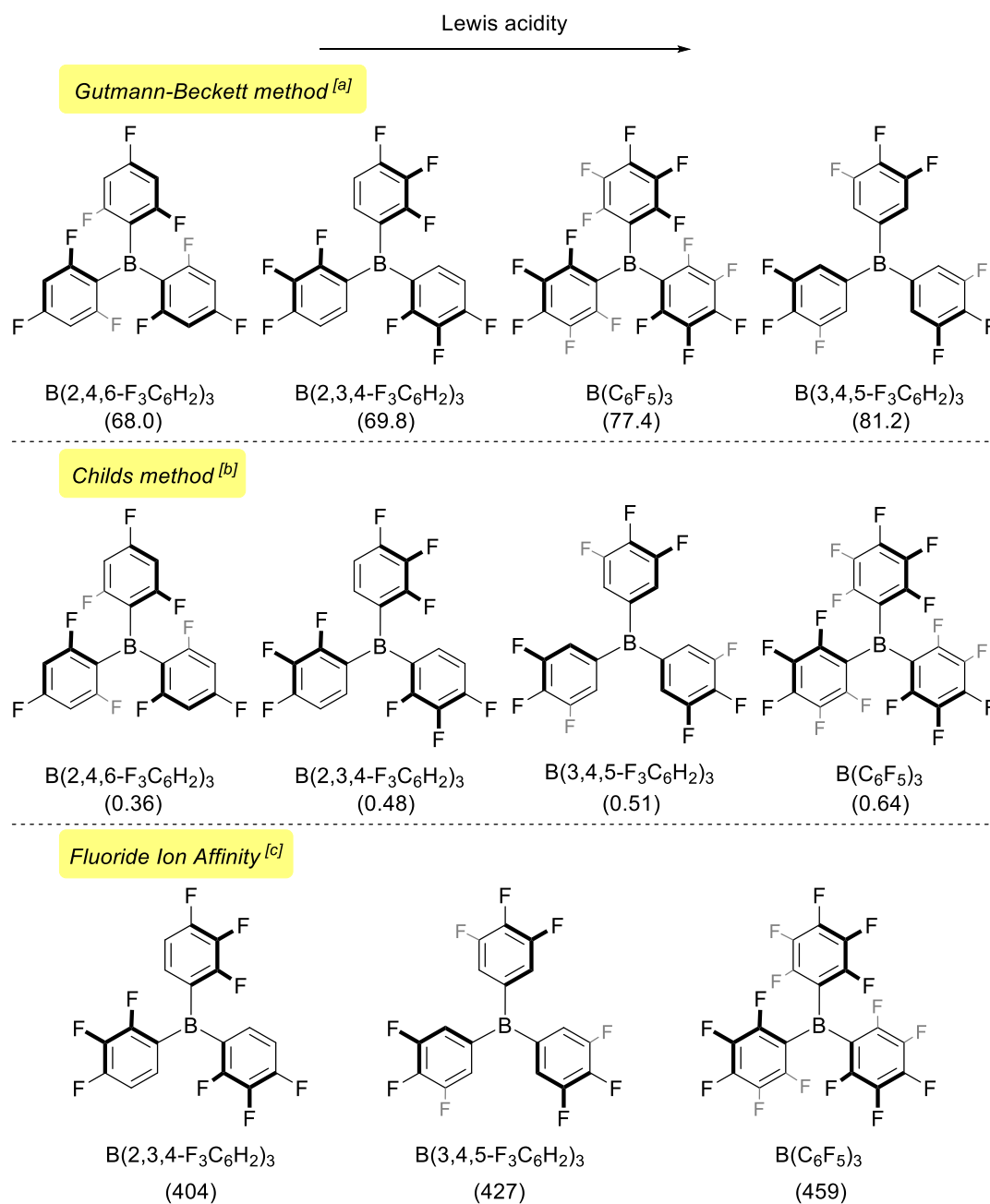


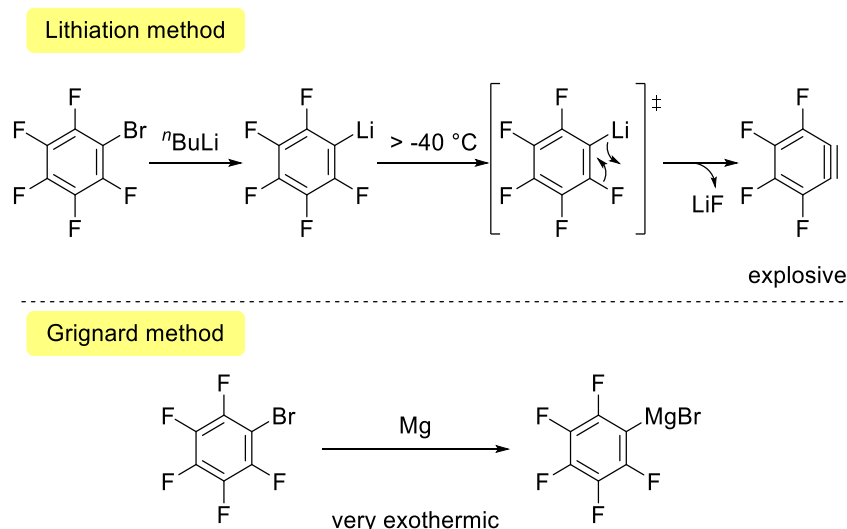
Figure 25 – Trends in Lewis acidity recorded through the Gutmann-Beckett method, the Childs method and fluoride ion affinity. Values in parentheses: ^[a] = acceptor number; ^[b] = relative acidity; ^[c] = kJmol⁻¹.

Chapter three – Synthesis of tris(pentafluorophenyl)borane using continuous flow technologies

3.1 Aims of this chapter

In this chapter, the attempted synthesis of the archetypal Lewis acid tris(pentafluorophenyl)borane $[B(C_6F_5)_3]$ using continuous flow techniques is described. $B(C_6F_5)_3$ is a desirable chemical in the main-group community due to its chemical stability, large steric bulk, and high Lewis acidity; however, as described in chapter two, its preparation suffers from several drawbacks. Factors of the $B(C_6F_5)_3$ synthetic procedures which can cause issues include:

- In the lithiation method, the intermediate (pentafluorophenyl)lithium (C_6F_5Li) is generated. C_6F_5Li has a propensity to decompose into the potentially explosive tetrafluorobenzyne through elimination of lithium fluoride above $-40\text{ }^\circ\text{C}$ and thus reaction temperature must be regulated (Scheme 43, top).
- In the Grignard method, the highly exothermic preparation of the Grignard reagent (pentafluorophenyl)magnesium bromide $[(C_6F_5)MgBr]$ can lead to run-away reaction and can be potentially explosive. As with the lithiation method reaction temperature must be tightly controlled (Scheme 43, bottom).
- In both methods, the twofold sublimation purification step is time-consuming.



Scheme 43 – Inherent problems of $B(C_6F_5)_3$ synthesis.

Whilst $B(C_6F_5)_3$ is a commercially available compound, the problems associated with its synthesis are reflected by its high price (£608 for 5 g).^{vii} In response to these issues, it was theorised that the benefits of continuous flow technologies could be applicable to the preparation of $B(C_6F_5)_3$, namely taking advantage of the increased scale-up and safety capabilities. Literature precedents suggested that the lithiation procedure would transfer smoothly to continuous flow, with successful preparations of boronic acids through organolithium intermediates.^{186,187,217–219} Moreover, it was theorised that the use of flow chemistry could potentially increase product yields through increased selectivity, and allow a translation towards scaled-up production.

3.2 Initial reactor design

The initial reactor design was composed of four modules (Figure 26). Firstly, the solutions were passed through a set of cooling coils, which reduced the temperature of the reagents to $-78\text{ }^\circ\text{C}$ before they were permitted to mix. Secondly, a reactor coil was connected, wherein $n\text{BuLi}$ was reacted with pentafluorobromobenzene ($C_6F_5\text{Br}$) at sub-ambient temperatures to form the organolithium intermediate $C_6F_5\text{Li}$. The outlet of this reactor coil was connected to a secondary reactor coil, also at sub-ambient temperature, wherein $C_6F_5\text{Li}$ was mixed with the desired electrophile. Finally, the fourth module consisted of a non-cooled coil where the products of the reaction were gradually returned to ambient temperature before collection.

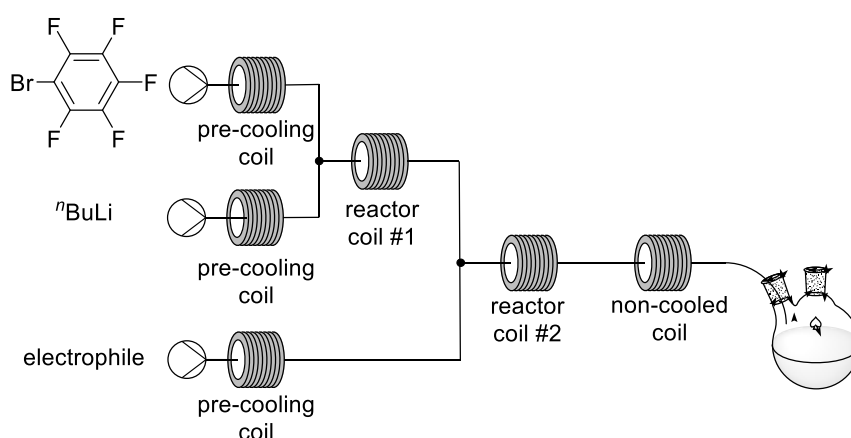


Figure 26 – Reactor design for $B(C_6F_5)_3$ synthesis.

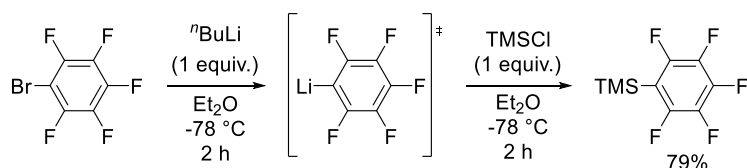
^{vii} Price taken from the Sigma Aldrich website on 31/12/2020.

Importantly, dry and degassed solvents were used, and the entire apparatus was flushed with nitrogen before initiating the reaction to prevent the decomposition of $n\text{BuLi}$ and $\text{BF}_3 \cdot \text{Et}_2\text{O}$. During the preparation of trimethyl(perfluorophenyl)silane ($\text{C}_6\text{F}_5\text{TMS}$) (section 3.3; section 3.5), the outlet stream was collected in an Erlenmeyer flask; however, during preparations of $\text{B}(\text{C}_6\text{F}_5)_3$ (section 3.4), the stream was collected within a Schlenk flask under a dry nitrogen atmosphere and the appropriate analysis was performed using air sensitive manipulation techniques to avoid decomposition and side-reactions.

3.3 Optimisation of lithiation procedure

The development of the process for $\text{B}(\text{C}_6\text{F}_5)_3$ synthesis in flow began with the optimisation of the lithiation step. Trimethylsilyl chloride (TMSCl) was chosen as an electrophile for this optimisation step due to its relative stability compared to $\text{BF}_3 \cdot \text{Et}_2\text{O}$ and other boron containing electrophiles, and for the air and moisture stability of the expected product $\text{C}_6\text{F}_5\text{TMS}$. Furthermore, the ^{19}F NMR spectrum of the product was easily distinguishable from the parent $\text{C}_6\text{F}_5\text{Br}$, allowing for facile *in situ* NMR monitoring and permitting quantitative determination of the reaction progress.

Initially, this reaction was performed in batch, to ensure the success of TMSCl as a surrogate electrophile. The reaction parameters are displayed in Scheme 44, and the crude reaction was followed by ^{19}F NMR spectroscopy. An NMR yield of 79% was recorded through analysis of the crude ^{19}F NMR spectrum. Gratifyingly, the only other ^{19}F NMR signals observed were assigned to the parent $\text{C}_6\text{F}_5\text{Br}$ and analysis of the crude ^1H NMR spectrum revealed only signals characteristic of the trimethylsilyl protons indicating a clean reaction with negligible decomposition.



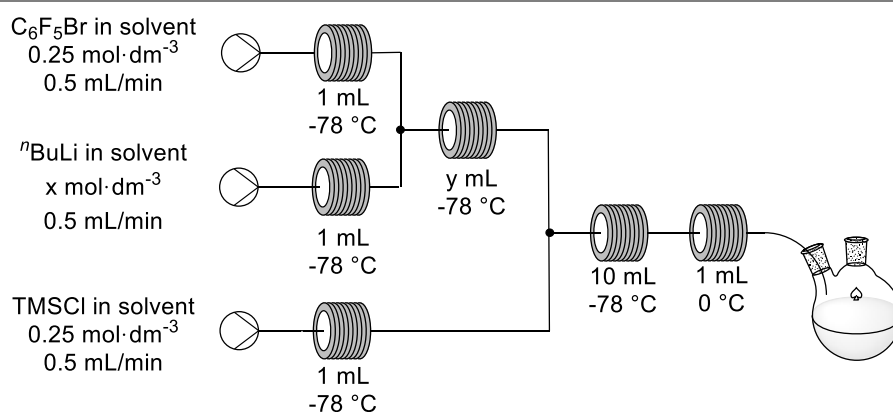
Scheme 44 – Initial batch preparation of $\text{C}_6\text{F}_5\text{TMS}$.

With promising results in hand, the reaction was translated towards continuous flow. The initial reactor plan was previously detailed in Figure 26. The reagents were initially cooled to $-78\text{ }^\circ\text{C}$, prior to the lithiation of $\text{C}_6\text{F}_5\text{Br}$ with $n\text{BuLi}$ in reactor coil one. Next, a stream of TMSCl was added to quench the organolithium intermediate in reactor coil two, before warming up in a coil at room temperature and being collected. In all runs, the ^{19}F NMR spectrum was taken immediately from the crude solution. A

secondary ^1H NMR spectrum was taken by removing the solvent *in vacuo*, dissolving the residual white solid in CDCl_3 , and passing this through a short cotton plug into an NMR tube to remove any suspended lithium chloride.

Initially, the reaction was performed with a 1:1:1 stoichiometry between the three reagents (Table 5, entry 1); however, this resulted in no reaction and only $\text{C}_6\text{F}_5\text{Br}$ was observed by ^{19}F NMR spectrum analysis. In response, the stoichiometry of $^n\text{BuLi}$ was increased to 1.6 equivalents, as reported by other literature lithiation procedures.^{186,187} This resulted in a remarkable increase in reaction progression, with 48% conversion into $\text{C}_6\text{F}_5\text{TMS}$ observed (Table 5, entry 2). Subsequently, the residence time was increased by increasing the volume of the reactor coil from 5 mL to 10 mL, which led to <95% conversion by ^{19}F NMR spectroscopy when a 10 mL reactor coil was employed (Table 5, entries 3–4). Additionally, ^1H NMR spectrum analysis of these runs found only trimethylsilane and residual ether solvent resonances. Therefore, the conditions in entry 4 were designated as optimal. Switching the solvent from Et_2O to THF (Table 5, entry 5) was not found to be significantly deleterious to the conversion.

Table 5 – Optimisation of lithiation step – initial optimisation.

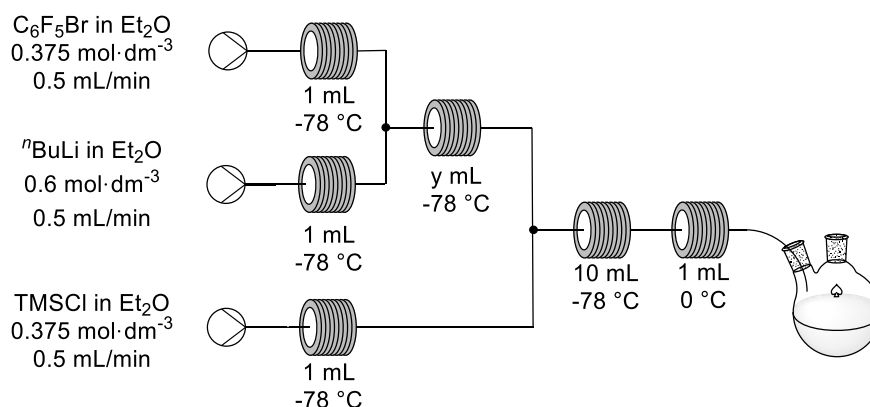


Run	Solvent	$^n\text{BuLi}$ molarity x ($\text{mol}\cdot\text{dm}^{-3}$)	Reactor coil volume y (mL)	Conversion by ^{19}F NMR spectroscopy (%)
1	Et_2O	0.25	5	<5
2	Et_2O	0.4	5	48
3	Et_2O	0.4	7.5	55
4	Et_2O	0.4	10	>95
5	THF	0.4	10	94

The concentration of the reaction was then increased by 1.5 equivalents, again with 1.6 equivalents of $^n\text{BuLi}$ per $\text{C}_6\text{F}_5\text{Br}$, with a view that increased molarities of reagents

would result in a greater product formation per unit time. The residence time of the reactor coil was reinvestigated by varying its volume (Table 6).

Table 6 – Optimisation of lithiation step – investigation into concentration.

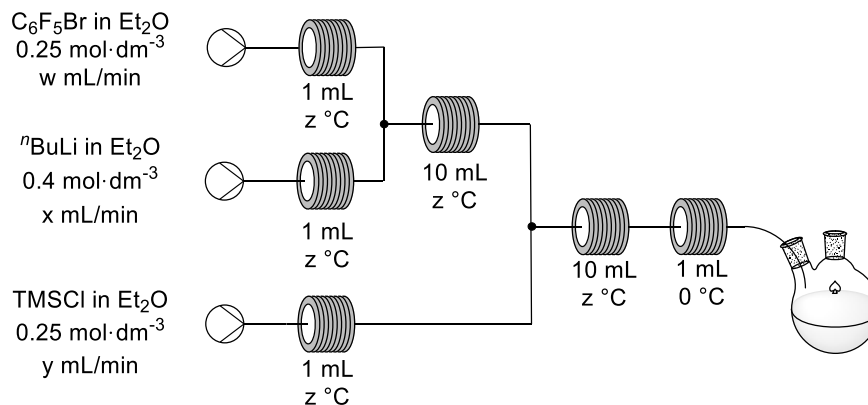


Run	Reactor coil volume y (mL)	Conversion by ^{19}F NMR spectroscopy (%)
1	5	73
2	7.5	66
3	10	70

Analysis of the ^{19}F NMR spectra revealed that increasing the molarity of all of the reagents did not have a positive impact towards the yield of $\text{C}_6\text{F}_5\text{TMS}$. On the contrary, the volume of the reactor coil did not register any effect upon the conversion rate, with all three experiments resulting in typical yields of 70% (Table 6, entries 1–3). This average conversion through a range of residence times suggested that the high concentration of reagents caused the reaction to be too exothermic upon mixing, causing some decomposition of the $\text{C}_6\text{F}_5\text{Li}$ intermediate as evidenced by new signals in the ^{19}F NMR spectra, despite the higher heat transfer present within the tubing compared to conventional batch reactions.

In response to these disappointing results, the concentration of the reagents was switched back to the optimal level (Table 5, entry 4) and temperature and flow rates were next investigated to further optimise the procedure (Table 7).

Table 7 – Optimisation of lithiation step – investigation of temperature and flow rates.



Run	C₆F₅Br flow rate w (mL/min)	ⁿBuLi flow rate x (mL/min)	TMSCl flow rate y (mL/min)	Temperature z (°C)	Conversion by ¹⁹ F NMR spectroscopy (%)
1	0.5	0.5	0.5	-60	53
2	0.33	0.33	0.33	-78	67
3	0.75	0.75	0.75	-78	43

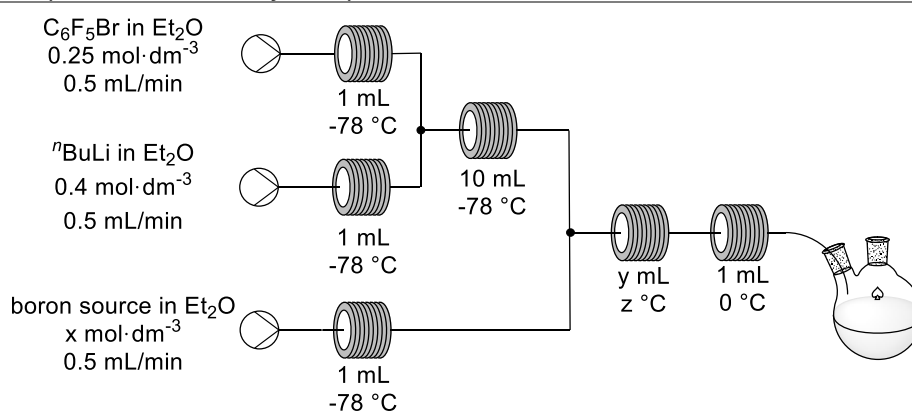
Increasing the temperature of the reactor to -60 °C (Table 7, entry 1) was detrimental towards the reaction giving 53% yield, presumably due to increased decomposition of C₆F₅Li upon decreased external temperature. Increasing the residence time of the reagents (Table 7, entry 2) also resulted in a sub-optimal conversion. This was attributed to the formation of solid side products upon decomposition of C₆F₅Li, which led to blockages hence inconsistent flow rates and unreliable residence times. Likewise, decreasing the residence time of the reagents (Table 7, entry 3) resulted in a low conversion, presumably as the C₆F₅Br and ⁿBuLi did not have sufficient time for mixing before getting quenched by the electrophile.

Overall, the optimal conditions were found in Table 5, entry 4. These conditions were carried forward to the optimisation of the second reactor coil as they allowed for a 95% conversion by ¹⁹F NMR spectroscopy to C₆F₅Li. It was hypothesised that any reduction in conversion during the investigation of the following borylation reaction would thus be a result of incomplete reaction within the second reactor coil.

3.4 Optimisation of the borylation procedure

With a quantitative preparation of C_6F_5Li , it appeared that the addition of $BF_3 \cdot Et_2O$ as an electrophile would easily produce the desired $B(C_6F_5)_3$. Unfortunately, this was not the case. Notably, whilst TMSCl was added in one equivalent to the generated organolithium compound, $BF_3 \cdot Et_2O$ was added in a third equivalent ratio to preserve the stoichiometry of the reaction. Table 8 displays the optimisation parameters that were investigated: the boron source; the molarity of the boron source; the temperature; and the reactor coil volume.

Table 8 – Optimisation of the borylation procedure.



Run	Boron source molarity x (mol·dm ⁻³)	Reactor coil volume y (mL)	Temperature z (°C)	Conversion by ¹⁹ F NMR spectroscopy (%)
1	$BF_3 \cdot Et_2O$ (0.0833)	5	-78	<5
2	$BF_3 \cdot Et_2O$ (0.0833)	10	-78	<5
3	$BF_3 \cdot Et_2O$ (0.0833)	15	-78	<5
4	$BF_3 \cdot Et_2O$ (0.1666)	10	-78	<5
5	$BF_3 \cdot Et_2O$ (0.0833)	10	5 ml at -78 5 ml at 0	<5
6	BCl_3 (0.0833)	5	-78	<5

Initially the volume of the second reactor coil was investigated (Table 8, entries 1–3), ranging from a 5 mL coil to a 15 mL coil; however, in all cases there was negligible presence of $B(C_6F_5)_3$. In response, the concentration of the electrophile was doubled (Table 8, entry 4); however, this still did not yield any of the desired borane. At this juncture it was theorised that the temperature of the tubing was too low for the

borylation to occur, thus the second reactor was split into two 5 mL coils, one at -78 °C and the other at 0 °C; however, this still did not yield any borane (Table 8, entry 5). Finally, the borane source was changed to a solution of BCl₃; however, also in this case no clear products were observed through multinuclear NMR probes (Table 8, entry 6). Surprisingly, NMR signals indicative of BF₃·Et₂O were not observed in any of these six experiments, suggesting it was participating in undesired reactions.

Figure 27 displays a typical ¹⁹F NMR spectrum from these reactions, in this case entry 1 in Table 8. The spectrum shows a myriad of signals; however, certain information can be derived. Signals indicative of B(C₆F₅)₃ (δ = -129, -145, -160 ppm), are clearly not present, revealing that the reaction was not successful.²²⁰ Partially arylated species, FB(C₆F₅)₂ and F₂B(C₆F₅), are not present either. In these cases the B–F fluorine atoms would produce signals around -73 and -30 ppm respectively.^{221,222} Likewise, the fluorine resonance of F₂B(ⁿBu) is produced around -54 ppm, which was not observed in the ¹⁹F NMR spectrum.²²³ FB(ⁿBu)₂ has not been previously characterised spectroscopically and so its presence in the crude material can not be ruled out.

It was postulated that the excess ⁿBuLi could result in the formation of the salt Li[B(C₆F₅)₄]; however, this species has indicative signals around -169, -159, and -134 ppm which are not present.²²⁴ Finally, the presence of BF₃·Et₂O would have been indicated by a signal at -153 ppm, which is not observed either. This suggests full consumption of BF₃·Et₂O which lends to the hypothesis that the intermediate organolithium compound was decomposing into tetrafluorobenzene. Further evidence towards this decomposition came from the broad signal at -204.75 ppm, indicative of lithium fluoride, the by-product of C₆F₅Li decomposition.²²⁵ The myriad of signals in the ¹⁹F NMR spectrum were thus likely a result of the uncontrollable runaway reactions of tetrafluorobenzene.

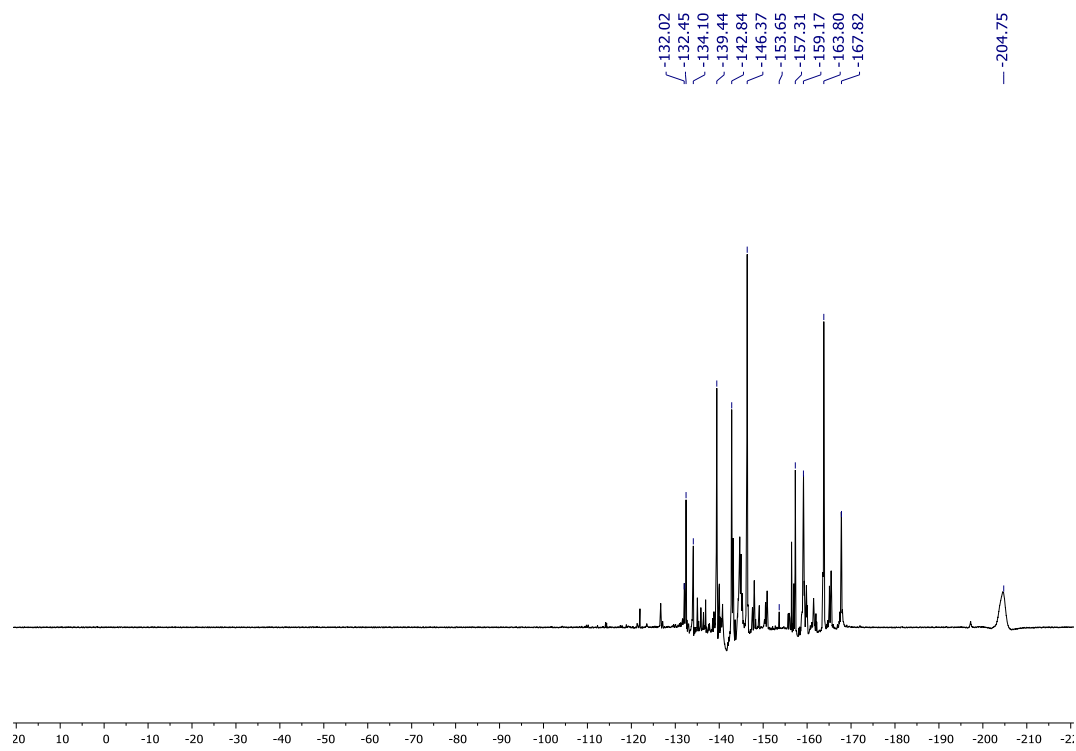


Figure 27 – ^{19}F NMR spectrum of typical failed $\text{B}(\text{C}_6\text{F}_5)_3$ synthesis.

Further confirmation that the reagents were not reacting as expected was determined through consideration of the ^{11}B NMR spectra, a typical example of which is displayed in Figure 28. The signal indicative of $\text{B}(\text{C}_6\text{F}_5)_3$ ($\delta = 59.0$ ppm) was clearly not present, indicating that the reaction was unsuccessful.²²⁰ Partially arylated species, $\text{FB}(\text{C}_6\text{F}_5)_2$ and $\text{F}_2\text{B}(\text{C}_6\text{F}_5)$, were not observable in the ^{19}F NMR spectrum (Figure 27) and thus unsurprisingly their resonances of 43.2 and 22.4 ppm respectively were not observable.²²⁶

The most downfield signal appeared at 86.7 ppm and was determined to be $\text{B}(\text{}^n\text{Bu})_3$.²²⁷ However, the signal was relatively broad and as $\text{B}(\text{C}_6\text{F}_5)(\text{alkyl})_2$ species are known to have ^{11}B NMR resonances between 80 and 90 ppm,²²⁸ the presence of these other species cannot be ruled out as they could be overlapped by the larger resonance characteristic of $\text{B}(\text{}^n\text{Bu})_3$.

Moreover, the most upfield signal in the spectrum was found at -13.03 ppm, which was indicative of a negatively charged borate species. This suggested the presence of a borate salt coupled to a lithium counterion, but the exact identity of this species could not be identified.

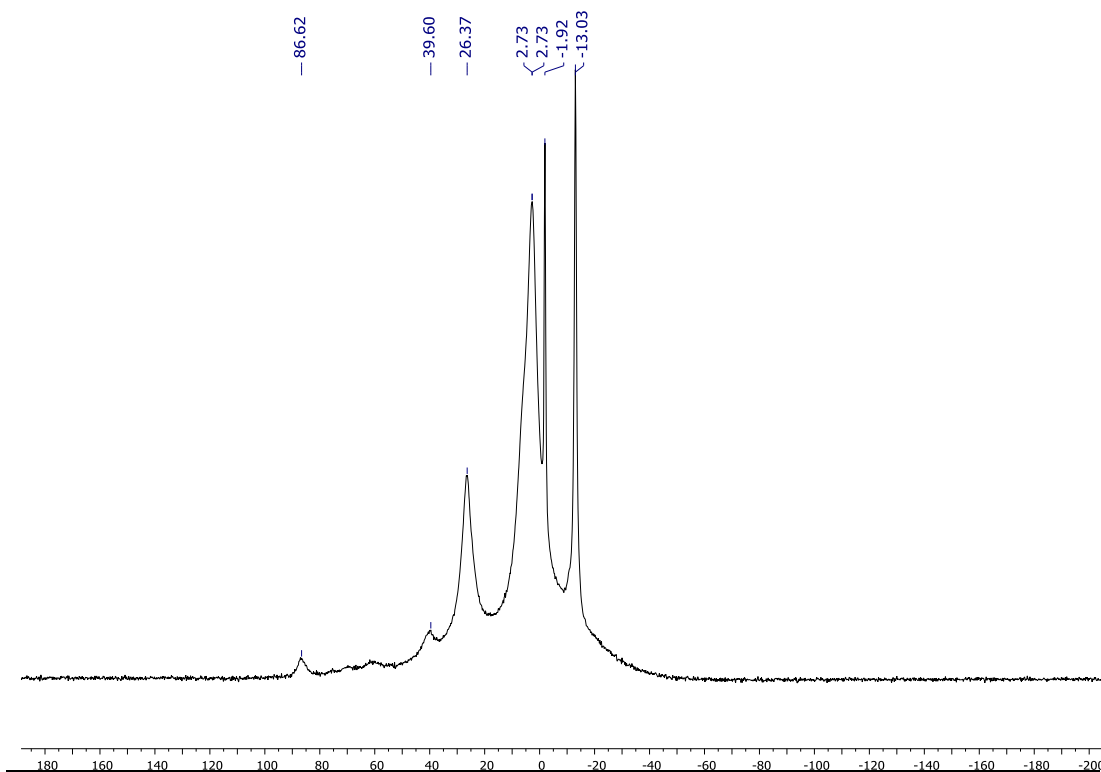


Figure 28 – ^{11}B NMR spectrum of typical failed $\text{B}(\text{C}_6\text{F}_5)_3$ synthesis.

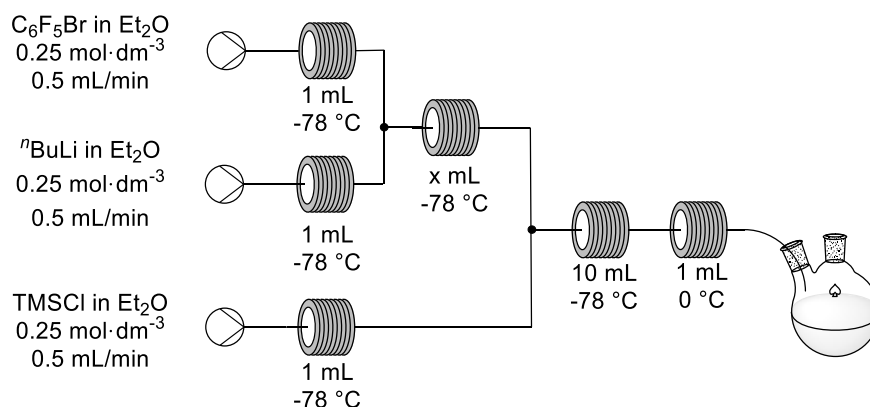
Whilst all the signals in the ^{19}F and ^{11}B NMR spectra could not be correctly identified, two important pieces of information were gleaned from these studies. First, it was determined that at some point in the reaction, the generated pentafluorophenyl(lithium) was decomposing into benzyne, which in turn participated in run-away reactions. Secondly, it was determined that the excess $^n\text{BuLi}$ was reacting with $\text{BF}_3 \cdot \text{Et}_2\text{O}$ to form $\text{B}(^n\text{Bu})_3$ and potentially mixed arylalkylborane species. With this knowledge in hand, it was decided to reinvestigate the lithiation procedure with stoichiometric $^n\text{BuLi}$ in an attempt to avoid these unwanted side-reactions.

3.5 Reinvestigation of lithiation procedure

To overcome the difficulties faced during the optimisation of the borylation step, the conditions of the initial reactor coil were reconsidered. The primary difference between the traditional batch preparation and the continuous flow adaptation was the equivalents of $^n\text{BuLi}$ per bromobenzene. Through the initial optimisation (Table 5) it was noted that stoichiometric combinations of $\text{C}_6\text{F}_5\text{Br}$ and $^n\text{BuLi}$ did not react to form the desired $\text{C}_6\text{F}_5\text{Li}$ in a 5 mL reactor coil. On the other hand, an excess of $^n\text{BuLi}$ was observed to be deleterious towards the optimisation of the second reactor step.

Therefore, the residence time of the reagents within the first reactor coil was re-evaluated (Table 9).

Table 9 – Reinvestigation of the lithiation step.



Run	Reactor coil volume x (mL)	Conversion by ¹⁹ F NMR spectroscopy (%)
1	5	<5
2	10	<5
3	15	<5

Unfortunately, there was no indication of C₆F₅TMS formation in any of the three experiments, with the ¹⁹F NMR spectra showing exclusively signals indicative of C₆F₅Br in all cases (Table 9, entries 1–3). Thus, it appeared that excess ⁿBuLi was required to promote the reaction under continuous flow conditions.

To elucidate further what was happening when excess ⁿBuLi was present in the reactant stream upon the addition of BF₃·Et₂O, a reaction was performed wherein the syringe pump that previously injected C₆F₅Br was replaced with a stream of pure Et₂O (Figure 29). It was speculated that any reaction between the two reagents would be responsible for the competing side reaction preventing B(C₆F₅)₃ synthesis.

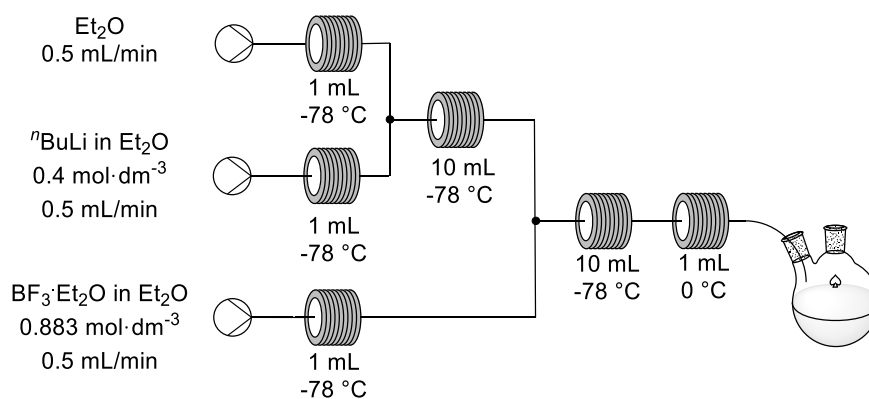


Figure 29 – Probe into the unwanted side-reaction preventing B(C₆F₅)₃ synthesis.

This reaction did not proceed smoothly. A white solid was visibly generated over a short period of time, which eventually blocked the tubing causing the syringe pumps to stall and leading to inconsistent flow rates. Despite this, a small amount of solution was collected in a Schlenk tube after one full residence time within the reactor. From an initial observation, the white solid was postulated to be lithium fluoride. This solid was completely insoluble in DCM, which further supported this hypothesis. From this observation it was suggested that the excess ⁿBuLi from the generation of C₆F₅Li was not innocent towards the electrophile in the second step of the reaction. Further analysis was taken by filtering the reaction mixture through a short cotton plug to remove the insoluble material. Multinuclear NMR spectroscopy and mass spectrometry was performed on this filtered sample.

The ¹⁹F NMR spectrum did not display any resonances. This result suggested that all the fluorine atoms present in BF₃·Et₂O had been transformed into something insoluble, presumably the lithium fluoride which had been filtered off prior to NMR analysis.

The ¹H NMR spectrum was also recorded and displayed resonances with multiplicity indicative of butyl protons. This confirmed that some reaction had indeed taken place; however, further information was required to fully elucidate what.

In the ¹¹B NMR spectrum (Figure 30), two signals were present, neither of which were at 0.0 ppm, a resonance which would have corresponded to the BF₃·Et₂O reagent. Importantly, both signals were present in all the experiments in Table 8, suggesting that the problems observed in the preparation of B(C₆F₅)₃ were a result of a competing side reaction between ⁿBuLi and the boron source. The most downfield signal appeared at 86.7 ppm and was determined to be B(ⁿBu)₃.²²⁷ This species was presumably formed through ligand exchange between the lithium and boron atoms.

A sharper resonance was also found at -18.4 ppm. Resonances in the ^{11}B NMR spectrum that are more upfield than 0 ppm are typically characteristic of negatively charged boron species. Notably, this signal was not observed in Figure 28, a typical ^{11}B NMR spectrum following an attempted but unsuccessful $\text{B}(\text{C}_6\text{F}_5)_3$ formation; however, in this spectrum a signal at -13.0 ppm is observable. It was thus theorised that this signal at -18.4 ppm was also reflective of a negatively charged boron species with a lithium counterion but with a different mixture of aryl and alkyl ligands on the boron atom.

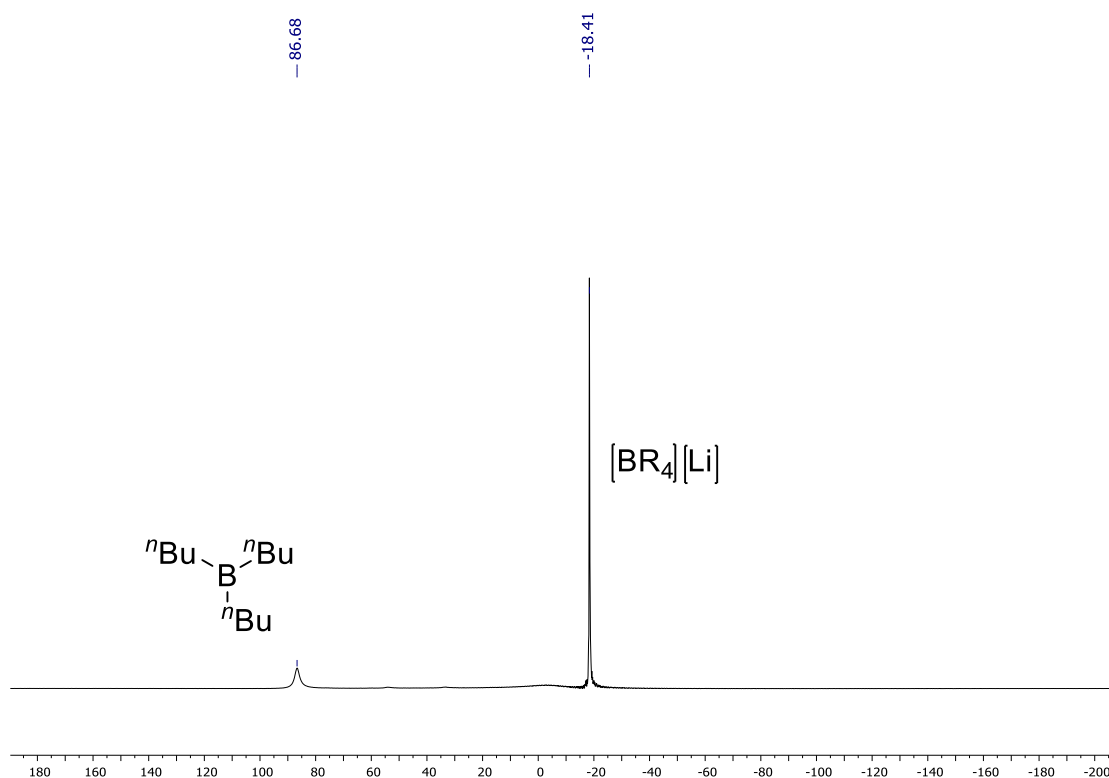


Figure 30 – ^{11}B NMR spectrum of reaction between $\text{BF}_3 \cdot \text{Et}_2\text{O}$ and $n\text{BuLi}$.

An EI (electrospray ionisation) mass spectrometry experiment was also run on the sample, which allowed further clarification on the identity of the negatively charged boron species (Figure 31). In the mass spectrum, the signal at $m/z = 375.3582$ was found to be indicative of a boron trimer, with each boron atom possessing two n Butyl ligands. Boron trimers of this type are highly unstable and this species was thus likely formed within the mass spectrometer by reaction of three $\text{B}(n\text{Bu})_2$ fragments.

Another prominent signal in the mass spectrum is that at $m/z = 250.3005$, which corresponds to the neutral diborane $(n\text{Bu})_2\text{B}-\text{B}(n\text{Bu})_2$. A literature search found that this species was not previously known, but similar tetra alkyl diboranes such as $(t\text{Bu})(t\text{BuCH}_2)\text{B}-\text{B}(t\text{Bu})(t\text{BuCH}_2)$ and $(i\text{Pr})_2\text{B}-\text{B}(i\text{Pr})_2$ corresponded to ^{11}B NMR signals

around 103–108 ppm.^{229,230} As there were no signals in the ^{11}B NMR spectrum (Figure 30) at such a downfield resonance, it is likely that this diborane was also formed in the mass spectrometer following the combination of two $\text{B}(n\text{Bu})_2$ fragments.

Whilst $\text{B}(n\text{Bu})_3$ itself was not observed, the observation of compounds which would have likely been formed *in situ* within the spectrometer following its fragmentation into $\text{B}(n\text{Bu})_2$ and subsequent recombination with other $\text{B}(n\text{Bu})_2$ fragments suggests that the formation of $\text{B}(n\text{Bu})_3$ was a likely side-reaction preventing the synthesis of $\text{B}(\text{C}_6\text{F}_5)_3$.

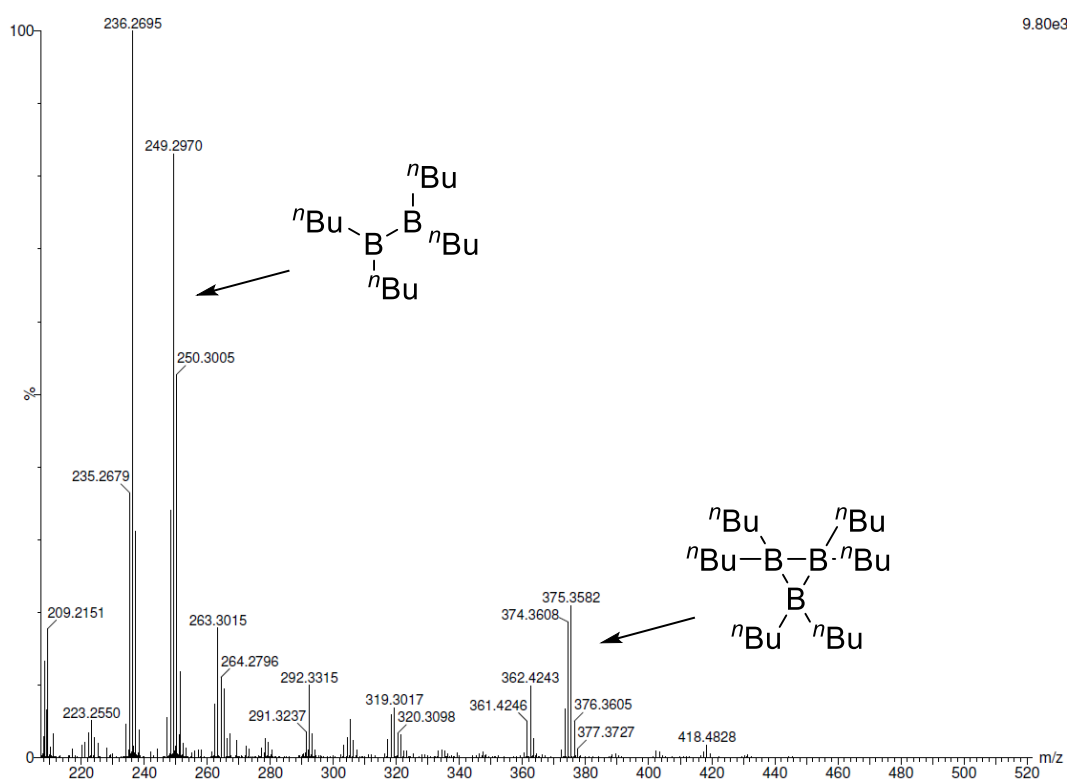
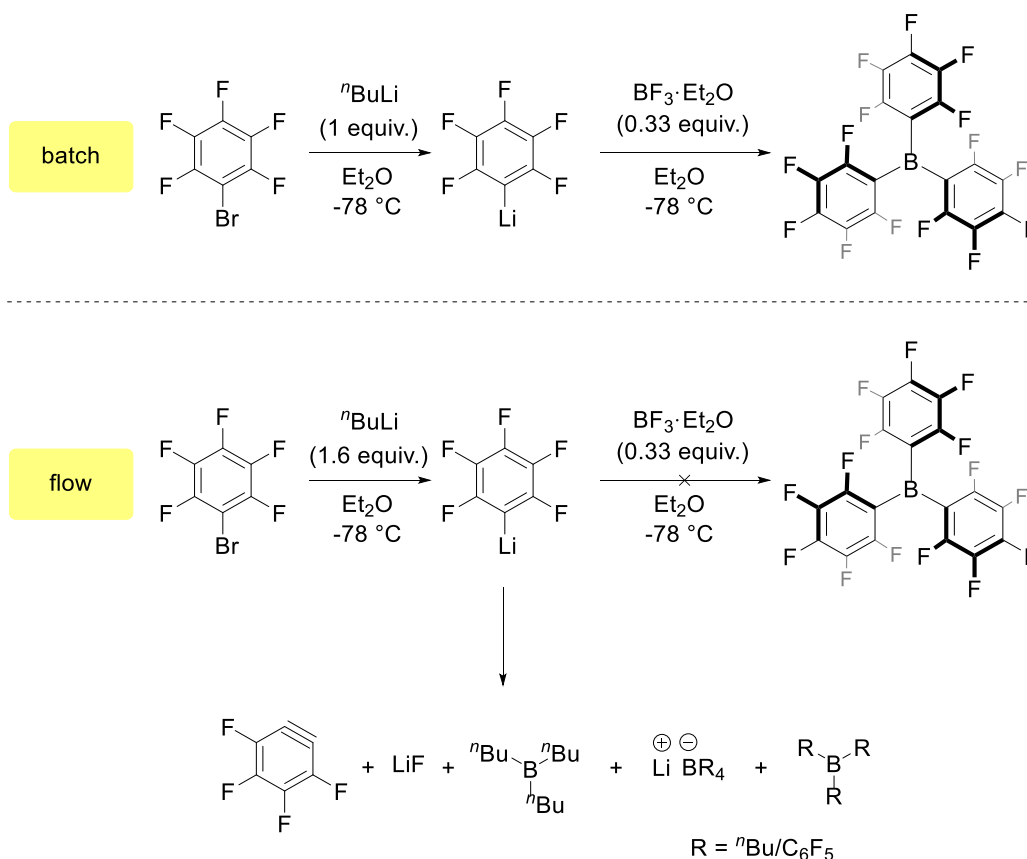


Figure 31 – Electrospray ionisation mass spectrum of reaction between $\text{BF}_3 \cdot \text{Et}_2\text{O}$ and $n\text{BuLi}$.

The result of this experiment suggested that there was indeed a competing reaction between the excess $n\text{BuLi}$ and $\text{BF}_3 \cdot \text{Et}_2\text{O}$, which occurred at a faster rate than the desired reaction of $\text{C}_6\text{F}_5\text{Li}$ with $\text{BF}_3 \cdot \text{Et}_2\text{O}$. At this juncture, the lithiation in flow project was abandoned to focus on more successful projects that are discussed in the following chapters.

3.6 Conclusions and outlook

In conclusion, the preparation of the Lewis acidic borane $B(C_6F_5)_3$ was attempted using continuous flow technologies, but unfortunately was not achieved. Whilst the highly unstable intermediate of the reaction, C_6F_5Li , could be safely generated and further transformed into C_6F_5TMS , it could not be readily transformed into the desired borane due to competing side reactions (Scheme 45).



Scheme 45 – Standard preparation of $B(C_6F_5)_3$ in batch and observed reactivity under continuous flow conditions.

A literature search into the use of a lithiation procedure for the preparation of boronic acids using flow chemistry found that an excess of $n\text{BuLi}$ was required for high yields.^{186,187,217–219} Clearly the excess $n\text{BuLi}$ did not have a detrimental effect upon the transference of one or two aryloxy groups in the same manner as it did upon the addition of three aryl moieties.

It was considered to re-optimize the procedure with only a small excess of $n\text{BuLi}$ (e.g. 1.1 equiv.); however, as any excess amount of $n\text{BuLi}$ would have promoted the side reactions, this would have resulted in a lower yield of $B(C_6F_5)_3$, making the use of flow chemistry redundant. In conclusion, although the initial idea of using flow chemistry

to enable the scale up of $B(C_6F_5)_3$ synthesis was promising, it was proven that the lithiation method is still not a viable route, and that the Grignard method is preferable in batch.

One final avenue for the synthesis of $B(C_6F_5)_3$ using continuous flow technologies that could be explored in the future is the use of isopropyl magnesium chloride and the Grignard method, instead of $nBuLi$ and the lithiation method used in this chapter. This was not explored due to time restraints but could offer an interesting continuation to the work described herein.

Chapter four – Hydroboration catalysis using conventional heating techniques

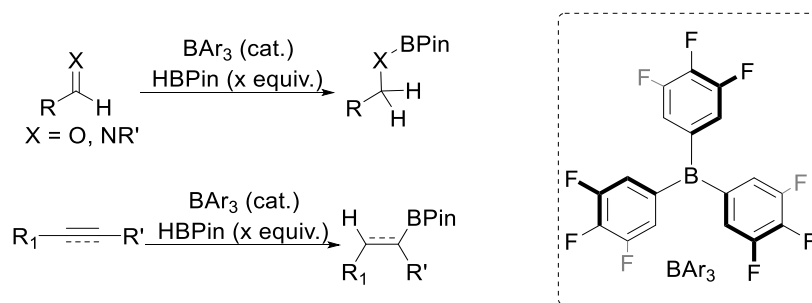
4.1 Aims of this chapter

This chapter investigates the efficiency of $B(3,4,5-F_3C_6H_2)_3$ and $Al(3,4,5-F_3C_6H_2)_3 \cdot Et_2O$ as catalysts and pre-catalysts for the hydroboration of unsaturated substrates. Oestreich proposed that strongly Lewis acidic triarylboranes without *ortho*-fluorine atoms on their aryl rings would make excellent hydroboration catalysts in the absence of a base, in cases where $B(C_6F_5)_3$, an example of a borane bearing these *ortho*-fluorine atoms, would be inactive.^{102,107} It was further suggested that these *ortho*-fluorine atoms precluded catalysis as they provided more steric exclusion than *ortho*-hydrogen atoms on the aryl rings.¹⁰⁷ Thus, as both $B(3,4,5-F_3C_6H_2)_3$ and $Al(3,4,5-F_3C_6H_2)_3 \cdot Et_2O$ were strong Lewis acids devoid of *ortho*-fluorine atoms around their aryl rings, it was hypothesised that they would act as efficient hydroboration catalysts.

This work began as an investigation into the use of $B(3,4,5-F_3C_6H_2)_3$ as an efficient hydroboration catalyst, but limitations were found in scope. Thus, the catalytic protocol was augmented with microwave irradiation (chapter five). Later investigations concerned the catalytic properties of the novel alane adduct $Al(3,4,5-F_3C_6H_2)_3 \cdot Et_2O$, to investigate if an increased Lewis acidity would impart a positive effect upon catalytic activity.

4.2 Hydroboration using tris(3,4,5-trifluorophenyl)borane as a catalyst

As discussed in chapter one, $B(3,4,5-F_3C_6H_2)_3$ had been previously synthesised by Melen and Oestreich; however, was employed in a solitary example of stoichiometric ketimine hydroboration.¹⁰⁷ To explore the borane's use as a catalyst, it was applied towards a large substrate scope (Scheme 46).

Scheme 46 – Overview of $B(3,4,5-F_3C_6H_2)_3$ -catalysed hydroboration.

4.2.1 Optimisation

The optimisation of the hydroboration procedure at room temperature was modelled on the hydroboration of acetophenone (Table 10). First, the hydroboration of acetophenone was attempted in the absence of catalyst (Table 10, entry 1). Satisfyingly, negligible conversion into the corresponding boronate ester was noted after 24 h. As $B(3,4,5-F_3C_6H_2)_3$ had already been targeted as a potential active catalyst following its stoichiometric application in the hydroboration transformation,¹⁰⁷ it was tested against a range of commercially available boranes such as BPh_3 and $BF_3 \cdot Et_2O$, along with the halogenated triarylboranes $B(C_6F_5)_3$ and $B(2,4,6-F_3C_6H_2)_3$ (Table 10, entries 2–6). When $B(3,4,5-F_3C_6H_2)_3$ was employed, quantitative conversion was observed after just one hour (Table 10, entry 2), designating it to be the best catalyst compared to the other boron-based catalysts which resulted in poor yields of the boronate ester after 24 h (3–27%).

Next, the conditions of the reaction were probed. In particular, the reaction was also found to be tolerant towards coordinating and non-coordinating solvents (Table 10, entries 7–8); however, $CDCl_3$ was chosen for the convenience of *in situ* monitoring through 1H NMR spectroscopy. A stoichiometric amount of HBPin was found to be deleterious to the conversion (Table 10, entry 9), thus a slight excess of the boron source was maintained throughout.

The catalyst loading was then increased to 5 mol% (Table 10, entry 10) but this did not significantly increase the rate of reaction, with quantitative conversion also recorded after one hour. Finally, HBPin was chosen as the boron source after 9-BBN failed to show reactivity after 24 hours (Table 10, entry 11).

Table 10 – Optimisation of $B(3,4,5-F_3C_6H_2)_3$ -catalysed hydroboration.

Run	Catalyst	Catalyst Loading (mol%)	Boron Source (equiv.)	Solvent	Time (h)	Conversion (%) ^[a]
1	No catalyst	-	HBPIn (1.1)	CDCl ₃	24	0
2	$B(3,4,5-F_3C_6H_2)_3$	2	HBPIn (1.1)	CDCl ₃	1	>95
3	BF ₃ ·Et ₂ O	2	HBPIn (1.1)	CDCl ₃	24	18
4	BPh ₃	2	HBPIn (1.1)	CDCl ₃	24	27
5	B(C ₆ F ₅) ₃	2	HBPIn (1.1)	CDCl ₃	24	3
6	$B(2,4,6-F_3C_6H_2)_3$	2	HBPIn (1.1)	CDCl ₃	24	21
7	$B(3,4,5-F_3C_6H_2)_3$	2	HBPIn (1.1)	Et ₂ O	2	>95
8	$B(3,4,5-F_3C_6H_2)_3$	2	HBPIn (1.1)	Toluene	16	>95
9	$B(3,4,5-F_3C_6H_2)_3$	2	HBPIn (1.0)	CDCl ₃	24	79
10	$B(3,4,5-F_3C_6H_2)_3$	5	HBPIn (1.1)	CDCl ₃	1	>95
11	$B(3,4,5-F_3C_6H_2)_3$	2	H-9-BBN (1.1)	CDCl ₃	24	0

Acetophenone (0.2 mmol, 24 mg). ^[a] Conversion determined by ¹H NMR spectroscopy with a mesitylene standard (0.1 mmol, 14 μL).

4.2.2 Scope of reaction

After establishing the optimal conditions for the catalytic transformation, a wide scope of aldehydes, ketones, and imines, bearing electron-donating, neutral, or electron-withdrawing groups were studied to explore the aptitude of the borane catalyst.^{viii} The reactions were set up inside a glove box and allowed to react at room temperature. The progression of the reaction was monitored by *in situ* ¹H NMR spectroscopy. Once conversion into the boronate ester products **1a–t** was observed, the corresponding alcohols or amines **2a–s** were yielded upon hydrolysis, followed by purification by flash column chromatography (Figure 32).

Aldehydes were first investigated, with both electron-withdrawing and electron-donating groups being tolerated by the borane catalyst. Full conversion into the

^{viii} Scope of hydroboration reactions was assisted by Masters student Lukas Gierlichs.

appropriate boronate esters was observed in less than 24 hours, and the corresponding alcohols **2a–e** were isolated in excellent yields (87–98%). Ketones were hydroborated at a faster rate than their aldehyde counterparts, with full conversion into the boronate esters noted within 2 hours. Also, the desired secondary alcohols **2f–i** were isolated in excellent yields (89–96%). Conversely, B(3,4,5-F₃C₆H₂)₃ was less active towards the sterically demanding substrate benzophenone, with 156 hours required for hydroboration, leading to the isolation of **2j** in 84% yield.

Aldimines with variation on both sides of the unsaturated heteronuclear bond were readily hydroborated and reduced into their respective amines **2k–s**. Quantitative conversions were achieved within 60 hours, with isolated yields recorded of 86–96%. One substrate, *N*-benzyl-1-phenylmethanimine, took 156 hours to completely convert into the intermediate boronate ester **1s**; however, the corresponding amine **2s** was still isolated in 96% yield. One ketimine, *N*-1-diphenylethan-1-imine, was also investigated, and was found to quantitatively form the appropriate boronate ester **1t** after 24 hours. Furthermore, **1t** was observed to be stable towards hydrolysis following a basic work-up and was isolated in lieu of the corresponding amine.

The reactivity of B(3,4,5-F₃C₆H₂)₃ gave mixed results; certain substrates responded excellently to the catalyst, whilst others were less responsive towards catalysis under room temperature conditions. In general, substrates containing electron-withdrawing functionalities underwent hydroboration more rapidly than those containing electron-donating functionalities, indicating that an electron deficient unsaturated bond was favourable towards rapid catalysis. This suggested that the HBPIn was more able to add across the substrate's unsaturated bond when it was already weakened by electron withdrawing groups on the adjacent aryl moiety.

Moreover, carbonyls were more readily reduced than imines, which suggested that the catalyst was more active towards more polarised unsaturated bonds. This inferred that the coordination of the borane to the oxygen of carbonyls was easier than the coordination of the borane to the nitrogen of imines. Presumably, this was a result of both the steric hinderance of the imine's nitrogen substituent and the increased electronegativity of the oxygen atom.

A 70 °C reaction was then employed to reduce the reaction time for less reactive substrates and to probe the reactivity of the catalyst at elevated temperature. As certain substrates appeared to react rapidly at room temperature, efforts were only focused on reactions that were observed to take longer than one hour under the previously optimised conditions (Figure 32).

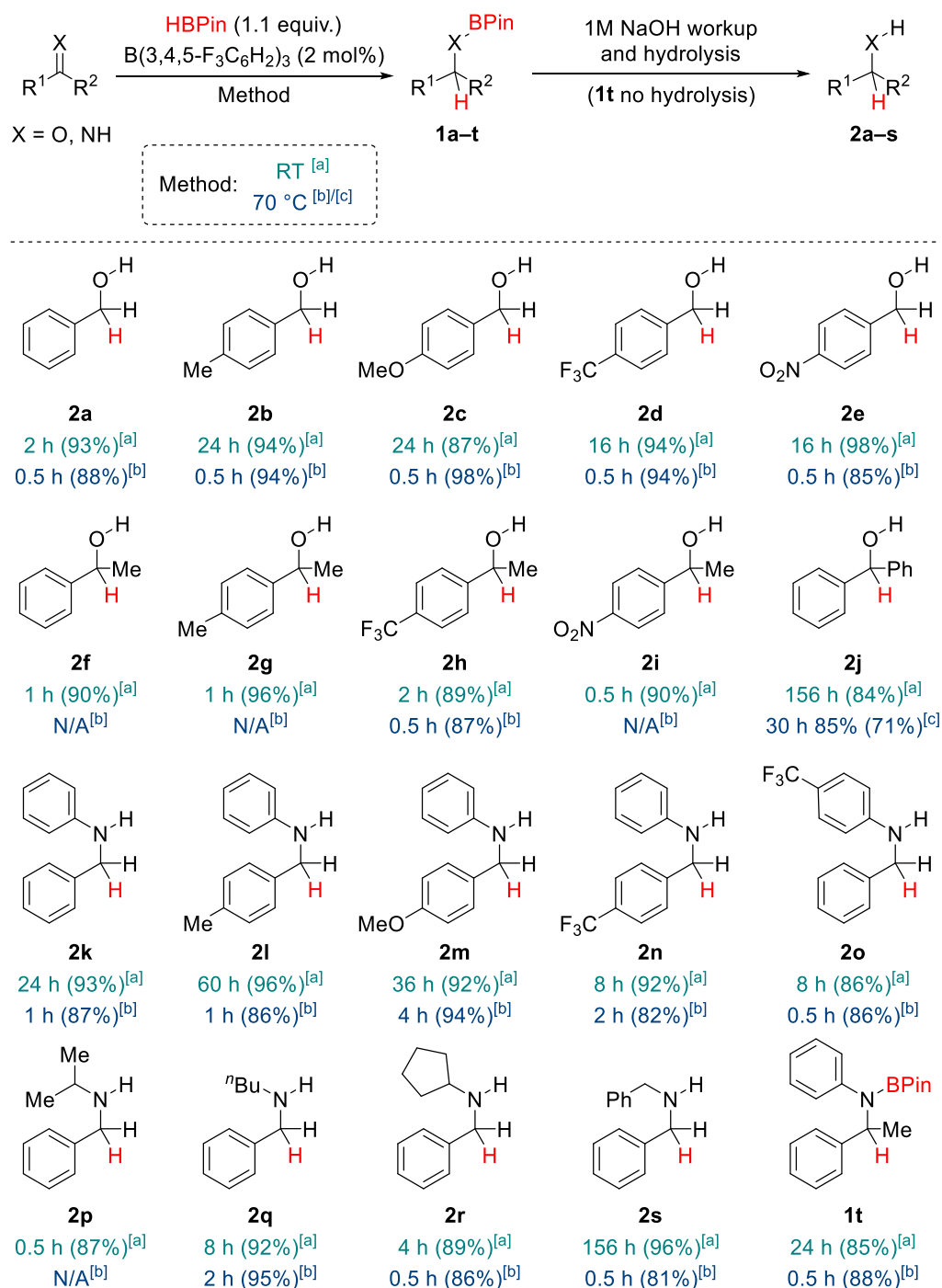


Figure 32 – Scope of borane-catalysed hydroboration using conventional heating techniques. Conversions determined by ¹H NMR spectroscopy. Isolated yields given in parentheses. ^[a] Time taken to reach quantitative conversion at room temperature. ^[b] Time taken to reach quantitative conversion at 70 °C. ^[c] Achieved maximum conversion of 85% at 70 °C and did not increase past this value.

A significant reduction in reaction time was observed upon heating the samples to 70 °C compared to when reactions were performed under room temperature conditions. The general reactivity trends for reactions at 70 °C remained the same for those at room temperature, with more rapid reactivity observed for carbonyls

compared to imines, and for substrates containing electron withdrawing functionalities compared to electron donating functionalities.

The quantitative conversion of aldehydes into their corresponding boronate esters **1a–e** was observed within 0.5 h and following hydrolysis and isolation, this formed alcohols **2a–e** in 85–98% isolated yield. Ketone 1-(4-(trifluoromethyl)-phenyl)ethan-1-one also showed quantitative conversion to **1h** within 0.5 h giving secondary alcohol **2h** in 87% isolated yield. Benzophenone was still slow to react due to the steric shielding around the carbonyl centre, and plateaued at 86% conversion to **1j** after 30 h. The desired product **2j** was isolated in 71% yield upon hydrolysis.

Secondary amines **2k–s** were also prepared quantitatively, within 0.5–4 h instead of up to 60 h. Additionally, *N*,1-diphenylethan-1-imine was also found to react faster at 70 °C, with quantitative conversion to **1s** after 0.5 h rather than the 24 h required at room temperature.

Homonuclear unsaturated bonds were then probed under the optimised conditions (Figure 33). Despite the satisfactory catalysis observed for carbonyls and imines, no reactivity was observed after 24 hours for any of the investigated alkenes or alkynes, demonstrating the limitation of $B(3,4,5-F_3C_6H_2)_3$ under conventional heating techniques. A test reaction with an increased catalytic loading concerning the reaction of phenyl acetylene with HBPi_n yielded full hydroboration after four days, proving the reaction to be possible. Therefore, in an attempt to promote reactivity with the rest of these substrates, the implementation of microwave irradiation was investigated to fully exploit the catalytic potential of the borane (chapter five).

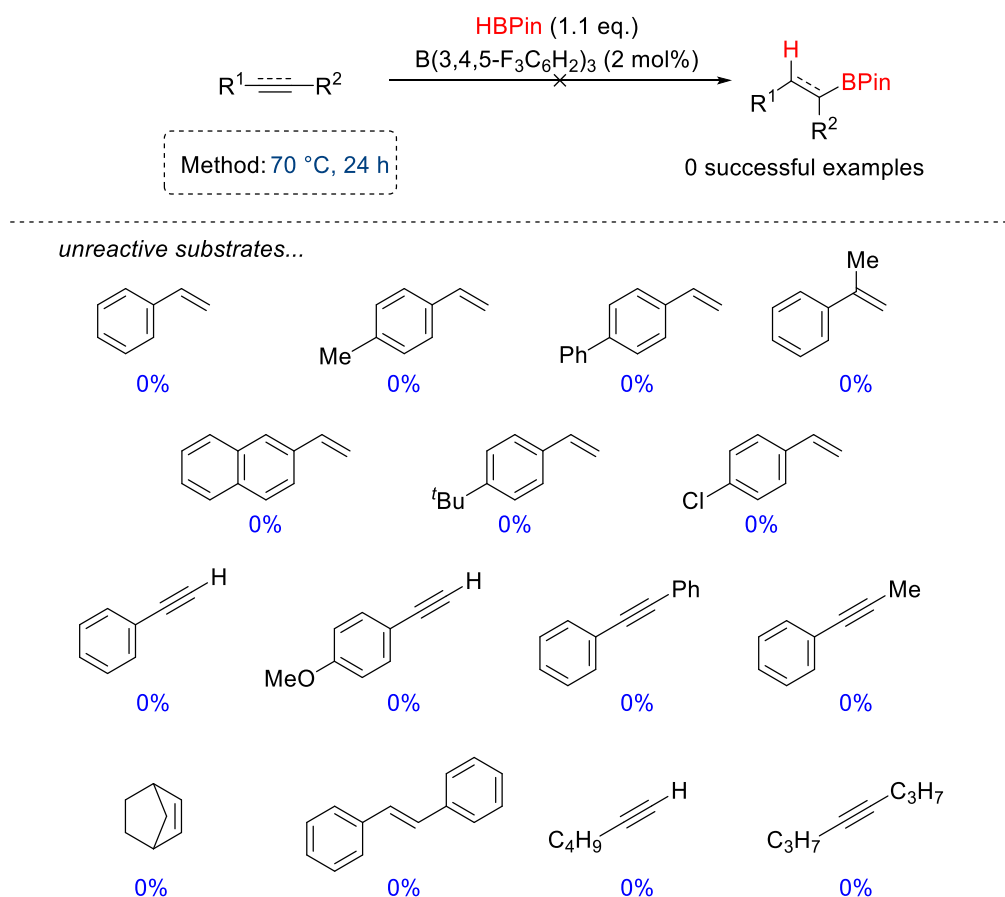


Figure 33 – Unsuccessful series of borane-catalysed hydroboration reactions using conventional heating techniques. Conversions determined from ^1H NMR spectroscopy.

4.2.3 Mechanism of hydroboration at room temperature

The initial consideration regarding the hydroboration reaction mechanism was the identity of the catalyst. Literature precedents has reported that many boron-based hydroboration ‘catalysts’ are in fact pre-catalysts, often forming a borohydride through ligand metathesis with HBPin, or even forming BH_3 *in situ*.^{102,110} To confirm the identity of the catalyst in the reaction as either the triarylborane or an *in situ* generated borohydride species, a stoichiometric mixture of HBPin with $\text{B(3,4,5-F}_3\text{C}_6\text{H}_2)_3$ was monitored by *in situ* ^{11}B NMR spectroscopy at room temperature (Figure 34).

Evidence of redistribution would have been immediately apparent through the presence of signals other than a broad singlet at 64.5 ppm and a doublet at 28.2 ppm, indicative of $\text{B(3,4,5-F}_3\text{C}_6\text{H}_2)_3$ and HBPin, respectively. As depicted in Figure 34, no metathesis was observed after 24 hours. Addition of acetophenone to this mixture resulted in immediate hydroboration at room temperature. This was evidenced by

depletion of the doublet at 28.2 ppm (HBPIn) and generation of a new singlet at 22.2 ppm (formed boronate ester).

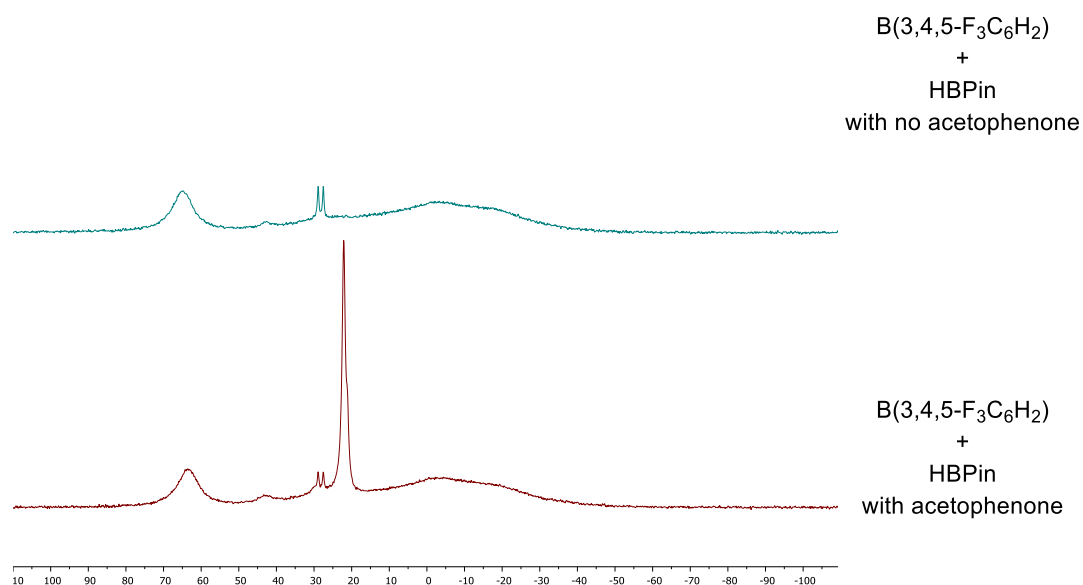
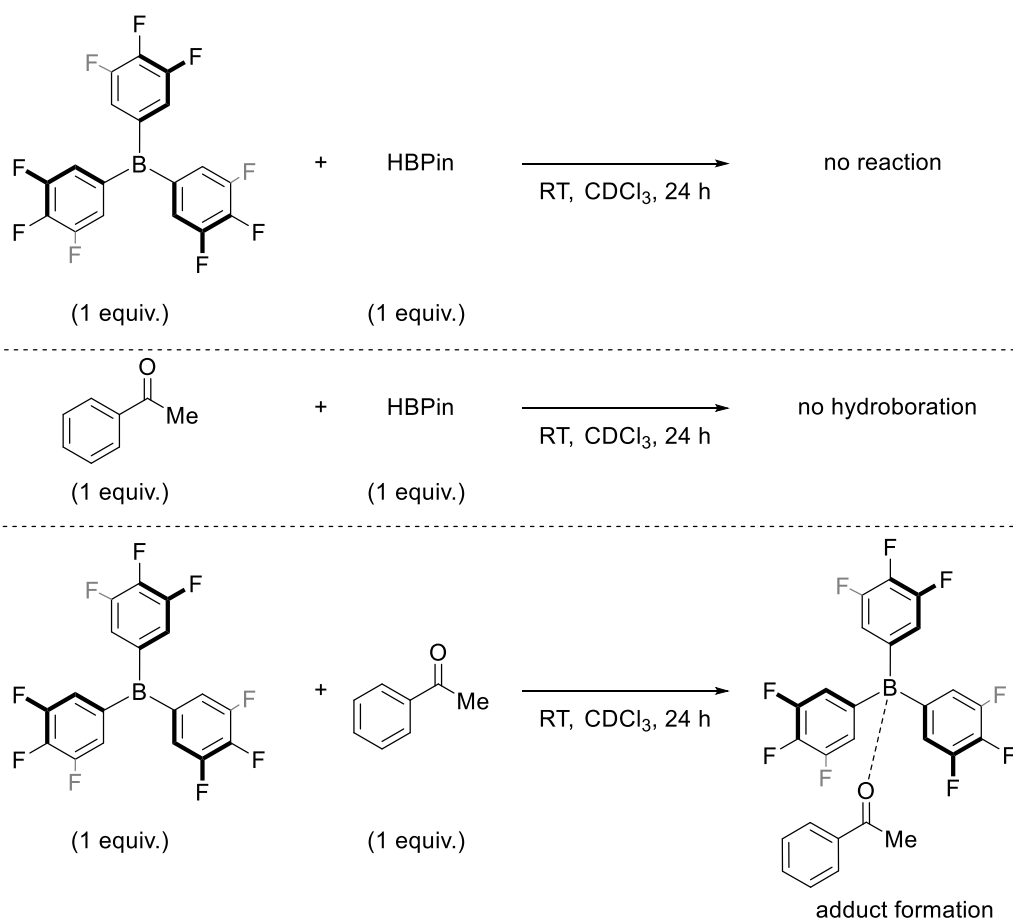


Figure 34 – ¹¹B NMR probes into the B(3,4,5-F₃C₆H₂)₃-catalysed hydroboration mechanism. Top – stoichiometric mixture of B(3,4,5-F₃C₆H₂)₃ with HBPIn left for 24 hours at room temperature. Bottom – stoichiometric mixture of B(3,4,5-F₃C₆H₂)₃ with HBPIn and acetophenone left for 30 minutes at room temperature.

Upon confirmation that the borane catalyst remained stable under exposure to HBPIn, further probes were made to elucidate the mechanism of the hydroboration reaction. Initially, three sets of stoichiometric reactions were set up, each of which missing a core component of the catalytic hydroboration reaction: acetophenone, HBPIn, or the B(3,4,5-F₃C₆H₂)₃ catalyst (Scheme 47).

As already confirmed, a stoichiometric mixture of the borane and HBPIn resulted in no ligand metathesis, confirming that at room temperature the B(3,4,5-F₃C₆H₂)₃ catalyst remained intact. A stoichiometric mixture of acetophenone and HBPIn was also monitored; however, negligible hydroboration was observed to occur in the absence of catalyst. Observation of a stoichiometric mixture of B(3,4,5-F₃C₆H₂)₃ and acetophenone garnered interest, as ¹H NMR probes suggested the formation of an adduct between the two compounds. This was evidenced through a shift of the acetophenone's methyl group from 2.50 ppm to 2.19 ppm. This upfield shift suggested a loss of electron density, presumably because the Lewis basic carbonyl functionality was now donating electron density into the borane's vacant *p*-orbital.

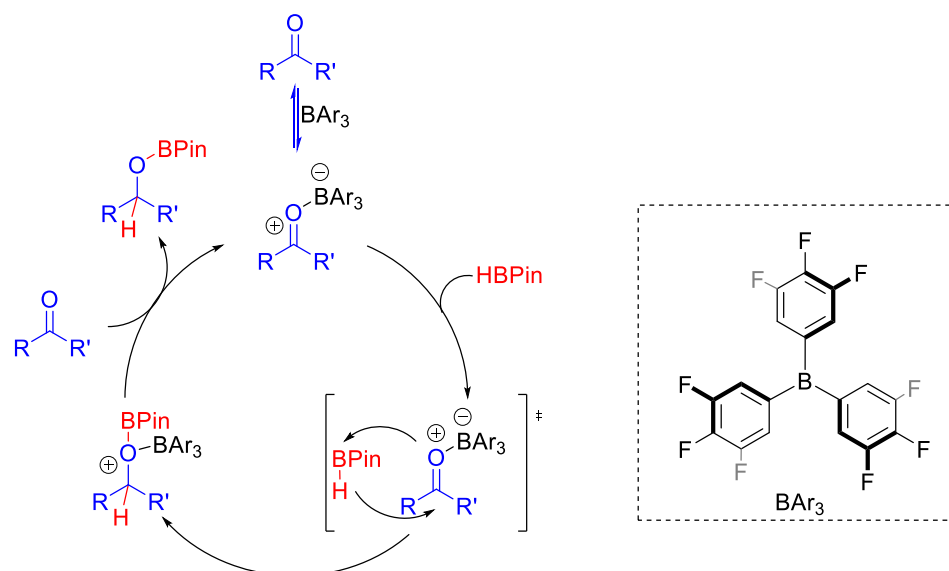


Scheme 47 – Stoichiometric probes into the $B(3,4,5-F_3C_6H_2)_3$ -catalysed hydroboration mechanism at room temperature.

Upon addition of HBPIn to the ketone-borane adduct, multinuclear NMR probes observed the presence of the boronate ester product. In the ^{11}B NMR spectrum, the doublet at 28.2 ppm indicative of HBPIn decreased in intensity, whilst a new signal at 22.2 ppm developed. In the 1H NMR spectrum, the progress of the reaction could be followed through loss of a signal at 2.50 ppm (corresponding to the acetophenone's methyl group), and a simultaneous appearance of a novel quartet and doublet (corresponding to the methyl group of the boronate ester and its new proton from reduction).

From these observations, a mechanism was proposed (Scheme 48). Herein, $B(3,4,5-F_3C_6H_2)_3$ was observed to form an adduct with the Lewis basic substrate. This interaction lowered the LUMO of the imine, making it more susceptible to reduction by HBPIn. Following hydroboration, the adduct between the boronate ester and the borane was made significantly weaker due to the decreased basicity of the boronate ester. Thus, the borane catalyst dissociated from the boronate ester to coordinate to a stronger base, in this case an unreduced substrate, closing the catalytic cycle.

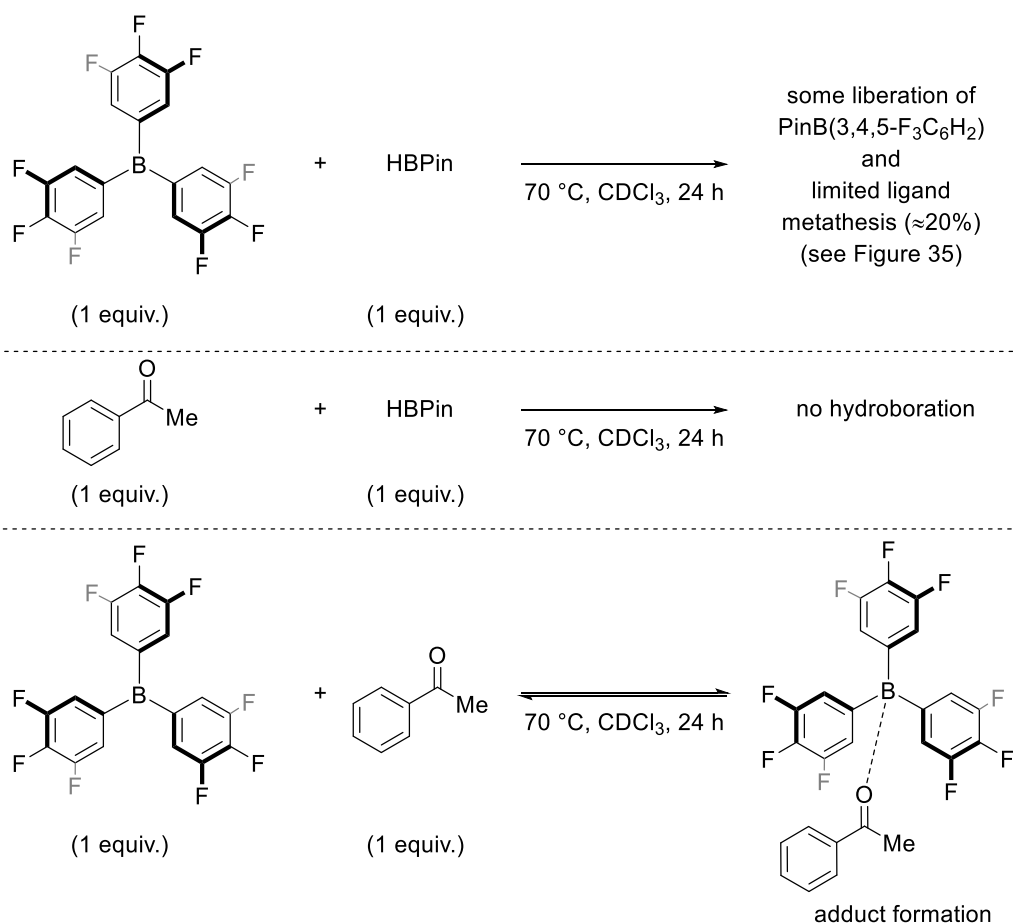
These observations concur with those proposed by Oestreich in the $B(3,5-(CF_3)_2C_6H_3)_3$ -catalysed hydroboration of ketimines.¹⁰⁷ Indeed, there was no evidence to suggest that any *in situ* generated alkoxide species had reacted with HBPIn to form trialkoxyborohydrides in line with the Clarke hydroboration mechanism.²³¹



Scheme 48 – Proposed mechanism for $B(3,4,5-F_3C_6H_2)_3$ -catalysed hydroboration at room temperature.

4.2.4 Mechanism of hydroboration at 70 °C

Multinuclear NMR experiments were performed to investigate whether the catalytic mechanism remained the same regardless of reaction temperature (Scheme 49). Initial experimental evidence confirmed that no hydroboration had occurred in the absence of a catalyst, confirming the necessity of the $B(3,4,5-F_3C_6H_2)_3$ catalyst even at elevated temperatures. Moreover, evidence that an adduct was generated between the borane and acetophenone before the hydroboration occurred was shown through a 1H NMR spectrum *via* the presence of a singlet at 2.19 ppm, mirroring what had been observed during the room temperature mechanistic studies. Notably, at 70 °C it appeared that this adduct existed in equilibrium between the free species, as the methyl signal indicative of free acetophenone (2.50 ppm) was also present in the 1H NMR spectrum. The rapid association and dissociation of the two molecules can be attributed to the elevated temperature of the reaction.



Scheme 49 – Stoichiometric probes into the B(3,4,5-F₃C₆H₂)₃-catalysed hydroboration mechanism at 70 °C.

When a stoichiometric mixture of B(3,4,5-F₃C₆H₂)₃ and HBPin was left to heat for 24 hours, evidence of ligand metathesis was observed. Analysis of the ¹⁹F NMR spectrum suggested that as much as 20% of the borane had undergone some form of ligand metathesis through loss of PinB(3,4,5-F₃C₆H₂) (Figure 35). This spectrum presented coupling patterns that were indicative of the 3,4,5-F₃C₆H₂ unit, suggesting that the aryl ring had remained intact and that the new fluorine resonances were not a result of aryl ring decomposition. The main signals in the spectrum were indicative of the borane, whilst the second largest set of signals were indicative of PinB(3,4,5-F₃C₆H₂) (literature values: δ/ppm : = -136.0 (d), -157.1 (t)).²³² Other smaller signals were also observed, which were attributed to the formation of hydroborane species.

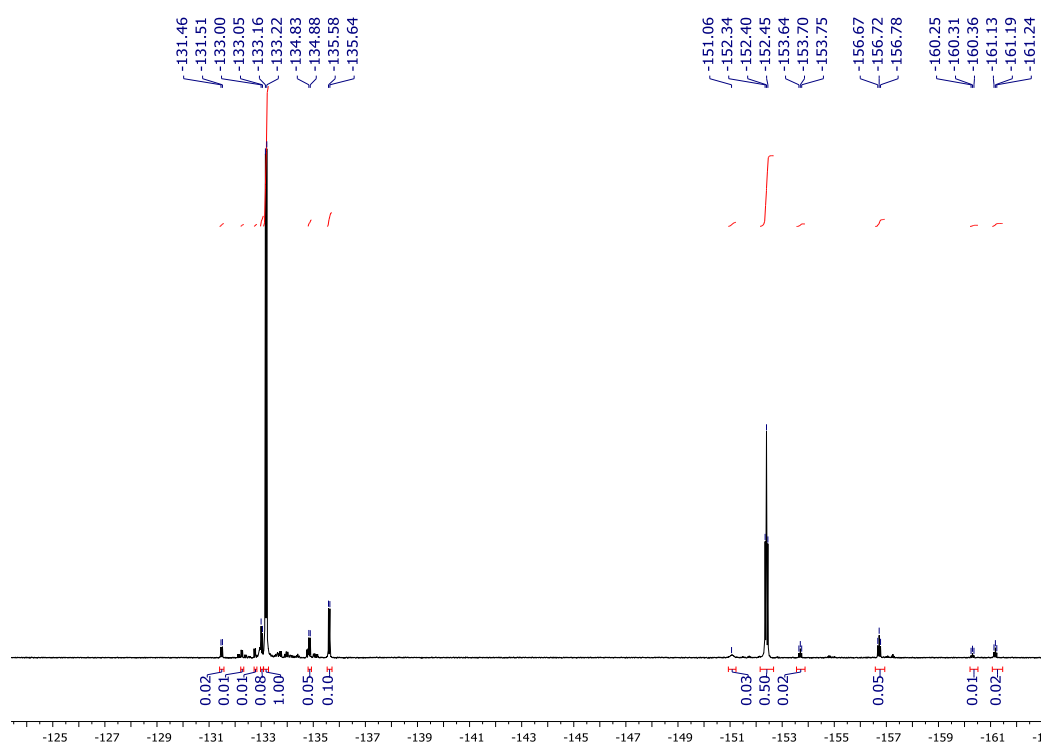
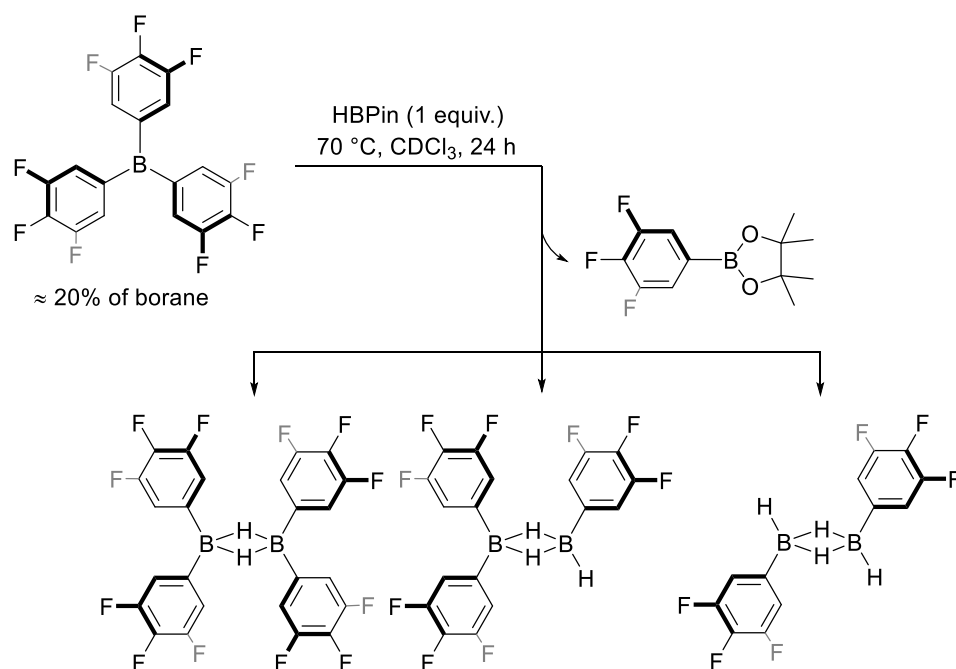


Figure 35 – ^{19}F NMR spectrum of a stoichiometric mixture of $\text{B}(3,4,5\text{-F}_3\text{C}_6\text{H}_2)_3$ and HBPIn; evidence of ligand redistribution forming catalytically active hydroboranes.

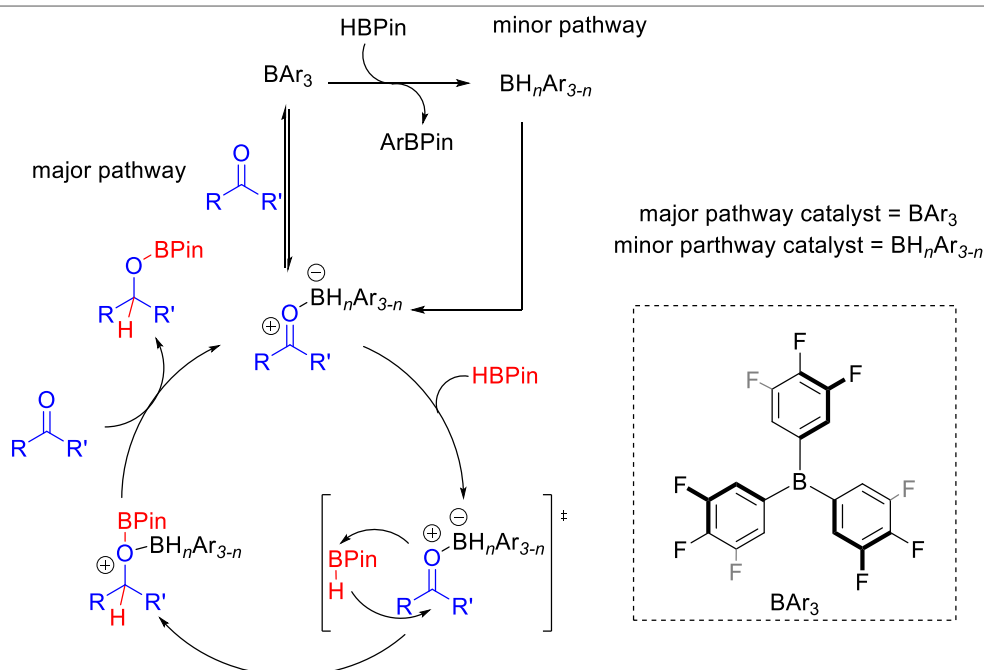
The ^{11}B NMR spectrum also revealed some small resonances between 16–30 ppm along with the HBPIn and borane reagents; however, these signals indicative of hydroborane species barely rose above the baseline, hence could not be individually assigned. The observations from the ^{11}B and ^{19}F NMR spectra bore a striking resemblance to the mechanism of alkene hydroboration promoted by a $\text{B}(3,5\text{-(CF}_3)_2\text{C}_6\text{H}_3)_3$ pre-catalyst, as proposed by Oestreich.¹⁰² Upon exposure of $\text{B}(3,5\text{-(CF}_3)_2\text{C}_6\text{H}_3)_3$ to HBPIn, it was known that ligand metathesis would occur, resulting in loss of $(3,5\text{-(CF}_3)_2\text{C}_6\text{H}_3)\text{BPIn}$ to form a range of catalytically active hydroboranes.¹⁰²

Therefore, it was suggested that σ -bond metathesis between the $\text{B}(3,4,5\text{-F}_3\text{C}_6\text{H}_2)_3$ and HBPIn had resulted in the formation of the same type of hydroborane species *via* loss of $(3,4,5\text{-F}_3\text{C}_6\text{H}_2)\text{BPIn}$ (Scheme 50). Thus, whilst most of the hydroboration catalysis was performed by the intact borane $\text{B}(3,4,5\text{-F}_3\text{C}_6\text{H}_2)_3$ at elevated temperatures, the possibility of other catalytically active boron-based species cannot be ruled out. The hydroborane species are proposed to be similar to those detected by Oestreich,¹⁰² with the sole difference being the fluorine substitution pattern around the aryl ring.



Scheme 50 – Suggested products from ligand metathesis between $\text{B}(\text{3,4,5-F}_3\text{C}_6\text{H}_2)_3$ and HBPIn at 70 °C.

As no other products were observed other than the boronate ester, it was confirmed that the identity of the catalyst did not affect the overall hydroboration reaction, with both hydroboranes and triarylborane species acting in a similar way. Thus, it was proposed that both the borane and the hydroborane products acted as Lewis acid catalysts towards the substrate by lowering the LUMO of acetophenone, making it more susceptible to σ -bond metathesis with HBPIn. A modified catalytic cycle was therefore proposed, which combines the elucidated mechanism of $\text{B}(\text{3,4,5-F}_3\text{C}_6\text{H}_2)_3$ with the inclusion of the formation and activity of the hydroborane species (Scheme 51).

Scheme 51 – Proposed mechanism for $B(3,4,5-F_3C_6H_2)_3$ -catalysed hydroboration at 70 °C.

4.3 Hydroboration using tris(3,4,5-trifluorophenyl)alane etherate as a catalyst

Upon the isolation of the novel alane adduct $Al(3,4,5-F_3C_6H_2)_3 \cdot OEt_2$, a short investigation was carried out to probe its potential as a catalyst. Due to previous study into the use of the alane's borane congener, $B(3,4,5-F_3C_6H_2)_3$, as a hydroboration catalyst, the first example of triarylalane assisted hydroboration was explored to compare the performance of the boron and aluminium based Lewis acids.

4.3.1 Optimisation

For the catalysis optimisation, the hydroboration of acetophenone by HBPIn was performed (Table 11). As expected, the reaction did not occur in the absence of a catalyst at room temperature (Table 11, entry 1). Upon introduction of $Al(3,4,5-F_3C_6H_2)_3 \cdot OEt_2$ at 5 mol% and 10 mol% respectively, negligible conversion to the corresponding boronate ester was observed (Table 11, entries 2–3). At this stage it was theorised that the ether was unable to dissociate from the alane under ambient conditions, precluding catalysis. In response, the temperature of the reaction medium was increased to 70 °C. At this temperature there was still negligible reduction in the absence of catalyst (Table 11, entry 4), but 68% NMR yield was observed after 24 h

in the presence of $\text{Al}(\text{3,4,5-F}_3\text{C}_6\text{H}_2)_3\cdot\text{OEt}_2$ at 5 mol% catalyst loading (Table 11, entry 5). A further improvement in reaction speed was noted when 10 mol% catalyst loading was employed, with quantitative conversion into the boronate ester after 6 h (Table 11, entry 6). When the reaction solvent was switched to benzene- d^6 , the reaction was again found to undergo quantitative hydroboration after 6 h (Table 11, entry 7). Furthermore, reducing the HBPIn to stoichiometric amounts gave a deleterious effect, resulting in only 84% conversion after 24 hours (Table 11, entry 8). Other boron sources such as HBCat and H-9-BBN were also probed; however, the alane was unreactive towards their reaction with acetophenone (Table 11, entries 9–10). Notably, the optimised conditions used for $\text{B}(\text{3,4,5-F}_3\text{C}_6\text{H}_2)_3$ -catalysed hydroboration promoted no reactivity when $\text{Al}(\text{3,4,5-F}_3\text{C}_6\text{H}_2)_3\cdot\text{OEt}_2$ was employed as a catalyst (Table 11, entry 11).

Table 11 – Optimisation of alane-catalysed hydroboration.

Entry	Catalyst loading (mol%)	Temperature (°C)	Boron source (equiv.)	Yield ^[a]	Time (h)
1	0	25	HBPIn (1.2)	<5%	24
2	5	25	HBPIn (1.2)	<5%	24
3	10	25	HBPIn (1.2)	<5%	24
4	0	70	HBPIn (1.2)	<5%	24
5	5	70	HBPIn (1.2)	68%	24
6	10	70	HBPIn (1.2)	>95%	6
7 ^[b]	10	70	HBPIn (1.2)	>95%	6
8	10	70	HBPIn (1.0)	85%	24
9	10	70	HBCat (1.2)	<5%	24
10	10	70	H-9-BBN (1.2)	<5%	24
11 ^[c]	2	25	HBPIn (1.1)	<5%	24

Acetophenone (0.2 mmol, 24 mg). ^[a] Conversion determined by ¹H NMR spectroscopy with internal mesitylene standard (0.1 mmol, 14 mL). ^[b] Benzene- d^6 solvent instead of CDCl_3 . ^[c] optimised conditions for $\text{B}(\text{3,4,5-F}_3\text{C}_6\text{H}_2)_3$ -catalysed hydroboration.

4.3.2 Scope

With optimised conditions in hand, a substrate scope was explored to determine the applicability of $\text{Al}(\text{3,4,5-F}_3\text{C}_6\text{H}_2)_3\cdot\text{OEt}_2$ as a hydroboration catalyst (Figure 36). As with the borane-catalysed hydroboration reactions, the reactions were set up inside a glove box and monitored through *in situ* ^1H NMR spectroscopy. Once >95% conversion into the boronate ester products was observed, a basic workup was performed to remove the catalyst. In the presence of aldehydes, ketones, and imines, the hydrolysis led to the reduction of the substrates into their respective alcohols and amines, and the products were further purified by flash column chromatography.

First, aldehydes were explored, with little variance in the activity of the catalyst for electron-donating, electron-withdrawing, and bulky substrates, leading to rapid conversion into the corresponding boronate esters within 2 hours in all cases. The resultant alcohols were isolated in 87–97% yield. Ketones and aldimines with the same structural features were slower to react under the optimised conditions, yet quantitative conversions were observed within 24 hours for ketones and 30 hours for aldimines, with isolated yields of 75–94%.

Further to this, alkenes and alkynes were investigated. The resultant boronate esters were formed exclusively as the *anti*-Markovnikov products, which were isolated in good to excellent yields and were found to be stable towards hydrolysis. Terminal alkynes performed well, with quantitative conversion to **4m–4p** noted within 48 hours. Following purification **4m–4p** were isolated in 68–94% yield. Conversely, no hydroboration was observed for the internal alkynes diphenylacetylene and 1-phenyl-1-propyne, likely due to the increased steric hindrance around the $\text{C}\equiv\text{C}$ triple bond.

Terminal alkenes also performed well, with full conversion of styrene derivatives into **4q–4t** within 48 hours. Following purification **4q–4t** were isolated in 73–91% yield. Conversely, 1,1-substituted alkenes were less tolerated, with only alpha-methyl styrene undergoing hydroboration. Alkenes possessing more steric bulk such as trans-stilbene and 1,1-diphenylethylene were unreactive under the conditions tested.

Whilst $\text{Al}(\text{3,4,5-F}_3\text{C}_6\text{H}_2)_3\cdot\text{OEt}_2$ was able to catalyse the hydroboration of a more varied scope of substrates than its boron-based analogue, it was noticeably slower at doing so, requiring five times the catalytic loading for efficient hydroboration to occur.

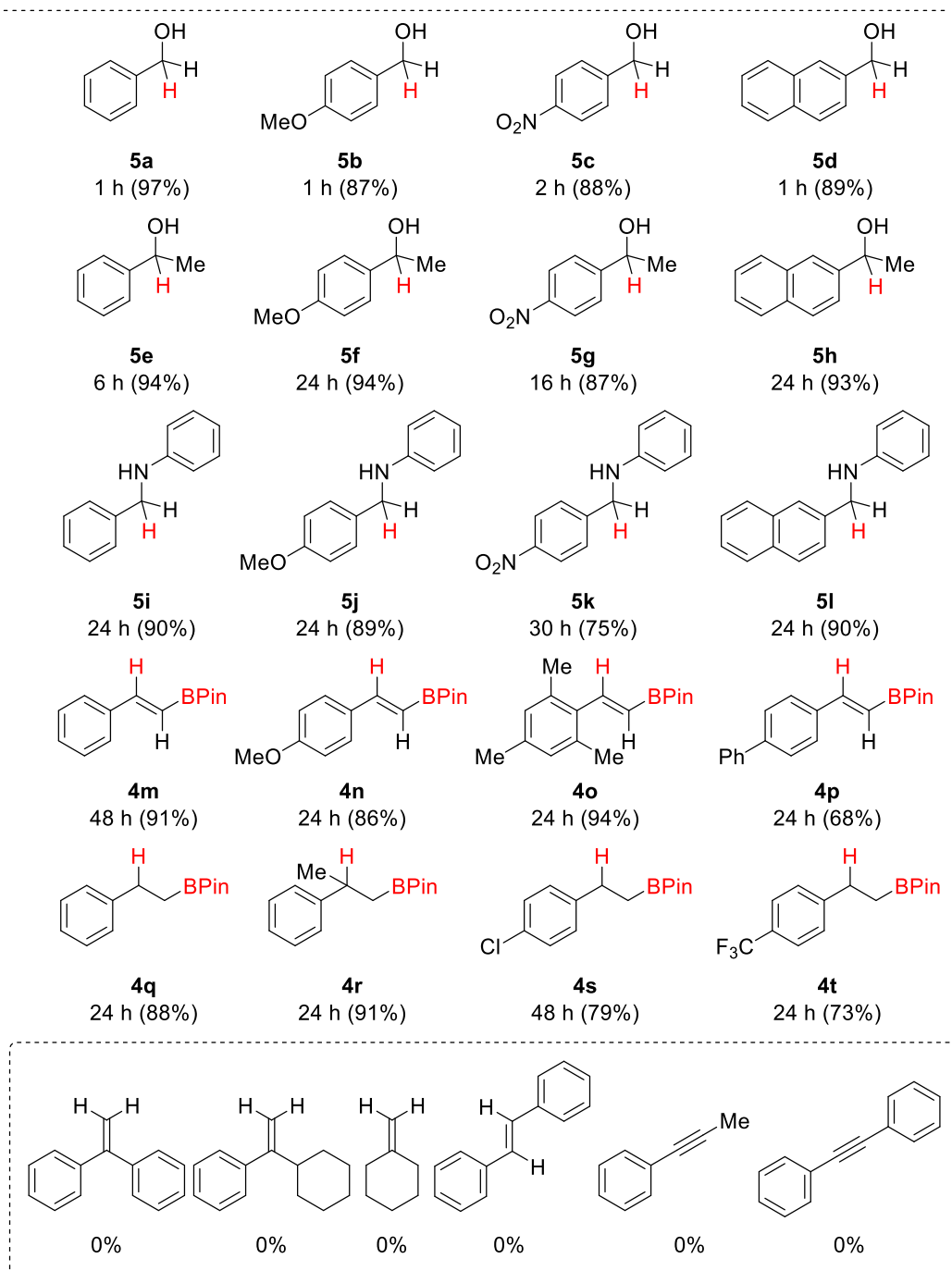
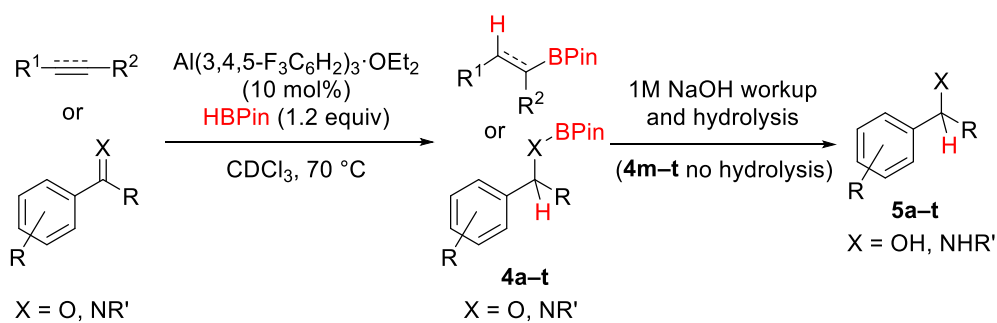
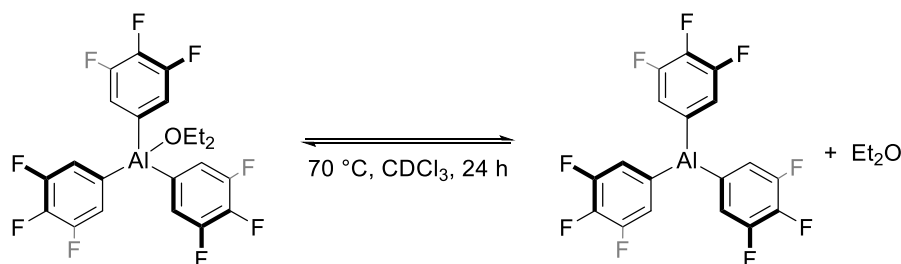


Figure 36 – Scope of alane-catalysed hydroboration. Time taken to reach quantitative conversion determined by 1H NMR spectroscopy. Isolated yields given in parentheses.

4.3.3 Mechanism of hydroboration

In comparison to its borane congener, $\text{Al}(\text{3,4,5-F}_3\text{C}_6\text{H}_2)_3\cdot\text{OEt}_2$ was notably slower at catalysing hydroboration. Whilst $\text{B}(\text{3,4,5-F}_3\text{C}_6\text{H}_2)_3$ was able to promote hydroboration at room temperature with a 2 mol% catalytic loading, there was negligible activity with $\text{Al}(\text{3,4,5-F}_3\text{C}_6\text{H}_2)_3\cdot\text{OEt}_2$ at the same temperature with an increased catalytic loading of 10 mol%. Initially, this was theorised to be due to the presence of the ether adduct hindering the ability of other substrates to bind to the aluminium centre. Thus, stoichiometric experiments were performed to elucidate the reaction mechanism.

$\text{Al}(\text{3,4,5-F}_3\text{C}_6\text{H}_2)_3\cdot\text{OEt}_2$ was placed in an NMR tube and left to heat at 70 °C for 24 hours to investigate if the ether could be liberated from the aluminium centre (Scheme 52). Indeed, a mixture of both the free alane and its adduct was observed by ^1H NMR spectroscopy as a quartet at 3.48 ppm and a triplet at 1.21 ppm for the free ether, and a quartet at 3.00 ppm and a triplet at 0.28 ppm for the alane etherate. The existence of two species was further confirmed by ^{19}F NMR spectroscopy, which displayed only two discrete sets of signals characteristic of the 3,4,5- $\text{F}_3\text{C}_6\text{H}_2$ aryl ring. One set of signals was attributed to the $\text{Al}(\text{3,4,5-F}_3\text{C}_6\text{H}_2)_3\cdot\text{OEt}_2$ adduct ($\delta = -135.5$ (d); -160.7 (t) ppm), whilst the other set ($\delta = -134.9$ (d); -161.2 (t) ppm) was assigned to the free alane. ^1H and ^{19}F NMR spectroscopy analyses suggested roughly 60% of the $\text{Al}(\text{3,4,5-F}_3\text{C}_6\text{H}_2)_3\cdot\text{OEt}_2$ had dissociated into the free alane.



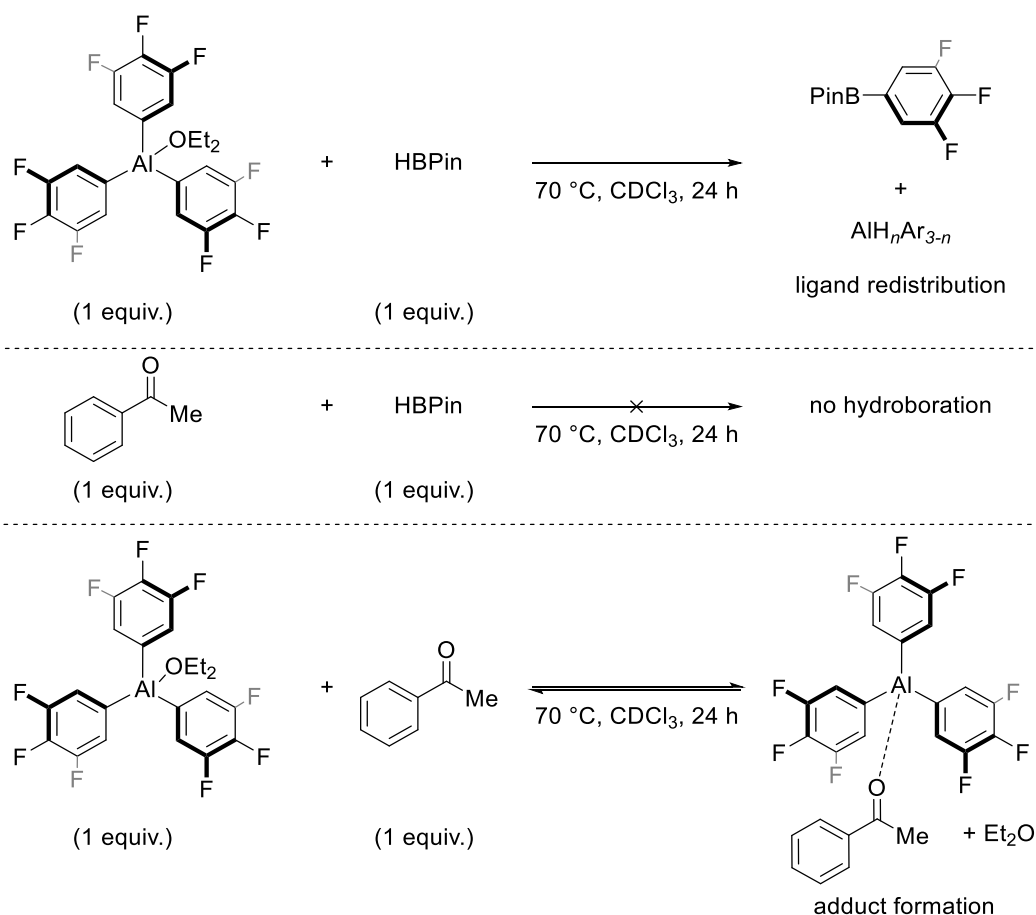
Scheme 52 – Liberation of ether from the $\text{Al}(\text{3,4,5-F}_3\text{C}_6\text{H}_2)_3\cdot\text{OEt}_2$ adduct at 70 °C.

After realisation that ether was liberated from the alane at elevated temperature, further stoichiometric probes were performed, each missing a core component of the hydroboration reaction: $\text{Al}(\text{3,4,5-F}_3\text{C}_6\text{H}_2)_3\cdot\text{OEt}_2$; acetophenone; and HBPIn (Scheme 53). As expected, there was no reaction between acetophenone and HBPIn in the absence of catalyst after 24 hours at 70 °C.

A mixture of $\text{Al}(\text{3,4,5-F}_3\text{C}_6\text{H}_2)_3\cdot\text{OEt}_2$ and acetophenone formed a mixture of the alane etherate and the alane carbonyl adducts, indicated by two discrete sets of ^{19}F NMR signals characteristic of the 3,4,5- $\text{F}_3\text{C}_6\text{H}_2$ aryl ring. One set of signals was indicative

of $\text{Al}(\text{3,4,5-F}_3\text{C}_6\text{H}_2)_3\cdot\text{OEt}_2$ and the other did not match the ^{19}F signals that had been assigned to the free alane. These signals were thus attributed to the alane acetophenone adduct ($\delta = -134.8$ (d), -161.6 (t) ppm). Further species were also observed by ^1H NMR spectroscopy as free ether ($\delta = 3.48$ (q); 1.21 (t) ppm), free acetophenone ($\delta = 2.50$ (s) ppm); the alane acetophenone adduct ($\delta = 2.36$ (s) ppm), and the alane etherate ($\delta = 2.78$ (q); 0.39 (t) ppm). It appeared that the equilibrium was shifted heavily in favour of the acetophenone alane adduct.

A mixture of $\text{Al}(\text{3,4,5-F}_3\text{C}_6\text{H}_2)_3\cdot\text{OEt}_2$ and HBPin at $70\text{ }^\circ\text{C}$ was found to form multiple products. Initial analysis of the ^{11}B NMR spectrum observed two signals. A signal at 42.7 ppm was indicative of boron-etherate adducts, which was attributed to the coordination of ether to boron containing species following the liberation of ether from the alane at elevated temperature. The other signal at 30.0 ppm was indicative of $\text{PinB}(\text{3,4,5-F}_3\text{C}_6\text{H}_2)$; fluorinated arylboronate esters such as $\text{PinB}(\text{3,4,5-F}_3\text{C}_6\text{H}_2)$ have characteristic sharp resonances around 30.0 ppm in the ^{11}B NMR spectrum, as observed by Marder.²³³ Moreover, the ^{19}F resonances for $\text{PinB}(\text{3,4,5-F}_3\text{C}_6\text{H}_2)$ were in accordance with the literature.²³² These signals were also observed following ligand distribution of HBPin with $\text{B}(\text{3,4,5-F}_3\text{C}_6\text{H}_2)_3$ in the aforementioned mechanistic studies for elevated temperature hydroborations (section 4.2.4), which further confirmed the identity of $\text{PinB}(\text{3,4,5-F}_3\text{C}_6\text{H}_2)$. The ^{19}F NMR spectrum of this experiment produced several signals, besides the ones assigned to $\text{Al}(\text{3,4,5-F}_3\text{C}_6\text{H}_2)_3$ and $\text{PinB}(\text{3,4,5-F}_3\text{C}_6\text{H}_2)$, which corresponded to a range of hydroalane species following ligand exchange between $\text{Al}(\text{3,4,5-F}_3\text{C}_6\text{H}_2)_3$ and HBPin.



Scheme 53 – Stoichiometric probes into the $\text{Al}(\text{3,4,5-F}_3\text{C}_6\text{H}_2)_3$ Et_2O -catalysed hydroboration mechanism at 70 °C.

The missing component of the hydroboration reaction was then added to each of these mixtures to elucidate the mechanism of hydroboration (Scheme 54).

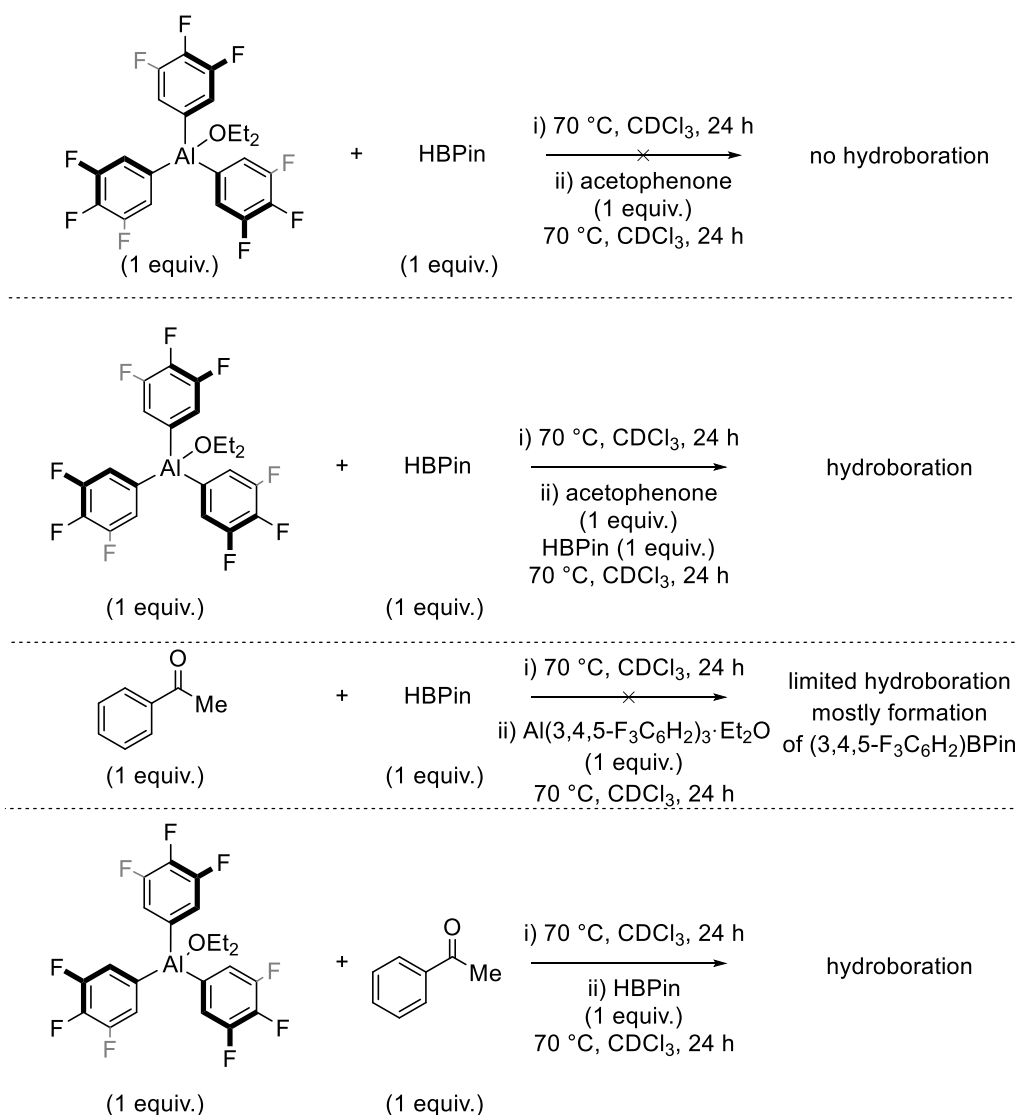
First, the mixture of hydroalane species formed from the addition of the alane with HBPIn was mixed with an equivalent of acetophenone. Surprisingly, no hydroboration was observed. Interpretation of the ^{11}B NMR spectrum found that no HBPIn was present in the solution, suggesting it had all reacted previously with $\text{Al}(\text{3,4,5-F}_3\text{C}_6\text{H}_2)_3$. Thus, a second equivalent of HBPIn was added and the solution was left for a further 24 hours at 70 °C. Analysis of the resultant NMR spectrum showed the formation of the boronate ester. During the catalytic scope, the ratio of HBPIn to alane was 12 to 1, suggesting that ligand exchange of the alane with HBPIn did not have a detrimental effect upon the catalytic activity.

Next, an equivalent of HBPIn was added to the mixture of $\text{Al}(\text{3,4,5-F}_3\text{C}_6\text{H}_2)_3$ and acetophenone. Surprisingly, no ligand redistribution was observed in this case. The ^{11}B NMR spectrum revealed signals only characteristic for the HBPIn and the boronate ester product. Further consultation of the ^{19}F NMR spectrum found that only

two sets of signals were present, which were in the same positions as they had been before the HBPIn was added. The two fluorine containing species in solution were thus assigned to the alane etherate and the alane acetophenone adduct. Therefore, it appears that once the alane acetophenone adduct has been generated, it is able to partake in the hydroboration mechanism without engaging in ligand metathesis with HBPIn to form PinB(3,4,5-F₃C₆H₂).

Finally, the mixture of HBPIn and acetophenone was mixed with a stoichiometric amount of catalyst. This founded incomplete hydroboration of the acetophenone as indicated by signals attributed to free acetophenone and its corresponding boronate ester. It appeared that some of the HBPIn had reacted with the alane to form hydroalane species, as indicated by the presence of signals indicative of PinB(3,4,5-F₃C₆H₂) in the ¹¹B and ¹⁹F NMR spectra. Analysis of the ¹H NMR spectrum found only minor signals attributed to the acetophenone Al(3,4,5-F₃C₆H₂)₃ adduct, thus suggesting the rate of ligand redistribution to form hydroalane species was significantly faster than the rate of acetophenone Al(3,4,5-F₃C₆H₂)₃ adduct formation.

These two competing reactions would likely not have been a problem during the hydroboration scope considering an excess of HBPIn was used; however, it highlighted that two mechanisms for hydroboration were plausible. In the catalysis optimisation, a maximum acetophenone conversion of 85% was noted when stoichiometric HBPIn was used (Table 11, entry 8). It is thus likely that some of this HBPIn had been consumed reacting with Al(3,4,5-F₃C₆H₂)₃ resulting in the lower conversion.

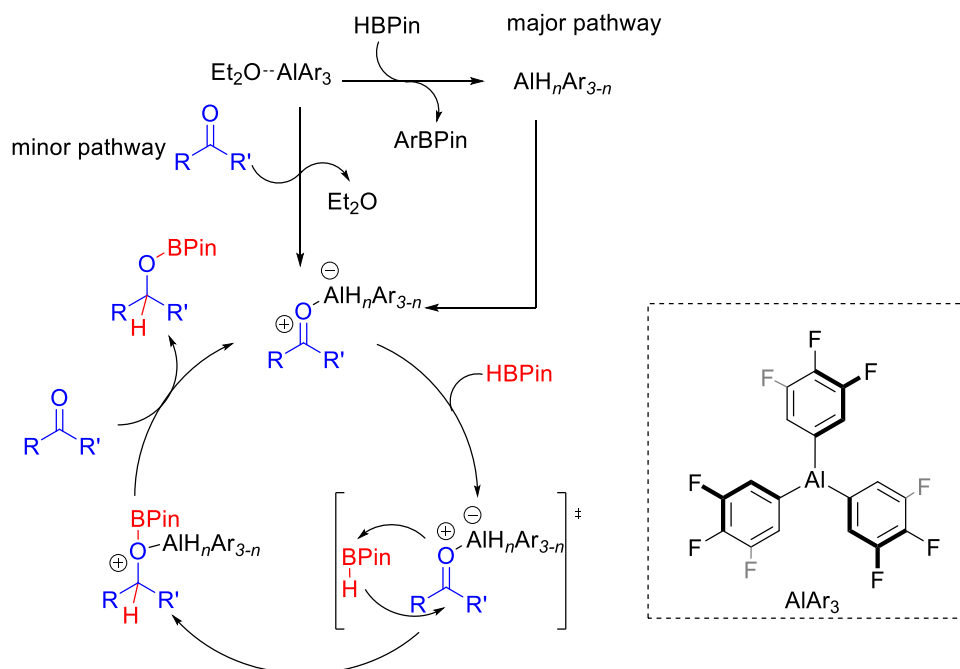


Scheme 54 – Further stoichiometric probes into the $\text{Al(3,4,5-F}_3\text{C}_6\text{H}_2)_3\text{-Et}_2\text{O}$ -catalysed hydroboration mechanism at 70 °C.

From these observations, two competing mechanisms can be postulated (Scheme 55). It appears that the reaction rate of ligand redistribution between $\text{Al(3,4,5-F}_3\text{C}_6\text{H}_2)_3$ and HBPIn is significantly higher than the rate of ligand redistribution between $\text{Al(3,4,5-F}_3\text{C}_6\text{H}_2)_3$ and acetophenone. Nevertheless, the latter reaction cannot be ruled out. It appears that most of the catalysis is performed by the hydroalane species generated *in situ* from ligand redistribution between $\text{Al(3,4,5-F}_3\text{C}_6\text{H}_2)_3$ and HBPIn. Thus, the LUMO of the substrate is significantly lowered upon coordination of the hydroalane to the acetophenone, facilitating σ -bond metathesis with HBPIn to form the boronate ester product.

The rapid mechanism bears similarity to that reported by Cowley and Thomas through the use of a triisobutyl aluminium pre-catalyst for hydroboration.¹¹⁹ This pre-catalyst

performed ligand exchange with HBPIn to liberate *i*BuBPIn and form a catalytically active diisobutyl aluminium hydride species, which was able to hydroborate a broad range of alkenes (chapter one, Scheme 16, right).



Scheme 55 – Proposed mechanism for $\text{Al}(\text{3,4,5-F}_3\text{C}_6\text{H}_2)_3 \cdot \text{Et}_2\text{O}$ -catalysed hydroboration.

4.4 Conclusions and outlook

In conclusion, two highly Lewis acidic catalysts prepared in chapter two were investigated for their activity towards hydroboration. In the first part of this chapter, $\text{B}(\text{3,4,5-F}_3\text{C}_6\text{H}_2)_3$ was found to act as an efficient catalyst both at room temperature and at 70 °C towards a range of carbonyls and imines. There was evidence of some ligand metathesis between $\text{B}(\text{3,4,5-F}_3\text{C}_6\text{H}_2)_3$ and HBPIn, forming active hydroborane catalysts *in situ*; however, this was minor in comparison to the $\text{B}(\text{3,4,5-F}_3\text{C}_6\text{H}_2)_3$ -catalysed hydroboration reaction. Whilst reaction times and isolated yields were satisfactory from the hydroboration transformation, a limitation in scope was noted upon the reaction with alkenes and alkynes. These limitations were offset with the assistance of microwave irradiation and will be further expanded upon in chapter five.

An interesting continuation to the research regarding $\text{B}(\text{3,4,5-F}_3\text{C}_6\text{H}_2)_3$ -catalysed hydroboration would be the synthesis of its diarylborane analogue $\text{HB}(\text{3,4,5-F}_3\text{C}_6\text{H}_2)_2$. Firstly, this borane be a candidate for promoting further catalytic reactions, in a similar way to how Piers borane and $\text{B}(\text{C}_6\text{F}_5)_3$ are often used as catalysts for different

reactions. More pertinent towards this thesis however, the synthesis and isolation of $\text{HB}(3,4,5\text{-F}_3\text{C}_6\text{H}_2)_2$ would allow confirmation of the mechanism proposed in Scheme 51, wherein $\text{B}(3,4,5\text{-F}_3\text{C}_6\text{H}_2)_3$ was suggested to generate hydroborane species such as $\text{HB}(3,4,5\text{-F}_3\text{C}_6\text{H}_2)_2$ *in situ* which could also catalyse the hydroboration reaction.

Indeed, kinetic studies could also be performed on the mechanism to determine the rate determining step of hydroboration. Upon consideration of the factors which hinder the rate of catalysis, it may be possible to design further borane catalysts that are more active than $\text{B}(3,4,5\text{-F}_3\text{C}_6\text{H}_2)_3$.

Moreover, in the second part of this chapter, $\text{Al}(3,4,5\text{-F}_3\text{C}_6\text{H}_2)_3\cdot\text{OEt}_2$ was found to act as an active pre-catalyst for the hydroboration of carbonyls, imines, alkynes, and alkenes. Whilst higher catalytic loadings and longer reaction times were required compared to its borane congener, the aluminium-based catalysts formed *in situ* were able to reduce substrates that the borane could not at 70 °C.

An extension to this research would be the isolation of the free alane $\text{Al}(3,4,5\text{-F}_3\text{C}_6\text{H}_2)_3$. Whilst time restraints prevented the ability to perform this experiment, one possible way of doing this would be to gently heat a sample of solvated $\text{Al}(3,4,5\text{-F}_3\text{C}_6\text{H}_2)_3\cdot\text{OEt}_2$ at 70 °C under a steady stream of nitrogen for an extended period of time. Stoichiometric studies found that the ether would partly dissociate from the alane at this temperature and thus it would be expected that upon dissociation the ether would be lost along with the stream of nitrogen gas.

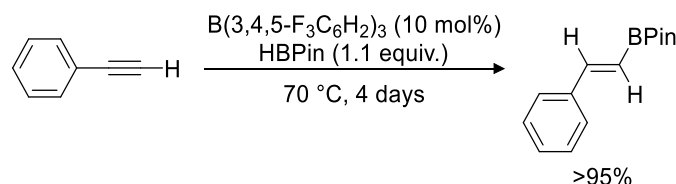
Moreover, further mechanistic studies could also be performed *via* computational methods to confirm the proposed mechanism. The proposed mechanism in Scheme 55 suggests that the hydroalane species coordinate to the substrate; however, there is the possibility that one step of the reaction could involve the hydroalane hydroaluminating the unsaturated bond before hydroboration with HBPi occurred. Whilst hydroalumination was not observed through multinuclear NMR spectroscopy, it would be interesting to investigate if hydroalumination was indeed a plausible in the hydroboration mechanism.

Chapter five – Hydroboration catalysis using microwave irradiation

5.1 Aims of this chapter

In continuation from the work described in chapter four regarding Lewis acid-catalysed hydroboration reactions using conventional heating techniques, this chapter investigates the use of microwave assisted heating to promote B(3,4,5-F₃C₆H₂)₃-catalysed hydroboration reactions.

Upon discovery that B(3,4,5-F₃C₆H₂)₃ was unable to hydroborate alkenes and alkynes at 70 °C under the previously optimised conditions (Table 10), further options were considered to promote the reaction. First, in effort to ensure that the reaction was feasible, the hydroboration of phenylacetylene was performed again with more forcing conditions (). Here, the catalyst loading was increased to 10 mol% and the reaction mixture heated at 70 °C until quantitative conversion was observed through multinuclear NMR spectroscopy. Although full conversion was observed only after four days, this proved the concept that harsher reaction conditions were able to promote the hydroboration transformation.



Scheme 56 – Hydroboration of phenylacetylene using conventional heating.

At this juncture, microwave irradiation was chosen as an enabling technology to promote hydroboration reactions which were difficult to achieve with traditional protocols. As discussed in chapter one, microwave radiation facilitates uniform heating and allows safe control over extreme reaction parameters such as high temperatures and pressures. For this purpose, a Biotage® Initiator+ 60 microwave instrument was employed to assist the catalytic reactions.

5.2 Investigation of B(3,4,5-F₃C₆H₂)₃ as a hydroboration catalyst for substrates with homonuclear unsaturated bonds using microwave irradiation

5.2.1 Optimisation

Once it was established that B(3,4,5-F₃C₆H₂)₃ could be employed as an active catalyst for the hydroboration of alkynes when left for longer periods of time, a Biotage® Initiator+ 60 microwave reactor was employed to safely heat samples to 180 °C. This accelerated the reactions and reduced the reaction timescale from days to hours or minutes. The reactions were performed in chloroform to allow a direct comparison to the conventionally heated reactions and to negate any possible solvent effects that could be introduced upon varying the reaction medium. Chloroform is an uncommon choice as a microwave solvent, due to its low loss factor and dielectric constant.¹⁴⁰ Thus, a more appropriate solvent such as ethylene glycol or ethanol should be employed instead if this reaction is to be optimised further in an industrial setting. The initial reaction temperature was set at 180 °C. The average pressure for these reactions was 20 bar, as measured by the internal pressure sensor on the microwave reactor. As the reaction vessels were only rated to 25 bar of pressure, safety considerations prevented the use of higher temperatures and pressures.

The optimisation considerations for the microwave assisted reactions are reported in Table 12, with phenylacetylene as the model substrate. First, the hydroboration reaction was attempted at 180 °C in the absence of catalyst; however, this failed to promote any product formation after 90 minutes (Table 12, entry 1). The addition of 2 mol% B(3,4,5-F₃C₆H₂)₃ resulted in successful hydroboration, with conversions of 47%, 63%, and 71% within 20, 40, and 90 minutes respectively (Table 12, entries 2–4). The reaction was further accelerated through increased catalytic loading, with 5 mol% B(3,4,5-F₃C₆H₂)₃ resulting in conversions of 77%, 88%, and >95% within 20, 40, and 90 minutes respectively (Table 12, entries 5–7).

To compare these results with conventional batch conditions, the hydroboration protocol was performed on phenylacetylene at 70 °C with 10 mol% catalyst (Table 12, entry 8). In this case, full conversion was achieved after four days. Moreover, when only 5 mol% catalyst was employed, the reaction reached only 50% conversion within the same period (Table 12, entry 9). By using a dedicated Parr reactor vessel at 180 °C for 90 minutes, only 40% conversion was observed

(Table 12, entry 10). This lower conversion is likely the result of a decreased temperature dissipation within the vessel and inefficient mixing. Attempts to reach 180 °C in a microwave vessel in a sand bath were unsuccessful, as the vessel's cap exploded off due to uncontrollable pressure build-up around 140 °C (Table 12, entry 11). When the reaction mixture was heated within the microwave reactor, an in-built system applied an external pressure to the vessel's cap thus preventing it from exploding. Unfortunately, this meant that there was no safe way of directly comparing the reactions that took place in the microwave to those that did not.

Table 12 – Optimisation of microwave reaction conditions for the hydroboration of phenylacetylene using HBPIn.

$$\text{Ph}-\text{C}\equiv\text{C}-\text{H} \xrightarrow[\text{Time (min)}]{\begin{array}{l} \text{Catalyst (x mol\%)} \\ \text{HBPIn (1.1 equiv.)} \\ \text{Temperature (x }^\circ\text{C)} \end{array}} \begin{array}{c} \text{H} \quad \text{BPIn} \\ \diagdown \quad / \\ \text{C}=\text{C} \\ / \quad \diagdown \\ \text{Ph} \quad \text{H} \end{array}$$

Entry	Catalyst	Loading (mol%)	Temperature (°C)	Time (min)	Conversion (%) ^[a]
1	None	-	180	90	<5
2	B(3,4,5-F ₃ C ₆ H ₂) ₃	2	180	20	47
3	B(3,4,5-F ₃ C ₆ H ₂) ₃	2	180	40	63
4	B(3,4,5-F ₃ C ₆ H ₂) ₃	2	180	90	71
5	B(3,4,5-F ₃ C ₆ H ₂) ₃	5	180	20	77
6	B(3,4,5-F ₃ C ₆ H ₂) ₃	5	180	40	86
7	B(3,4,5-F ₃ C ₆ H ₂) ₃	5	180	90	>95
8	B(3,4,5-F ₃ C ₆ H ₂) ₃	5	70 (no MW)	5760 (96 h)	50
9	B(3,4,5-F ₃ C ₆ H ₂) ₃	10	70 (no MW)	5760 (96 h)	>95
10	B(3,4,5-F ₃ C ₆ H ₂) ₃	5	180 (no MW) ^[b]	90	40
11	B(3,4,5-F ₃ C ₆ H ₂) ₃	5	180 (no MW) ^[c]	-	-

Phenylacetylene (0.4 mmol, 40.8 mg), HBPIn (0.44 mmol, 63.8 μL), chloroform solvent (2 mL). Microwave reaction conditions – 180 °C, 20 bar. ^[a] Conversion determined by ¹H NMR spectroscopy. ^[b] Reaction completed in an oven heated Parr acid digestion vessel. ^[c] Reaction vessel heated in a sand bath; however, vessel exploded before reaching 180 °C.

5.2.2 Scope

The optimal conditions were then applied to a range of alkenes and alkynes, which were found to undergo hydroboration in as little as 90 minutes, a remarkable increase in reaction speed. Mono- and disubstituted terminal alkenes were first probed and gave the *anti*-Markovnikov boronate esters **3a–d** in quantitative yields. Further styrene derivatives also underwent hydroboration to form their respective boronate

esters as the *anti*-Markovnikov product (**3e–g**); however, no quantitative conversions were observed after 90 minutes.

Terminal alkynes also performed well, forming **3h** and **3i** in high isolated yields (83–92%). Internal alkynes were less receptive towards the optimised conditions. Diphenylacetylene only reached 50% conversion to **3j** after 90 minutes at 180 °C. Meanwhile, prop-1-yn-1-ylbenzene produced an inseparable mixture of both the Markovnikov and *anti*-Markovnikov products in a 3:1 ratio (**3k**). Notably, no over-reduction into diboronate esters was observed during the hydroboration of alkynes and other than **3k**, exclusively the *anti*-Markovnikov product was formed.

The use of microwave irradiation still had some limitation towards certain alkenes and alkynes, with norbornene, *trans*-stilbene, 1-hexyne and 4-octyne resistant towards reduction.

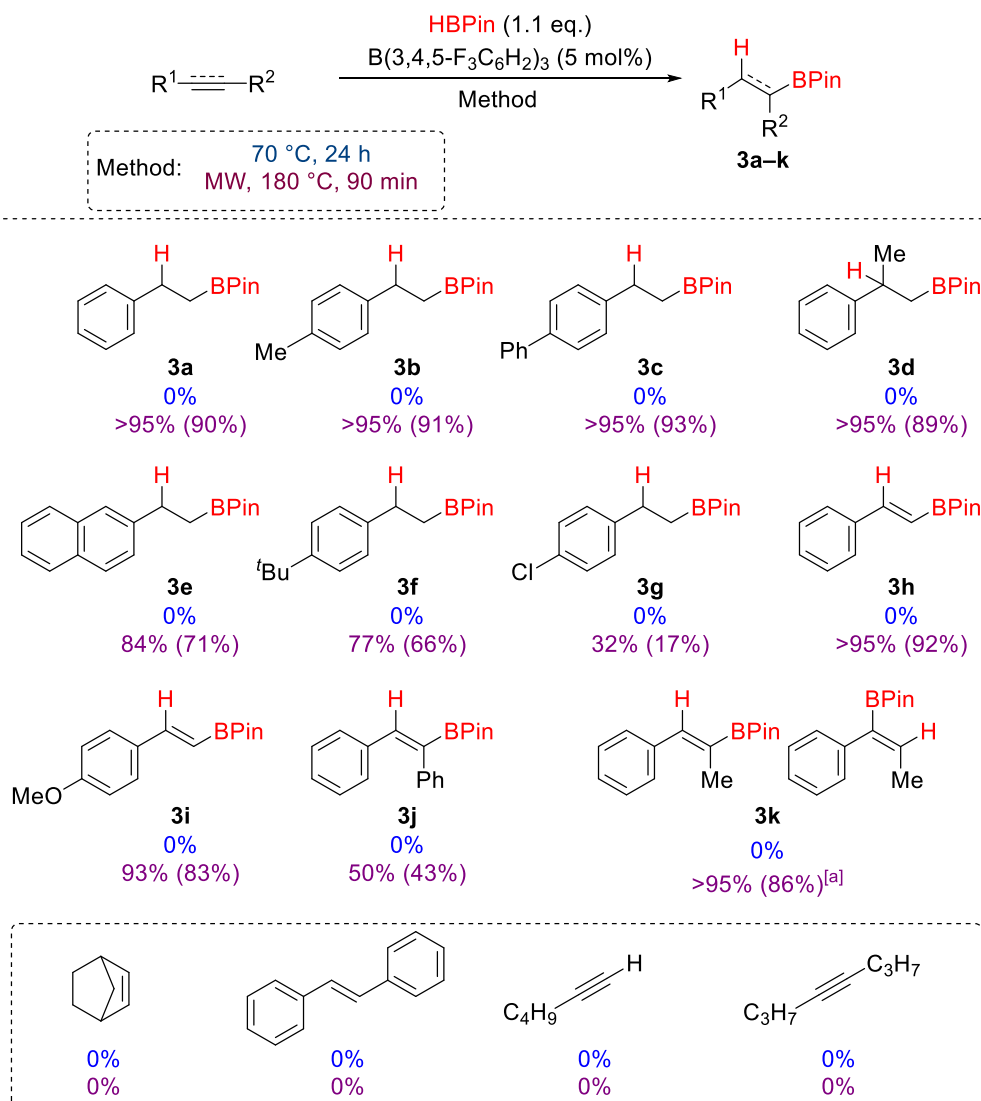


Figure 37 – Hydroboration of alkenes and alkynes. Conversions for **3a–k** determined from ¹H NMR spectroscopy, isolated yield in parentheses. ^[a] two regioisomers formed in a 3:1 product ratio.

5.3 Investigation of $B(3,4,5-F_3C_6H_2)_3$ as a hydroboration catalyst for substrates with heteronuclear unsaturated bonds using microwave irradiation

5.3.1 Optimisation

As the benefits of microwave irradiation towards the hydroboration of homonuclear carbon bonds became clear, it was decided to investigate the use of this enabling technology towards other hydroboration reactions which were already feasible using conventional heating conditions. Whilst it was apparent that increasing the reaction temperature increased the reaction rate, it was theorised that applying the harsher conditions within the microwave reactor could result in exceptionally rapid reactions.

Anisaldehyde was chosen as the model substrate for the optimisation studies, as it took 24 hours to undergo complete hydroboration at room temperature. The reactions were immediately quenched with a basic workup to analyse solely the effect of microwave heating inside the reaction vessel, excluding the continuation of the reaction at room temperature. This basic workup was required to remove the catalyst and to hydrolyse the formed boronate ester into 4-methoxybenzyl alcohol.

Initially, the reaction was attempted in the absence of catalyst (Table 13, entry 1). Surprisingly, 11% conversion was observed after 5 minutes. This can be attributed to the forcing conditions present within the microwave reactor, which allowed for the activation energy of the hydroboration reaction to be overcome even without a catalyst. At 0.5 mol% catalyst loading, there was a significant improvement with 40%, 60%, and 73% conversion into the boronate ester after 1, 3, and 5 minutes at 180 °C respectively (Table 13, entries 2–4). Whilst promising, quantitative conversion was targeted and thus the catalyst loading was increased to 1 mol%, which led to 90% conversion into the boronate ester after 5 minutes (Table 13, entries 5–7). At this juncture, 2 mol% catalyst loading was investigated (Table 13, entries 8–10), in line with the reactions under conventional heating. In this case, full conversion into the corresponding boronate ester was observed after only 5 minutes (Table 13, entry 10).

The optimised conditions were then applied in the presence of a $B(C_6F_5)_3$ catalyst. This resulted in a conversion of 30%, which was greater than the amount of hydroboration observed in the absence of catalyst (Table 13, entry 11). This suggested that the borane could act as a catalyst under the extreme conditions

applied by the microwave reactor; however, it was notably not as active as $B(3,4,5-F_3C_6H_2)_3$.

Table 13 – Optimisation of microwave reaction conditions for the hydroboration of anisaldehyde using HBPIn.

Entry	Catalyst	Catalyst loading (mol%)	Time (min)	Conversion (%) ^[a]
1	No catalyst	-	5	11
2	$B(3,4,5-F_3C_6H_2)_3$	0.5	1	40
3	$B(3,4,5-F_3C_6H_2)_3$	0.5	3	60
4	$B(3,4,5-F_3C_6H_2)_3$	0.5	5	73
5	$B(3,4,5-F_3C_6H_2)_3$	1	1	70
6	$B(3,4,5-F_3C_6H_2)_3$	1	3	80
7	$B(3,4,5-F_3C_6H_2)_3$	1	5	90
8	$B(3,4,5-F_3C_6H_2)_3$	2	1	80
9	$B(3,4,5-F_3C_6H_2)_3$	2	3	93
10	$B(3,4,5-F_3C_6H_2)_3$	2	5	>95
11	$B(C_6F_5)_3$	2	5	30

Anisaldehyde (0.4 mmol, 54.4 mg), HBPIn (0.44 mmol, 63.8 μ L). Microwave reaction conditions - 180 °C, 20 bar. Pressure and temperature were measured by the microwave's in-built sensors
^[a] Conversion determined by ¹H NMR spectroscopy.

5.3.2 Scope

With optimised conditions in hand, attention was returned to the initial scope of aldehyde, ketone and imine substrates for examples which took longer than one hour to undergo hydroboration at room temperature. The reactions were heated in the microwave at 180 °C for five minutes and quenched immediately with a basic workup. Most substrates displayed much improved reactivity under microwave irradiation, with quantitative conversion (>95%) observed within five minutes in the majority of cases, a significant reduction in reaction time compared to conventionally heated reactions.

There were few exceptions to the rapid hydroboration. In cases of very electron deficient substrates there was a decline in activity: **2h** was isolated in only 71% yield after five minutes, whilst **2n** was isolated in 95% yield after one hour under microwave irradiation. Moreover, the steric encumberment of benzophenone caused slow reactivity as also observed using conventional heating techniques, with only 25%

conversion to **2j** noted after five minutes at 180 °C. Attempts to improve this yield by increasing the reaction time to 30 minutes or one hour showed small increases in yield to 38% and 45% respectively. Notably, there was no change in functional group tolerance, and the trends in reactivity of electron-withdrawing/electron-donating substituents remained the same between the microwave-assisted reactions and the standard heated reactions.

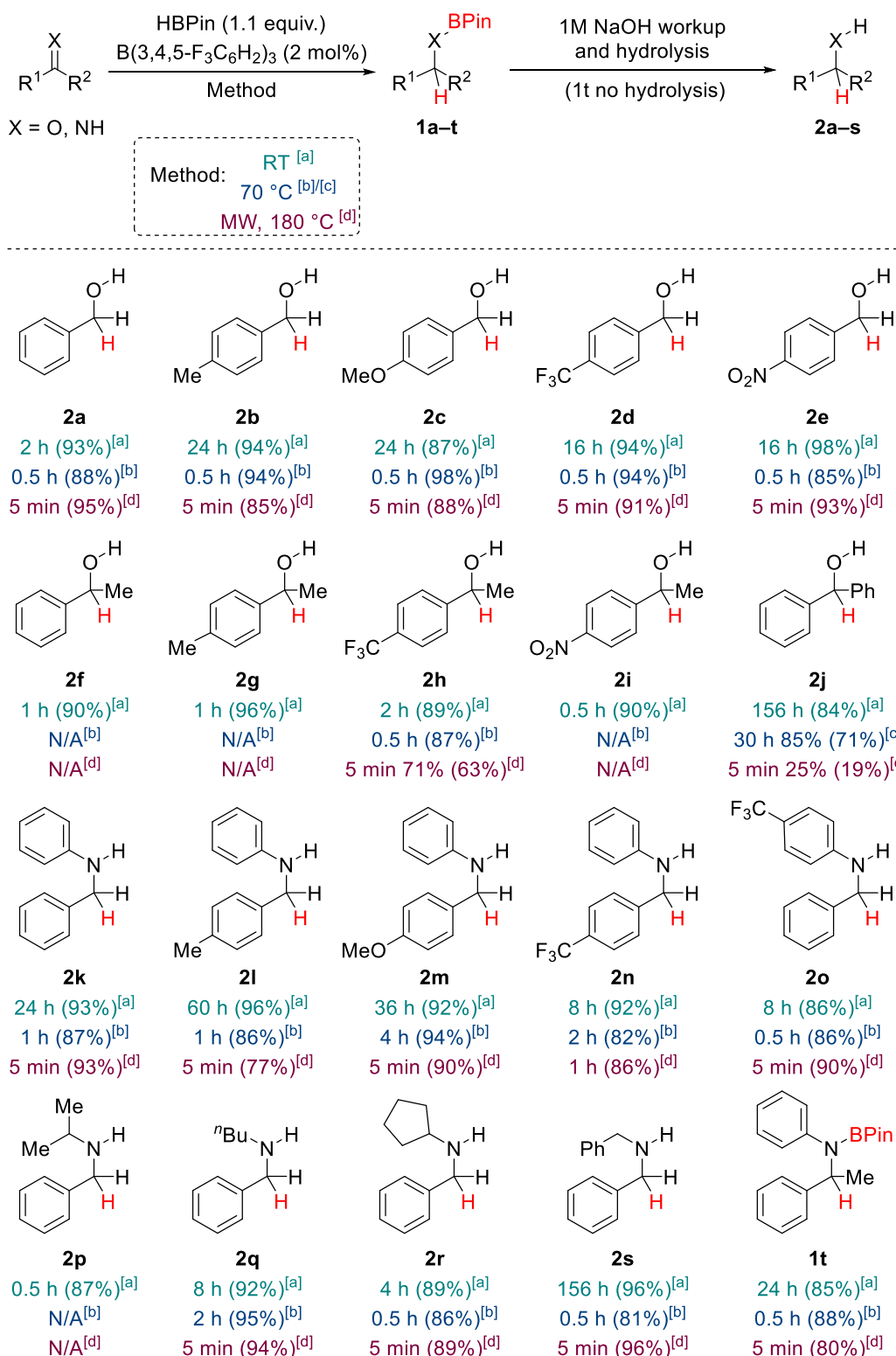


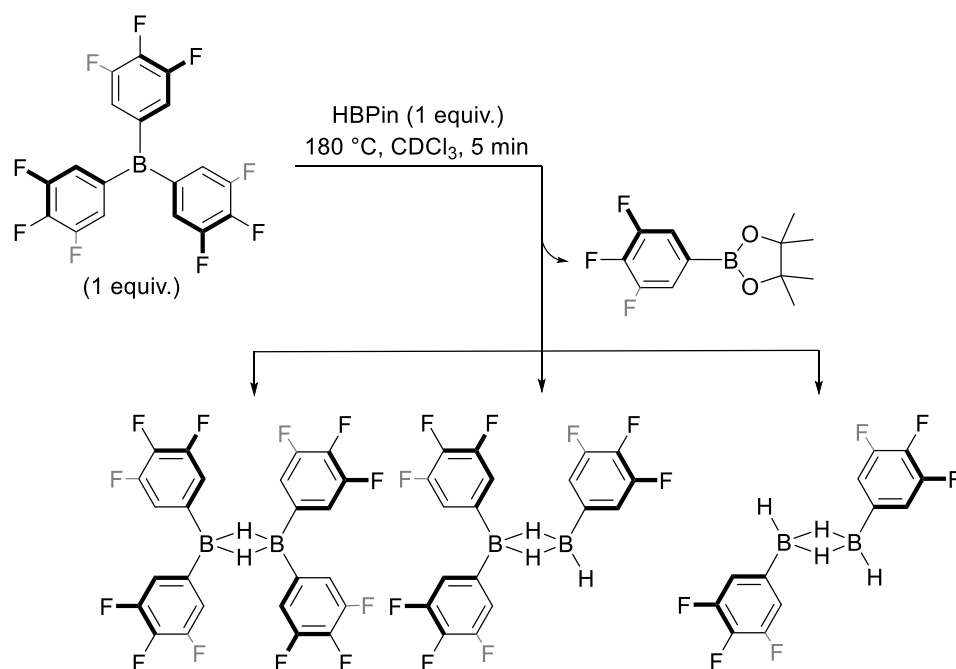
Figure 38 – Scope of borane-catalysed hydroboration, comparing conventional heating techniques to microwave assisted heating. Conversions determined by ¹H NMR spectroscopy. Isolated yields given in parentheses. ^[a] Time taken to reach quantitative conversion at room temperature. ^[b] Time taken to reach quantitative conversion at 70 °C. ^[c] Achieved maximum conversion of 85% at 70 °C and did not increase past this value. ^[d] Time taken and conversion in microwave at 180 °C.

5.4 Mechanism of hydroboration under microwave irradiation

5.4.1 Mechanism of hydroboration in the microwave for substrates containing heteronuclear unsaturated bonds

Investigation into the mechanism of $B(3,4,5-F_3C_6H_2)_3$ -catalysed hydroboration of acetophenone at 70 °C suggested that at elevated temperatures the borane catalyst had a propensity to perform ligand exchange with the HBPIn reagent to form a range of catalytically active hydroborane species. At 70 °C, an estimated 20% of the borane was observed to undergo this transformation. It was thus theorised that the elevated temperatures applied by microwave irradiation would promote further ligand metathesis between HBPIn and $B(3,4,5-F_3C_6H_2)_3$, pushing towards the full conversion of the triarylborane into a range of catalytically active hydroborane species.

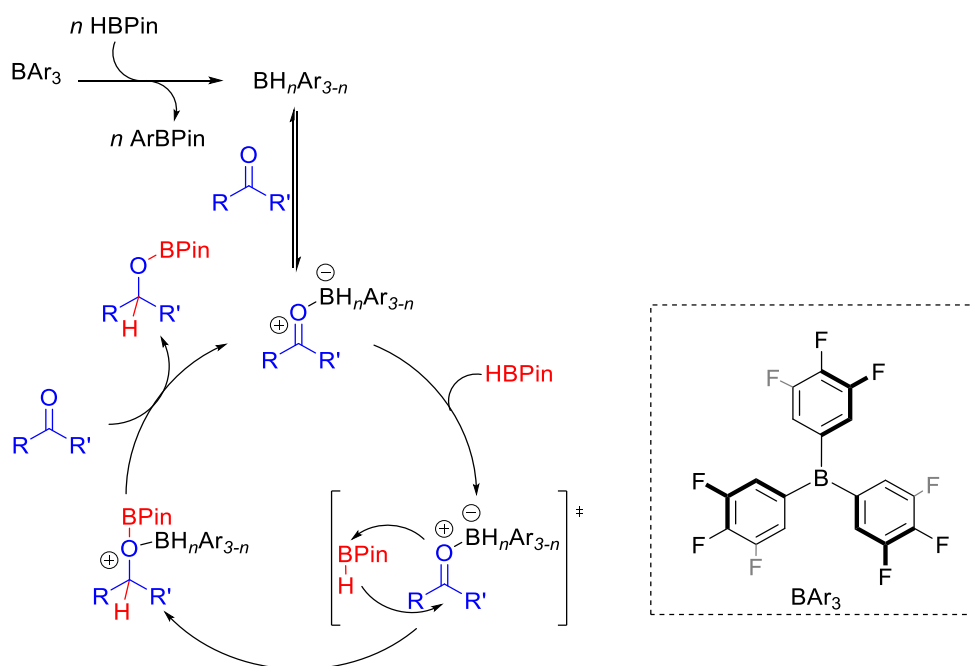
Indeed, when a stoichiometric mixture of $B(3,4,5-F_3C_6H_2)_3$ and HBPIn was heated to 180 °C for five minutes in the microwave reactor, clear generation of $(3,4,5-F_3C_6H_2)BPIn$ was evidenced by ^{19}F and ^{11}B NMR spectroscopy. Several low intensity signals were also observed and were attributed to the formation of the catalytically active hydroborane species; however, further investigations are required to fully elucidate the identity of these structures. No signals indicative of HBPIn were recorded, suggesting full consumption of the borane catalyst and thus a greater concentration of hydroborane species in the microwave heated reactions at 180 °C compared to the classically heated reactions at 70 °C. Unfortunately, attempts to isolate the generated hydroborane species were unsuccessful. Nevertheless, it was thus proposed that the borane acted as a pre-catalyst when exposed to the high temperatures and pressures applied by the microwave reactor, forming a range of catalytically active hydroborane species (Scheme 57). The suggested hydroborane species are modelled on those detected by Oestreich following ligand metathesis between $B(3,5-(CF_3)_2C_6H_3)_3$ and HBPIn.¹⁰²



Scheme 57 – Suggested products from ligand metathesis between $B(3,4,5-F_3C_6H_2)_3$ and HBPIn at 180 °C.

The same stoichiometric hydroboration experiments that were carried out at 70 °C to elucidate the mechanism (Scheme 51) were then repeated with microwave heating for five minutes. The resultant multinuclear NMR spectra from these studies were near identical to those performed at 70 °C, with the one exception being that $B(3,4,5-F_3C_6H_2)_3$ was no longer observed, and that $(3,4,5-F_3C_6H_2)BPIn$ and its corresponding hydroborane species were observable instead.

Therefore, the proposed minor pathway of carbonyl hydroboration by a $B(3,4,5-F_3C_6H_2)_3$ pre-catalyst at 70 °C (Scheme 51) was suggested to be the sole mechanism when the reaction took place under microwave irradiation (Scheme 58). It was proposed that the borane initially performed ligand exchange with HBPIn to form a range of catalytically active hydroborane species. These hydroborane species acted as Lewis acid catalysts, coordinating to the substrate, lowering its LUMO, hence making it susceptible to σ -bond metathesis by HBPIn.



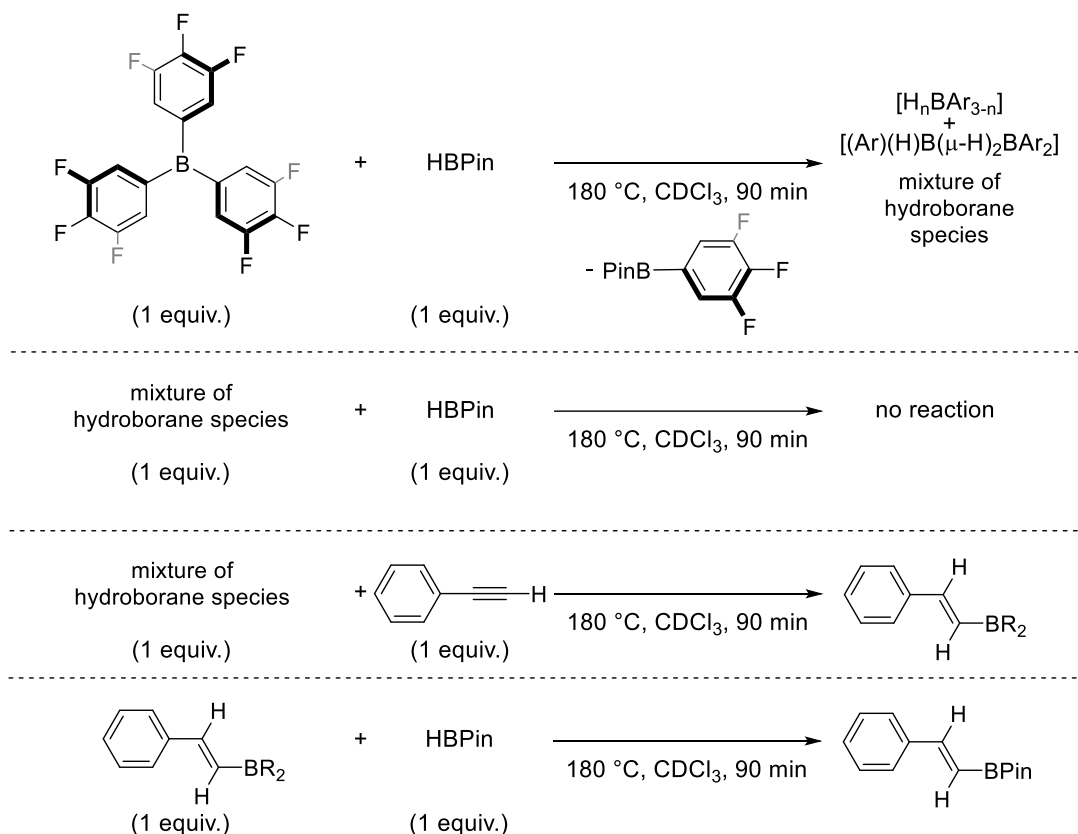
Scheme 58 – Proposed mechanism for $B(3,4,5-F_3C_6H_2)_3$ -catalysed hydroboration.

5.4.2 Mechanism of hydroboration in the microwave for substrates containing homonuclear unsaturated bonds

Investigation into the mechanism of $B(3,4,5-F_3C_6H_2)_3$ -catalysed hydroboration of acetophenone at $180\text{ }^\circ\text{C}$ revealed that at elevated temperatures the borane catalyst would perform ligand exchange with the $HBPIn$ reagent to form a range of catalytically active hydroborane species. Thus, under microwave irradiation the reaction mechanism for the hydroboration of alkenes by $B(3,4,5-F_3C_6H_2)_3$ appeared to be identical to the hydroboration reaction mechanism when promoted by $B(3,5-(CF_3)_2C_6H_3)_3$. Here, the borane was catalytically innocent and acted only as a pre-catalyst to a mixture of highly catalytically active hydroborane species (Scheme 12).¹⁰²

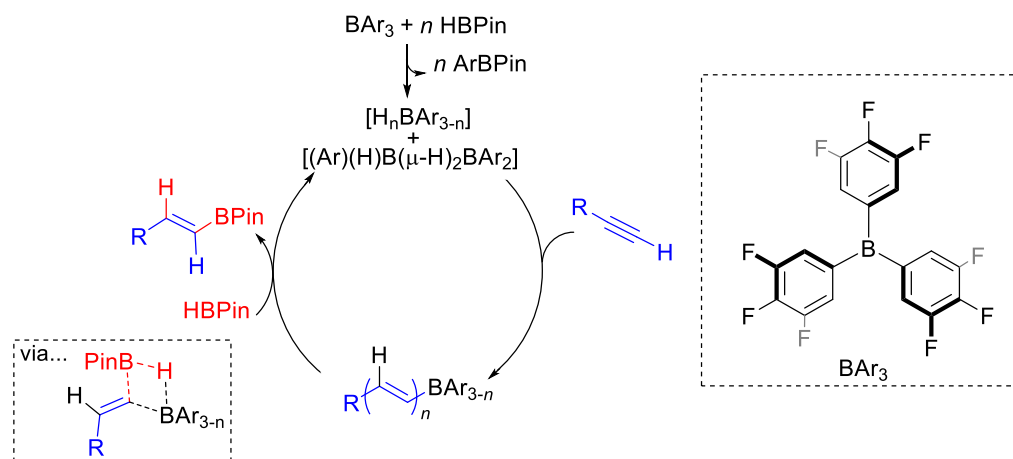
As discussed in section 5.4.1, the isolation of the hydroborane species was not possible; however, brief stoichiometric probes were performed to elucidate the mechanism (Scheme 59). First, a second equivalent of $HBPIn$ was introduced to the mixture of hydroborane species, but no reactivity was observed by multinuclear NMR spectroscopy. Phenylacetylene was then added to the mixture of hydroborane species and allowed to react in the microwave for 90 minutes. Analysis of the 1H NMR spectrum observed depletion of the terminal alkyne proton at 3.00 ppm, and the generation of two doublets at 7.33 and 6.10 ppm, which were attributed to vicinal olefin protons. Therefore, it was suggested that the hydroborane species were able

to hydroborate the alkyne bond. Addition of a second equivalent of HBPIn to this sample and a further 90 minutes in the microwave did not warrant any observable change in the NMR spectrum; however, as exclusively 4,4,5,5-tetramethyl-2-styryl-1,3,2-dioxaborolane was isolated following the catalytic reaction it would suggest that ligand metathesis between HBPIn and the hydroborane hydroborated species occurred at this step.



Scheme 59 – Stoichiometric probes into the $\text{B}(3,4,5\text{-F}_3\text{C}_6\text{H}_2)_3$ -catalysed hydroboration mechanism at 180 °C.

Based on these results and considering previous studies of other triarylborane catalysed hydroborations,^{102,106} the following mechanism was proposed. Once generated under microwave conditions, the catalytically active hydroborane species were proposed to undergo a concerted 1,2-*syn*-addition over the $\text{C}\equiv\text{C}$ triple bond, followed by ligand metathesis with HBPIn to generate the desired boronate ester (Scheme 60). Mechanistic studies by Lloyd-George and Thomas concerning the hydroboration of alkynes by a HBCy_2 found that the retention of boronate ester stereochemistry originated from a 2-electron-3-centre intermediate. As stereochemistry is also retained when a $\text{B}(3,4,5\text{-F}_3\text{C}_6\text{H}_2)_3$ precatalyst is used, it is proposed that a similar 2-electron-3-centre intermediate is formed in this catalytic system.

Scheme 60 – Proposed mechanism for $B(3,4,5-F_3C_6H_2)_3$ -catalysed hydroboration.

5.5 Conclusions and outlook

In conclusion, the use of microwave irradiation was able to notably improve the catalytic activity of $B(3,4,5-F_3C_6H_2)_3$. Not only did it enable the safe increase of the temperature of the reaction medium to 180 °C, it also decreased reaction times from hours to minutes. Furthermore, the forcing reaction parameters allowed for substrates that were formerly unreactive to be reduced efficiently and rapidly.

The work presented within this chapter acts as a new benchmark in the field of enabling technologies and main-group chemistry, where the use of microwave irradiation was proven to promote reactions that are otherwise challenging using conventional conditions. Considering the inherent challenges of main-group chemistry as an alternative to traditional transition metal catalysts, microwave irradiation can offer a facile approach that can assist main-group catalysts to rival the activity of conventional platinum group metals.

Further work in this area could be performed to confirm the proposed mechanism either *via* deuteration studies or by using computational methods.

Chapter six – Hydroamination catalysis with $B(C_6F_5)_3$

6.1 Aims of this chapter

This chapter investigates the use of the archetypal strong Lewis acid triarylborane $B(C_6F_5)_3$ as a hydroamination catalyst for alkenes. Literature precedents revealed that $B(C_6F_5)_3$ was an active hydroamination catalyst for alkynes, promoting a variety of inter- and intra-molecular reactions.^{130–132} Thus, it was proposed that alkenes could also be subjected towards the $B(C_6F_5)_3$ -catalysed hydroamination reaction.

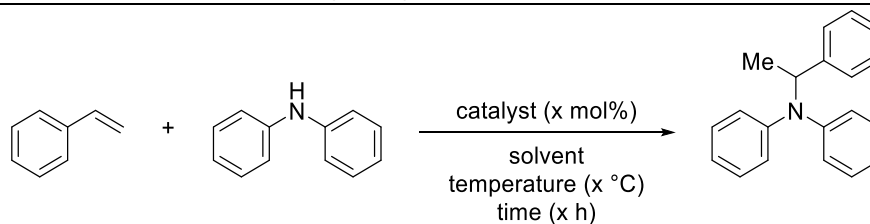
6.2 Optimisation

Diphenylamine and styrene were selected as reagents to optimise the hydroamination transformation. First, the hydroamination procedure was attempted in the absence of catalyst at room temperature; however, no reactivity was observed (Table 14, entry 1). Literature precedents had observed that $B(C_6F_5)_3$ was an active catalyst for the hydroamination of alkynes,^{130–132} hence this borane was targeted for the analogous reaction with alkenes. Unfortunately, the introduction of $B(C_6F_5)_3$ as a catalyst was not observed to promote reactivity at room temperature regardless of catalytic loading (Table 14, entries 2–4).

The temperature of reaction was thus increased to 70 °C to help promote reactivity. Still, no conversion was observed after 24 hours in experiments with no catalyst or with 2 mol% catalytic loading (Table 14, entries 5–6). Increasing the amount of $B(C_6F_5)_3$ to 5 mol% and 10 mol% initiated reactivity between styrene and diphenylamine into the Markovnikov addition product, in 26% and 62% conversion after 24 hours respectively (Table 14, entries 7–8). Attention was then turned towards alternate Lewis acidic borane catalysts to investigate if increased reactivity could be achieved by tuning Lewis acidity or steric factors. Using the same conditions that allowed for 62% conversion by $B(C_6F_5)_3$ founded no reactivity for any of the tested catalysts after 24 hours at 70 °C (Table 14, entries 9–13).

As increased conversion of diphenylamine was observed by increasing the temperature from ambient conditions to 70 °C, it was proposed that reaching higher temperatures could attain better results. Thus, C_6D_5Br was employed as a solvent, and the hydroamination reaction proceeded for 24 hours at 160 °C with 10 mol% catalytic loading of $B(C_6F_5)_3$ (Table 14, entry 14). Surprisingly, hydroamination did not occur and instead signals indicative of polystyrene were observed in the 1H NMR spectrum. It was speculated that at greatly elevated temperatures, $B(C_6F_5)_3$ acted as a polymerisation catalyst rather than a hydroamination catalyst. Indeed, $B(C_6F_5)_3$ was classically used as a polymerisation initiator before its widespread use in frustrated Lewis pair chemistry.⁵¹ To investigate if hydroamination could be achieved at greatly elevated temperatures in a shorter time period, the hydroamination reaction was attempted with the assistance of microwave irradiation; using similar conditions as had been optimised for the hydroboration of alkenes in chapter five (Table 14, entry 15). Indeed, polymerisation was also observed following this reaction and thus the use of microwave irradiation as an enabling technology was not pursued further for the hydroamination transformation.

It was thus decided that to attain better conversions, either the catalytic loading of $B(C_6F_5)_3$, or the timescale of reaction had to be increased. By applying 20 mol% of $B(C_6F_5)_3$, full conversion into the Markovnikov product was observed after 24 hours (Table 14, entry 16). Whilst a promising result, such a high catalytic loading was deemed impractical. Instead, the timescale of reaction with 10 mol% catalytic loading was increased to 48 h (Table 14, entry 17). At this stage, 92% conversion into the tertiary amine was observed and thus these conditions were designated as optimal.

Table 14 – Optimisation of borane-catalysed hydroamination.^{ix}

Run	Catalyst	Catalyst Loading (mol %)	Temperature (°C)	Time (h)	Conversion (%) ^[a]
1	-	-	25	24	<5
2	$B(C_6F_5)_3$	2	25	24	<5
3	$B(C_6F_5)_3$	5	25	24	<5
4	$B(C_6F_5)_3$	10	25	24	<5
5	-	-	70	24	<5
6	$B(C_6F_5)_3$	2	70	24	<5
7	$B(C_6F_5)_3$	5	70	24	26
8	$B(C_6F_5)_3$	10	70	24	62
9	$B(2,4,6-F_3C_6H_2)_3$	10	70	24	<5
10	$B(3,4,5-F_3C_6H_2)_3$	10	70	24	<5
11	BPh_3	10	70	24	<5
12	$BH_3 \cdot THF$	10	70	24	<5
13	BCl_3	10	70	24	<5
14	$B(C_6F_5)_3$ ^[b]	10	160	24	<5 ^[c]
15	$B(C_6F_5)_3$ ^[d]	10	180	1.5	<5 ^[c]
16	$B(C_6F_5)_3$	20	70	24	100
17	$B(C_6F_5)_3$	10	70	48	92

Styrene (0.2 mmol, 22.9 μ L), diphenylamine (0.2 mmol, 33.8 mg). ^[a] Conversion determined by ¹H NMR spectroscopy with mesitylene standard (0.1 mmol, 14 μ L). ^[b] C_6D_6Br used as solvent ^[c] polymerisation of styrene noted instead of hydroamination ^[d] Reaction performed in a microwave vessel; styrene (0.4 mmol, 45.8 μ L), diphenylamine (0.4 mmol, 67.6 mg).

6.3 Scope

After establishing optimised conditions for $B(C_6F_5)_3$ -catalysed hydroamination, the scope of reactivity was probed (Figure 39). A variety of olefins and amines with electron donating and electron withdrawing properties were investigated to explore the aptitude of the $B(C_6F_5)_3$ catalyst. The reagents were combined inside a glove box and allowed to react at 70 °C for 48 hours, at which point ¹H NMR spectroscopy was used to monitor the progression of the reaction. Unfortunately, the versatility of the catalyst was observed to be rather limited and thus only six out of a total fifteen attempted substrate combinations were shown to form the desired hydroamination product. These products were purified through flash column chromatography.

^{ix} Entries 9–17 of the optimisation process were performed by Masters student Jessica Stone.

Initially, the reactivity of styrene with a range of amines was investigated. As already observed through the optimisation procedure, the addition of a $B(C_6F_5)_3$ catalyst permitted the reaction of styrene with diphenylamine to form **6a** in 73% isolated yield. The only other amines that were observed to undergo reactivity with styrene were installed with electron donating functionalities, with di-4-tolylamine and bis(4-(*tert*-butyl)phenyl)amine reacting to form **6b** and **6c** in 30% and 61% respectively.

Attention was then focused on the reaction of diphenylamine with different olefins. Styrene derivatives with *para*-electron-donating groups reacted well with diphenylamine, with 1H NMR spectroscopy recording full conversion into the hydroamination product after 48 hours. Tertiary amines **6d–6e** were thus isolated in 89% and 80% respectively. 1-Vinylnaphthalene was also able to partake in the hydroamination reaction in a limited fashion with diphenylamine, forming **6f** in 22% isolated yield.

Unfortunately, there was no observable reactivity after 48 hours for nine further combinations of substrates, highlighting the difficulty of the reaction. The cyclic amines quinoline and morpholine failed to form **6g** and **6h** upon reaction with styrene. Moreover, the non-sterically hindered amines aniline and *N*-methylaniline were also unable to react with styrene to form **6i** and **6j**. It is likely that these amines were unable to dissociate from the borane catalyst to perform the hydroamination due to their higher basicity in comparison to diphenylamine.

Styrene derivatives bearing electron-withdrawing substituents were observed to be unreactive with diphenylamine and thus no evidence of **6k–6m** formation was observed after 48 hours. As electron donating styrene derivatives had been previously observed to react, 2-methyl styrene was also reacted with diphenylamine, but was recalcitrant under the performed reaction conditions and **6n** was not observed. Finally, the natural product α -pinene was also subjected towards the reaction conditions; however, this was unable to form **6o** upon reaction with diphenylamine.^x

^x Reactions to form **6a** and **6l–6o** were performed by Masters student Jessica Stone.

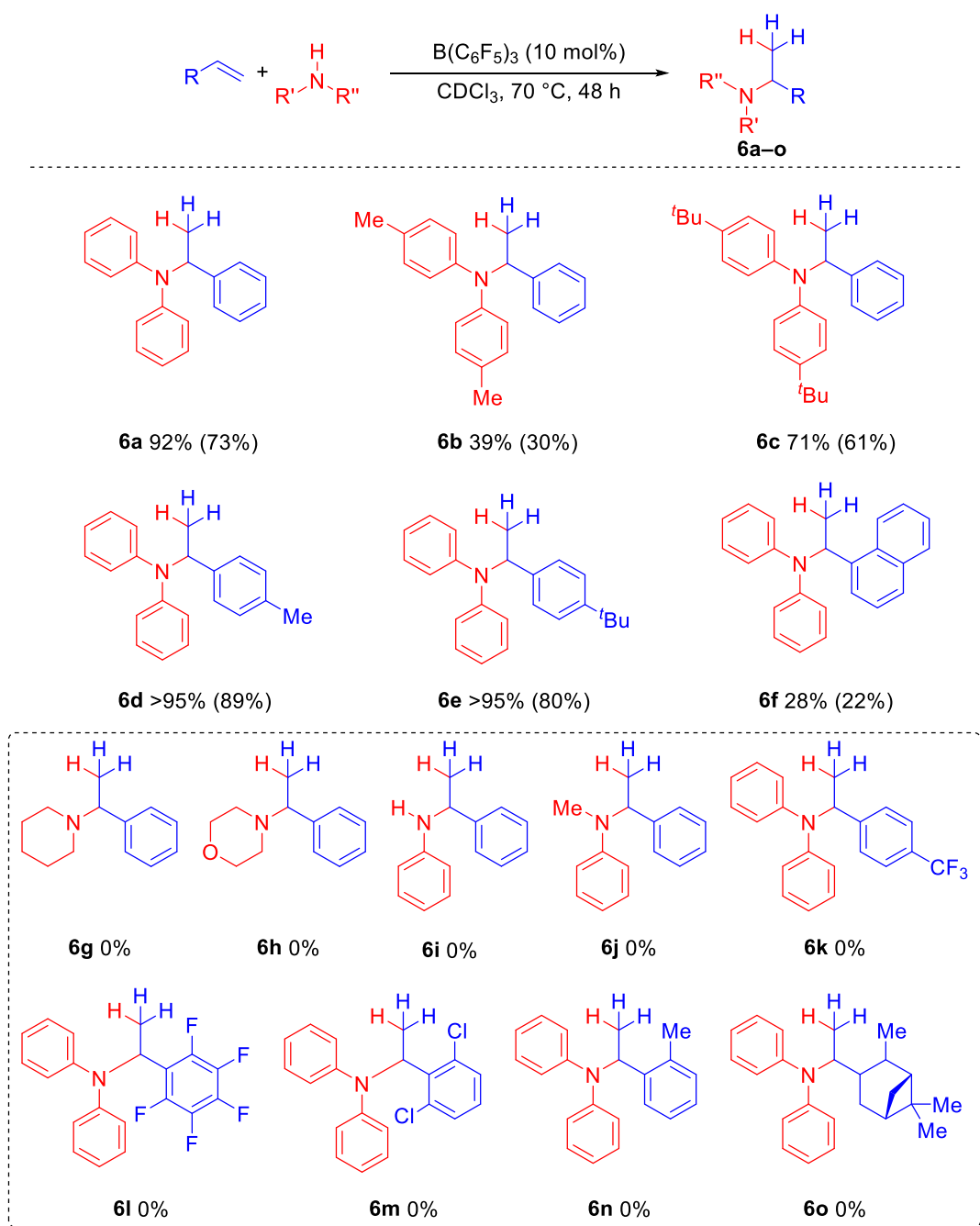


Figure 39 – Scope of borane-catalysed hydroamination. Conversions determined by 1H NMR spectroscopy. Isolated yields given in parentheses.

6.4 Mechanism

The mechanism of $B(C_6F_5)_3$ -catalysed hydroamination of olefins was proposed to be similar to that suggested by Stephan for the $B(C_6F_5)_3$ -catalysed hydroamination of alkynes (chapter one, Scheme 24). Stephan's system suggested that the observed Markovnikov products were the result of FLP-like activation of the alkyne between the acidic and basic sites of the borane and the amine respectively.¹³⁰ As exclusively

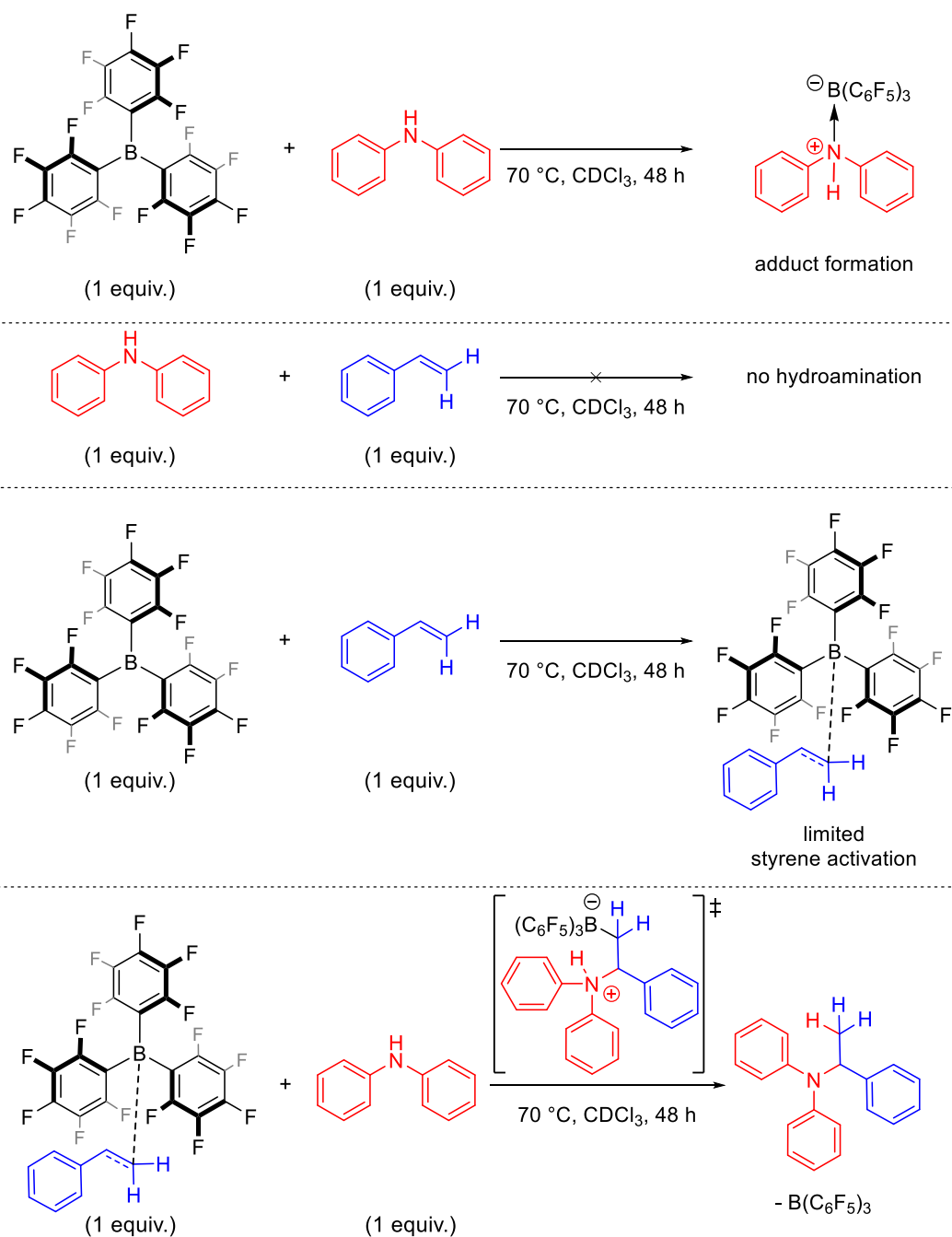
Markovnikov tertiary amines were observed following the hydroamination of olefins in Figure 39, an FLP-like catalytic process was suggested to be present.

To elucidate the mechanism, stoichiometric reactions between the reagents were performed (Scheme 61). As expected, a mixture of diphenylamine and styrene failed to react in the absence of a catalyst.

Predictably, a stoichiometric mixture of $B(C_6F_5)_3$ and diphenylamine registered the formation of an adduct. This was indicated by the single resonance in the ^{11}B NMR spectrum shifting upfield from 58.5 to 50.7 ppm, following its acceptance of electron density from the amine. This result was unsurprising, due to the propensity of acidic and basic compounds to form adducts. Indeed, this adduct was previously reported in the literature as an intermediate towards N–H bond cleavage by a borane/NHC FLP.²³⁴

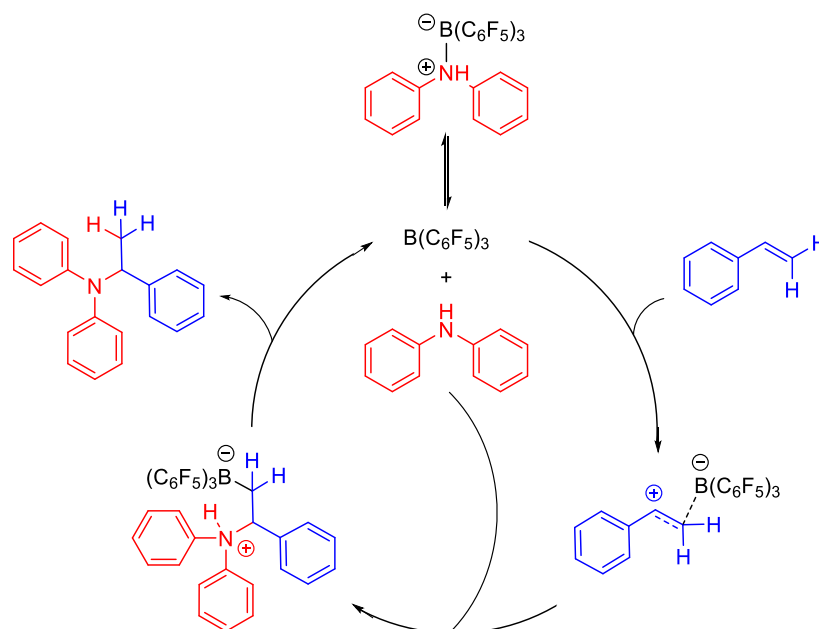
A stoichiometric mixture of $B(C_6F_5)_3$ and styrene registered limited formation of an activated styrene complex. Next to each of the three sets of resonances characteristic of olefinic styrene protons in the 1H NMR spectrum, a low intensity multiplet of the same coupling pattern was situated slightly downfield. It was suggested that these smaller resonances were indicative of the borane activating the olefin.

When the missing component of each of these reactions was introduced, hydroamination was observed after the resultant mixtures were heated at 70 °C for 48 hours. Scheme 61 details only the addition of diphenylamine to the activated styrene complex for clarity. In every case, *in situ* ^{11}B NMR probes recorded the observation of a new, low intensity sharp singlet at 36.6 ppm, which was attributed to the zwitterionic FLP-like activated complex. After 48 hours had elapsed, consumption of the styrene and diphenylamine reagents was observed in the 1H NMR spectrum, with newly generated signals indicative of *N*-phenyl-*N*-(1-phenylethyl)aniline observed instead. Likewise, following 48 hours uncoordinated $B(C_6F_5)_3$ was again observed in the ^{11}B NMR spectrum indicating that it had been released from the substrate.

Scheme 61 – Stoichiometric probes into the $B(C_6F_5)_3$ -catalysed hydroamination mechanism.

It was thus suggested that an equilibrium existed between the borane and the amine in solution. As the borane was relinquished from the adduct it was able to instead activate the olefin substrate at the terminal carbon position. This coordination then resulted in the formation of a partial carbocation on the styrene's alpha-carbon. Reintroduction of the amine resulted in a zwitterionic FLP-like complex, wherein the olefin bond is opened to provide a new C–B and a new C–N bond with the acidic and basic centres of the borane and amine respectively. A resultant 1,3-hydride shift from the nitrogen atom to the terminal carbon atom and concomitant dissociation of the

borane resulted in the tertiary amine product (Scheme 62). These observations suggest that the $B(C_6F_5)_3$ -catalysed hydroamination of olefins closely resembled that of the $B(C_6F_5)_3$ -catalysed hydroamination of alkynes (chapter one, Scheme 24).¹³⁰ Indeed the key steps were also mirrored in intramolecular alkyne hydroamination mechanisms.^{41,132}



Scheme 62 – Proposed mechanism of $B(C_6F_5)_3$ mediated hydroamination of alkenes.

This proposed mechanism explains why highly basic amines were recalcitrant towards the reaction conditions. It is likely that these amines were not able to dissociate themselves from the borane adduct, precluding themselves from performing in the hydroamination reaction by shutting down the catalytic cycle. It also explains why electron donating styrene derivatives performed well, as they were more able to coordinate to the borane catalyst. Moreover, the long timescale of reaction is explained by the high energy required to initially dissociate the $B(C_6F_5)_3$ from the amine to allow both to participate in the catalytic reaction. As this dissociation is energetically intense, it is a very rate limiting step.

6.5 Conclusions and outlook

In conclusion, the ability of $B(C_6F_5)_3$ as an olefin hydroamination catalyst was explored in response to literature precedents which revealed it was able to hydroaminate alkynes. Whilst the scope of the reaction was not as varied as intended, this chapter has shown that this difficult protocol is indeed feasible.

Unfortunately, due to time restraints the scope of olefin hydroamination reactions could not be increased. Bis(4-methoxyphenyl)amine had been ordered; however, this chemical did not arrive in time to be applied towards the reaction conditions. Future work on this project is ongoing within the Melen lab, investigating further conditions which would allow $B(C_6F_5)_3$ to promote the hydroamination of ammonia and primary amines such as aniline.

Chapter seven – Conclusions and outlook

In this thesis a range of Lewis acids based upon boron and aluminium were prepared and a selection of these were shown to act as excellent catalysts for 1,2-functionalisation reactions. Moreover, microwave assisted heating and flow chemistry were employed to augment classical methodologies to mixed degrees of success.

In chapter two, the synthesis of a range of boron and aluminium based Lewis acids were described. The Lewis acidity of these compounds was then compared using a combination of experimental and theoretical probes.

In chapter three, the attempted synthesis of $B(C_6F_5)_3$ via an organolithium intermediate was described when flow chemistry was employed as an enabling technology. Whilst quantitative production of the (pentafluorophenyl)lithium intermediate was recorded, difficulties arose when this intermediate was further reacted with a boron source. Ultimately it was discovered that the excess *n*-butyl lithium reagent required to form the (pentafluorophenyl)lithium intermediate participated in rapid side-reactions with the boron source, precluding the formation of the desired triarylborane. Unfortunately, it was concluded that batch chemistry was more successful for the preparation of triarylboranes than flow chemistry.

Chapter four found that two Lewis acids, $B(3,4,5-F_3C_6H_2)_3$ and $Al(3,4,5-F_3C_6H_2)_3 \cdot Et_2O$ could be used as efficient hydroboration catalysts. $B(3,4,5-F_3C_6H_2)_3$ was recorded to hydroborate a range of aldehydes, ketones, and imines at both room temperature and at 70 °C, with quantitative conversions noted in most cases; however, a limitation in scope was noted, as substrates containing unsaturated homonuclear bonds were found inactive towards reduction. Moreover, $Al(3,4,5-F_3C_6H_2)_3 \cdot Et_2O$ was observed to hydroborate a range of substrates containing unsaturated homonuclear and heteronuclear bonds.

In chapter five, the hydroboration catalysis promoted by $B(3,4,5-F_3C_6H_2)_3$ was improved with the introduction of microwave irradiation. By performing reactions in a microwave reactor at 180 °C, reaction timescale was reduced significantly for all reactions and previously recalcitrant substrates displayed reactivity.

Finally, chapter six discussed the use of $B(C_6F_5)_3$ as a hydroamination catalyst for olefins, expanding upon the literature known alkyne scope. Whilst limitations were

observed in the catalyst versatility, this work recorded the first example of borane-catalysed alkene hydroamination.

The initial aim of this thesis was to investigate further the use of Lewis acidic compounds based upon boron and aluminium, with an emphasis on how enabling technologies could be applied to improve conventional reactions. A clear success story within this thesis is discussed within chapters four and five, wherein the scope of $B(3,4,5-F_3C_6H_2)_3$ -catalysed hydroboration was broadened when microwave irradiation was applied as a heating source; however, further progression can be made. As described in chapter one, the combined fields of main-group catalysis and enabling technologies investigated in unison are rather unexplored and thus the scope of further reactivity is expansive. Below are suggested avenues which could be explored to continue upon the results described within this thesis:

Borane synthesis in flow – Chapter three discussed the attempted synthesis of $B(C_6F_5)_3$ using continuous flow chemistry. This project could be reattempted using the Grignard method of borane synthesis, using a commercial solvated Grignard reagent such as *isopropylmagnesium chloride*, rather than the lithiation method with *n*-butyl lithium. Conventional batch borane synthesis is often limited by lengthy reaction times, low selectivity, and safety risks. Thus, the ability to prepare these versatile main-group catalysts in flow would be a huge asset to the main-group chemist.

Borane-catalysed hydroamination – Chapter six discussed the first forays into the $B(C_6F_5)_3$ -catalysed hydroamination of alkenes. Limitations in scope were observed, with only styrenes containing electron donating functionalities and weakly basic amines amenable to reaction. Further research in the Melen group concerns methods to expand reactivity towards more basic reagents such as aniline and ammonia. One potential avenue which could allow the promotion of this difficult reaction is flow chemistry, wherein enhanced temperature and pressure control could allow for increased selectivity towards hydroamination rather than adduct formation or styrene polymerisation.

Further enabling technologies – This thesis discussed only the enabling technologies of microwave assisted synthesis and flow chemistry; however, there are many more enabling technologies that can be exploited further by the main-group chemist. For example, mechanochemistry and photochemistry are often used in organocatalysis and thus their use to enhance main-group element-catalysed reactions will undoubtedly be realised in the future.

To summarise, this thesis has investigated the reactivity of frustrated Lewis pairs and Lewis acid catalysts, and has used enabling technologies to improve existing reaction protocols.

Chapter eight – Experimental

8.1 General experimental

With the exception of starting material synthesis and column chromatography, all reactions and manipulations were carried out under an atmosphere of dry, O₂-free nitrogen using standard double-manifold techniques with a rotary oil pump. A nitrogen-filled glove box (MBraun) was used to manipulate solids including the storage of starting materials, room temperature reactions, product recovery and sample preparation for analysis. Reagents were purchased from commercial sources (Sigma-Aldrich, Alfa Aesar, Acros, Fluorochem, TCI) and were used as received without purification. The solvents were either used straight from the solvent purification system MB SPS-800 (toluene, dichloromethane, hexane, pentane) or distilled after stirring over sodium/benzophenone (Et₂O), potassium (THF) or calcium hydride (CHCl₃). All solvents were stored over molecular sieves (3 Å). Deuterated solvents were distilled and dried over molecular sieves before use. Microwave synthesis was carried out using a Biotage® Initiator+ Robot 60 Microwave Synthesizer. ¹H, ¹³C{¹H}, ¹¹B, ¹¹B{¹H}, ¹⁹F, ¹⁹F{¹H}, and ³¹P NMR spectra were recorded on a Bruker Avance 500 or a Bruker Avance II 400 spectrometer. Chemical shifts are expressed as parts per million (ppm, δ) downfield of tetramethylsilane (TMS) and are referenced to CDCl₃ (7.26/77.2 ppm) or C₆D₆ (7.16/128.1 ppm) as internal standards. Multinuclear NMR spectra were referenced to BF₃·Et₂O/CDCl₃ (¹¹B), and CFC₃ (¹⁹F), 85% H₃PO₄ (³¹P). The description of signals includes: s = singlet, d = doublet, t = triplet, q = quartet, p = pentet, hept = heptet, dd = doublet of doublets, ov dd = overlapping doublet of doublets, dm = doublet of multiplets, m = multiplet and br = broad. All coupling constants are absolute values and are expressed in Hertz (Hz). IR-Spectra were measured on a Shimadzu IR Affinity-1 photospectrometer. The description of signals includes s = strong, m = medium, w = weak, sh = shoulder, and br = broad. Mass spectra were measured by the School of Chemistry in Cardiff University on a Waters LCT Premier/XE or a Waters GCT Premier spectrometer. Elemental analysis was performed by Dr Nigel Howard at Cambridge University.

DFT calculations were performed using the graphical interface WebMO computational platform, which employed the Gaussian 09 package.^{xi}

Al(2,3,4-F₃C₆H₂)₃, Al(3,4,5-F₃C₆H₂)₃, B(2,3,4-F₃C₆H₂)₃, B(3,4,5-F₃C₆H₂)₃, Al(C₆F₅)₃, and B(C₆F₅)₃ were initially geometry optimised using the meta-hybrid M06-2X functional,²³⁵ and Dunning's correlation-consistent polarised double zeta (cc-pVDZ) basis set on all atoms.²³⁶ After this a vibrational frequency calculation was undertaken to ensure each structure was a minimum on the potential energy landscape.

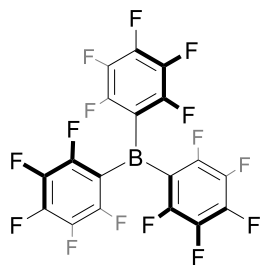
Fluoride ion affinity (FIA) calculations were then performed.²³⁷ This was done by calculating the enthalpy of the triarylalane/triarylborane, fluoride ion and triarylalane–F/triarylborane–F complex. A counterpoise correction was then performed to give a basis set superposition error (BSSE) value, which was added to the enthalpy of the reaction to give the final FIA value. Note that FIA is the negative of the reaction enthalpy plus BSSE.^{xii}

^{xi} Gaussian 09, Revision D.01, Frisch, M. J.; Trucks, G. W.; Schlegel, H. B.; Scuseria, G. E.; Robb, M. A.; Cheeseman, J. R.; Scalmani, G.; Barone, V.; Petersson, G. A.; Nakatsuji, H.; Li, X.; Caricato, M.; Marenich, A.; Bloino, J.; Janesko, B. G.; Gomperts, R.; Mennucci, B.; Hratchian, H. P.; Ortiz, J. V.; Izmaylov, A. F.; Sonnenberg, J. L.; Williams-Young, D.; Ding, F.; Lipparini, F.; Egidi, F.; Goings, J.; Peng, B.; Petrone, A.; Henderson, T.; Ranasinghe, D.; Zakrzewski, V. G.; Gao, J.; Rega, N.; Zheng, G.; Liang, W.; Hada, M.; Ehara, M.; Toyota, K.; Fukuda, R.; Hasegawa, J.; Ishida, M.; Nakajima, T.; Honda, Y.; Kitao, O.; Nakai, H.; Vreven, T.; Throssell, K.; Montgomery, Jr, J. A.; Peralta, J. E.; Ogliaro, F.; Bearpark, M.; Heyd, J. J.; Brothers, E.; Kudin, K. N.; Staroverov, V. N.; Keith, T.; Kobayashi, R.; Normand, J.; Raghavachari, K.; Rendell, A.; Burant, J. C.; Iyengar, S. S.; Tomasi, J.; Cossi, M.; Millam, J. M.; Klene, M.; Adamo, C.; Cammi, R.; Ochterski, J. W.; Martin, R. L.; Morokuma, K.; Farkas, O.; Foresman, J. B.; Fox, D. J. Gaussian, Inc., Wallingford CT, 2016.

^{xii} All DFT calculations were performed by Dr Darren Ould.

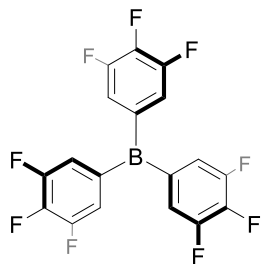
8.2 Synthesis and characterisation of boranes

Tris(pentafluorophenyl)borane $B(C_6F_5)_3$



According to the Lancaster procedure,²⁰¹ Mg turnings (3.05 g, 126 mmol, 1.0 equiv.) were suspended in Et₂O and cooled to 0 °C. 1,2-dibromoethane (0.1 mL, 1.17 mmol) and 1-bromo-pentafluorobenzene (15.7 mL, 126 mmol, 1.0 equiv.) were added dropwise with vigorous stirring. After addition, the reaction mixture was allowed to warm to room temperature and stirred until all magnesium turnings were consumed. The solution was then cooled to 0 °C and added dropwise to a solution of BF₃·Et₂O (5.18 mL, 42 mmol, 0.33 equiv.) in toluene, also at 0 °C. The solution was allowed to warm to room temperature and stirred for a further hour. The diethyl ether solvent was removed *in vacuo* and the resulting toluene solution was heated to reflux for three hours. After this time the reaction was allowed to stir for 16 hours at ambient temperature, after which all volatiles were removed *in vacuo*. This crude material was washed with warm hexane (~45 °C, 200 mL × 3), in which the crude etherate was mildly soluble. The crude etherate solution was passed through a filter canula and all volatiles were removed *in vacuo*. Sublimation of the resultant solid (120 °C, 1 × 10⁻³ mbar) resulted in oily yellow crystals. These yellow crystals were washed with pentane (3 × 5 mL), and sublimed again (120 °C, 1 × 10⁻³ mbar) to afford tris(pentafluorophenyl)borane as colourless crystals. **Yield:** 13.07 g, 25.5 mmol, 61%. Spectroscopic data agrees with literature values.²²⁰

¹¹B NMR (160 MHz, CDCl₃, 298 K) δ/ppm: 59.0 (s). ¹³C NMR (126 MHz, CDCl₃, 298 K) δ/ppm: 148.4 (dm, ¹J_{FC} = 252 Hz, 6C, *o*C), 145.2 (dm, ¹J_{FC} = 248 Hz, 3C, *p*C), 137.7 (dm, ¹J_{FC} = 250 Hz, 6C, *m*C), 113.2 (br, 3C, *i*C). ¹⁹F NMR (471 MHz, CDCl₃, 298 K) δ/ppm: -127.81 (d, ³J_{FF} = 19.8 Hz, 6F, *o*F), -142.60 (s, 3F, *p*F), -159.86 (td, ³J_{FF} = 20.8, ³J_{FF} = 7.4 Hz, 6F, *m*F).

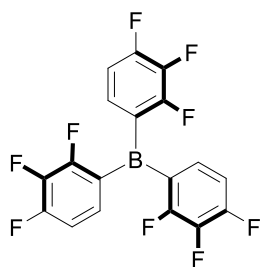
Tris(3,4,5-trifluorophenyl)borane B(3,4,5-F₃C₆H₂)₃*Grignard Method*

Mg turnings (3.05 g, 126 mmol, 1.0 equiv.) were suspended in Et₂O and cooled to 0 °C. 1,2-dibromoethane (0.1 mL, 1.17 mmol) and 1-bromo-3,4,5-fluorobenzene (15.0 mL, 126 mmol, 1.0 equiv.) were added dropwise with vigorous stirring. After addition, the reaction mixture was allowed to warm to room temperature and stirred until all magnesium turnings were consumed. The solution was then cooled to 0 °C and added dropwise to a solution of BF₃·Et₂O (5.18 mL, 42 mmol, 0.33 equiv.) in toluene, also at 0 °C. The solution was allowed to warm to room temperature and stirred for a further hour. The diethyl ether solvent was removed *in vacuo* and the resulting toluene solution was heated to reflux for three hours. After this time the reaction was allowed to stir for 16 hours at ambient temperature, after which all volatiles were removed *in vacuo*. Sublimation of the resultant solid (120 °C, 1 × 10⁻³ mbar) resulted in oily yellow crystals. These yellow crystals were washed with pentane (3 × 5 mL), and sublimed again (120 °C, 1 × 10⁻³ mbar) to afford tris(3,4,5-trifluorophenyl)borane as colourless crystals. **Yield:** 4.92 g, 12.2 mmol, 29%.

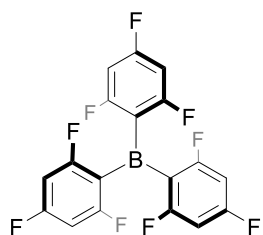
Lithiation Method

1-bromo-3,4,5-fluorobenzene (5 mL, 42 mmol) was suspended in Et₂O and cooled to -78 °C. ⁿBuLi was added dropwise (16.8 mL, 2.5 M, 42 mmol) with vigorous stirring. After addition, the reaction mixture was allowed to stir at -78 °C for two hours. BF₃·Et₂O (1.7 mL, 14 mmol) was then added dropwise with vigorous stirring. The solution was allowed to warm to room temperature, and was then stirred for 16 hours, after which all volatiles were removed *in vacuo*. Sublimation of the resultant solid (120 °C, 1 × 10⁻³ mbar) resulted in oily yellow crystals. These yellow crystals were washed with pentane (3 × 5 mL), and sublimed again (120 °C, 1 × 10⁻³ mbar) to afford tris(3,4,5-trifluorophenyl)borane as colourless crystals. **Yield:** 1.351 g, 3.34 mmol, 24%.

Spectroscopic data agrees with literature values.¹⁰⁷ ¹H NMR (500 MHz, CDCl₃, 298 K) δ/ppm: 7.19–7.16 (m, 6H, Ar–H). ¹¹B{¹H} NMR (160 MHz, CDCl₃, 298 K) δ/ppm: 64.5 (s). ¹³C{¹H} NMR (126 MHz, CDCl₃, 298 K) δ/ppm: 151.5 (ddd, ¹J_{FC} = 253.8 Hz, ²J_{FC} = 10.0 Hz, ³J_{FC} = 3.1 Hz, mC), 142.9 (dt, ¹J_{FC} = 260.8 Hz, ²J_{FC} = 16.7 Hz, pC), 136.4–136.0, (m, iC), 121.9 (dd, ²J_{FC} = 13.6 Hz, ³J_{FC} = 5.0 Hz, oC). ¹⁹F NMR (471 MHz, CDCl₃, 298 K) δ/ppm: -133.3 (dd, ³J_{FF} = 20.0 Hz, ³J_{FH} = 7.2 Hz, 6F, mF), -158.2 (tt, ³J_{FF} = 20.0 Hz, ⁴J_{FH} = 6.8 Hz, 3F, pF). **EA** calcd for C₁₈H₆BF₉: C, 53.51; H, 1.50; N, 0.00. Found: C, 53.27; H, 1.41; N, 0.00.

Tris(2,3,4-trifluorophenyl)borane B(2,3,4-F₃C₆H₂)₃

Mg turnings (486 mg, 20 mmol, 1.0 equiv.) were suspended in Et₂O and cooled to 0 °C. 1,2-dibromoethane (0.1 mL, 1.17 mmol) and 1-bromo-2,3,4-fluorobenzene (2.37 mL, 20 mmol, 1.0 equiv.) were added dropwise with vigorous stirring. After addition, the reaction mixture was allowed to warm to room temperature and stirred until all magnesium turnings were consumed. The solution was then cooled to 0 °C and added dropwise to a solution of BF₃·Et₂O (0.83 mL, 6.7 mmol, 0.33 equiv.) in toluene, also at 0 °C. The solution was allowed to warm to room temperature and stirred for a further hour. The diethyl ether solvent was removed *in vacuo* and the resulting toluene solution was heated to reflux for three hours. After this time the reaction was allowed to stir for 16 hours at ambient temperature, after which all volatiles were removed *in vacuo*. Sublimation of the resultant solid (120 °C, 1 × 10⁻³ mbar) resulted in oily yellow crystals. These yellow crystals were washed with pentane (3 × 5 mL), and sublimed again (120 °C, 1 × 10⁻³ mbar) to afford tris(2,3,4-trifluorophenyl)borane as colourless crystals. **Yield:** 376 mg, 0.93 mmol, 14%. **¹H NMR** (400 MHz, C₆D₆, 298 K) δ/ppm: 6.43–6.38 (m, 6H, Ar–H). **¹¹B{¹H} NMR** (128 MHz, C₆D₆, 298 K) δ/ppm: 62.6 (s). **¹³C{¹H} NMR** (126 MHz, C₆D₆, 298 K) δ/ppm: 156.2 (ddd, ¹J_{FC} = 59.3 Hz, ³J_{FC} = 9.3 Hz, ⁴J_{FC} = 3.8 Hz, 3C, oC–F), 153.7 (ddd, ¹J_{FC} = 62.9 Hz, ³J_{FC} = 9.4 Hz, ⁴J_{FC} = 3.9 Hz, 3C, pC–F), 140.0 (ddd, ¹J_{FC} = 254.1 Hz, ³J_{FC} = 17.1 Hz, ³J_{FC} = 14.6 Hz, 3C, mC–F), 132.4–132.0 (m, 3C, oC–H), 126.2 (br, 3C, iC), 112.9 (dd, ³J_{FC} = 16.8 Hz, ⁴J_{FC} = 3.2 Hz, 3C, mC). **¹⁹F{¹H} NMR** (376 MHz, C₆D₆, 298 K) δ/ppm: -121.6 (dd, ³J_{FF} = 20.9 Hz, ⁴J_{FF} = 12.4 Hz, 3F, oF), -126.0 (dd, ³J_{FF} = 20.9 Hz, ⁴J_{FF} = 12.4 Hz, 3F, pF), -160.8 (t, ³J_{FF} = 20.9 Hz, 3F, mF). **HRMS (EI⁺) [M]⁺ [C₁₈H₆BF₉]⁺:** calculated 404.0419, found, 404.0410. **EA** calcd for C₁₈H₆BF₉: C, 53.51; H, 1.50; N, 0.00. Found: C, 53.31; H, 1.51; N, 0.00.

Tris(2,4,6-trifluorophenyl)borane B(2,4,6-F₃C₆H₂)₃

Mg turnings (486 mg, 20 mmol, 1.0 equiv.) were suspended in Et₂O and cooled to 0 °C. 1,2-dibromoethane (0.1 mL, 1.17 mmol) and 1-bromo-2,4,6-fluorobenzene (2.36 mL, 20 mmol, 1.0 equiv.) were added dropwise with vigorous stirring. After addition, the reaction mixture was allowed to warm to room temperature and stirred until all magnesium turnings were consumed. The solution was then cooled to 0 °C and added dropwise to a solution of BF₃·Et₂O (0.83 mL, 6.7 mmol, 0.33 equiv.) in toluene, also at 0 °C. The solution was allowed to warm to room temperature and stirred for a further hour. The diethyl ether solvent was removed *in vacuo* and the resulting toluene solution was heated to reflux for three hours. After this time the reaction was allowed to stir for 16 hours at ambient temperature, after which all volatiles were removed *in vacuo*. Sublimation of the resultant solid (120 °C, 1 × 10⁻³ mbar) resulted in oily yellow crystals. These yellow crystals were washed with pentane (3 × 5 mL), and sublimed again (120 °C, 1 × 10⁻³ mbar) to afford tris(2,4,6-trifluorophenyl)borane as colourless crystals. **Yield:** 620 mg, 1.53 mmol, 23%. Spectroscopic data agrees with literature values.²³⁸ **¹H NMR** (500 MHz, CDCl₃, 298 K) δ/ppm: 6.60–6.67 (m, 6H, Ar–H). **¹¹B{¹H} NMR** (160 MHz, CDCl₃, 298 K) δ/ppm: 59.5 (br). **¹³C{¹H} NMR** (126 MHz, CDCl₃, 298 K) δ/ppm: 168.1–167.2 (m, 3C, *p*C), 165.4–164.6 (m, 6C, *o*C), 114.3 (br, 3C, *i*C) 100.8–100.2 (m, 6C, *m*C). **¹⁹F NMR** (471 MHz, CDCl₃, 298 K) δ/ppm: -95.77 (d, ³J_{FF} = 11.4 Hz, 6F, *o*F), -100.37 (t, ³J_{FF} = 11.3 Hz, 3F, *p*F).

Crystal refinement data for novel boranes:

Compound	B(2,3,4-F₃C₆H₂)₃
Empirical formula	C ₁₈ H ₆ BF ₉
Formula Weight	404.04
Temperature/ K	150(2)
Wavelength /Å	0.71073
Crystal System	Monoclinic
Space Group	<i>P</i> 2 ₁ / <i>n</i>
<i>a</i> / Å	8.6982(5)
<i>b</i> / Å	16.8822(9)
<i>c</i> / Å	10.6039(5)
α / °	90
β / °	90.014(5)
γ / °	90
Volume/ Å ³	1557.13(15)
Z	4
Density (calc)/ g cm ⁻³	1.723
Absorption coefficient/ mm ⁻¹	0.175
F(000)	800
Crystal size/ mm ³	0.479 × 0.301 × 0.199
θ range/ °	3.363 to 29.900
Index ranges	-11 ≤ <i>h</i> ≤ 11 -23 ≤ <i>k</i> ≤ 21 -14 ≤ <i>l</i> ≤ 14
Reflections collected	16055
Independent reflections	3966

R(int)	0.0724
Absorption Correction	Semi-empirical from equivalents
Data / restraints / parameters	3966 / 0 / 254
Goodness of fit, S	1.117
Final R indices [$I > 2\sigma(I)$]	$R_1 = 0.0488$ $wR_2 = 0.1182$
R indices (all data)	$R_1 = 0.0687$ $wR_2 = 0.1376$
Max/min residual electron density/ $e\text{\AA}^{-3}$	+0.643 -0.256

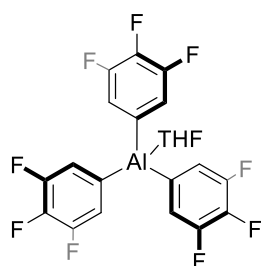
8.3 Synthesis and characterisation of alanes

CAUTION

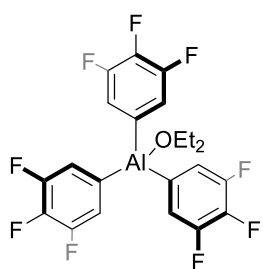
The alane compounds described herein are potentially shock and thermally sensitive due to their potential to decompose into benzyne derivatives.

Appropriate care should be taken upon their synthesis.

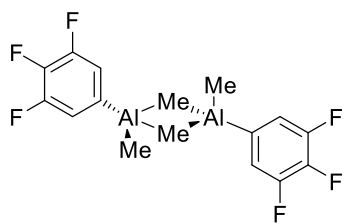
Tetrahydrofuran adduct of tris(3,4,5-trifluorophenyl)alane $\text{Al}(\text{3,4,5-F}_3\text{C}_6\text{H}_2)_3 \cdot \text{THF}$



Mg turnings (486 mg, 20 mmol, 1.0 equiv.) were suspended in THF and cooled to 0 °C. 1,2-dibromoethane (0.1 mL, 1.17 mmol) and 1-bromo-3,4,5-trifluorobenzene (2.39 mL, 20.0 mmol, 1.0 equiv.) were added dropwise with vigorous stirring. After addition, the reaction mixture was allowed to warm to room temperature and stirred until all magnesium turnings were consumed. The solution was then cooled to 0 °C and added dropwise to a solution of AlCl_3 (889 mg, 6.7 mmol, 0.33 equiv.) in toluene, also at 0 °C. The solution was allowed to warm to room temperature and stirred for a further hour. The diethyl ether solvent was removed *in vacuo* and the resulting toluene solution was heated to reflux for three hours. After this time the reaction was allowed to stir for 16 hours at ambient temperature. After this the solution was filtered *via* a filter cannula and the toluene solvent removed *in vacuo*. The resulting solid was washed with pentane and dried *in vacuo* to give the tetrahydrofuran adduct of tris(3,4,5-trifluorophenyl)alane as an off-white powder. **Yield:** 342 mg, 0.693 mmol, 10.4%. Due to the potential for benzyne formation the product was not sublimed. **$^1\text{H NMR}$** (500 MHz, C_6D_6 , 298 K) δ /ppm: 7.14–7.06 (m, 6H, Ar–H), 3.10 (br, 4H, THF), 0.46–0.34 (m, 4H, THF). **$^{13}\text{C}\{^1\text{H}\}$ NMR** (101 MHz, C_6D_6 , 298 K) δ /ppm: 152.1 (dd, $^1J_{\text{FC}} = 254.5$ Hz, $^2J_{\text{FC}} = 9.0$ Hz, 6C, *m*C), 141.9 (br, 3C, *i*C), 140.9 (dd, $^1J_{\text{FC}} = 252.8$ Hz, $^2J_{\text{FC}} = 30.7$ Hz, 3C, *p*C), 120.7 (d, $^2J_{\text{FC}} = 9.1$ Hz, 6C, *o*C), 69.4 (s, 2C, THF), 13.4 (s, 2C, THF). **$^{19}\text{F NMR}$** (471 MHz, C_6D_6 , 298 K) δ /ppm: -135.54 (s, 6F, *m*F), -160.69 (s, 3F, *p*F).

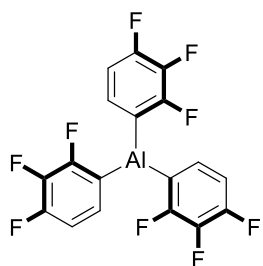
Tris(3,4,5-trifluorophenyl)alane etherate $\text{Al}(\text{3,4,5-F}_3\text{C}_6\text{H}_2)_3 \cdot \text{Et}_2\text{O}$ 

Mg turnings (486 mg, 20 mmol, 1.0 equiv.) were suspended in Et_2O and cooled to 0 °C. 1,2-dibromoethane (0.1 mL, 1.17 mmol) and 5-bromo-1,2,3-trifluorobenzene (2.39 mL, 20.0 mmol, 1.0 equiv.) were added dropwise with vigorous stirring. After addition, the reaction mixture was allowed to warm to room temperature and stirred until all magnesium turnings were consumed. The solution was then cooled to 0 °C and added dropwise to a solution of AlCl_3 (888 mg, 6.7 mmol, 0.33 equiv.) in toluene, also at 0 °C. The solution was allowed to warm to room temperature and stirred for a further hour. The diethyl ether solvent was removed *in vacuo* and the resulting toluene solution was heated to reflux for three hours. After this time the reaction was allowed to stir for 16 hours at ambient temperature. After this the solution was filtered *via* a filter cannula and the toluene solvent removed *in vacuo*. The resulting solid was washed with pentane and dried *in vacuo* to give the etherate product tris(3,4,5-trifluorophenyl)alane as an off-white powder. **Yield:** 1.58 g, 3.2 mmol, 48%. Crystals suitable for single crystal X-ray diffraction were grown from a saturated solution of toluene with a few drops of pentane added and cooled to -40 °C. Due to the potential for benzyne formation the product was not sublimed. **Mp:** 126–134 °C. **$^1\text{H NMR}$** (400 MHz, C_6D_6 , 298 K) δ /ppm: 6.99 (ov dd, $J = 7.0$ Hz, 6H, Ar-H), 3.00 (q, $^3J_{\text{HH}} = 7.0$ Hz, 4H, CH_2), 0.28 (t, $^3J_{\text{HH}} = 7.0$ Hz, 4H, CH_3). **$^{13}\text{C}\{^1\text{H}\}$ NMR** (101 MHz, C_6D_6 , 298 K) δ /ppm: 151.4 (dd, $^1J_{\text{FC}} = 254$ Hz, $^2J_{\text{FC}} = 11.8$ Hz, 6C, *mC*), 140.4 (m, 3C, *iC*), 140.3 (dt, $^1J_{\text{FC}} = 252$ Hz, $^2J_{\text{FC}} = 11.8$ Hz, 3C, *pC*), 120.2 (dd, $^2J_{\text{FC}} = 11.1$ Hz, $^3J_{\text{FC}} = 4.2$ Hz, 6C, *oC*), 68.2 (s, 2C, CH_2), 12.5 (s, 2C, CH_3). **$^{19}\text{F NMR}$** (376 MHz, C_6D_6 , 298 K) δ /ppm: -135.5 (d, $^3J_{\text{FF}} = 19.9$ Hz, 6F, *mF*), -160.7 (t, $^3J_{\text{FF}} = 19.9$ Hz, 3F, *pF*). **IR** ν_{max} (cm^{-1}): 1601 (m), 1512 (s), 1387 (s), 1302 (s), 1267 (w), 1223 (w), 1190 (w), 1148 (w), 1088 (s), 1028 (s), 1015 (s), 887 (m), 878 (m), 849 (s), 772 (m), 745 (m), 710 (m), 600 (s), 584 (s), 519 (s), 503 (sh). **HRMS (EI $^+$)** $[\text{M-OEt}_2]^+ [\text{C}_{18}\text{H}_6\text{AlF}_9]^+$: calculated 420.0141, found 419.1153.

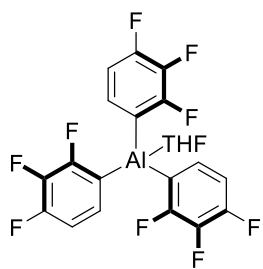
μ_2 -Dimethyl-bis[(3,4,5-trifluorophenyl)methyl-alane] μ_2 -[Al(3,4,5-F₃C₆H₂)Me]₂

Tris(3,4,5-trifluorophenyl)borane (206 mg, 0.51 mmol, 1.0 equiv.) was suspended in hexane (3 mL). To this, trimethylaluminium (0.25 mL, 0.51 mmol, 1.0 equiv., 2.0 M solution in hexanes) was added dropwise and the reaction was left undisturbed for two days. During this

time, crystals of the alane were developed. The solvent level was reduced by removal *in vacuo* and placed in the freezer at -40 °C to ensure all the product had crystallised out. The hexane solvent was removed *via* pipette and the crystals dried *in vacuo* to give μ_2 -dimethyl-bis[(3,4,5-trifluorophenyl)methyl-alane] as an off-white solid. **Yield:** 158 mg, 0.42 mmol, 83%. **Mp:** 105–110 °C. **¹H NMR** (500 MHz, C₆D₆, 298 K) δ /ppm: 6.87 (ov dd, $J = 7.0$ Hz, 4H, Ar–H), -0.39 (s, 12H, Me). **¹³C{¹H} NMR** (126 MHz, C₆D₆, 298 K) δ /ppm: 151.5 (ddd, $^1J_{FC} = 256$ Hz, $^2J_{FC} = 12.3$ Hz, $^3J_{FC} = 1.6$ Hz, 4C, *mC*), 141.4 (dt, $^1J_{FC} = 254$ Hz, $^2J_{FC} = 12.3$ Hz, 2C, *pC*), 138.5 (2C, *iC*), 121.9 (dd, $^2J_{FC} = 11.6$ Hz, $^3J_{FC} = 3.0$ Hz, 6C, *oC*), -7.9 (4C, Me). **¹⁹F NMR** (376 MHz, C₆D₆, 298 K) δ /ppm: -135.3 (dd, $^3J_{FF} = 19.8$ Hz, $^3J_{FH} = 5.8$ Hz, 4F, *mF*), -158.2 (s, 2F, *pF*). **IR ν_{max}** (cm⁻¹): 1516 (m), 1387 (m), 1302 (m), 1198 (w), 1088 (m), 1030 (m), 878 (m), 849 (m), 654 (br, m), 579 (br, m).

Tris(2,3,4-trifluorophenyl)alane Al(2,3,4-F₃C₆H₂)₃

Tris(2,3,4-trifluorophenyl)borane (300 mg, 0.74 mmol, 1.0 equiv.) was suspended in hexane (3 mL). To this, trimethylaluminium (0.37 mL, 0.74 mmol, 1.0 equiv., 2.0 M solution in hexanes) was added dropwise and the reaction was left undisturbed for four days. During this time, crystals of the alane were developed. The solvent level was reduced by removal *in vacuo* and placed in the freezer at -40 °C to ensure all the product had crystallised out. The hexane solvent was removed *via* pipette and the crystals dried *in vacuo* to give tris(2,3,4-trifluorophenyl)alane as an off-white solid. **Yield:** 243 mg, 0.58 mmol, 78%. Crystals suitable for single crystal X-ray diffraction were collected from the hexane solution. **Mp:** 145–147 °C. **¹H NMR** (400 MHz, C₆D₆, 298 K) δ/ppm: 6.74 (br, 3H, Ar–H), 6.53 (dd, ³J_{FH} = 14.8 Hz, ³J_{HH} = 8.5 Hz, 3H, Ar–H). **¹³C{¹H} NMR** (126 MHz, C₆D₆, 298 K) δ/ppm: 156.9 (d, ¹J_{FC} = 235 Hz, 3C, Ar, oC–F), 152.8 (d, ¹J_{FC} = 252 Hz, 3C, Ar, pC–F), 139.4 (ddd, ¹J_{FC} = 255 Hz, ²J_{FC} = 21.4 Hz, ²J_{FC} = 14.7 Hz, 3C, Ar, mC–F), 132.1 (s, 3C, oC–H), 130.7 (s, 3C, iC), 113.5 (d, ²J_{FC} = 14.9 Hz, 3C, mC–H). **¹⁹F NMR** (376 MHz, C₆D₆, 298 K) δ/ppm: -115.1 (s, 3F, Ar–F), -132.9 (s, 3F, Ar–F), -162.1–162.2 (m, 3F, Ar–F). **HRMS (ES⁺):** [M]⁺ [C₁₈H₆AlF₉]⁺: calculated 420.0141, found 419.3153. **EA** calcd for C₁₈H₆AlF₉: C, 51.45; H, 1.44; N, 0.00. Found: C, 51.49; H, 1.43; N, 0.00

Tetrahydrofuran adduct of tris(2,3,4-trifluorophenyl)alane $\text{Al}(\text{2,3,4-F}_3\text{C}_6\text{H}_2)_3\cdot\text{THF}$ 

1-bromo-3,4,5-fluorobenzene (5 mL, 42 mmol) was suspended in Et_2O and cooled to $-78\text{ }^\circ\text{C}$. $^n\text{BuLi}$ was added dropwise (16.8 mL, 2.5 M, 42 mmol) with vigorous stirring. After addition, the reaction mixture was allowed to stir at $-78\text{ }^\circ\text{C}$ for two hours. AlCl_3 (1.86 g, 14 mmol, 0.33 equiv.) was then added *via* a powder funnel in four increments with vigorous stirring. The solution was allowed to warm to room temperature and was then stirred for 16 hours. The yellow solution was passed through a filter canula and all solvents were removed *in vacuo*. DCM was added to the resultant yellow solid, and the solution was isolated through a filter canula. All volatiles were removed *in vacuo* to form a crude yellow powder, which were dissolved in a 10:1 mixture of DCM and pentane. Crystals of the THF adduct of tris(2,3,4-trifluorophenyl)alane which were suitable for single crystal X-ray diffraction were grown from this mixture. **Yield:** 78 mg, 0.16 mmol, 1.1%. **$^1\text{H NMR}$** (400 MHz, CDCl_3 , 298 K) δ /ppm: 7.10–7.00 (m, 3H, Ar–H), 6.99–6.88 (m, 3H, Ar–H), 4.39 (s, 6H, THF), 2.64–2.13 (m, 6H, THF). **$^{13}\text{C}\{^1\text{H}\}$ NMR** (101 MHz, CDCl_3 , 298 K) δ /ppm: 156.5 (ddd, $^1J_{\text{FC}} = 232.6\text{ Hz}$, $^2J_{\text{FC}} = 6.6\text{ Hz}$, $^3J_{\text{FC}} = 2.9\text{ Hz}$, 3C, oC–F), 152.2 (ddd, $^1J_{\text{FC}} = 249.5\text{ Hz}$, $^2J_{\text{FC}} = 10.0\text{ Hz}$, $^3J_{\text{FC}} = 3.9\text{ Hz}$, 3C, pC), 139.4 (ddd, $^1J_{\text{FC}} = 253.9\text{ Hz}$, $^2J_{\text{FC}} = 22.3\text{ Hz}$, $^2J_{\text{FC}} = 14.4\text{ Hz}$, 3C, mC–F), 132.5–132.2 (m, 3C, oC–H), 126.2 (d, $^2J_{\text{FC}} = 51.5\text{ Hz}$, 3C, iC), 113.4 (d, $^2J_{\text{FC}} = 15.5\text{ Hz}$, 3C, mC–H), 74.0 (s, 4C, THF), 25.7 (s, 4C, THF). **$^{19}\text{F NMR}$** (376 MHz, CDCl_3 , 298 K) δ /ppm: -117.89 (dd, $^3J_{\text{FF}} = 26.9\text{ Hz}$, $^4J_{\text{FF}} = 8.3\text{ Hz}$, 3F, pF), -135.21 (dd, $^3J_{\text{FF}} = 19.1\text{ Hz}$, $^4J_{\text{FF}} = 8.3\text{ Hz}$, 3F, oF), -163.21 (dd, $^3J_{\text{FF}} = 26.9\text{ Hz}$, $^4J_{\text{FF}} = 19.1\text{ Hz}$, 3F, mF).

Crystal refinement data for novel alanes:

Compound	μ_2 -[Al(3,4,5-F ₃ C ₆ H ₂)Me] ₂	Al(3,4,5-F ₃ C ₆ H ₂) ₃ ·OEt ₂
Empirical formula	C ₈ H ₈ AlF ₃	C ₂₂ H ₁₆ AlF ₉ O
Formula Weight	188.12	494.33
Temperature/ K	150(2)	150(2)
Wavelength /Å	0.71073	1.54178
Crystal System	Triclinic	Triclinic
Space Group	<i>P</i> -1	<i>P</i> -1
<i>a</i> / Å	6.9009(10)	10.2941(10)
<i>b</i> / Å	7.4059(12)	10.3687(8)
<i>c</i> / Å	9.7517(11)	10.6335(7)
α / °	68.597(13)	99.732(6)
β / °	71.726(12)	98.186(7)
γ / °	72.199(14)	90.099(7)
Volume/ Å ³	430.18(12)	1106.85(16)
Z	1	2
Density (calc)/ g cm ⁻³	1.452	1.483
Absorption coefficient/ mm ⁻¹	0.223	1.625
F(000)	192	500
Crystal size/ mm ³	0.307 × 0.219 × 0.134	0.327 × 0.176 × 0.145
θ range/ °	3.480 to 29.439	4.263 to 72.675
Index ranges	-9 ≤ <i>h</i> ≤ 9	-10 ≤ <i>h</i> ≤ 12
	-9 ≤ <i>k</i> ≤ 8	-12 ≤ <i>k</i> ≤ 12
	-12 ≤ <i>l</i> ≤ 12	-13 ≤ <i>l</i> ≤ 9
Reflections collected	3077	7493
Independent reflections	3077	4250
R(int)	0.0476	0.0311

Absorption Correction	Multi-scan	Gaussian
Data / restraints / parameters	3077 / 6 / 122	4250 / 58 / 366
Goodness of fit, S	0.982	1.047
Final R indices [$I > 2\sigma(I)$]	$R_1 = 0.0585$ $wR_2 = 0.1349$	$R_1 = 0.0690$ $wR_2 = 0.1902$
R indices (all data)	$R_1 = 0.1024$ $wR_2 = 0.1489$	$R_1 = 0.0946$ $wR_2 = 0.2175$
Max/min residual electron density/ $e\text{\AA}^{-3}$	+0.305 -0.345	+0.327 -0.448

Compound	Al(2,3,4-F₃C₆H₂)₃	Al(2,3,4-F₃C₆H₂)₃·THF
Empirical formula	C ₁₈ H ₆ AlF ₉	C ₂₂ H ₁₄ Al F ₉ O
Formula Weight	420.21	492.31
Temperature/ K	150(2)	150(2)
Wavelength /Å	0.71073	0.71073
Crystal System	Orthorhombic	Triclinic
Space Group	<i>Pbca</i>	<i>P</i> -1
<i>a</i> / Å	9.8089(7)	10.3004(5)
<i>b</i> / Å	17.9147(13)	10.3101(6)
<i>c</i> / Å	18.0420(19)	10.3293(6)
α / °	90	71.348(5)
β / °	90	84.423(4)
γ / °	90	78.631(4)
Volume/ Å ³	3170.4(5)	1018.25(10)
Z	8	2
Density (calc)/ g cm ⁻³	1.761	1.606
Absorption coefficient/ mm ⁻¹	0.228	0.194
F(000)	1664	496
Crystal size/ mm ³	0.252 × 0.240 × 0.187	0.445 × 0.286 × 0.210
θ range/ °	3.272 to 27.498	3.398 to 29.527
Index ranges	-12 ≤ <i>h</i> ≤ 12 -22 ≤ <i>k</i> ≤ 23 -23 ≤ <i>l</i> ≤ 17	-14 ≤ <i>h</i> ≤ 14, -14 ≤ <i>k</i> ≤ 11, -14 ≤ <i>l</i> ≤ 12
Reflections collected	16279	7939
Independent reflections	3616	4742
R(int)	0.0922	0.0233

Absorption Correction	Semi-empirical from equivalents	Gaussian
Data / restraints / parameters	3616 / 12 / 266	4742 / 0 / 298
Goodness of fit, S	1.027	1.024
Final R indices [$I > 2\sigma(I)$]	$R_1 = 0.0839$ $wR_2 = 0.1960$	$R_1 = 0.0469$ $wR_2 = 0.1008$
R indices (all data)	$R_1 = 0.1391$ $wR_2 = 0.2413$	$R_1 = 0.0720$ $wR_2 = 0.1158$
Max/min residual electron density/ $e\text{\AA}^{-3}$	+0.672 -0.567	+0.437 -0.323

8.4 Lewis acidity determination

8.4.1 The Gutmann-Beckett method of Lewis acidity determination

General procedure 1

The Lewis acid (0.0625 mmol, 1.0 equiv.) was dissolved in CDCl_3 (0.7 mL) and added to an NMR tube. Triethyl phosphine oxide (5 mg, 0.0375 mmol, 0.6 equiv.) and a capillary containing a PPh_3 standard in CDCl_3 were also added, before the NMR tube was sealed and inverted several times. The ^{31}P NMR spectrum was recorded, and the signals were referenced to PPh_3 in CDCl_3 ($\delta = -5.21$ ppm).¹⁴ The acceptor number was calculated through the Gutmann-Beckett procedure.^{7,8}

Tris(pentafluorophenyl)borane

According to *general procedure 1*, tris(pentafluorophenyl)borane (32.0 mg, 0.0625 mmol) was combined with triethylphosphine oxide to form the corresponding adduct. ^{31}P NMR (162 MHz, CDCl_3 , 298 K) δ/ppm : 75.96 (s). **AN** = 77.45.

Tris(3,4,5-trifluorophenyl)borane

According to *general procedure 1*, tris(3,4,5-trifluorophenyl)borane (25.3 mg, 0.0625 mmol) was combined with triethylphosphine oxide to form the corresponding adduct. ^{31}P NMR (162 MHz, CDCl_3 , 298 K) δ/ppm : 77.67 (s). **AN** = 81.24.

Tris(2,3,4-trifluorophenyl)borane

According to *general procedure 1*, tris(2,3,4-trifluorophenyl)borane (25.3 mg, 0.0625 mmol) was combined with triethylphosphine oxide to form the corresponding adduct. ^{31}P NMR (162 MHz, CDCl_3 , 298 K) δ/ppm : 72.53 (s). **AN** = 69.85.

Tris(2,4,6-trifluorophenyl)borane

According to *general procedure 1*, tris(2,3,4-trifluorophenyl)borane (25.3 mg, 0.0625 mmol) was combined with triethylphosphine oxide to form the corresponding adduct. ^{31}P NMR (162 MHz, CDCl_3 , 298 K) δ/ppm : 71.70 (s). **AN** = 68.01.

8.4.2 The Childs method of Lewis acidity determination

General procedure 2

The Lewis acid (0.0625 mmol, 1.0 equiv.) was dissolved in CDCl_3 (0.7 mL) and added to an NMR tube. Crotonaldehyde (5.2 μL , 0.0625 mmol, 1.0 equiv.) was also added, before the NMR tube was sealed and inverted several times. The ^1H NMR spectrum was recorded, and the signals were referenced to CDCl_3 ($\delta = 7.26$ ppm). The relative acidity was calculated through the Childs procedure.⁹

Tris(pentafluorophenyl)borane

According to *general procedure 2*, tris(pentafluorophenyl)borane (32.0 mg, 0.0625 mmol) was combined with crotonaldehyde to form the corresponding adduct. ^1H NMR (400 MHz, CDCl_3 , 298 K) $\Delta\delta$ of H^3 : 0.96 ppm. **Relative acidity** = 0.64.

Tris(3,4,5-trifluorophenyl)borane

According to *general procedure 2*, tris(3,4,5-trifluorophenyl)borane (25.3 mg, 0.0625 mmol) was combined with crotonaldehyde to form the corresponding adduct. ^1H NMR (400 MHz, CDCl_3 , 298 K) $\Delta\delta$ of H^3 : 0.76 ppm. **Relative acidity** = 0.51.

Tris(2,3,4-trifluorophenyl)borane

According to *general procedure 2*, tris(2,3,4-trifluorophenyl)borane (25.3 mg, 0.0625 mmol) was combined with crotonaldehyde to form the corresponding adduct: ^1H NMR (400 MHz, CDCl_3 , 298 K) $\Delta\delta$ of H^3 : 0.72 ppm. **Relative acidity** = 0.48.

Tris(2,4,6-trifluorophenyl)borane

According to *general procedure 2*, tris(2,4,6-trifluorophenyl)borane (25.3 mg, 0.0625 mmol) was combined with crotonaldehyde to form the corresponding adduct. ^1H NMR (400 MHz, CDCl_3 , 298 K) $\Delta\delta$ of H^3 : 0.53 ppm. **Relative acidity** = 0.36.

Triphenylborane

According to *general procedure 2*, triphenylborane (15.1 mg, 0.0625 mmol) was combined with crotonaldehyde to form the corresponding adduct. ^1H NMR (400 MHz, CDCl_3 , 298 K) $\Delta\delta$ of H^3 : 0.03 ppm. **Relative acidity** = 0.02.

8.4.3 FIA calculations for Lewis acidity determination

Table 15 – Enthalpy values for determining the fluoride ion affinity of select boranes and alanes.

Definition of FIA		$E(\text{Ar})_3 + \text{F}^- \rightarrow \text{F}-E(\text{Ar})_3^-$			FIA = $-\Delta H$
Species	$\text{Al}(3,4,5\text{-F}_3\text{C}_6\text{H}_2)_3$ (Ha)	F^- (Ha)	$^-\text{Al}(3,4,5\text{-F}_3\text{C}_6\text{H}_2)_3\text{F}$ (Ha)	BSSE (Ha)	FIA (KJ mol ⁻¹)
Enthalpy	-1829.83018	-99.738167	-1929.824575	0.061640431	511
Species	$\text{Al}(2,3,4\text{-F}_3\text{C}_6\text{H}_2)_3$ (Ha)	F^- (Ha)	$^-\text{Al}(2,3,4\text{-F}_3\text{C}_6\text{H}_2)_3\text{F}$ (Ha)	BSSE (Ha)	FIA (KJ mol ⁻¹)
Enthalpy	-1829.846028	-99.738167	-1929.837331	0.06221322	501
Species	$\text{B}(3,4,5\text{-F}_3\text{C}_6\text{H}_2)_3$ (Ha)	F^- (Ha)	$^-\text{B}(3,4,5\text{-F}_3\text{C}_6\text{H}_2)_3\text{F}$ (Ha)	BSSE (Ha)	FIA (KJ mol ⁻¹)
Enthalpy	-1612.267807	-99.738167	-1712.237861	0.069153069	427
Species	$\text{B}(2,3,4\text{-F}_3\text{C}_6\text{H}_2)_3$ (Ha)	F^- (Ha)	$^-\text{B}(2,3,4\text{-F}_3\text{C}_6\text{H}_2)_3\text{F}$ (Ha)	BSSE (Ha)	FIA (KJ mol ⁻¹)
Enthalpy	-1612.273944	-99.738167	-1712.233613	0.067797654	404
Species	$\text{Al}(\text{C}_6\text{F}_5)_3$ (Ha)	F^- (Ha)	$^-\text{Al}(\text{C}_6\text{F}_5)_3\text{F}$ (Ha)	BSSE (Ha)	FIA (KJ mol ⁻¹)
Enthalpy	-2425.144391	-99.738167	-2525.149834	0.061262443	541
Species	$\text{B}(\text{C}_6\text{F}_5)_3$ (Ha)	F^- (Ha)	$^-\text{B}(\text{C}_6\text{F}_5)_3\text{F}$ (Ha)	BSSE (Ha)	FIA (KJ mol ⁻¹)
Enthalpy	-2207.560101	-99.738167	-2307.539725	0.066692489151	459

Ha = Hartree units, BSSE = basis set superposition error value

8.5 B(3,4,5-F₃C₆H₂)₃-catalysed hydroboration

General procedure 3

Synthesised in accordance with the literature known procedure,²³⁹ the necessary aldehyde (10 mmol) was dissolved in CH₂Cl₂ (10 mL) along with 3 Å molecular sieves. To this the required amine (10 mmol) was added. The reaction was left at ambient temperature for two hours at which point MgSO₄ was added with subsequent filtration. Volatiles were removed *in vacuo* to leave the pure imine.

General procedure 4

In an NMR tube, pinacolborane (31.9 mg, 220 μmol) and the substrate (aldehyde/ketone/imine) (200 μmol) were combined in deuterated chloroform (0.7 mL). To this, tris(3,4,5-trifluorophenyl)borane (1.6 mg, 2 mol%, 4 μmol) was added, and the NMR tube sealed. The mixture was left at room temperature and conversion was monitored *via in situ* ¹H NMR spectroscopy using mesitylene (13.9 μL, 100 μmol) as an internal standard until the desired boronate ester had been formed in >95% yield. A parallel reaction with the same amounts of reagents and catalyst, but without a mesitylene internal standard was also prepared and upon quantitative conversion the boronate ester was hydrolysed, either by passing the solution through a silica plug, or *via* washing with 1 M NaOH (3 × 10 mL), to isolate the desired alcohol or imine.

General procedure 5

In an NMR tube, pinacolborane (31.9 mg, 220 μmol) and the substrate (aldehyde/ketone/imine) (200 μmol) were combined in deuterated chloroform (0.7 mL). To this, tris(3,4,5-trifluorophenyl)borane (1.6 mg, 2 mol%, 4 μmol) was added, and the NMR tube sealed. The mixture was heated to 70 °C and conversion was monitored *via in situ* ¹H NMR spectroscopy using mesitylene (13.9 μL, 100 μmol) as an internal standard until the desired boronate ester had been formed in >95% yield. A parallel reaction with the same amounts of reagents and catalyst, but without a mesitylene internal standard was also prepared and upon quantitative conversion the boronate ester was hydrolysed, either by passing the solution through a silica plug, or *via* washing with 1 M NaOH (3 × 10 mL), to isolate the desired alcohol or imine.

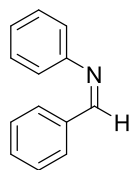
General procedure 6

In a 2 mL microwave vial, pinacolborane (62.8 mg, 440 μmol), and the substrate (aldehyde/ketone/imine) (400 μmol) were combined in chloroform (2 mL). To this, tris(3,4,5-trifluorophenyl)borane (3.2 mg, 2 mol%, 8 μmol) was added, and the microwave vial sealed and placed into the microwave. The reaction was heated to 180 °C for five minutes, and the catalyst was removed by the addition of 1 M NaOH (5 mL) immediately after the microwave allowed the removal of the vial. The solution was washed with 1 M NaOH (3×5 mL), and the solvent was removed *in vacuo* to yield the desired product. For further purification, the desired alcohol/amine was isolated using flash column chromatography using a suitable eluent.

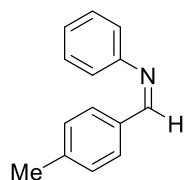
General procedure 7

In a 2 mL microwave vial, pinacolborane (62.8 mg, 440 μmol), and the substrate (alkene/alkyne) (400 μmol) were combined in chloroform (2 mL). To this, tris(3,4,5-trifluorophenyl)borane (8.1 mg, 5 mol%, 20 μmol) was added, and the microwave vial sealed and placed into the microwave. The reaction was heated to 180 °C for 90 minutes, and the catalyst was removed by passing the solution through a silica plug. The solvent was subsequently removed *in vacuo* to yield the desired boronate ester. For further purification, the desired boronate ester was isolated using flash column chromatography using a suitable eluent.

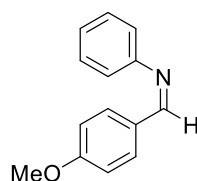
8.5.1 Synthesis of starting materials

(Z)-N,1-diphenylmethanimine

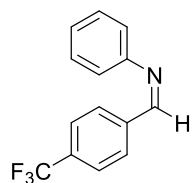
Synthesised in accordance with *general procedure 3* using benzaldehyde (1.02 mL, 10 mmol) and aniline (913 μ L, 10 mmol). Spectroscopic analyses agree with literature values.²⁴⁰ **Yield:** 1.63 g, 9.0 mmol, 90%. **¹H NMR** (400 MHz, CDCl₃, 298 K) δ /ppm: 8.43 (s, 1H, C–H), 7.90–7.80 (m, 2H, Ar–H), 7.55–7.31 (m, 5H, Ar–H), 7.28–7.05 (m, 3H, Ar–H).

(Z)-N-phenyl-1-(p-tolyl)methanimine

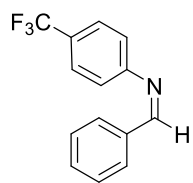
Synthesised in accordance with *general procedure 3* using 4-tolualdehyde (1.18 mL, 10 mmol) and aniline (913 μ L, 10 mmol). Spectroscopic analyses agree with literature values.¹⁰⁸ **Yield:** 1.79 g, 9.2 mmol, 92%. **¹H NMR** (400 MHz, CDCl₃, 298 K) δ /ppm: 8.42 (s, 1H, C–H), 7.76 (d, ³J_{HH} = 8.9 Hz, 1H, Ar–H), 7.12–7.05 (m, 2H, Ar–H), 7.03 (dd, ³J_{HH} = 7.4 Hz, ⁴J_{HH} = 1.6 Hz, 1H, Ar–H), 6.99 (d, ³J_{HH} = 7.9 Hz, 1H, Ar–H), 6.96–6.87 (m, 4H, Ar–H), 2.26 (s, 3H, Me).

(Z)-1-(4-methoxyphenyl)-N-phenylmethanimine

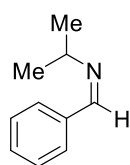
Synthesised in accordance with *general procedure 3* using 4-anisaldehyde (1.22 mL, 10 mmol) and aniline (913 μ L, 10 mmol). Spectroscopic analyses agree with literature values.¹⁰⁸ **Yield:** 1.88 g, 8.9 mmol, 89%. **¹H NMR** (400 MHz, CDCl₃, 298 K) δ /ppm: 8.44 (s, 1H, C–H), 7.91 (d, ³J_{HH} = 8.9 Hz, 2H, Ar–H), 7.50–7.41 (m, 2H, Ar–H), 7.30–7.23 (m, 3H, Ar–H), 7.04 (d, ³J_{HH} = 8.8 Hz, 2H, Ar–H), 3.92 (s, 3H, OMe).

(Z)-1-(4-(trifluoromethyl)phenyl)-N-phenylmethanimine

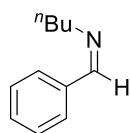
Synthesised in accordance with *general procedure 3* using 4-(trifluoromethyl)benzaldehyde (1.36 mL, 10 mmol) and aniline (913 μ L, 10 mmol). Spectroscopic analyses agree with literature values.¹⁰⁸ **Yield:** 2.34 g, 9.4 mmol, 94%. **¹H NMR** (400 MHz, CDCl₃, 298 K) δ /ppm: 8.44 (s, 1H, C–H), 7.95 (d, ³J_{HH} = 8.0 Hz, 2H, Ar–H), 7.66 (d, ³J_{HH} = 8.2 Hz, 2H, Ar–H), 7.47–7.28 (m, 2H, Ar–H), 7.25–7.11 (m, 3H, Ar–H). **¹⁹F NMR** (376 MHz, CDCl₃, 298 K) δ /ppm: 62.81 (s, 3F, *p*-CF₃).

(Z)-1-phenyl-N-(4-(trifluoromethyl)phenyl)methanimine

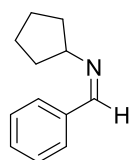
Synthesised in accordance with *general procedure 3* using benzaldehyde (1.02 mL, 10 mmol) and 4-trifluoromethylaniline (1.26 mL, 10 mmol). Spectroscopic analyses agree with literature values.¹⁰⁸ **Yield** 2.32 g, 9.3 mmol, 93%. **¹H NMR** (400 MHz, CDCl₃, 298 K) δ /ppm: 8.43 (s, 1H, C–H), 7.92 (dd, ³J_{HH} = 7.8 Hz, ⁴J_{HH} = 1.8 Hz, 2H, Ar–H), 7.65 (d, ³J_{HH} = 8.3 Hz, 2H, Ar–H), 7.58–7.46 (m, 3H, Ar–H), 7.26 (d, ³J_{HH} = 8.1 Hz, 2H, Ar–H). **¹⁹F NMR** (376 MHz, CDCl₃, 298 K) δ /ppm: 62.00 (s, 3F, *p*-CF₃).

(Z)-N-isopropyl-1-phenylmethanimine

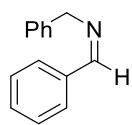
Synthesised in accordance with *general procedure 3* using benzaldehyde (1.02 mL, 10 mmol) and isopropylamine (859 μ L, 10 mmol). Spectroscopic analyses agree with literature values.¹⁰⁸ **Yield**: 1.32 g, 9.0 mmol, 90%. **¹H NMR** (400 MHz, CDCl₃, 298 K) δ /ppm: 8.31 (s, 1H, C–H), 7.79–7.68 (m, 2H, Ar–H), 7.51–7.35 (m, 3H, Ar–H), 3.54 (hept, ³J_{HH} = 6.4 Hz, 1H, CH(CH₃)₂), 1.27 (d, ³J_{HH} = 6.3 Hz, 6H, CH(CH₃)₂).

(Z)-N-butyl-1-phenylmethanimine

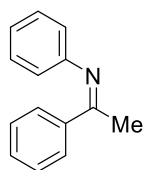
Synthesised in accordance with *general procedure 3* using benzaldehyde (1.02 mL, 10 mmol) and *n*-butylamine (988 μ L, 10 mmol). Spectroscopic analyses agree with literature values.¹⁰⁸ **Yield**: 1.47 g, 9.1 mmol, 91%. **¹H NMR** (400 MHz, CDCl₃, 298 K) δ /ppm: 8.19 (s, 1H, C–H), 7.93–7.56 (m, 2H, Ar–H), 7.36–7.29 (m, 3H, Ar–H), 3.54 (t, ³J_{HH} = 7.0 Hz, 2H, NCH₂), 1.67–1.58 (m, 2H, CH₂), 1.38–1.27 (m, 2H, CH₂), 0.88 (t, ³J_{HH} = 7.4 Hz, 3H, CH₃).

(Z)-N-cyclopentyl-1-phenylmethanimine

Synthesised in accordance with *general procedure 3* using benzaldehyde (1.02 mL, 10 mmol) and cyclopentylamine (987 μ L, 10 mmol). Spectroscopic analyses agree with literature values.¹⁰⁸ **Yield**: 1.61 g, 9.3 mmol, 93%. **¹H NMR** (400 MHz, CDCl₃, 298 K) δ /ppm: 8.29 (s, 1H, C–H), 7.73 (dd, ³J_{HH} = 6.7 Hz, ⁴J_{HH} = 3.0 Hz, 2H, Ar–H), 7.75–6.58 (m, 3H, Ar–H), 3.77 (p, ³J_{HH} = 6.3 Hz, 1H), 1.96–1.83 (m, 4H, cyclopentyl H), 1.80–1.63 (m, 4H, cyclopentyl H).

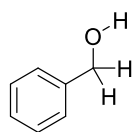
(Z)-N-benzyl-1-phenylmethanimine

Synthesised in accordance with *general procedure 3* using benzaldehyde (1.02 mL, 10 mmol) and benzylamine (1.09 mL, 10 mmol). Spectroscopic analyses agree with literature values.¹⁰⁸ **Yield:** 1.72 g, 8.8 mmol, 88%. **¹H NMR** (400 MHz, CDCl₃, 298 K) δ /ppm: 8.30 (s, 1H, C–H), 7.71 (dd, ³J_{HH} = 6.8 Hz, ⁴J_{HH} = 2.9 Hz, 2H, Ar–H), 7.37–7.28 (m, 3H, Ar–H), 7.26 (d, ²J_{HH} = 4.4 Hz, 4H, Ar–H), 7.23–7.16 (m, 1H, Ar–H), 4.74 (s, 2H, CH₂).

(E)-N,1-diphenylethan-1-imine

Synthesised in accordance with the literature known procedure,²⁴¹ a flame dried Schlenk flask was charged with dry toluene, dry 3 Å molecular sieves, acetophenone (2 mL, 17.1 mmol), and aniline (3 mL, 32.9 mmol). The reaction was heated to reflux for 18 h and filtered to remove molecular sieves. The volatiles were removed *in vacuo*, and the product was purified by Kugelrohr distillation to yield the pure imine. Spectroscopic analyses agree with literature values.²⁴¹ **Yield:** 1.17 g, 5.9 mmol, 35%. **¹H NMR** (400 MHz, CDCl₃, 298 K) δ /ppm: 8.05–7.96 (m, 2H, Ar–H), 7.50–7.42 (m, 3H, Ar–H), 7.36 (t, ³J_{HH} = 7.9 Hz, 2H), 7.10 (t, ³J_{HH} = 7.4 Hz, 1H, Ar–H), 6.81 (d, ³J_{HH} = 7.8 Hz, 2H), 2.25 (s, 3H, Me).

8.5.2 Synthesis of reduction products

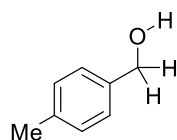
Phenylmethanol (2a)

Synthesised in accordance with *general procedure 4*, using benzaldehyde (21.2 mg, 200 μmol) as the substrate gave the corresponding boronate ester after 2 h. The boronate ester was hydrolysed through a silica plug to isolate the title compound as a colourless oil. **Yield:** 20 mg, 185 μmol , 93%.

Synthesised in accordance with *general procedure 5*, using benzaldehyde (21.2 mg, 200 μmol) as the substrate gave the corresponding boronate ester after 0.5 h. The boronate ester was hydrolysed through a silica plug to isolate the title compound as a colourless oil. **Yield:** 19 mg, 175 μmol , 88%.

Synthesised in accordance with *general procedure 6*, using benzaldehyde (42.2 mg, 400 μmol) as the substrate gave the corresponding boronate ester after 5 min. Crude ^1H NMR spectrum analysis of the hydrolysed material revealed >95% conversion. The crude material was purified by flash-column chromatography using hexane/ethyl acetate (5:1) as the eluent to afford the title compound as a colourless oil. **Yield:** 41 mg, 379 μmol , 95%.

Spectroscopic data agrees with literature values.²⁴² **^1H NMR** (400 MHz, CDCl_3 , 298 K) δ /ppm: 7.65–6.96 (m, 5H, Ar–H), 4.55 (s, 2H, CH_2), 2.17 (s, 1H, OH). **$^{13}\text{C}\{^1\text{H}\}$ NMR** (101 MHz, CDCl_3 , 298 K) δ /ppm: 140.9 (s, Ar), 128.6 (s, Ar), 127.7 (s, Ar), 127.1 (s, Ar), 65.3 (s, CH_2).

p-Tolylmethanol (2b)

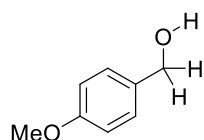
Synthesised in accordance with *general procedure 4*, using 4-methylbenzaldehyde (24.0 mg, 200 μmol) as the substrate gave the corresponding boronate ester after 24 h. The boronate ester was hydrolysed through a silica plug to isolate the title compound as a colourless oil. **Yield:** 23 mg, 188 μmol , 94%.

Synthesised in accordance with *general procedure 5*, using 4-methylbenzaldehyde (24.0 mg, 200 μmol) as the substrate gave the corresponding boronate ester after 0.5 h. The boronate ester was hydrolysed through a silica plug to isolate the title compound as a colourless oil. **Yield:** 23 mg, 188 μmol , 94%.

Synthesised in accordance with *general procedure 6*, using 4-methylbenzaldehyde (48.0 mg, 400 μmol) as the substrate gave the corresponding boronate ester after 5 min. Crude ^1H NMR spectrum analysis of the hydrolysed material revealed >95% conversion. The crude material was purified by flash-column chromatography using hexane/ethyl acetate (5:1) as the eluent to afford the title compound as a colourless oil. **Yield:** 42 mg, 341 μmol , 85%.

Spectroscopic data agrees with literature values.²⁴² ^1H NMR (400 MHz, CDCl_3 , 298 K) δ/ppm : 7.26 (d, $^3J_{\text{HH}} = 8.0$ Hz, 2H, Ar–H), 7.18 (d, $^3J_{\text{HH}} = 7.9$ Hz, 2H, Ar–H), 4.64 (s, 2H, CH_2), 2.36 (s, 3H, Me), 1.81 (s, 1H, OH). $^{13}\text{C}\{^1\text{H}\}$ NMR (101 MHz, CDCl_3 , 298 K) δ/ppm : 138.0 (s, Ar), 137.5 (s, Ar), 129.4 (s, Ar), 127.2 (s, Ar), 65.4 (s, CH_2), 21.3 (s, Me).

(4-Methoxyphenyl)methanol (2c)

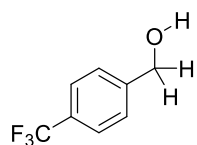


Synthesised in accordance with *general procedure 4*, using 4-methoxybenzaldehyde (27.2 mg, 200 μmol) as the substrate gave the corresponding boronate ester after 24 h. The boronate ester was hydrolysed through a silica plug to isolate the title compound as a colourless oil. **Yield:** 24 mg, 174 μmol , 87%.

Synthesised in accordance with *general procedure 5*, using 4-methoxybenzaldehyde (27.2 mg, 200 μmol) as the substrate gave the corresponding boronate ester after 0.5 h. The boronate ester was hydrolysed through a silica plug to isolate the title compound as a colourless oil. **Yield:** 27 mg, 196 μmol , 98%.

Synthesised in accordance with *general procedure 6*, using 4-methoxybenzaldehyde (54.5 mg, 400 μmol) as the substrate gave the corresponding boronate ester after 5 min. Crude ^1H NMR spectrum analysis of the hydrolysed material revealed >95% conversion. The crude material was purified by flash-column chromatography using hexane/ethyl acetate (5:1) as the eluent to afford the title compound as a colourless oil. **Yield:** 49 mg, 355 μmol , 88%.

Spectroscopic data agrees with literature values.²⁴² ^1H NMR (400 MHz, CDCl_3 , 298 K) δ/ppm : 7.15 (d, $^3J_{\text{HH}} = 8.8$ Hz, 2H, Ar–H), 6.77 (d, $^3J_{\text{HH}} = 8.7$ Hz, 2H, Ar–H), 4.44 (s, 2H, CH_2), 3.68 (s, 3H, OMe), 2.41 (s, 1H, OH). $^{13}\text{C}\{^1\text{H}\}$ NMR (101 MHz, CDCl_3 , 298 K) δ/ppm : 159.1 (s, Ar), 133.2 (s, Ar), 128.7 (s, Ar), 113.9 (s, Ar), 64.8 (s, CH_2), 55.3 (s, OMe).

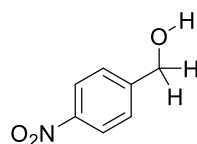
(4-(Trifluoromethyl)phenyl)methanol (2d)

Synthesised in accordance with *general procedure 4*, using 4-(trifluoromethyl)benzaldehyde (34.8 mg, 200 μmol) as the substrate gave the corresponding boronate ester after 16 h. The boronate ester was hydrolysed through a silica plug to isolate the title compound as a colourless oil. **Yield:** 33 mg, 187 μmol , 94%.

Synthesised in accordance with *general procedure 5*, using 4-(trifluoromethyl)benzaldehyde (34.8 mg, 200 μmol) as the substrate gave the corresponding boronate ester after 0.5 h. The boronate ester was hydrolysed through a silica plug to isolate the title compound as a colourless oil. **Yield:** 33 mg, 187 μmol , 94%.

Synthesised in accordance with *general procedure 6*, using 4-(trifluoromethyl)benzaldehyde (69.6 mg, 400 μmol) as the substrate gave the corresponding boronate ester after 5 min. Crude ^1H NMR spectrum analysis of the hydrolysed material revealed >95% conversion. The crude material was purified by flash-column chromatography using hexane/ethyl acetate (5:1) as the eluent to afford the title compound as a colourless oil. **Yield:** 64 mg, 364 μmol , 91%.

Spectroscopic data agrees with literature values.²⁴³ **^1H NMR** (400 MHz, CDCl_3 , 298 K) δ/ppm : 7.58 (d, $^3J_{\text{HH}} = 7.6$ Hz, 2H, Ar-H), 7.42 (d, $^3J_{\text{HH}} = 7.6$ Hz, 2H, Ar-H), 4.69 (s, 2H, CH_2), 2.76 (s, 1H, OH). **$^{13}\text{C}\{^1\text{H}\}$ NMR** (101 MHz, CDCl_3 , 298 K) δ/ppm : 144.8 (s, Ar), 129.8 (q, $^2J_{\text{FC}} = 32.4$ Hz, Ar), 126.9 (s, Ar), 125.5 (q, $^1J_{\text{FC}} = 3.8$ Hz, CF_3), 64.4 (s, CH_2). **^{19}F NMR** (376 MHz, CDCl_3 , 298 K) δ/ppm : -62.51 (s, 3F, *p*- CF_3).

(4-Nitrophenyl)methanol (2e)

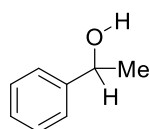
Synthesised in accordance with *general procedure 4*, using 4-nitrobenzaldehyde (30.2 mg, 200 μmol) as the substrate gave the corresponding boronate ester after 16 h. The boronate ester was hydrolysed through a silica plug to isolate the title compound as a brown oil. **Yield:** 30 mg, 196 μmol , 98%.

Synthesised in accordance with *general procedure 5*, using 4-nitrobenzaldehyde (30.2 mg, 200 μmol) as the substrate gave the corresponding boronate ester after 0.5 h. The boronate ester was hydrolysed through a silica plug to isolate the title compound as a brown oil. **Yield:** 26 mg, 170 μmol , 85%.

Synthesised in accordance with *general procedure 6*, using 4-nitrobenzaldehyde (60.4 mg, 400 μmol) as the substrate gave the corresponding boronate ester after 5 min. Crude ^1H NMR spectrum analysis of the hydrolysed material revealed >95% conversion. The crude material was purified by flash-column chromatography using hexane/ethyl acetate (5:1) as the eluent to afford the title compound as a brown oil. **Yield:** 57 mg, 372 μmol , 93%.

Spectroscopic data agrees with literature values.²⁴² **^1H NMR** (400 MHz, CDCl_3 , 298 K) δ/ppm : 8.18 (d, $^3J_{\text{HH}} = 7.5$ Hz, 2H, Ar–H), 7.51 (d, $^3J_{\text{HH}} = 7.7$ Hz, 2H, Ar–H), 4.82 (s, 2H, CH_2), 2.30 (s, 1H, OH). **$^{13}\text{C}\{^1\text{H}\}$ NMR** (101 MHz, CDCl_3 , 298 K) δ/ppm : 148.4 (s, Ar), 147.3 (s, Ar), 127.1 (s, Ar), 123.8 (s, Ar), 64.1 (s, CH_2).

1-Phenylethanol (2f)

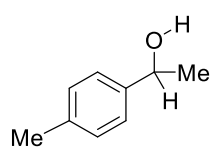


Synthesised in accordance with *general procedure 4*, using acetophenone (24.0 mg, 200 μmol) as the substrate gave the corresponding boronate ester after 1 h. The boronate ester was hydrolysed through a silica plug to isolate the title compound as a colourless oil. **Yield:** 22 mg, 180 μmol , 90%.

General procedure 5 and *general procedure 6* were not required due to rapid reaction at room temperature.

Spectroscopic data agrees with literature values.²⁴⁴ **^1H NMR** (400 MHz, CDCl_3 , 298K) δ/ppm : 7.38–7.32 (m, 4H, Ar–H), 7.28–7.24 (m, 1H, Ar–H), 4.88 (q, $^3J_{\text{HH}} = 6.2$ Hz, 1H, C–H), 1.87 (s, 1H, OH), 1.49 (d, $^3J_{\text{HH}} = 6.5$ Hz, 3H, Me). **$^{13}\text{C}\{^1\text{H}\}$ NMR** (101 MHz, CDCl_3 , 298K) δ/ppm : 145.9 (s, Ar), 128.6 (s, Ar), 127.6 (s, Ar), 125.5 (s, Ar), 70.6 (s, C–H), 25.3 (Me).

1-(*p*-Tolyl)ethan-1-ol (2g)

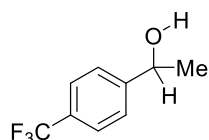


Synthesised in accordance with *general procedure 4*, using 4-methylacetophenone (26.8 mg, 200 μmol) as the substrate gave the corresponding boronate ester after 1 h. The boronate ester was hydrolysed through a silica plug to isolate the title compound as a colourless oil. **Yield:** 26 mg, 191 μmol , 96%.

General procedure 5 and *general procedure 6* were not required due to rapid reaction at room temperature.

Spectroscopic data agrees with literature values.²⁴⁴ **¹H NMR** (400 MHz, CDCl₃, 298K) δ /ppm: 7.19 (d, ³J_{HH} = 8.1 Hz, 2H, Ar–H), 7.08 (d, ³J_{HH} = 7.9 Hz, 2H, Ar–H), 4.79 (q, ³J_{HH} = 6.4 Hz, 1H, C–H), 2.27 (s, 3H, Me), 1.77 (s, 1H, OH), 1.41 (d, ³J_{HH} = 6.5 Hz, 3H, Me). **¹³C{¹H} NMR** (101 MHz, CDCl₃, 298K) δ /ppm: 142.9 (s, Ar), 137.2 (s, Ar), 129.2 (s, Ar), 125.4 (s, Ar), 70.3 (s, C–H), 25.1 (s, Me), 21.1 (s, Me).

1-(4-Trifluoromethyl)phenyl)ethan-1-ol (2h)

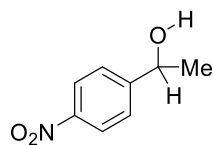


Synthesised in accordance with *general procedure 4*, using 4-(trifluoromethyl)acetophenone (37.6 mg, 200 μ mol) as the substrate gave the corresponding boronate ester after 2 h. The boronate ester was hydrolysed through a silica plug to isolate the title compound as a colourless oil. **Yield:** 34 mg, 179 μ mol, 89%.

Synthesised in accordance with *general procedure 5*, using 4-(trifluoromethyl)acetophenone (37.6 mg, 200 μ mol) as the substrate gave the corresponding boronate ester after 0.5 h. The boronate ester was hydrolysed through a silica plug to isolate the title compound as a colourless oil. **Yield:** 33 mg, 174 μ mol, 87%.

Synthesised in accordance with *general procedure 6*, using 4-(trifluoromethyl)acetophenone (75.2 mg, 400 μ mol) as the substrate gave the corresponding boronate ester after 5 min. Crude ¹H NMR spectrum analysis of the hydrolysed material revealed 71% conversion. The crude material was purified by flash-column chromatography using hexane/ethyl acetate (5:1) as the eluent to afford the title compound as a colourless oil. **Yield:** 48 mg, 253 μ mol, 63%.

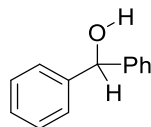
Spectroscopic data agrees with literature values.²⁴³ **¹H NMR** (400 MHz, CDCl₃, 298 K) δ /ppm: 7.61 (d, ³J_{HH} = 8.1 Hz, 2H, Ar–H), 7.49 (d, ³J_{HH} = 8.1 Hz, 2H, Ar–H), 4.97 (q, ³J_{HH} = 6.5 Hz, 1H, C–H), 1.90 (s, 1H, OH), 1.51 (d, ³J_{HH} = 6.5 Hz, 3H, Me). **¹³C{¹H} NMR** (101 MHz, CDCl₃, 298 K) δ /ppm: 149.8 (s, Ar), 129.8 (q, ²J_{FC} = 32.3 Hz, Ar), 125.8 (s, Ar), 125.6 (q, ¹J_{FC} = 3.7 Hz, CF₃), 70.0 (s, C–H), 25.6 (s, Me). **¹⁹F NMR** (376 MHz, CDCl₃, 298 K) δ /ppm: -62.46 (s, 3F, *p*-CF₃).

1-(4-Nitrophenyl)ethan-1-ol (2i)

Synthesised in accordance with *general procedure 4*, using 4-nitroacetophenone (33.0 mg, 200 μmol) as the substrate gave the corresponding boronate ester after 0.5 h. The boronate ester was hydrolysed through a silica plug to isolate the title compound as a brown oil. **Yield:** 30 mg, 180 μmol , 90%.

General procedure 5 and *general procedure 6* were not required due to rapid reaction at room temperature.

Spectroscopic data agrees with literature values.²⁴⁴ **^1H NMR** (400 MHz, CDCl_3 , 298 K) δ/ppm : 8.18 (d, $^3J_{\text{HH}} = 8.8$ Hz, 2H, Ar–H), 7.53 (d, $^3J_{\text{HH}} = 8.8$ Hz, 2H, Ar–H), 5.02 (q, $^3J_{\text{HH}} = 6.4$ Hz, 1H, C–H), 1.51 (d, $^3J_{\text{HH}} = 6.5$ Hz, 3H, Me). **$^{13}\text{C}\{^1\text{H}\}$ NMR** (101 MHz, CDCl_3 , 298 K) δ/ppm : 153.2 (s, Ar), 147.3 (s, Ar), 126.2 (s, Ar), 123.9 (s, Ar), 69.6 (s, C–H), 25.6 (s, Me).

Diphenylmethanol (2j)

Synthesised in accordance with *general procedure 4*, using benzophenone (36.4 mg, 200 μmol) as the substrate gave the corresponding boronate ester after 156 h. The boronate ester was hydrolysed through a silica plug to isolate the title compound as a colourless oil. **Yield:** 31 mg, 168 μmol , 85%.

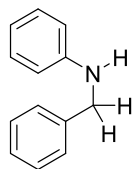
Synthesised in accordance with *general procedure 5*, using benzophenone (36.4 mg, 200 μmol) as the substrate gave the corresponding boronate ester after 30 h. Between 30 h and 72 h there was no increase in conversion from 85%, and the title compound was isolated by flash-column chromatography using hexane/ethyl acetate (5:1) as the eluent. **Yield:** 26 mg, 141 μmol , 71%.

Synthesised in accordance with *general procedure 6*, using benzophenone (72.8 mg, 400 μmol) as the substrate gave the corresponding boronate ester after 5 min. Crude ^1H NMR spectrum analysis of the hydrolysed material revealed 25% conversion. The crude material was purified by flash-column chromatography using hexane/ethyl acetate (5:1) as the eluent to afford the title compound as a colourless oil. **Yield:** 14 mg, 76 μmol , 19%.

Spectroscopic data agrees with literature values.²⁴⁵ **^1H NMR** (400 MHz, CDCl_3 , 298 K) δ/ppm : 7.34–7.22 (m, 8H, Ar–H), 7.21–7.15 (m, 2H, Ar–H), 5.75 (s, 1H, C–H), 2.20

(s, 1H, OH). $^{13}\text{C}\{^1\text{H}\}$ NMR (101 MHz, CDCl_3 , 298 K) δ /ppm: 143.9 (s, Ar), 128.6 (s, Ar), 127.7 (s, Ar), 126.7 (s, Ar), 76.4 (s, C–H).

N-Benzylaniline (2k)



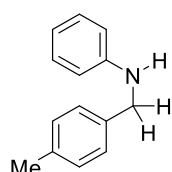
Synthesised in accordance with *general procedure 4*, using (*Z*)-*N*,1-diphenylmethanimine (36.2 mg, 200 μmol) as the substrate gave the corresponding boronate ester after 24 h. The boronate ester was hydrolysed *via* a basic workup (3 \times 10 mL 1 M NaOH washings) to isolate the title compound as a colourless oil. **Yield:** 34 mg, 186 μmol , 93%.

Synthesised in accordance with *general procedure 5*, using (*Z*)-*N*,1-diphenylmethanimine (36.2 mg, 200 μmol) as the substrate gave the corresponding boronate ester after 1 h. The boronate ester was hydrolysed *via* a basic workup (3 \times 10 mL 1 M NaOH washings) to isolate the title compound as a colourless oil. **Yield:** 32 mg, 175 μmol , 87%.

Synthesised in accordance with *general procedure 6*, using (*Z*)-*N*,1-diphenylmethanimine (72.4 mg, 400 μmol) as the substrate gave the corresponding boronate ester after 5 min. Crude ^1H NMR spectrum analysis of the hydrolysed material revealed >95% conversion. The crude material was purified by flash-column chromatography using hexane/ethyl acetate (5:1) as the eluent to afford the title compound as a colourless oil. **Yield:** 68 mg, 371 μmol , 93%.

Spectroscopic data agrees with literature values.¹⁰⁷ ^1H NMR (400 MHz, CDCl_3 , 298 K) δ /ppm: 7.39 (q, $^3J_{\text{HH}} = 8.2$ Hz, 4H, Ar–H), 7.32 (d, $^3J_{\text{HH}} = 6.7$ Hz, 1H, Ar–H), 7.22 (t, $^3J_{\text{HH}} = 7.4$ Hz, 2H, Ar–H), 6.76 (t, $^3J_{\text{HH}} = 7.3$ Hz, 1H, Ar–H), 6.68 (d, $^3J_{\text{HH}} = 9.4$ Hz, 2H, Ar–H), 4.36 (s, 2H, CH_2), 4.05 (s, 1H, N–H). $^{13}\text{C}\{^1\text{H}\}$ NMR (101 MHz, CDCl_3 , 298 K) δ /ppm: 148.3 (s, Ar), 139.6 (s, Ar), 129.4 (s, Ar), 128.8 (s, Ar), 127.6 (s, Ar), 127.3 (s, Ar), 117.7 (s, Ar), 113.0 (s, Ar), 48.4 (s, CH_2).

N-(4-Methylbenzyl)aniline (2l)



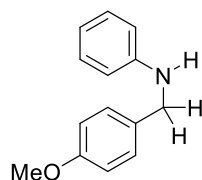
Synthesised in accordance with *general procedure 4*, using (*Z*)-*N*-phenyl-1-(*p*-tolyl)methanimine (39.0 mg, 200 μmol) as the substrate gave the corresponding boronate ester after 60 h. The boronate ester was hydrolysed *via* a basic workup (3 \times 10 mL 1 M NaOH washings) to isolate the title compound as a colourless oil. **Yield:** 38 mg, 193 μmol , 96%.

Synthesised in accordance with *general procedure 5*, using (*Z*)-*N*-phenyl-1-(*p*-tolyl)methanimine (39.0 mg, 200 μ mol) as the substrate gave the corresponding boronate ester after 4 h. The boronate ester was hydrolysed *via* a basic workup (3 \times 10 mL 1 M NaOH washings) to isolate the title compound as a colourless oil. **Yield:** 34 mg, 172 μ mol, 86%.

Synthesised in accordance with *general procedure 6*, using (*Z*)-*N*-phenyl-1-(*p*-tolyl)methanimine (78.0 mg, 400 μ mol) as the substrate gave the corresponding boronate ester after 5 min. Crude ^1H NMR spectrum analysis of the hydrolysed material revealed >95% conversion. The crude material was purified by flash-column chromatography using hexane/ethyl acetate (5:1) as the eluent to afford the title compound as a colourless oil. **Yield:** 61 mg, 309 μ mol, 77%.

Spectroscopic data agrees with literature values.²⁴⁶ **^1H NMR** (400 MHz, CDCl_3 , 298 K) δ /ppm: 7.29–7.24 (m, 2H, Ar–H), 7.22–7.11 (m, 4H, Ar–H), 6.71 (t, $^3J_{\text{HH}} = 7.4$ Hz, 1H, Ar–H), 6.66–6.62 (m, 2H, Ar–H), 4.29 (s, 2H, CH_2), 3.98 (s, 1H, N–H), 2.35 (s, 3H, Me). **$^{13}\text{C}\{^1\text{H}\}$ NMR** (101 MHz, CDCl_3 , 298 K) δ /ppm: 148.3 (s, Ar), 137.0 (s, Ar), 136.5 (s, Ar), 129.4 (s, Ar), 129.4 (s, Ar), 127.7 (s, Ar), 117.6 (s, Ar), 112.9 (s, Ar), 48.2 (s, CH_2), 21.3 (s, Me).

***N*-(4-Methoxybenzyl)aniline (2m)**



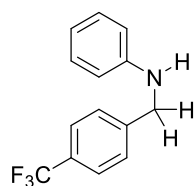
Synthesised in accordance with *general procedure 4*, using (*Z*)-1-(4-methoxyphenyl)-*N*-phenylmethanimine (42.2 mg, 200 μ mol) as the substrate gave the corresponding boronate ester after 36 h. The boronate ester was hydrolysed through a silica plug to isolate the title compound as a colourless oil. **Yield:** 39 mg, 183 μ mol, 92%.

Synthesised in accordance with *general procedure 5*, using (*Z*)-1-(4-methoxyphenyl)-*N*-phenylmethanimine (42.2 mg, 200 μ mol) as the substrate gave the corresponding boronate ester after 4 h. The boronate ester was hydrolysed through a silica plug to isolate the title compound as a colourless oil. **Yield:** 40 mg, 188 μ mol, 94%.

Synthesised in accordance with *general procedure 6*, using (*Z*)-1-(4-methoxyphenyl)-*N*-phenylmethanimine (84.4 mg, 400 μ mol) as the substrate gave the corresponding boronate ester after 5 min. Crude ^1H NMR spectrum analysis of the hydrolysed material revealed >95% conversion. The crude material was purified by flash-column chromatography using hexane/ethyl acetate (5:1) as the eluent to afford the title compound as a colourless oil. **Yield:** 77 mg, 361 μ mol, 90%.

Spectroscopic data agrees with literature values.²⁴⁷ **¹H NMR** (400 MHz, CDCl₃, 298 K) δ /ppm: 7.31 (d, ³J_{HH} = 8.8 Hz, 2H, Ar–H), 7.24–7.15 (m, 2H, Ar–H), 6.90 (d, ³J_{HH} = 8.7 Hz, 2H, Ar–H), 6.73 (t, ³J_{HH} = 7.3 Hz, 1H, Ar–H), 6.65 (d, ³J_{HH} = 9.7 Hz, 2H, Ar–H), 4.27 (s, 2H, CH₂), 3.96 (s, 1H, N–H), 3.82 (s, 3H, OMe). **¹³C{¹H} NMR** (101 MHz, CDCl₃, 298 K) δ /ppm: 159.0 (s, Ar), 148.3 (s, Ar), 131.5 (s, Ar), 129.4 (s, Ar), 128.9 (s, Ar), 117.6 (s, Ar), 114.1 (s, Ar), 113.0 (s, Ar), 55.4 (s, CH₂), 47.9 (s, OMe).

***N*-(4-Trifluoromethyl)benzyl)aniline (2n)**

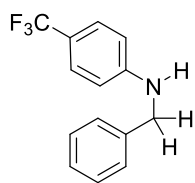


Synthesised in accordance with *general procedure 4*, using (*Z*)-1-(4-(trifluoromethyl)phenyl)-*N*-phenylmethanimine (49.8 mg, 200 μ mol) as the substrate gave the corresponding boronate ester after 8 h. The boronate ester was hydrolysed *via* a basic workup (3 \times 10 mL 1 M NaOH washings) to isolate the title compound as a colourless oil. **Yield:** 46 mg, 183 μ mol, 92%.

Synthesised in accordance with *general procedure 5*, using (*Z*)-1-(4-(trifluoromethyl)phenyl)-*N*-phenylmethanimine (49.8 mg, 200 μ mol) as the substrate gave the corresponding boronate ester after 2 h. The boronate ester was hydrolysed *via* a basic workup (3 \times 10 mL 1 M NaOH washings) to isolate the title compound as a colourless oil. **Yield:** 41 mg, 163 μ mol, 82%.

Synthesised in accordance with *general procedure 6*, using (*Z*)-1-(4-(trifluoromethyl)phenyl)-*N*-phenylmethanimine (99.6 mg, 400 μ mol) as the substrate gave the corresponding boronate ester after 1 h. Crude ¹H NMR spectrum analysis of the hydrolysed material revealed >95% conversion. The crude material was purified by flash-column chromatography using hexane/ethyl acetate (5:1) as the eluent to afford the title compound as a colourless oil. **Yield:** 86 mg, 343 μ mol, 86%.

Spectroscopic data agrees with literature values.²⁴⁷ **¹H NMR** (400 MHz, CDCl₃, 298 K) δ /ppm: 7.59 (d, ³J_{HH} = 8.1 Hz, 2H, Ar–H), 7.49 (d, ³J_{HH} = 8.0 Hz, 2H, Ar–H), 7.23–7.08 (m, 2H, Ar–H), 6.91–6.64 (m, 1H, Ar–H), 6.61 (d, ³J_{HH} = 8.6 Hz, 2H, Ar–H), 4.42 (s, 2H, CH₂), 4.16 (s, 1H, N–H). **¹³C{¹H} NMR** (101 MHz, CDCl₃, 298 K) δ /ppm: 147.8 (s, Ar), 143.9 (s, Ar), 129.5 (s, Ar), 127.6 (s, Ar), 125.7 (q, ¹J_{FC} = 3.8 Hz, CF₃), 118.1 (s, Ar), 113.0 (s, Ar), 47.9 (s, CH₂). **¹⁹F NMR** (376 MHz, CDCl₃, 298 K) δ /ppm: -62.39 (s, 3F, *p*-CF₃).

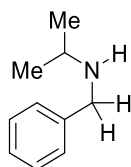
***N*-Benzyl-4-(trifluoromethyl)aniline (2o)**

Synthesised in accordance with *general procedure 4*, using (*Z*)-1-phenyl-*N*-(4-(trifluoromethyl)phenyl)methanimine (49.8 mg, 200 μ mol) as the substrate gave the corresponding boronate ester after 8 h. The boronate ester was hydrolysed *via* a basic workup (3 \times 10 mL 1 M NaOH washings) to isolate the title compound as a colourless oil. **Yield:** 43 mg, 171 μ mol, 86%.

Synthesised in accordance with *general procedure 5*, using (*Z*)-1-phenyl-*N*-(4-(trifluoromethyl)phenyl)methanimine (49.8 mg, 200 μ mol) as the substrate gave the corresponding boronate ester after 0.5 h. The boronate ester was hydrolysed *via* a basic workup (3 \times 10 mL 1 M NaOH washings) to isolate the title compound as a colourless oil. **Yield:** 43 mg, 171 μ mol, 86%.

Synthesised in accordance with *general procedure 6*, using (*Z*)-1-phenyl-*N*-(4-(trifluoromethyl)phenyl)methanimine (99.6 mg, 400 μ mol) as the substrate gave the corresponding boronate ester after 5 min. Crude ^1H NMR spectrum analysis of the hydrolysed material revealed >95% conversion. The crude material was purified by flash-column chromatography using hexane/ethyl acetate (5:1) as the eluent to afford the title compound as a colourless oil. **Yield:** 90 mg, 358 μ mol, 90%.

Spectroscopic data agrees with literature values.²⁴⁷ ^1H NMR (400 MHz, CDCl_3 , 298 K) δ /ppm: 7.83 (d, $^3J_{\text{HH}} = 7.7$ Hz, 1H, Ar-H), 7.56 (d, $^3J_{\text{HH}} = 8.2$ Hz, 1H, Ar-H), 7.47–7.37 (m, 1H, Ar-H), 7.33–7.26 (m, 3H, Ar-H), 7.25–7.14 (m, 2H, Ar-H), 6.53 (d, $^3J_{\text{HH}} = 8.5$ Hz, 2H, Ar-H) 4.27 (s, 2H, CH_2). $^{13}\text{C}\{^1\text{H}\}$ NMR (101 MHz, CDCl_3 , 298 K) δ /ppm: 147.8 (s, Ar), 143.9 (s, Ar), 129.5 (s, Ar), 127.6 (s, Ar), 125.8 (s, Ar), 125.7 (q, $^1J_{\text{FC}} = 3.8$ Hz, CF_3), 118.1 (s, Ar), 113.0 (s, Ar), 47.9 (s, CH_2). ^{19}F NMR (376 MHz, CDCl_3 , 298 K) δ /ppm: -61.01 (s, 3F, *p*- CF_3).

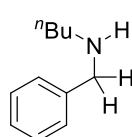
***N*-Benzylpropan-2-amine (2p)**

Synthesised in accordance with *general procedure 4*, using (*Z*)-*N*-isopropyl-1-phenylmethanimine (29.4 mg, 200 μ mol) as the substrate gave the corresponding boronate ester after 0.5 h. The boronate ester was hydrolysed *via* a basic workup (3 \times 10 mL 1 M NaOH washings) to isolate the title compound as a colourless oil. **Yield:** 26 mg, 174 μ mol, 87%.

General procedure 5 and *general procedure 6* were not required due to rapid reaction at room temperature.

Spectroscopic data agrees with literature values.²⁴⁸ **¹H NMR** (400 MHz, CDCl₃, 298 K) δ /ppm: 7.27 (d, ³J_{HH} = 4.4 Hz, 4H, Ar–H), 7.21–7.16 (m, 1H, Ar–H), 3.73 (d, ²J_{HH} = 6.6 Hz, 2H, CH₂), 2.86–2.74 (m, 1H, C–H), 1.20 (s, 1H, N–H), 1.05 (d, ³J_{HH} = 6.3 Hz, 6H, Me). **¹³C{¹H} NMR** (101 MHz, CDCl₃, 298 K) δ /ppm: 141.0 (s, Ar), 128.5 (s, Ar), 128.2 (s, Ar), 126.9 (s, Ar), 51.8 (s, CH₂), 48.2 (s, CH(CH₃)₂), 23.1 (s, CH(CH₃)₂).

N-Benzylbutan-1-amine (2q)

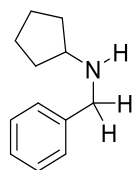


Synthesised in accordance with *general procedure 4*, using (*Z*)-*N*-butyl-1-phenylmethanimine (32.2 mg, 200 μ mol) as the substrate gave the corresponding boronate ester after 8 h. The boronate ester was hydrolysed *via* a basic workup (3 \times 10 mL 1 M NaOH washings) to isolate the title compound as a colourless oil. **Yield:** 30 mg, 184 μ mol, 92%.

Synthesised in accordance with *general procedure 5*, using (*Z*)-*N*-butyl-1-phenylmethanimine (32.2 mg, 200 μ mol) as the substrate gave the corresponding boronate ester after 2 h. The boronate ester was hydrolysed *via* a basic workup (3 \times 10 mL 1 M NaOH washings) to isolate the title compound as a colourless oil. **Yield:** 31 mg, 190 μ mol, 95%.

Synthesised in accordance with *general procedure 6*, using (*Z*)-*N*-butyl-1-phenylmethanimine (64.4 mg, 400 μ mol) as the substrate gave the corresponding boronate ester after 5 min. Crude ¹H NMR spectrum analysis of the hydrolysed material revealed >95% conversion. The title compound was purified by flash-column chromatography using hexane/ethyl acetate (5:1) as the eluent to afford the title compound as a colourless oil. **Yield:** 61 mg, 374 μ mol, 94%.

Spectroscopic data agrees with literature values.²⁴⁹ **¹H NMR** (400 MHz, CDCl₃, 298 K) δ /ppm: 7.58 (d, ³J_{HH} = 6.6 Hz, 2H, Ar–H), 7.42–7.30 (m, 3H, Ar–H), 4.04 (s, 2H, CH₂), 2.82–2.63 (m, 2H, CH₂), 1.87–1.73 (m, 2H, CH₂), 1.31 (hept, ³J_{HH} = 7.4 Hz, 2H, CH₂), 0.86 (t, ³J_{HH} = 7.4 Hz, 3H, Me). **¹³C{¹H} NMR** (101 MHz, CDCl₃, 298 K) δ /ppm: 130.5 (s, Ar), 130.4 (s, Ar), 129.5 (s, Ar), 129.2 (s, Ar), 50.7 (s, CH₂), 45.9 (s, ⁿBu), 28.0 (s, ⁿBu), 20.2 (s, ⁿBu), 13.6 (s, ⁿBu).

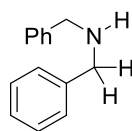
N-Benzylcyclopentanamine (2r)

Synthesised in accordance with *general procedure 4*, using (*Z*)-*N*-cyclopentyl-1-phenylmethanimine (34.6 mg, 200 μmol) as the substrate gave the corresponding boronate ester after 4 h. The boronate ester was hydrolysed *via* a basic workup (3 \times 10 mL 1 M NaOH washings) to isolate the title compound as a colourless oil. **Yield:** 31 mg, 177 μmol , 89%.

Synthesised in accordance with *general procedure 5*, using (*Z*)-*N*-cyclopentyl-1-phenylmethanimine (34.6 mg, 200 μmol) as the substrate gave the corresponding boronate ester after 0.5 h. The boronate ester was hydrolysed *via* a basic workup (3 \times 10 mL 1 M NaOH washings) to isolate the title compound as a colourless oil. **Yield:** 30 mg, 171 μmol , 86%.

Synthesised in accordance with *general procedure 6*, using (*Z*)-*N*-cyclopentyl-1-phenylmethanimine (69.2 mg, 400 μmol) as the substrate gave the corresponding boronate ester after 5 min. Crude ^1H NMR spectrum analysis of the hydrolysed material revealed >95% conversion. The crude material was purified by flash-column chromatography using hexane/ethyl acetate (5:1) as the eluent to afford the title compound as a colourless oil. **Yield:** 62 mg, 354 μmol , 89%.

Spectroscopic data agrees with literature values.²⁴⁹ **^1H NMR** (400 MHz, CDCl_3 , 298 K) δ /ppm: 7.54 (m, 2H, Ar-H), 7.46–7.28 (m, 3H, Ar-H), 3.93 (s, 2H, CH_2), 3.20 (q, $^3J_{\text{HH}} = 7.0$ Hz, 1H, C-H), 1.96 (s, 1H, N-H), 1.96–1.87 (m, 2H, cyclopentyl H), 1.88–1.72 (m, 4H, cyclopentyl H), 1.63–1.42 (m, 2H, cyclopentyl H). **$^{13}\text{C}\{^1\text{H}\}$ NMR** (101 MHz, CDCl_3 , 298 K) δ /ppm: 140.7 (s, Ar), 132.0 (s, Ar), 130.3 (s, Ar), 129.1 (s, Ar), 57.7 (s, CH_2), 50.2 (s, cyclopentyl), 30.1 (s, cyclopentyl), 24.0 (s, cyclopentyl).

Dibenzylamine (2s)

Synthesised in accordance with *general procedure 4*, using (*Z*)-*N*-benzyl-1-phenylmethanimine (39.0 mg, 200 μmol) as the substrate gave the corresponding boronate ester after 156 h. The boronate ester was hydrolysed *via* a basic workup (3 \times 10 mL 1 M NaOH washings) to isolate the title compound as a colourless oil. **Yield:** 38 mg, 193 μmol , 96%.

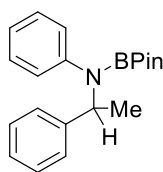
Synthesised in accordance with *general procedure 5*, using (*Z*)-*N*-benzyl-1-phenylmethanimine (39.0 mg, 200 μmol) as the substrate gave the corresponding boronate ester after 0.5 h. The boronate ester was hydrolysed *via* a basic workup (3

× 10 mL 1 M NaOH washings) to isolate the title compound as a colourless oil. **Yield:** 31 mg, 178 μmol , 89%.

Synthesised in accordance with *general procedure 6*, using (*Z*)-*N*-benzyl-1-phenylmethanimine (78.0 mg, 400 μmol) as the substrate gave the corresponding boronate ester after 5 min. Crude ^1H NMR spectrum analysis of the hydrolysed material revealed >95% conversion. The crude material was purified by flash-column chromatography using hexane/ethyl acetate (5:1) as the eluent to afford the title compound as a colourless oil. **Yield:** 76 mg, 386 μmol , 96%.

Spectroscopic data agrees with literature values.²⁴⁷ **^1H NMR** (400 MHz, CDCl_3 , 298 K) δ/ppm : 7.29–7.21 (m, 8H, Ar–H), 7.20–7.12 (m, 2H, Ar–H), 3.72 (s, 4H, CH_2), 1.78 (s, 1H, N–H). **$^{13}\text{C}\{^1\text{H}\}$ NMR** (101 MHz, CDCl_3 , 298 K) δ/ppm : 140.4 (s, Ar), 128.5 (s, Ar), 128.3 (s, Ar), 127.1 (s, Ar), 53.3 (s, CH_2).

4,4,5,5-Tetramethyl-*N*-phenyl-*N*-(1-phenylethyl)-1,3,2-dioxaborolan-2-amine (1t)



Synthesised in accordance with *general procedure 4*, using (*E*)-*N*,1-diphenylethan-1-imine (39.0 mg, 200 μmol) as the substrate gave the corresponding boronate ester after 24 h. The boronate ester was purified *via* a basic workup (3 × 10 mL 1 M NaOH washings) but not hydrolysed to isolate the title compound as a colourless oil. **Yield:** 55 mg, 170 μmol , 85%.

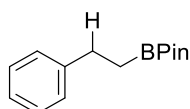
Synthesised in accordance with *general procedure 5*, using (*E*)-*N*,1-diphenylethan-1-imine (39.0 mg, 200 μmol) as the substrate gave the corresponding boronate ester after 0.5 h. The boronate ester was purified *via* a basic workup (3 × 10 mL 1 M NaOH washings) but not hydrolysed to isolate the title compound as a colourless oil. **Yield:** 57 mg, 176 μmol , 88%.

Synthesised in accordance with *general procedure 6*, using (*E*)-*N*,1-diphenylethan-1-imine (78.0 mg, 400 μmol) as the substrate gave the corresponding boronate ester after 5 min. Crude ^1H NMR spectrum analysis of the hydrolysed material revealed >95% conversion. The crude material was purified by flash-column chromatography using hexane/ethyl acetate (5:1) as the eluent to afford the title compound as a colourless oil. **Yield:** 104 mg, 322 μmol , 80%.

Spectroscopic data agrees with literature values.²⁵⁰ **^1H NMR** (400 MHz, CDCl_3 , 298 K) δ/ppm : 7.28 (dd, $^3J_{\text{HH}} = 8.3$ Hz, $^4J_{\text{HH}} = 1.3$ Hz, 2H, Ar–H), 7.22 (td, $^3J_{\text{HH}} = 6.8$ Hz,

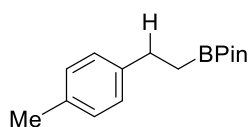
$^4J_{\text{HH}} = 1.8$ Hz, 2H, Ar–H), 7.13 (tt, $^3J_{\text{HH}} = 6.4$ Hz, $^4J_{\text{HH}} = 1.4$ Hz, 1H, Ar–H), 7.04–6.95 (m, 2H, Ar–H), 6.55 (tt, $^3J_{\text{HH}} = 7.4$ Hz, $^4J_{\text{HH}} = 1.1$ Hz, 1H, Ar–H), 6.47–6.38 (m, 2H, Ar–H), 4.39 (q, $^3J_{\text{HH}} = 6.7$ Hz, 1H, C–H), 1.42 (d, $^3J_{\text{HH}} = 6.7$ Hz, 3H, Me), 1.18 (s, 12H, pinacol). $^{11}\text{B NMR}$ (128 MHz, CDCl_3 , 298 K) δ /ppm: 22.3 (s). $^{13}\text{C}\{^1\text{H}\}$ NMR (101 MHz, CDCl_3 , 298 K) δ /ppm: 147.4 (s, Ar), 145.3 (s, Ar), 129.2 (s, Ar), 128.7 (s, Ar), 127.0 (s, Ar), 125.9 (s, Ar), 117.3 (s, Ar), 113.4 (s, Ar), 83.2 (s, pinacol), 53.6 (s, C–H), 25.1 (s, pinacol), 24.7 (s, Me).

4,4,5,5-Tetramethyl-2-phenethyl-1,3,2-dioxaborolane (3a)

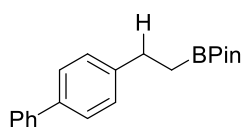


Synthesised in accordance with *general procedure 7*, using styrene (41.6 mg, 400 μmol) as the substrate gave the title compound. Crude conversion by NMR spectroscopy >95%. The crude material was purified by flash-column chromatography using hexane/ethyl acetate (20:1) as the eluent to afford **3a** as a colourless oil. **Yield:** 84 mg, 362 μmol , 90%. Spectroscopic data agrees with literature values.²⁵¹ $^1\text{H NMR}$ (400 MHz, CDCl_3 , 298 K) δ /ppm: 7.29–7.20 (m, 4H, Ar–H), 7.15 (t, $^3J_{\text{HH}} = 7.0$ Hz, 1H, Ar–H), 2.81–2.67 (m, 2H, CH_2), 1.22 (s, 12H, pinacol), 1.19–1.10 (m, 2H, CH_2). $^{11}\text{B NMR}$ (128 MHz, CDCl_3 , 298 K) δ /ppm: 33.9 (s). $^{13}\text{C}\{^1\text{H}\}$ NMR *partial* (101 MHz, CDCl_3 , 298 K) δ /ppm: 144.5 (s, Ar), 128.3 (s, Ar), 128.1 (s, Ar), 125.6 (s, Ar), 83.2 (s, pinacol), 30.1 (s, CH_2), 25.0 (s, pinacol). Note, the carbon adjacent to the boron atom was not observed due to quadrupolar relaxation.

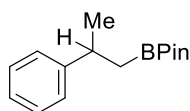
4,4,5,5-Tetramethyl-2-(4-methylphenethyl)-1,3,2-dioxaborolane (3b)



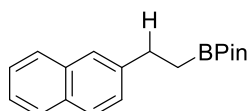
Synthesised in accordance with *general procedure 7*, using 4-methylstyrene (47.2 mg, 400 μmol) as the substrate gave the title compound. Crude conversion by NMR spectroscopy >95%. The crude material was purified by flash-column chromatography using hexane/ethyl acetate (20:1) as the eluent to afford **3b** as a colourless oil. **Yield:** 90 mg, 366 μmol , 91%. Spectroscopic data agrees with literature values.²⁵¹ $^1\text{H NMR}$ (400 MHz, CDCl_3 , 298 K) δ /ppm: 7.09 (q, $^3J_{\text{HH}} = 8.1$ Hz, 4H, Ar–H), 2.71 (m, 2H, CH_2), 2.31 (s, 3H, Me), 1.23 (s, 12H, pinacol), 1.12 (m, 2H, CH_2). $^{11}\text{B NMR}$ (128 MHz, CDCl_3 , 298 K) δ /ppm: 33.9 (s). $^{13}\text{C}\{^1\text{H}\}$ NMR *partial* (101 MHz, CDCl_3 , 298 K) δ /ppm: 141.5 (s, Ar), 135.0 (s, Ar), 129.0 (s, Ar), 128.0 (s, Ar), 83.2 (s, pinacol), 29.7 (s, CH_2), 25.0 (s, pinacol), 21.1 (s, Me). Note, the carbon adjacent to the boron atom was not observed due to quadrupolar relaxation.

4,4,5,5-Tetramethyl-2-(2-([1,1'-biphenyl]4-yl)ethyl)-1,3,2-dioxaborolane (3c)

Synthesised in accordance with *general procedure 7*, using 4-vinylbiphenyl (72.0 mg, 400 μmol) as the substrate gave the title compound. Crude conversion by NMR spectroscopy >95%. The crude material was purified by flash-column chromatography using hexane/ethyl acetate (20:1) as the eluent to afford **3c** as a colourless oil. **Yield:** 115 mg, 372 μmol , 93%. Spectroscopic data agrees with literature values.¹²⁵ **^1H NMR** (400 MHz, CDCl_3 , 298 K) δ /ppm: 7.65–7.57 (m, 2H, Ar–H), 7.55–7.49 (m, 2H, Ar–H), 7.48–7.40 (m, 2H, Ar–H), 7.37–7.29 (m, 3H, Ar–H), 3.02–2.70 (m, 2H, CH_2), 1.25 (s, 12H, pinacol), 1.20 (dd, $^3J_{\text{HH}} = 8.8$ Hz, $^3J_{\text{HH}} = 7.5$ Hz, 2H, CH_2). **^{11}B NMR** (128 MHz, CDCl_3 , 298 K) δ /ppm: 34.0 (s). **$^{13}\text{C}\{^1\text{H}\}$ NMR** (101 MHz, CDCl_3 , 298 K) δ /ppm: 143.7 (s, Ar), 141.4 (s, Ar), 138.6 (s, Ar), 128.8 (s, Ar), 128.6 (s, Ar), 127.1 (s, Ar), 127.1 (s, Ar), 127.0 (s, Ar), 83.3 (s, pinacol), 77.2 (s, CH_2), 29.8 (s, CH_2), 25.0 (s, pinacol).

4,4,5,5-Tetramethyl-2-(2-phenylpropyl)-1,3,2-dioxaborolane (3d)

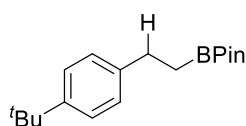
Synthesised in accordance with *general procedure 7*, using α -methylstyrene (47.3 mg, 400 μmol) as the substrate gave the title compound. Crude conversion by NMR spectroscopy >95%. The crude material was purified by flash-column chromatography using hexane/ethyl acetate (20:1) as the eluent to afford **3d** as a colourless oil. **Yield:** 88 mg, 357 μmol , 89%. Spectroscopic data agrees with literature values.²⁵² **^1H NMR** (400 MHz, CDCl_3 , 298 K) δ /ppm: 7.28–7.22 (m, 4H, Ar–H), 7.06–7.00 (m, 1H, Ar–H), 3.14–2.98 (m, 1H, C–H), 1.28 (d, $^3J_{\text{HH}} = 6.9$ Hz, 3H, Me), 1.16 (s, 12H, pinacol), 1.00–0.83 (m, 2H, CH_2). **^{11}B NMR** (128 MHz, CDCl_3 , 298 K) δ /ppm: 33.7 (s). **$^{13}\text{C}\{^1\text{H}\}$ NMR** (101 MHz, CDCl_3 , 298 K) δ /ppm: 149.4 (s, Ar), 128.3 (s, Ar), 126.8 (s, Ar), 125.8 (s, Ar), 83.1 (s, pinacol), 36.0 (s, CH_2), 25.1 (s, pinacol), 24.9 (s, C–H), 24.8 (s, Me).

4,4,5,5-Tetramethyl-2-(2-(naphthalen-2-yl)ethyl)-1,3,2-dioxaborolane (3e)

Synthesised in accordance with *general procedure 7*, using 2-vinylnaphthalene (61.6 mg, 400 μmol) as the substrate gave the title compound. Crude conversion by NMR spectroscopy 84%. The crude material was purified by flash-column chromatography using hexane/ethyl acetate (20:1) as the eluent to afford **3e** as a colourless oil. **Yield:** 80 mg, 284 μmol , 71%. Spectroscopic data agrees with literature values.²⁵³ **^1H NMR** (400 MHz, CDCl_3 ,

298 K) δ /ppm: 7.82–7.73 (m, 3H, Ar–H), 7.66 (s, 1H, Ar–H), 7.47–7.35 (m, 3H, Ar–H), 2.98–2.89 (m, 2H, CH₂), 1.29–1.25 (m, 2H, CH₂), 1.23 (s, 12H, pinacol). ¹¹B NMR (128 MHz, CDCl₃, 298 K) δ /ppm: 34.0 (s). ¹³C{¹H} NMR partial (101 MHz, CDCl₃, 298 K) δ /ppm: 142.1 (s, Ar), 133.8 (s, Ar), 132.0 (s, Ar), 127.8 (s, Ar), 127.7 (s, Ar), 127.6 (s, Ar), 127.4 (s, Ar), 125.8 (s, Ar), 125.8 (s, Ar), 125.0 (s, Ar), 83.3 (s, pinacol), 30.3 (s, CH₂), 25.0 (s, pinacol). Note, the carbon adjacent to the boron atom was not observed due to quadrupolar relaxation.

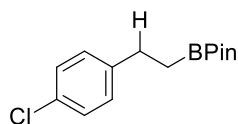
4,4,5,5-Tetramethyl-2-(4-(*tert*-butyl)phenethyl)-1,3,2-dioxaborolane (3f)



Synthesised in accordance with *general procedure 7*, using 4-*tert*-butylstyrene (64.1 mg, 400 μ mol) as the substrate gave the title compound. Crude conversion by NMR spectroscopy 77%.

The crude material was purified by flash-column chromatography using hexane/ethyl acetate (20:1) as the eluent to afford **3f** as a colourless oil. **Yield:** 76 mg, 264 μ mol, 66%. Spectroscopic data agrees with literature values.¹²⁵ ¹H NMR (400 MHz, CDCl₃, 298 K) δ /ppm: 7.29 (d, ³J_{HH} = 8.4 Hz, 2H, Ar–H), 7.15 (d, ³J_{HH} = 8.5 Hz, 2H, Ar–H), 2.84–2.63 (m, 2H, CH₂), 1.30 (s, 9H, ^tBu), 1.22 (s, 12H, pinacol), 1.14 (dd, ³J_{HH} = 9.0 Hz, ³J_{HH} = 7.5 Hz, 2H, CH₂). ¹¹B NMR (128 MHz, CDCl₃, 298 K) δ /ppm: 34.0 (s). ¹³C{¹H} NMR partial (101 MHz, CDCl₃, 298 K) δ /ppm: 148.4 (s, Ar), 141.5 (s, Ar), 127.8 (s, Ar), 125.2 (s, Ar), 83.2 (s, pinacol), 34.5 (s, ^tBu), 31.6 (s, ^tBu), 29.5 (s, CH₂), 25.0 (s, pinacol). Note, the carbon adjacent to the boron atom was not observed due to quadrupolar relaxation.

4,4,5,5-Tetramethyl-2-(4-chlorophenethyl)-1,3,2-dioxaborolane (3g)

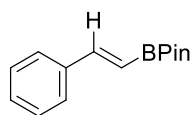


Synthesised in accordance with *general procedure 7*, using 4-chlorostyrene (55.2 mg, 400 μ mol) as the substrate gave the title compound. Crude conversion by NMR spectroscopy 32%. The

crude material was purified by flash-column chromatography using hexane/ethyl acetate (20:1) as the eluent to afford **3g** as a colourless oil. **Yield:** 18 mg, 68 μ mol, 17%. Spectroscopic data agrees with literature values.²⁵⁴ ¹H NMR (400 MHz, CDCl₃, 298 K) δ /ppm: 7.22 (d, ³J_{HH} = 8.4 Hz, 2H, Ar–H), 7.14 (d, ³J_{HH} = 8.4 Hz, 2H, Ar–H), 2.71 (m, 2H, CH₂), 1.21 (s, 12H, pinacol), 1.11 (m, 2H, CH₂). ¹¹B NMR (128 MHz, CDCl₃, 298 K) δ /ppm: 33.9 (s). ¹³C{¹H} NMR partial (101 MHz, CDCl₃, 298 K) δ /ppm: 143.0 (s, Ar), 131.3 (s, Ar), 129.5 (s, Ar), 128.4 (s, Ar), 83.3 (s, pinacol), 29.5 (s, CH₂),

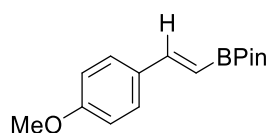
25.0 (s, pinacol). Note, the carbon adjacent to the boron atom was not observed due to quadrupolar relaxation.

(E)-4,4,5,5-Tetramethyl-2-styryl-1,3,2-dioxaborolane (3h)

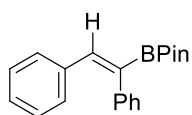


Synthesised in accordance with *general procedure 7*, using phenylacetylene (40.8 mg, 400 μmol) as the substrate gave the title compound. Crude conversion by NMR spectroscopy >95%. The crude material was purified by flash-column chromatography using hexane/ethyl acetate (20:1) as the eluent to afford **3h** as a colourless oil. **Yield:** 85 mg, 369 μmol , 92%. Spectroscopic data agrees with literature values.¹⁰⁸ **^1H NMR** (400 MHz, CDCl_3 , 298 K) δ/ppm : 7.41 (d, $^3J_{\text{HH}} = 7.7$ Hz, 2H, Ar–H), 7.33 (d, $^3J_{\text{HH}} = 18.5$ Hz, 1H, C=C–H), 7.29–7.19 (m, 3H, Ar–H), 6.10 (d, $^3J_{\text{HH}} = 18.4$ Hz, 1H, C=C–H), 1.24 (s, 12H, pinacol). **^{11}B NMR** (128 MHz, CDCl_3 , 298 K) δ/ppm : 30.2 (s). **$^{13}\text{C}\{^1\text{H}\}$ NMR** *partial* (101 MHz, CDCl_3 , 298 K) δ/ppm : 149.6 (s, C=C), 137.6 (s, Ar), 129.0 (s, Ar), 128.7 (s, Ar), 127.2 (s, Ar), 83.5 (s, pinacol), 24.9 (s, pinacol). Note, the carbon adjacent to the boron atom was not observed due to quadrupolar relaxation.

(E)-2-(4-Methoxystyryl)-4,4,5,5-tetramethyl-1,3,2-dioxaborolane (3i)

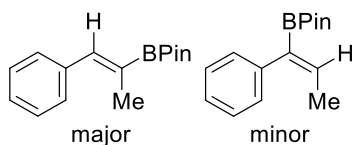


Synthesised in accordance with *general procedure 7*, using 4-ethynylanisole (52.8 mg, 400 μmol) as the substrate gave the title compound. Crude conversion by NMR spectroscopy 93%. The crude material was purified by flash-column chromatography using hexane/ethyl acetate (20:1) as the eluent to afford **3i** as a colourless oil. **Yield:** 86 mg, 331 μmol , 83%. Spectroscopic data agrees with literature values.¹⁰⁹ **^1H NMR** (400 MHz, CDCl_3 , 298 K) δ/ppm : 7.43 (d, $^3J_{\text{HH}} = 8.6$ Hz, 2H, Ar–H), 7.36 (d, $^3J_{\text{HH}} = 18.4$ Hz, 1H, C=C–H), 6.86 (d, $^3J_{\text{HH}} = 8.8$ Hz, 2H, Ar–H), 6.01 (d, $^3J_{\text{HH}} = 18.4$ Hz, 1H, C=C–H), 3.80 (s, 3H, OMe), 1.31 (s, 12H, pinacol). **^{11}B NMR** (128 MHz, CDCl_3 , 298K) δ/ppm : 30.3 (s). **$^{13}\text{C}\{^1\text{H}\}$ NMR** (101 MHz, CDCl_3 , 298 K) δ/ppm : 160.4 (s, C=C), 149.2 (s, Ar), 130.5 (s, Ar), 128.5 (s, Ar), 114.0 (s, Ar), 83.3 (s, pinacol), 77.4 (s, C=C), 55.3 (s, OMe), 24.9 (s, pinacol).

(Z)-2-(1,2-Diphenylvinyl)-4,4,5,5-tetramethyl-1,3,2-dioxaborolane (3j)

Synthesised in accordance with *general procedure 7*, using diphenylacetylene (71.2 mg, 400 μmol) as the substrate gave the title compound. Crude conversion by NMR spectroscopy 50%. The crude material was purified by flash-column chromatography using hexane/ethyl acetate (20:1) as the eluent to afford **3j** as a colourless oil. **Yield:** 53 mg, 173 μmol , 43%. Spectroscopic data agrees with literature values.¹⁰⁸ **^1H NMR** (400 MHz, CDCl_3 , 298 K) δ/ppm : 7.29 (s, 1H, Ar-H), 7.24–7.14 (m, 3H, Ar-H), 7.14–7.08 (m, 2H, Ar-H, C=C-H), 7.06–7.02 (m, 3H, Ar-H), 7.01–6.95 (m, 2H, Ar-H), 1.24 (s, 12H, pinacol). **^{11}B NMR** (128 MHz, CDCl_3 , 298 K) δ/ppm : 30.6 (s). **$^{13}\text{C}\{^1\text{H}\}$ NMR partial** (101 MHz, CDCl_3 , 298 K) δ/ppm : 143.3 (s, C=C), 140.5 (s, Ar), 137.1 (s, Ar), 130.1 (s, Ar), 129.0 (s, Ar), 128.4 (s, Ar), 128.0 (s, Ar), 127.7 (s, Ar), 126.4 (s, Ar), 83.9 (s, pinacol), 24.9 (s, pinacol). Note, the carbon adjacent to the boron atom was not observed due to quadrupolar relaxation.

**(Z)-4,4,5,5-Tetramethyl-2-(1-phenylprop-1-en-2-yl)-1,3,2-dioxaborolane and
(Z)-4,4,5,5-tetramethyl-2-(1-phenylprop-1-en-1-yl)-1,3,2-dioxaborolane (3k)**



Synthesised in accordance with *general procedure 7*, using 1-phenyl-1-propyne (46.4 mg, 400 μmol) as the substrate gave the title compounds. Crude conversion by NMR spectroscopy >95%. The crude material was purified by flash-column chromatography using hexane/ethyl acetate (20:1) as the eluent to afford **3k** as a colourless oil. **Yield:** 84 mg, 344 μmol , 86%. Isolated as a mix of regioisomers (3:1 linear:branched). Spectroscopic data agrees with literature values.¹⁰⁹

Major isomer - **^1H NMR** (400 MHz, CDCl_3 , 298 K) δ/ppm : 7.44–7.29 (m, 5H, Ar-H), 7.24–7.23 (m, 1H, C=C-H), 1.99 (d, $^3J_{\text{HH}} = 1.8$ Hz, 3H, Me), 1.32 (s, 12H, pinacol). **^{11}B NMR** (128 MHz, CDCl_3 , 298 K) δ/ppm : 30.7 (s). **$^{13}\text{C}\{^1\text{H}\}$ NMR partial** (101 MHz, CDCl_3 , 298 K) δ/ppm : 142.5 (s, C=C), 138.0 (s, Ar), 129.5 (s, Ar), 128.2 (s, Ar), 127.3 (s, Ar), 83.7 (s, pinacol), 25.0 (s, pinacol), 16.1 (s, Me). Note, the carbon adjacent to the boron atom was not observed due to quadrupolar relaxation.

Minor isomer - **^1H NMR** (400 MHz, CDCl_3 , 298 K) δ/ppm : 7.22–7.13 (m, 5H, Ar-H), 6.72 (q, $^2J_{\text{HH}} = 6.9$ Hz, 1H, C=C-H), 1.77 (d, $^3J_{\text{HH}} = 7.0$ Hz, 3H, Me), 1.27 (s, 12H, pinacol). **^{11}B NMR** (128 MHz, CDCl_3 , 298 K) δ/ppm : 30.7 (s). **$^{13}\text{C}\{^1\text{H}\}$ NMR partial** (101 MHz, CDCl_3 , 298 K) δ/ppm : 142.9 (s, C=C), 139.9 (s, Ar), 129.2 (s, Ar), 127.9

(s, Ar), 126.0 (s, Ar), 83.6 (s, pinacol), 24.9 (s, pinacol), 16.1 (s, Me). Note, the carbon adjacent to the boron atom was not observed due to quadrupolar relaxation.

8.6 Al(3,4,5-F₃C₆H₂)₃·Et₂O-catalysed hydroboration

General procedure 8

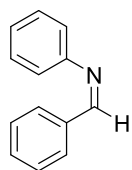
Synthesised in accordance with the literature known procedure,²³⁹ the necessary aldehyde (10 mmol) was dissolved in CH₂Cl₂ (10 mL) along with 3 Å molecular sieves. To this the required amine (10 mmol) was added. The reaction was left at ambient temperature for two hours at which point MgSO₄ was added with subsequent filtration. Volatiles were removed *in vacuo* to leave the pure imine.

General procedure 9

In an NMR tube, pinacolborane (34.8 µL, 240 µmol, 1.2 equiv.) and the substrate (200 µmol, 1.0 equiv.) were combined in deuterated chloroform (0.7 mL). To this, tris(3,4,5-trifluorophenyl)alane etherate (9.9 mg, 10 mol%, 20 µmol, 0.1 equiv.) was added, and the NMR tube sealed. The mixture was heated to 70 °C and conversion was monitored *via in situ* ¹H NMR spectroscopy until the desired boronate ester had been formed in >95% yield. Upon completion of the reaction, the catalyst was removed (and for aldehyde, ketone and imine substrates, the boronate ester was hydrolysed) by washing with 1 M NaOH (3 × 10 mL) and was further purified using flash column chromatography.

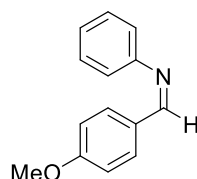
8.6.1 Synthesis of starting materials

***N*,1-Diphenylmethanimine**

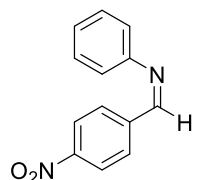


Synthesised in accordance with *general procedure 8* using benzaldehyde (1.06 g, 10 mmol, 1.0 equiv.) and aniline (933 mL, 10 mmol, 1.0 equiv.).

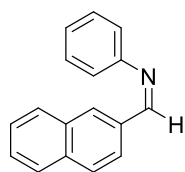
Yield: 1.74 g, 9.60 mmol, 96%. Spectroscopic analyses agree with literature values.²⁴⁰ **¹H NMR** (500 MHz, CDCl₃, 298 K) δ/ppm: 8.46 (s, 1H, N=CH), 7.92 (dd, ³J_{HH} = 6.6 Hz, ⁴J_{HH} = 2.8 Hz, 2H, Ar-H), 7.61–7.43 (m, 3H, Ar-H), 7.41 (t, ³J_{HH} = 7.7 Hz, 2H, Ar-H), 7.23 (d, ³J_{HH} = 8.4 Hz, 3H, Ar-H).

1-(4-Methoxyphenyl)-*N*-phenylmethanimine

Synthesised in accordance with *general procedure 8* using 4-methoxybenzaldehyde (1.36 g, 10 mmol, 1.0 equiv.) and aniline (933 mL, 10 mmol, 1.0 equiv.). **Yield:** 2.04 g, 9.67 mmol, 96.7%. Spectroscopic analyses agree with literature values.¹⁰⁸ **¹H NMR** (500 MHz, CDCl₃, 298 K) δ /ppm: 8.39 (s, 1H, N=CH), 7.86 (d, ³J_{HH} = 8.9 Hz, 2H, Ar–H), 7.50–7.33 (m, 2H, Ar–H), 7.25–7.18 (m, 3H, Ar–H), 6.99 (d, ³J_{HH} = 8.8 Hz, 2H, Ar–H), 3.88 (s, 3H, OMe).

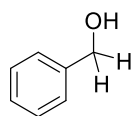
1-(4-Nitrophenyl)-*N*-phenylmethanimine

Synthesised in accordance with *general procedure 8* using 4-nitrobenzaldehyde (1.51 g, 10 mmol, 1.0 equiv.) and aniline (933 mL, 10 mmol, 1.0 equiv.). **Yield:** 2.11 g, 9.32 mmol, 93.2%. Spectroscopic analyses agree with literature values.¹⁰⁸ **¹H NMR** (500 MHz, CDCl₃, 298 K) δ /ppm: 8.49 (s, 1H, CH=N), 8.26 (d, ³J_{HH} = 9.0 Hz, 2H, Ar–H), 8.01 (d, ³J_{HH} = 9.3 Hz, 2H, Ar–H), 7.41–7.33 (m, 2H, Ar–H), 7.23 (t, ³J_{HH} = 7.4 Hz, 1H, Ar–H), 7.20 (d, ³J_{HH} = 7.6 Hz, 2H, Ar–H).

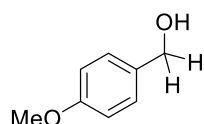
1-(Naphthalen-2-yl)-*N*-phenylmethanimine

Synthesised in accordance with *general procedure 8* using 4-naphthaldehyde (1.56 g, 10 mmol, 1.0 equiv.) and aniline (933 mL, 10 mmol, 1.0 equiv.). **Yield:** 2.18 g, 9.43 mmol, 94.3%. Spectroscopic analyses agree with literature values.¹⁰⁸ **¹H NMR** (500 MHz, CDCl₃, 298 K) δ /ppm: 8.63 (s, 1H, CH=N), 8.21 (s, 1H, Ar–H), 8.18 (dd, ³J_{HH} = 8.5 Hz, ⁴J_{HH} = 1.6 Hz, 1H, Ar–H), 7.94 (t, ³J_{HH} = 8.1 Hz, 2H, Ar–H), 7.89 (d, ³J_{HH} = 7.8 Hz, 1H, Ar–H), 7.59–7.51 (m, 2H, Ar–H), 7.43 (dd, ³J_{HH} = 8.3 Hz, ³J_{HH} = 7.2 Hz, 2H, Ar–H), 7.31–7.22 (m, 3H, Ar–H).

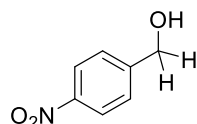
8.6.2 Synthesis of reduction products

Phenylmethanol (5a)

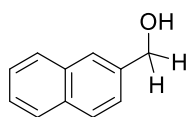
Synthesised in accordance with *general procedure 9* using benzaldehyde (20.4 μL , 200 μmol). The crude material was purified by flash-column chromatography using hexane/ethyl acetate (5:1) as the eluent to afford the title compound as a colourless oil. **Yield:** 21 mg, 193 μmol , 97%. Spectroscopic analyses agree with literature values.²⁴² **$^1\text{H NMR}$** (500 MHz, CDCl_3 , 298 K) δ/ppm : 7.39–7.34 (m, 4H, Ar–H), 7.31 (t, $^3J_{\text{HH}} = 6.7$ Hz, 1H, Ar–H), 4.63 (s, 2H, CH_2), 2.71 (br, 1H, OH). **$^{13}\text{C}\{^1\text{H}\}$ NMR** (126 MHz, CDCl_3 , 298 K) δ/ppm : 140.9 (s, Ar), 128.6 (s, Ar), 127.6 (s, Ar), 127.0 (s, Ar), 65.1 (s, CH_2).

(4-Methoxyphenyl)methanol (5b)

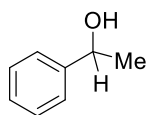
Synthesised in accordance with *general procedure 9* using 4-methoxybenzaldehyde (24.3 μL , 200 μmol). The crude material was purified by flash-column chromatography using hexane/ethyl acetate (5:1) as the eluent to afford the title compound as a colourless oil. **Yield:** 24 mg, 174 μmol , 87%. Spectroscopic analyses agree with literature values.²⁴² **$^1\text{H NMR}$** (500 MHz, CDCl_3 , 298 K) δ/ppm : 7.30 (d, $^3J_{\text{HH}} = 8.8$ Hz, 2H, Ar–H), 6.90 (d, $^3J_{\text{HH}} = 8.7$ Hz, 2H, Ar–H), 4.62 (s, 2H, CH_2), 3.81 (s, 3H, OMe). **$^{13}\text{C}\{^1\text{H}\}$ NMR** (126 MHz, CDCl_3 , 298 K) δ/ppm : 159.4 (s, Ar), 133.3 (s, Ar), 128.8 (s, Ar), 114.1 (s, Ar), 65.2 (s, OMe), 55.5 (s, CH_2).

(4-Nitrophenyl)methanol (5c)

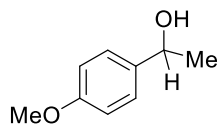
Synthesised in accordance with *general procedure 9* using 4-nitrobenzaldehyde (31.1 mg, 200 μmol). The crude material was purified by flash-column chromatography using hexane/ethyl acetate (5:1) as the eluent to afford the title compound as a yellow solid. **Yield:** 27 mg, 176 μmol , 88%. Spectroscopic analyses agree with literature values.²⁴² **$^1\text{H NMR}$** (500 MHz, CDCl_3 , 298 K) δ/ppm : 8.22 (d, $^3J_{\text{HH}} = 8.8$ Hz, 2H, Ar–H), 7.54 (d, $^3J_{\text{HH}} = 8.8$ Hz, 2H, Ar–H), 4.84 (d, $^3J_{\text{HH}} = 5.5$ Hz, 2H, CH_2), 1.90 (t, $^3J_{\text{HH}} = 5.5$ Hz, 1H, OH). **$^{13}\text{C}\{^1\text{H}\}$ NMR** (126 MHz, CDCl_3 , 298 K) δ/ppm : 148.2 (s, Ar), 147.5 (s, Ar), 127.1 (s, Ar), 123.9 (s, Ar), 64.2 (s, CH_2).

Napthalen-2-ylmethanol (5d)

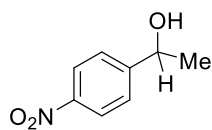
Synthesised in accordance with *general procedure 9* using 2-napthaldehyde (31.2 mg, 200 μmol). The crude material was purified by flash-column chromatography using hexane/ethyl acetate (5:1) as the eluent to afford the title compound as a colourless oil. **Yield:** 28 mg, 177 μmol , 89%. Spectroscopic analyses agree with literature values.²⁵⁵ **$^1\text{H NMR}$** (500 MHz, CDCl_3 , 298 K) δ/ppm : 7.87–7.81 (m, 4H, Ar–H), 7.51–7.46 (m, 3H, Ar–H), 4.87 (d, $^3J_{\text{HH}} = 6.0$ Hz, 2H, CH_2), 1.73 (t, $^3J_{\text{HH}} = 6.0$ Hz, 1H, OH). **$^{13}\text{C}\{^1\text{H}\}$ NMR** (126 MHz, CDCl_3 , 298 K) δ/ppm : 138.4 (s, Ar), 133.5 (s, Ar), 133.1 (s, Ar), 128.5 (s, Ar), 128.0 (s, Ar), 127.9 (s, Ar), 126.4 (s, Ar), 126.1 (s, Ar), 125.6 (s, Ar), 125.3 (s, Ar), 65.7 (s, CH_2).

1-Phenylethanol (5e)

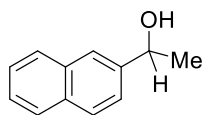
Synthesised in accordance with *general procedure 9* using acetophenone (23.4 μL , 200 μmol). The crude material was purified by flash-column chromatography using hexane/ethyl acetate (5:1) as the eluent to afford the title compound as a colourless oil. **Yield:** 23 mg, 188 μmol , 94%. Spectroscopic analyses agree with literature values.²⁴⁴ **$^1\text{H NMR}$** (500 MHz, CDCl_3 , 298 K) δ/ppm : 7.41–7.32 (m, 4H, Ar–H), 7.32–7.24 (m, 1H, Ar–H), 4.90 (q, $^3J_{\text{HH}} = 6.4$ Hz, 1H, CH_2), 1.92 (br, 1H, OH), 1.50 (d, $^3J_{\text{HH}} = 6.5$ Hz, 3H, Me). **$^{13}\text{C}\{^1\text{H}\}$ NMR** (126 MHz, CDCl_3 , 298 K) δ/ppm : 145.9 (s, Ar), 128.6 (s, Ar), 127.6 (s, Ar), 125.5 (s, Ar), 70.5 (s, C–H), 25.3 (s, Me).

1-(4-Methoxyphenyl)ethanol (5f)

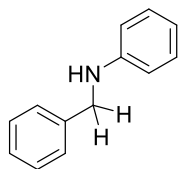
Synthesised in accordance with *general procedure 9* using 4-methoxyacetophenone (27.5 μL , 200 μmol). The crude material was purified by flash-column chromatography using hexane/ethyl acetate (5:1) as the eluent to afford the title compound as a colourless oil. **Yield:** 29 mg, 191 μmol , 95%. Spectroscopic analyses agree with literature values.²⁵⁶ **$^1\text{H NMR}$** (500 MHz, CDCl_3 , 298 K) δ/ppm : 7.31 (d, $^3J_{\text{HH}} = 8.8$ Hz, 2H, Ar–H), 6.89 (d, $^3J_{\text{HH}} = 8.8$ Hz, 2H, Ar–H), 4.86 (q, $^3J_{\text{HH}} = 6.4$ Hz, 1H, CH_2), 3.81 (s, 3H, OMe), 1.74 (br, 1H, OH), 1.48 (d, $^3J_{\text{HH}} = 6.4$ Hz, 3H, Me). **$^{13}\text{C}\{^1\text{H}\}$ NMR** (126 MHz, CDCl_3 , 298 K) δ/ppm : 159.0 (s, Ar), 138.0 (s, Ar), 126.7 (s, Ar), 113.9 (s, Ar), 70.0 (s, C–H), 55.3 (s, OMe), 25.0 (s, Me).

1-(4-Nitrophenyl)ethanol (5g)

Synthesised in accordance with *general procedure 9* using 4-nitroacetophenone (33.0 mg, 200 μmol). The crude material was purified by flash-column chromatography using hexane/ethyl acetate (5:1) as the eluent to afford the title compound as a yellow solid. **Yield:** 29 mg, 174 μmol , 87%. Spectroscopic analyses agree with literature values.²⁴⁴ **$^1\text{H NMR}$** (500 MHz, CDCl_3 , 298 K) δ/ppm : 8.20 (d, $^3J_{\text{HH}} = 8.8$ Hz, 2H, Ar-H), 7.54 (d, $^3J_{\text{HH}} = 8.3$ Hz, 2H, Ar-H), 5.02 (q, $^3J_{\text{HH}} = 6.5$ Hz, 1H, CH_2), 2.05 (br, 1H, OH), 1.52 (d, $^3J_{\text{HH}} = 6.5$ Hz, 3H, Me). **$^{13}\text{C}\{^1\text{H}\}$ NMR** (126 MHz, CDCl_3 , 298 K) δ/ppm : 153.2 (s, Ar), 147.3 (s, Ar), 126.3 (s, Ar), 123.9 (s, Ar), 69.7 (s, C-H), 25.7 (s, Me).

1-(Naphthalen-2-yl)ethanol (5h)

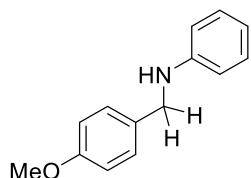
Synthesised in accordance with *general procedure 9* using 2-acetylnaphthalene (36.4 mg, 200 μmol). The crude material was purified by flash-column chromatography using hexane/ethyl acetate (5:1) as the eluent to afford the title compound as a colourless oil. **Yield:** 32 mg, 186 μmol , 93%. Spectroscopic analyses agree with literature values.²⁵⁶ **$^1\text{H NMR}$** (500 MHz, CDCl_3 , 298 K) δ/ppm : 7.88–7.79 (m, 4H, Ar-H), 7.54–7.43 (m, 3H, Ar-H), 5.08 (qd, $^3J_{\text{HH}} = 6.4$ Hz, $^3J_{\text{HH}} = 3.3$ Hz, 1H, CH_2), 1.92 (d, $^3J_{\text{HH}} = 3.5$ Hz, 1H, OH), 1.59 (d, $^3J_{\text{HH}} = 6.5$ Hz, 3H, Me). **$^{13}\text{C}\{^1\text{H}\}$ NMR** (126 MHz, CDCl_3 , 298 K) δ/ppm : 143.3 (s, Ar), 133.5 (s, Ar), 133.1 (s, Ar), 128.5 (s, Ar), 128.1 (s, Ar), 127.8 (s, Ar), 126.3 (s, Ar), 125.9 (s, Ar), 123.9 (s, Ar), 123.9 (s, Ar), 70.7 (s, C-H), 25.3 (s, Me).

N-Benzylaniline (5i)

Synthesised in accordance with *general procedure 9* using *N*,1-diphenylmethanimine (36.2 mg, 200 μmol). The crude material was purified by flash-column chromatography using hexane/ethyl acetate (5:1) as the eluent to afford the title compound as a colourless oil. **Yield:** 33 mg, 180 μmol , 90%. Spectroscopic analyses agree with literature values.¹⁰⁷ **$^1\text{H NMR}$** (500 MHz, CDCl_3 , 298 K) δ/ppm : 7.41–7.33 (m, 4H, Ar-H), 7.32–7.26 (m, 1H, Ar-H), 7.19 (dd, $^3J_{\text{HH}} = 8.6$ Hz, $^3J_{\text{HH}} = 7.3$ Hz, 2H, Ar-H), 6.73 (t, $^3J_{\text{HH}} = 7.4$ Hz, 1H, Ar-H), 6.69–6.64 (m, 2H, Ar-H), 4.34 (s, 2H, CH_2), 4.03 (br, 1H, N-H). **$^{13}\text{C}\{^1\text{H}\}$ NMR** (126 MHz, CDCl_3 , 298 K) δ/ppm : 148.3 (s, Ar), 139.6 (s, Ar), 129.4 (s,

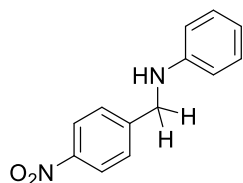
Ar), 128.8 (s, Ar), 127.7 (s, Ar), 127.4 (s, Ar), 117.7 (s, Ar), 113.0 (s, Ar), 48.5 (s, CH₂).

***N*-(4-Methoxybenzyl)aniline (5j)**

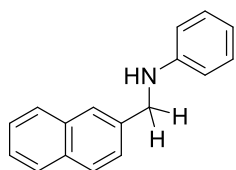


Synthesised in accordance with *general procedure 9* using 1-(4-methoxyphenyl)-*N*-phenylmethanimine (42.2 mg, 200 μmol). The crude material was purified by flash-column chromatography using hexane/ethyl acetate (5:1) as the eluent to afford the title compound as a colourless oil. **Yield:** 38 mg, 178 μmol, 89%. Spectroscopic analyses agree with literature values.²⁴⁷ **¹H NMR** (500 MHz, CDCl₃, 298 K) δ/ppm: 7.30 (d, ³J_{HH} = 8.4 Hz, 2H, Ar–H), 7.19 (t, ³J_{HH} = 7.8 Hz, 2H, Ar–H), 6.89 (d, ³J_{HH} = 8.5 Hz, 2H, Ar–H), 6.72 (t, ³J_{HH} = 7.3 Hz, 1H, Ar–H), 6.65 (d, ³J_{HH} = 8.3 Hz, 2H, Ar–H), 4.26 (s, 2H, CH₂), 3.95 (br, 1H, N–H), 3.81 (s, 3H, OMe). **¹³C{¹H} NMR** (126 MHz, CDCl₃, 298 K) δ/ppm: 159.0 (s, Ar), 148.3 (s, Ar), 131.5 (s, Ar), 129.4 (s, Ar), 128.9 (s, Ar), 117.6 (s, Ar), 114.2 (s, Ar), 113.0 (s, Ar), 55.4 (s, OMe), 47.9 (s, CH₂).

***N*-(4-Nitrobenzyl)aniline (5k)**



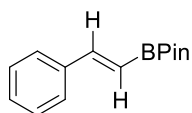
Synthesised in accordance with *general procedure 9* using 1-(4-nitrophenyl)-*N*-phenylmethanimine (45.2 mg, 200 μmol). The crude material was purified by flash-column chromatography using hexane/ethyl acetate (5:1) as the eluent to afford the title compound as a colourless oil. **Yield:** 35 mg, 153 μmol, 77%. Spectroscopic analyses agree with literature values.²⁵⁷ **¹H NMR** (500 MHz, CDCl₃, 298 K) δ/ppm: 8.20 (d, ³J_{HH} = 8.8 Hz, 2H, Ar–H), 7.55–7.53 (m, 2H, Ar–H), 7.17 (dd, ³J_{HH} = 8.6 Hz, ³J_{HH} = 7.4 Hz, 2H, Ar–H), 6.75 (t, ³J_{HH} = 7.4 Hz, 1H, Ar–H), 6.60–6.55 (m, 2H, Ar–H), 4.48 (s, 2H, CH₂), 4.26 (br, 1H, N–H). **¹³C{¹H} NMR** (126 MHz, CDCl₃, 298 K) δ/ppm: 147.6 (s, Ar), 147.4 (s, Ar), 147.2 (s, Ar), 129.5 (s, Ar), 127.8 (s, Ar), 124.0 (s, Ar), 118.3 (s, Ar), 113.0 (s, Ar), 47.7 (s, CH₂).

***N*-(Naphthalen-2-ylmethyl)aniline (5l)**

Synthesised in accordance with *general procedure 9* using 1-(naphthalen-2-yl)-*N*-phenylmethanimine (46.2 mg, 200 μ mol).

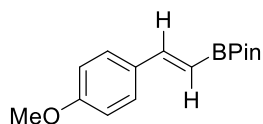
The crude material was purified by flash-column chromatography using hexane/ethyl acetate (5:1) as the eluent to afford the title

compound as a colourless oil. **Yield:** 42 mg, 180 μ mol, 90%. Spectroscopic analyses agree with literature values.²⁵⁷ **$^1\text{H NMR}$** (500 MHz, CDCl_3 , 298 K) δ /ppm: 7.85–7.80 (m, 4H, Ar–H), 7.51–7.44 (m, 3H, Ar–H), 7.22–7.17 (m, 2H, Ar–H), 6.74 (t, $^3J_{\text{HH}} = 7.3$ Hz, 1H, Ar–H), 6.69 (d, $^3J_{\text{HH}} = 8.6$ Hz, 2H, Ar–H), 4.51 (s, 2H, CH_2), 4.16 (s, 1H, N–H). **$^{13}\text{C}\{^1\text{H}\}$ NMR** (126 MHz, CDCl_3 , 298 K) δ /ppm: 148.2 (s, Ar), 137.0 (s, Ar), 133.6 (s, Ar), 132.8 (s, Ar), 129.4 (s, Ar), 128.5 (s, Ar), 127.9 (s, Ar), 127.8 (s, Ar), 126.3 (s, Ar), 126.0 (s, Ar), 125.9 (s, Ar), 117.7 (s, Ar), 113.0 (s, Ar), 48.6 (s, CH_2).

4,4,5,5-Tetramethyl-2-styryl-1,3,2-dioxaborolane (4m)

Synthesised in accordance with *general procedure 9* using phenylacetylene (22.0 μL , 200 μmol). The crude material was purified by flash-column chromatography using hexane/ethyl acetate

(20:1) as the eluent to afford the title compound as a colourless oil. **Yield:** 42 mg, 182 μmol , 91%. Spectroscopic analyses agree with literature values.¹⁰⁸ **$^1\text{H NMR}$** (500 MHz, CDCl_3 , 298 K) δ /ppm: 7.52–7.28 (m, 6H, Ar–H and $\text{HC}=\text{C}$), 6.17 (d, $^3J_{\text{HH}} = 18.4$ Hz, 1H, $\text{HC}=\text{C}$), 1.32 (s, 12H, pinacol). **$^{11}\text{B NMR}$** (160 MHz, CDCl_3 , 298 K) δ /ppm: 30.1 (s). **$^{13}\text{C}\{^1\text{H}\}$ NMR** *partial* (126 MHz, CDCl_3 , 298 K) δ /ppm: 149.6 (s, $\text{C}=\text{C}$), 137.6 (s, Ar), 129.0 (s, Ar), 128.7 (s, Ar), 127.2 (s, Ar), 83.5 (s, pinacol), 25.0 (s, pinacol). Note, the carbon atom adjacent to the boron atom was not observed due to quadrupolar relaxation.

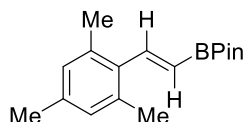
2-(4-Methoxystyryl)-4,4,5,5-tetramethyl-1,3,2-dioxaborolane (4n)

Synthesised in accordance with *general procedure 9* using 1-ethynyl-4-methoxybenzene (25.9 μL , 200 μmol). The crude material was purified by flash-column chromatography using

hexane/ethyl acetate (20:1) as the eluent to afford the title compound as a colourless oil. **Yield:** 45 mg, 173 μmol , 86%. Spectroscopic analyses agree with literature values.¹⁰⁹ **$^1\text{H NMR}$** (500 MHz, CDCl_3 , 298 K) δ /ppm: 7.44 (d, $^3J_{\text{HH}} = 8.7$ Hz, 2H, Ar–H), 7.35 (d, $^3J_{\text{HH}} = 18.4$ Hz, 1H, $\text{CH}=\text{C}$), 6.87 (d, $^3J_{\text{HH}} = 8.8$ Hz, 2H, Ar–H), 6.01 (d,

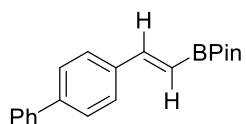
$^3J_{\text{HH}} = 18.4$ Hz, 1H, CH=C), 3.81 (s, 3H, OMe), 1.31 (s, 12H, pinacol). $^{11}\text{B NMR}$ (160 MHz, CDCl_3 , 298 K) δ/ppm : 30.1 (s). $^{13}\text{C}\{^1\text{H}\}$ NMR *partial* (126 MHz, CDCl_3 , 298 K) δ/ppm : 160.4 (s, C=C), 149.2 (s, Ar), 130.4 (s, Ar), 128.6 (s, Ar), 114.1 (s, Ar), 83.4 (s, pinacol), 55.4 (s, OMe), 24.9 (s, pinacol). Note, the carbon atom adjacent to the boron atom was not observed due to quadrupolar relaxation.

2-(2,4,6-Trimethylstyryl)-4,4,5,5-tetramethyl-1,3,2-dioxaborolane (4o)

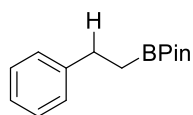


Synthesised in accordance with *general procedure 9* using 2-ethynyl-1,3,5-trimethylbenzene (28.8 mg, 200 μmol). The crude material was purified by flash-column chromatography using hexane/ethyl acetate (20:1) as the eluent to afford the title compound as a colourless oil. **Yield:** 51 mg, 187 μmol , 94%. Spectroscopic analyses agree with literature values.¹⁰⁵ $^1\text{H NMR}$ (500 MHz, CDCl_3 , 298 K) δ/ppm : 7.44 (d, $^3J_{\text{HH}} = 18.8$ Hz, 1H, CH=C), 6.86 (s, 2H, Ar-H), 5.68 (d, $^3J_{\text{HH}} = 18.8$ Hz, 1H, CH=C), 2.30 (s, 6H, mesityl), 2.27 (s, 3H, mesityl), 1.33 (s, 12H, pinacol). $^{11}\text{B NMR}$ (160 MHz, CDCl_3 , 298 K) δ/ppm : 29.9 (s). $^{13}\text{C}\{^1\text{H}\}$ NMR *partial* (126 MHz, CDCl_3 , 298 K) δ/ppm : 148.6 (s, C=C), 136.9 (s, Ar), 136.0 (s, Ar), 135.2 (s, Ar), 128.8 (s, Ar), 83.4 (s, pinacol), 25.0 (s, pinacol), 21.1 (s, Me), 21.1 (s, Me). Note, the carbon atom adjacent to the boron atom was not observed due to quadrupolar relaxation.

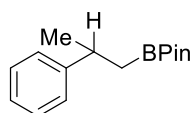
2-(2-(Biphenyl-4-yl)vinyl)-4,4,5,5-tetramethyl-1,3,2-dioxaborolane (4p)



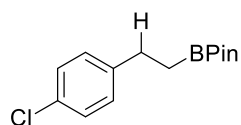
Synthesised in accordance with *general procedure 9* using 4-ethynyl-1,1'-biphenyl (35.6 mg, 200 μmol). The crude material was purified by flash-column chromatography using hexane/ethyl acetate (20:1) as the eluent to afford the title compound as a colourless oil. **Yield:** 49 mg, 136 μmol , 68%. Spectroscopic analyses agree with literature values.²⁵⁸ $^1\text{H NMR}$ (500 MHz, CDCl_3 , 298 K) δ/ppm : 7.62–7.57 (m, 6H, Ar-H), 7.47–7.42 (m, 3H, Ar-H), 7.36 (m, 1H, HC=C), 6.22 (d, $^3J_{\text{HH}} = 18.4$ Hz, 1H, HC=C), 1.34 (s, 12H, pinacol). $^{11}\text{B NMR}$ (160 MHz, CDCl_3 , 298 K) δ/ppm : 30.1 (s). $^{13}\text{C}\{^1\text{H}\}$ NMR *partial* (126 MHz, CDCl_3 , 298 K) δ/ppm : 149.1 (s, C=C), 141.7 (s, Ar), 140.7 (s, Ar), 136.5 (s, Ar), 128.9 (s, Ar), 127.7 (s, Ar), 127.6 (s, Ar), 127.4 (s, Ar), 127.1 (s, Ar), 83.5 (s, pinacol), 25.0 (s, pinacol). Note, the carbon adjacent to the boron atom was not observed due to quadrupolar relaxation.

4,4,5,5-Tetramethyl-2-phenethyl-1,3,2-dioxaborolane (4q)

Synthesised in accordance with *general procedure 9* using styrene (22.9 μL , 200 μmol). The crude material was purified by flash-column chromatography using hexane/ethyl acetate (20:1) as the eluent to afford the title compound as a colourless oil. **Yield:** 41 mg, 177 μmol , 88%. Spectroscopic analyses agree with literature values.²⁵¹ **$^1\text{H NMR}$** (400 MHz, CDCl_3 , 298 K) δ/ppm : 7.29–7.20 (m, 4H, Ar–H), 7.15 (t, $^3J_{\text{HH}} = 7.0$ Hz, 1H, Ar–H), 2.81–2.67 (m, 2H, CH_2), 1.22 (s, 12H, pinacol), 1.19–1.10 (m, 2H, CH_2). **$^{11}\text{B NMR}$** (128 MHz, CDCl_3 , 298 K) δ/ppm : 33.9 (s). **$^{13}\text{C}\{^1\text{H}\}$ NMR** *partial* (101 MHz, CDCl_3 , 298 K) δ/ppm : 144.5 (s, Ar), 128.3 (s, Ar), 128.1 (s, Ar), 125.6 (s, Ar), 83.2 (s, pinacol), 30.1 (s, CH_2), 25.0 (s, pinacol). Note, the carbon adjacent to the boron atom was not observed due to quadrupolar relaxation.

4,4,5,5-Tetramethyl-2-(2-phenylpropyl)-1,3,2-dioxaborolane (4r)

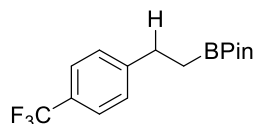
Synthesised in accordance with *general procedure 9*, using alpha-methylstyrene (26.0 μL , 400 μmol). The crude material was purified by flash-column chromatography using hexane/ethyl acetate (20:1) as the eluent to afford **3d** as a colourless oil. **Yield:** 45 mg, 183 μmol , 91%. Spectroscopic data agrees with literature values.²⁵² **$^1\text{H NMR}$** (400 MHz, CDCl_3 , 298 K) δ/ppm : 7.28–7.22 (m, 4H, Ar–H), 7.06–7.00 (m, 1H, Ar–H), 3.14–2.98 (m, 1H, C–H), 1.28 (d, $^3J_{\text{HH}} = 6.9$ Hz, 3H, Me), 1.16 (s, 12H, pinacol), 1.00–0.83 (m, 2H, CH_2). **$^{11}\text{B NMR}$** (128 MHz, CDCl_3 , 298 K) δ/ppm : 33.7 (s). **$^{13}\text{C}\{^1\text{H}\}$ NMR** (101 MHz, CDCl_3 , 298 K) δ/ppm : 149.4 (s, Ar), 128.3 (s, Ar), 126.8 (s, Ar), 125.8 (s, Ar), 83.1 (s, pinacol), 36.0 (s, CH_2), 25.1 (s, pinacol), 24.9 (s, C–H), 24.8 (s, Me).

4,4,5,5-Tetramethyl-2-(4-chlorophenethyl)-1,3,2-dioxaborolane (4s)

Synthesised in accordance with *general procedure 9* using 4-chlorostyrene (24.0 μL , 200 μmol). The crude material was purified by flash-column chromatography using hexane/ethyl acetate (20:1) as the eluent to afford the title compound as a colourless oil. **Yield:** 42 mg, 158 μmol , 79%. Spectroscopic data agrees with literature values.²⁵⁴ **$^1\text{H NMR}$** (400 MHz, CDCl_3 , 298 K) δ/ppm : 7.22 (d, $^3J_{\text{HH}} = 8.4$ Hz, 2H, Ar–H), 7.14 (d, $^3J_{\text{HH}} = 8.4$ Hz, 2H, Ar–H), 2.71 (m, 2H, CH_2), 1.21 (s, 12H, pinacol), 1.11 (m, 2H, CH_2). **$^{11}\text{B NMR}$** (128 MHz, CDCl_3 , 298 K) δ/ppm : 33.9 (s). **$^{13}\text{C}\{^1\text{H}\}$ NMR** *partial* (101 MHz, CDCl_3 , 298

K) δ /ppm: 143.0 (s, Ar), 131.3 (s, Ar), 129.5 (s, Ar), 128.4 (s, Ar), 83.3 (s, pinacol), 29.5 (s, CH₂), 25.0 (s, pinacol). Note, the carbon adjacent to the boron atom was not observed due to quadrupolar relaxation.

4,4,5,5-Tetramethyl-2-(4-(trifluoromethyl)phenethyl)-1,3,2-dioxaborolane (4t)



Synthesised in accordance with *general procedure 9* using 4-(trifluoromethyl)styrene (29.6 μ L, 200 μ mol). The crude material was purified by flash-column chromatography using hexane/ethyl acetate (20:1) as the eluent to afford the title compound as a colourless oil. **Yield:** 44 mg, 147 μ mol, 73%. Spectroscopic data agrees with literature values.¹¹⁹ **¹H NMR** (400 MHz, CDCl₃, 298 K) δ /ppm: 7.51 (d, ³J_{HH} = 8.0 Hz, 2H, Ar-H), 7.32 (d, ³J_{HH} = 7.9 Hz, 2H, Ar-H), 2.84–2.76 (m, 2H, CH₂), 1.22 (s, 12H, pinacol), 1.18–1.12 (m, 2H, CH₂). **¹¹B NMR** (128 MHz, CDCl₃, 298 K) δ /ppm: 33.7 (s). **¹³C{¹H} NMR partial** (101 MHz, CDCl₃, 298 K) δ /ppm: 148.6 (s, Ar), 128.5 (s, Ar), 128.0 (s, Ar), 125.3 (q, ¹J_{FC} = 3.8 Hz, CF₃), 123.5 (s, Ar), 83.4 (s, pinacol), 30.0 (s, CH₂), 25.0 (s, pinacol). Note, the carbon adjacent to the boron atom was not observed due to quadrupolar relaxation. **¹⁹F NMR** (376 MHz, CDCl₃, 298 K) δ /ppm: -62.25 (s, 3F, *p*-CF₃).

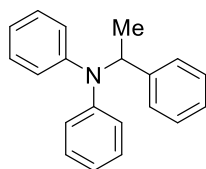
8.7 B(C₆F₅)₃-catalysed hydroamination

General procedure 10

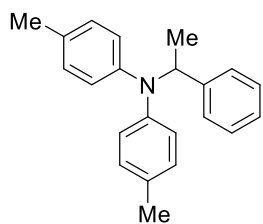
In an NMR tube, an olefin (200 μmol) and an amine (200 μmol) were combined in deuterated chloroform (0.7 mL). To this, tris(pentafluorophenyl)borane (10.2 mg, 10 mol%, 20 μmol) and a mesitylene internal standard (13.9 μL, 100 μmol) were added, and the NMR tube sealed. The mixture was left to heat at 70 °C for 48 h, at which point *in situ* ¹H NMR spectroscopy was used to observe the reaction progression. The resultant hydroamination product was then isolated through flash column chromatography.

8.7.1 Synthesis of reduction products

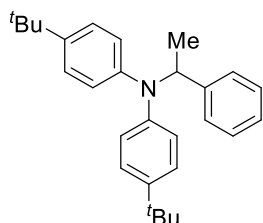
N-Phenyl-*N*-(1-phenylethyl)aniline (6a)



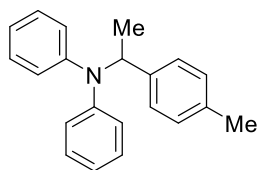
Synthesised in accordance with *general procedure 10* using styrene (22.9 μL, 200 μmol) and diphenylamine (33.8 mg, 200 μmol). The crude material was purified by flash-column chromatography using a hexane/ethyl acetate mixture as the eluent (10:1 then 50:1) to afford the title compound as a colourless oil. **Yield:** 40 mg, 146 μmol, 73%. Spectroscopic analyses agree with literature values.²⁵⁹ **¹H NMR** (400 MHz, CDCl₃, 298 K) δ/ppm: 7.44 (d, ³J_{HH} = 7.7 Hz, 1H, Ar–H), 7.31 (ov dd, ³J_{HH} = 6.5 Hz, ³J_{HH} = 5.9 Hz, 3H, Ar–H), 7.24–7.15 (m, 6H, Ar–H), 7.09 (t, ³J_{HH} = 7.4 Hz, 1H), 7.04–6.95 (m, 1H, Ar–H), 6.84 (t, ³J_{HH} = 7.2 Hz, 2H, Ar–H), 6.75 (d, ³J_{HH} = 8.2 Hz, 2H, Ar–H), 4.25 (q, ³J_{HH} = 6.9 Hz, 1H, CH–N), 1.63 (d, ³J_{HH} = 7.2 Hz, 3H, Me). **¹³C{¹H} NMR** (101 MHz, CDCl₃, 298 K) δ/ppm: 145.6 (s, Ar), 144.3 (s, Ar), 129.4 (s, Ar), 129.0 (s, Ar), 127.8 (s, Ar), 127.6 (s, Ar), 127.2 (s, Ar), 126.6 (s, Ar), 122.5 (s, Ar), 120.6 (s, Ar), 120.2 (s, Ar), 116.9 (s, Ar), 40.5 (s, C–N), 22.0 (s, Me). **HRMS (ES⁺):** [M]⁺ [C₂₀H₁₉N]⁺: calculated 274.1518, found 274.1601.

4-Methyl-N-phenyl-N-(1-phenylethyl)aniline (6b)

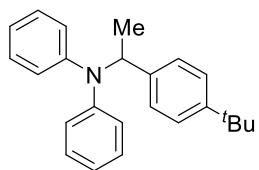
Synthesised in accordance with *general procedure 10* using styrene (22.9 μL , 200 μmol) and di-4-tolylamine (39.5 mg, 200 μmol). The crude material was purified by flash-column chromatography using a hexane/ethyl acetate mixture as the eluent (10:1 then 50:1) to afford the title compound as a colourless oil. **Yield:** 18 mg, 59 μmol , 30%. **$^1\text{H NMR}$** (400 MHz, CDCl_3 , 298 K) δ /ppm: 7.31–7.09 (m, 7H, Ar–H), 7.10–7.01 (m, 1H, Ar–H), 6.97–6.85 (m, 3H, Ar–H), 6.61–6.53 (m, 2H, Ar–H), 4.17 (q, $^3J_{\text{HH}} = 6.8$ Hz, 1H, CH–N), 2.30 (s, 3H, Ar–Me), 2.18 (s, 3H, Ar–Me), 1.53 (d, $^3J_{\text{HH}} = 6.7$ Hz, 3H, Me). **$^{13}\text{C}\{^1\text{H}\}$ NMR** (101 MHz, CDCl_3 , 298 K) δ /ppm: 145.7 (s, Ar), 129.7 (s, Ar), 128.8 (s, Ar), 128.6 (s, Ar), 128.5 (s, Ar), 128.4 (s, Ar), 127.6 (s, Ar), 127.5 (s, Ar), 127.5 (s, Ar), 126.3 (s, Ar), 121.1 (s, Ar), 116.7 (s, Ar), 40.2 (s, C–N), 21.84 (s, Me), 21.1 (s, Ar–Me), 20.5 (s, Ar–Me). **HRMS (ES $^+$):** $[\text{M}]^+$ $[\text{C}_{22}\text{H}_{23}\text{N}]^+$: calculated 302.1831, found 302.1913.

4-(Tert-butyl)-N-(4-tert-butyl)phenyl)-N-(1-phenylethyl)aniline (6c)

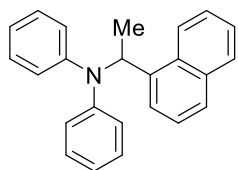
Synthesised in accordance with *general procedure 10* using styrene (22.9 μL , 200 μmol) and bis(4-*tert*-butyl)phenylamine (56.2 mg, 200 μmol). The crude material was purified by flash-column chromatography using a hexane/ethyl acetate mixture as the eluent (10:1 then 50:1) to afford the title compound as a colourless oil. **Yield:** 47 mg, 122 μmol , 61%. **$^1\text{H NMR}$** (400 MHz, CDCl_3 , 298 K) δ /ppm: 7.55–7.50 (m, 1H, Ar–H), 7.41–7.35 (m, 2H, Ar–H), 7.34–7.31 (m, 1H, Ar–H), 7.29–7.23 (m, 5H, Ar–H), 7.19–7.14 (m, 1H, Ar–H), 7.12–7.02 (m, 1H, Ar–H), 6.99–6.89 (m, 1H, Ar–H), 6.80–6.72 (m, 1H, Ar–H), 4.59–4.26 (m, 1H, CH–N), 1.70 (d, $^3J_{\text{HH}} = 7.0$ Hz, 3H, Me), 1.42 (s, 6H, ^tBu), 1.36 (s, 12H, ^tBu). **$^{13}\text{C}\{^1\text{H}\}$ NMR** (101 MHz, CDCl_3 , 298 K) δ /ppm: 145.8 (s, Ar), 129.0 (s, Ar), 128.7 (s, Ar), 128.6 (s, Ar), 128.4 (s, Ar), 127.6 (s, Ar), 127.6 (s, Ar), 127.3 (s, Ar), 126.5 (s, Ar), 126.2 (s, Ar), 126.1 (s, Ar), 124.8 (s, Ar), 124.7 (s, Ar), 123.9 (s, Ar), 123.7 (s, Ar), 119.2 (s, Ar), 119.0 (s, Ar), 116.8 (s, Ar), 40.8 (s, C–N), 34.6 (s, ^tBu), 34.4 (s, ^tBu), 34.2 (s, ^tBu), 34.1 (s, ^tBu), 31.7 (s, ^tBu), 31.7 (s, ^tBu), 31.7 (s, ^tBu), 31.6 (s, ^tBu), 22.1 (s, Me). **HRMS (ES $^+$):** $[\text{M}]^+$ $[\text{C}_{28}\text{H}_{23}\text{N}]^+$: calculated 386.2769, found 386.2848.

***N*-Phenyl-(*N*-(1-*p*-tolyl)ethyl)aniline (6d)**

Synthesised in accordance with *general procedure 10* using *p*-methylstyrene (26.3 μL , 200 μmol) and diphenylamine (33.8 mg, 200 μmol). The crude material was purified by flash-column chromatography using a hexane/ethyl acetate mixture as the eluent (10:1 then 50:1) to afford the title compound as a brown oil. **Yield:** 51 mg, 178 μmol , 89%. **$^1\text{H NMR}$** (400 MHz, CDCl_3 , 298 K) δ/ppm : 7.24–7.14 (m, 4H, Ar–H), 7.10–7.02 (m, 6H, Ar–H), 7.00–6.92 (m, 4H, Ar–H), 6.87–6.80 (m, 1H, Ar–H), 4.00 (q, $^3J_{\text{HH}} = 6.0$ Hz, 1H, CH–N), 2.24 (d, $^3J_{\text{HH}} = 2.6$ Hz, 3H, Me), 1.61–1.47 (m, 3H, Ar–Me). **$^{13}\text{C}\{^1\text{H}\}$ NMR** (101 MHz, CDCl_3 , 298 K) δ/ppm : 140.7 (s, Ar), 135.6 (s, Ar), 129.5 (s, Ar), 129.2 (s, Ar), 128.5 (s, Ar), 127.6 (s, Ar), 118.7 (s, Ar), 117.6 (s, Ar), 43.9 (s, C–N), 22.2 (s, Ar–Me), 21.1 (s, Me). **HRMS (ASAP⁺):** $[\text{M}]^+$ $[\text{C}_{21}\text{H}_{21}\text{N}]^+$: calculated 288.1674, found 288.1768.

***N*-(1-(4-(Tert-butyl)phenyl)ethyl)-*N*-phenylaniline (6e)**

Synthesised in accordance with *general procedure 10* using *p*-methylstyrene (26.3 μL , 200 μmol) and diphenylamine (33.8 mg, 200 μmol). The crude material was purified by flash-column chromatography using a hexane/ethyl acetate mixture as the eluent (10:1 then 50:1) to afford the title compound as a brown oil. **Yield:** 53 mg, 161 μmol , 80%. **$^1\text{H NMR}$** (500 MHz, CDCl_3 , 298 K) δ/ppm : 7.23 (d, $^3J_{\text{HH}} = 8.5$ Hz, 2H, Ar–H), 7.18–7.15 (m, 3H, Ar–H), 7.10–7.04 (m, 4H, Ar–H), 6.98 (dd, $^3J_{\text{HH}} = 10.7$ Hz, $^3J_{\text{HH}} = 8.3$ Hz, 4H, Ar–H), 6.84 (t, $^3J_{\text{HH}} = 7.2$ Hz, 1H, Ar–H), 4.00 (q, $^3J_{\text{HH}} = 7.2$ Hz, 1H, CH–N), 1.54 (d, $^3J_{\text{HH}} = 7.2$ Hz, 3H, Me), 1.23 (s, 9H, ^tBu). **$^{13}\text{C}\{^1\text{H}\}$ NMR** (126 MHz, CDCl_3 , 298 K) δ/ppm : 148.8 (s, Ar), 143.6 (s, Ar), 129.5 (s, Ar), 128.6 (s, Ar), 127.2 (s, Ar), 125.4 (s, Ar), 118.8 (s, Ar), 117.8 (s, Ar), 43.8 (s, C–N), 34.5 (s, ^tBu), 31.6 (s, ^tBu), 22.2 (s, ^tBu). **HRMS (ES⁺):** $[\text{M}]^+$ $[\text{C}_{24}\text{H}_{27}\text{N}]^+$: calculated 330.2144, found 330.1994.

***N*-(1-(Naphthalen-1-yl)ethyl)-*N*-phenylaniline (6f)**

Synthesised in accordance with *general procedure 10* using 1-vinylnaphthalene (30.8 mg, 200 μmol) and diphenylamine (33.8 mg, 200 μmol). The crude material was purified by flash-column chromatography using a hexane/ethyl acetate mixture as the eluent (10:1 then 50:1) to afford the title compound as a brown oil. **Yield:** 14 mg, 43 μmol , 22 %. **^1H NMR** (500 MHz, CDCl_3 , 298 K) δ/ppm : 7.91–7.67 (m, 4H, Ar–H), 7.54–7.41 (m, 2H, Ar–H), 7.38–7.30 (m, 1H, Ar–H), 7.30–7.22 (m, 4H, Ar–H), 7.20–7.14 (m, 2H, Ar–H), 7.10–7.01 (m, 3H, Ar–H), 6.96–6.86 (m, 1H, Ar–H), 4.67–3.88 (m, 1H, CH–N), 1.73 (d, $^3J_{\text{HH}} = 6.7$ Hz, 3H, Me). **$^{13}\text{C}\{^1\text{H}\}$ NMR** (126 MHz, CDCl_3 , 298 K) δ/ppm : 144.0 (s, Ar), 129.4 (s, Ar), 129.3 (s, Ar), 128.6 (s, Ar), 128.6 (s, Ar), 127.9 (s, Ar), 127.7 (s, Ar), 127.6 (s, Ar), 126.8 (s, Ar), 125.9 (s, Ar), 125.3 (s, Ar), 125.2 (s, Ar), 118.5 (s, Ar), 117.6 (s, Ar), 44.2 (s, C–N), 21.9 (s, Me). **HRMS (ES $^+$):** $[\text{M}]^+$ $[\text{C}_{24}\text{H}_{21}\text{N}]^+$: calculated 324.1674, found 324.1751.

V – References

- 1 G. N. Lewis, *Valence and the Structure of Atoms and Molecules*, The Chemical Catalogue Company, Inc., New York, 1923.
- 2 J. N. Brønsted, *Recl. des Trav. Chim. des Pays-Bas*, 1923, **42**, 718–728.
- 3 T. M. Lowry, *J. Soc. Chem. Ind.*, 1923, **42**, 43–47.
- 4 R. G. Pearson, *J. Am. Chem. Soc.*, 1963, **85**, 3533–3539.
- 5 T. L. Ho, *Chem. Rev.*, 1975, **75**, 1–20.
- 6 M. Nič, J. Jirát, B. Košata, A. Jenkins and A. McNaught, Eds., *IUPAC Compendium of Chemical Terminology*, IUPAC, Research Triangle Park, NC, 2009.
- 7 U. Mayer, V. Gutmann and W. Gerger, *Monatshefte für Chemie*, 1975, **106**, 1235–1257.
- 8 M. A. Beckett, G. C. Strickland, J. R. Holland and K. S. Varma, *Polymer*, 1996, **37**, 4629–4631.
- 9 R. F. Childs, D. L. Mulholland and A. Nixon, *Can. J. Chem.*, 1982, **60**, 801–808.
- 10 J. R. Gaffen, J. N. Bentley, L. C. Torres, C. Chu, T. Baumgartner and C. B. Caputo, *Chem*, 2019, **5**, 1567–1583.
- 11 K. O. Christe, D. A. Dixon, D. McLemore, W. W. Wilson, J. A. Sheehy and J. A. Boatz, *J. Fluor. Chem.*, 2000, **101**, 151–153.
- 12 M. T. Mock, R. G. Potter, D. M. Camaioni, J. Li, W. G. Dougherty, W. S. Kassel, B. Twamley and D. L. DuBois, *J. Am. Chem. Soc.*, 2009, **131**, 14454–14465.
- 13 A. R. Jupp, T. C. Johnstone and D. W. Stephan, *Dalton Trans.*, 2018, **47**, 7029–7035.
- 14 O. M. Demchuk, W. Świerczyńska, K. Dziuba, S. Frynas, A. Flis and K. M. Pietrusiewicz, *Phosphorus, Sulfur Silicon Relat. Elem.*, 2017, **192**, 64–68.
- 15 G. Hilt and A. Nödling, *Eur. J. Org. Chem.*, 2011, 7071–7075.
- 16 D. C. Bradley, I. S. Harding, A. D. Keefe, M. Motevalli and D. H. Zheng, *J. Chem. Soc., Dalton Trans.*, 1996, 3931–3936.
- 17 J. N. Bentley, S. A. Elgadi, J. R. Gaffen, P. Demay-Drouhard, T. Baumgartner and C. B. Caputo, *Organometallics*, 2020, **39**, 3645–3655.
- 18 G. J. P. Britovsek, J. Ugoletti and A. J. P. White, *Organometallics*, 2005, **24**, 1685–1691.
- 19 T. E. Mallouk, G. L. Rosenthal, G. Muller, R. Brusasco and N. Bartlett, *Inorg. Chem.*, 1984, **23**, 3167–3173.
- 20 R. S. Mulliken, *J. Chem. Phys.*, 1934, **2**, 782–793.
- 21 A. Y. Timoshkin and G. Frenking, *Organometallics*, 2008, **27**, 371–380.
- 22 Z. M. Heiden and A. P. Lathem, *Organometallics*, 2015, **34**, 1818–1827.
- 23 H. Böhler, N. Trapp, D. Himmel, M. Schleep and I. Krossing, *Dalton Trans.*, 2015, **44**, 7489–7499.

- 24 T. A. Rokob, A. Hamza and I. Pápai, *J. Am. Chem. Soc.*, 2009, **131**, 10701–10710.
- 25 P. Erdmann, J. Leitner, J. Schwarz and L. Greb, *ChemPhysChem*, 2020, **21**, 987–994.
- 26 H. Yamamoto, *Lewis acids in organic synthesis*, Wiley, 2008.
- 27 A. Corma and H. García, *Chem. Rev.*, 2003, **103**, 4307–4365.
- 28 P. Vermeeren, T. A. Hamlin, I. Fernández and F. M. Bickelhaupt, *Angew. Chem. Int. Ed.*, 2020, **59**, 6201–6206.
- 29 D. W. Stephan, *Org. Biomol. Chem.*, 2012, **10**, 5740–5746.
- 30 J. Lam, K. M. Szkop, E. Mosaféri and D. W. Stephan, *Chem. Soc. Rev.*, 2019, **48**, 3592–3612.
- 31 D. W. Stephan and G. Erker, *Chem. Sci.*, 2014, **5**, 2625–2641.
- 32 H. C. Brown, H. I. Schlesinger and S. Z. Cardon, *J. Am. Chem. Soc.*, 1942, **64**, 325–329.
- 33 G. Wittig and E. Benz, *Chem. Ber.*, 1959, **92**, 1999–2013.
- 34 W. Tochtermann, *Angew. Chem. Int. Ed.*, 1966, **5**, 351–371.
- 35 D. J. Parks and W. E. Piers, *J. Am. Chem. Soc.*, 1996, **118**, 9440–9441.
- 36 G. C. Welch, R. R. San Juan, J. D. Masuda and D. W. Stephan, *Science*, 2006, **314**, 1124–1126.
- 37 D. W. Stephan, *J. Chem. Soc., Dalton Trans.*, 2009, 3129–3136.
- 38 F.-G. Fontaine, M.-A. Courtemanche, M.-A. Légaré and É. Rochette, *Coord. Chem. Rev.*, 2017, **334**, 124–135.
- 39 M.-A. Légaré, G. Bélanger-Chabot, R. D. Dewhurst, E. Welz, I. Krummenacher, B. Engels and H. Braunschweig, *Science*, 2018, **359**, 896–900.
- 40 M. A. Légaré, M. A. Courtemanche, É. Rochette and F. G. Fontaine, *Science*, 2015, **349**, 513–516.
- 41 J. Paradies, *Eur. J. Org. Chem.*, 2019, **2019**, 283–294.
- 42 O. J. Metters, S. J. K. Forrest, H. A. Sparkes, I. Manners and D. F. Wass, *J. Am. Chem. Soc.*, 2016, **138**, 1994–2003.
- 43 A. M. Chapman, M. F. Haddow and D. F. Wass, *J. Am. Chem. Soc.*, 2011, **133**, 8826–8829.
- 44 A. M. Chapman, M. F. Haddow and D. F. Wass, *Eur. J. Inorg. Chem.*, 2012, **2012**, 1546–1554.
- 45 Y. Ma, S. Zhang, C.-R. Chang, Z.-Q. Huang, J. C. Ho and Y. Qu, *Chem. Soc. Rev.*, 2018, **47**, 5541–5553.
- 46 K. K. Ghuman, L. B. Hoch, T. E. Wood, C. Mims, C. V. Singh and G. A. Ozin, *ACS Catal.*, 2016, **6**, 5764–5770.
- 47 L. Wang, T. Yan, R. Song, W. Sun, Y. Dong, J. Guo, Z. Zhang, X. Wang and G. A. Ozin, *Angew. Chem. Int. Ed.*, 2019, **58**, 9501–9505.
- 48 S. Zhang, Z. Q. Huang, Y. Ma, W. Gao, J. Li, F. Cao, L. Li, C. R. Chang and Y. Qu, *Nat. Commun.*, 2017, **8**, 1–11.
- 49 H. C. Brown and R. R. Holmes, *J. Am. Chem. Soc.*, 1956, **78**, 2173–2176.

- 50 T. Brinck, J. S. Murray and P. Politzer, *Inorg. Chem.*, 1993, **32**, 2622–2625.
- 51 W. E. Piers and T. Chivers, *Chem. Soc. Rev.*, 1997, **26**, 345–354.
- 52 A. R. Siedle, R. A. Newmark, W. M. Lamanna and J. C. Huffman, *Organometallics*, 1993, **12**, 1491–1492.
- 53 J. L. Carden, A. Dasgupta and R. L. Melen, *Chem. Soc. Rev.*, 2020, **49**, 1706–1725.
- 54 B. L. Dufrey and T. M. Gilbert, *Inorg. Chem.*, 2011, **50**, 7871–7879.
- 55 M. V. Metz, D. J. Schwartz, C. L. Stern, P. N. Nickias and T. J. Marks, *Angew. Chem. Int. Ed.*, 2000, **39**, 1312–1316.
- 56 M. V. Metz, D. J. Schwartz, C. L. Stern, T. J. Marks and P. N. Nickias, *Organometallics*, 2002, **21**, 4159–4168.
- 57 A. E. Ashley, T. J. Herrington, G. G. Wildgoose, H. Zaher, A. L. Thompson, N. H. Rees, T. Krämer and D. O'Hare, *J. Am. Chem. Soc.*, 2011, **133**, 14727–14740.
- 58 É. Dorkó, M. Szabó, B. Kótai, I. Pápai, A. Domján and T. Soós, *Angew. Chem. Int. Ed.*, 2017, **56**, 9512–9516.
- 59 É. Dorkó, B. Kótai, T. Földes, Á. Gyömöre, I. Pápai and T. Soós, *J. Organomet. Chem.*, 2017, **847**, 258–262.
- 60 L. A. Mück, A. Y. Timoshkin and G. Frenking, *Inorg. Chem.*, 2012, **51**, 640–646.
- 61 T. K. Wood, W. E. Piers, B. A. Keay and M. Parvez, *Org. Lett.*, 2006, **8**, 2875–2878.
- 62 M. Yasuda, S. Yoshioka, S. Yamasaki, T. Somyo, K. Chiba and A. Baba, *Org. Lett.*, 2006, **8**, 761–764.
- 63 I. B. Sivaev and V. I. Bregadze, *Coord. Chem. Rev.*, 2014, **270–271**, 75–88.
- 64 W. E. Piers, S. C. Bourke and K. D. Conroy, *Angew. Chem. Int. Ed.*, 2005, **44**, 5016–5036.
- 65 L. O. Müller, D. Himmel, J. Stauffer, G. Steinfeld, J. Slattery, G. Santiso-Quiñones, V. Brecht and I. Krossing, *Angew. Chem. Int. Ed.*, 2008, **47**, 7659–7663.
- 66 N. G. Stahl, M. R. Salata and T. J. Marks, *J. Am. Chem. Soc.*, 2005, **127**, 10898–10909.
- 67 C. H. Lee, S. J. Lee, J. W. Park, K. H. Kim, B. Y. Lee and J. S. Oh, *J. Mol. Catal. A Chem.*, 1998, **132**, 231–239.
- 68 G. S. Hair, A. H. Cowley, R. A. Jones, B. G. McBurnett and A. Voigt, *J. Am. Chem. Soc.*, 1999, **121**, 4922–4923.
- 69 E. Y.-X. Chen, W. J. Kruper, G. Roof and D. R. Wilson, *J. Am. Chem. Soc.*, 2001, **123**, 745–746.
- 70 J. Chen and E. Y.-X. Chen, *Angew. Chem. Int. Ed.*, 2015, **54**, 6842–6846.
- 71 S. Feng, G. R. Roof and E. Y.-X. Chen, *Organometallics*, 2002, **21**, 832–839.
- 72 K. Vanka, M. S. W. Chan, C. C. Pye and T. Ziegler, *Organometallics*, 2000, **19**, 1841–1849.
- 73 S. Sato, N. Takeda, M. Ueda and O. Miyata, *Synth.*, 2016, **48**, 882–892.

- 74 T. Miyoshi, S. Matsuya, M. Tsugawa, S. Sato, M. Ueda and O. Miyata, *Org. Lett.*, 2013, **15**, 3374–3377.
- 75 G. Ménard, L. Tran and D. W. Stephan, *Dalton Trans.*, 2013, **42**, 13685–13691.
- 76 A. J. B. Robertson, *Platin. Met. Rev.*, 1975, **19**, 64–69.
- 77 J. J. Berzelius, *Ann. Chim. Phys.*, 1835, **61**, 146–151.
- 78 P. T. Anastas and M. M. Kirchhoff, *Acc. Chem. Res.*, 2002, **35**, 686–694.
- 79 H. Dong, J. Zhao, J. Chen, Y. Wu and B. Li, *Int. J. Miner. Process.*, 2015, **145**, 108–113.
- 80 R. L. Melen, *Science*, 2019, **363**, 479–484.
- 81 L. C. Wilkins and R. L. Melen, *Coord. Chem. Rev.*, 2016, **324**, 123–139.
- 82 P. P. Power, *Nature*, 2010, **463**, 171–177.
- 83 M. S. Hill, D. J. Liptrot and C. Weetman, *Chem. Soc. Rev.*, 2016, **45**, 972–988.
- 84 H. C. Brown and B. C. Subba Rao, *J. Am. Chem. Soc.*, 1956, **78**, 2582–2588.
- 85 H. C. Brown, *Tetrahedron*, 1961, **12**, 117–138.
- 86 H. C. Brown and S. K. Gupta, *J. Am. Chem. Soc.*, 1972, **94**, 4370–4371.
- 87 H. C. Brown and S. K. Gupta, *J. Am. Chem. Soc.*, 1975, **97**, 5249–5255.
- 88 C. E. Tucker, J. Davidson and P. Knochel, *J. Org. Chem.*, 1992, **57**, 3482–3485.
- 89 N. Miyaura and A. Suzuki, *Chem. Rev.*, 1995, **95**, 2457–2483.
- 90 R. Barbeyron, E. Benedetti, J. Cossy, J. J. Vasseur, S. Arseniyadis and M. Smietana, *Tetrahedron*, 2014, **70**, 8431–8452.
- 91 M. L. Shegavi and S. K. Bose, *Catal. Sci. Technol.*, 2019, **9**, 3307–3336.
- 92 J. V. Obligacion and P. J. Chirik, *Nat. Rev. Chem.*, 2018, **2**, 15–34.
- 93 Y. Suseela, A. S. B. Prasad and M. Periasamy, *J. Chem. Soc. Chem. Commun.*, 1990, 446–447.
- 94 Y. Suseela and M. Periasamy, *J. Organomet. Chem.*, 1993, **450**, 47–52.
- 95 A. Prokofjevs, A. Boussonnière, L. Li, H. Bonin, E. Lacôte, D. P. Curran and E. Vedejs, *J. Am. Chem. Soc.*, 2012, **134**, 12281–12288.
- 96 P. Eisenberger, A. M. Bailey and C. M. Crudden, *J. Am. Chem. Soc.*, 2012, **134**, 17384–17387.
- 97 P. Eisenberger and C. M. Crudden, *Dalton Trans.*, 2017, **46**, 4874–4887.
- 98 K. Stefkova, L. Gierlichs, D. Willcox and R. L. Melen, in *Encyclopedia of Inorganic and Bioinorganic Chemistry*, Wiley, 2020, pp. 1–37.
- 99 X. Fan, J. Zheng, Z. H. Li and H. Wang, *J. Am. Chem. Soc.*, 2015, **137**, 4916–4919.
- 100 J. S. McGough, S. M. Butler, I. A. Cade and M. J. Ingleson, *Chem. Sci.*, 2016, **7**, 3384–3389.
- 101 L. Fan and D. W. Stephan, *Dalton Trans.*, 2016, **45**, 9229–9234.
- 102 Q. Yin, S. Kemper, H. F. T. Klare and M. Oestreich, *Chem. Eur. J.*, 2016, **22**,

- 13840–13844.
- 103 K. Shirakawa, A. Arase and M. Hoshi, *Synthesis (Stuttg.)*, 2004, **2004**, 1814–1820.
- 104 G. A. Molander and N. M. Ellis, *J. Org. Chem.*, 2008, **73**, 6841–6844.
- 105 M. Fleige, J. Möbus, T. Vom Stein, F. Glorius and D. W. Stephan, *Chem. Commun.*, 2016, **52**, 10830–10833.
- 106 E. Nieto-Sepulveda, A. D. Bage, L. A. Evans, T. A. Hunt, A. G. Leach, S. P. Thomas and G. C. Lloyd-Jones, *J. Am. Chem. Soc.*, 2019, **141**, 18600–18611.
- 107 Q. Yin, Y. Soltani, R. L. Melen and M. Oestreich, *Organometallics*, 2017, **36**, 2381–2384.
- 108 J. R. Lawson, L. C. Wilkins and R. L. Melen, *Chem. Eur. J.*, 2017, **23**, 10997–11000.
- 109 N. W. J. Ang, C. S. Buettner, S. Docherty, A. Bismuto, J. R. Carney, J. H. Docherty, M. J. Cowley and S. P. Thomas, *Synth.*, 2018, **50**, 803–808.
- 110 A. D. Bage, T. A. Hunt and S. P. Thomas, *Org. Lett.*, 2020, **22**, 4107–4112.
- 111 L. Hu, J. He, Y. Zhang and E. Y.-X. Chen, *Macromolecules*, 2018, **51**, 1296–1307.
- 112 G. Ménard and D. W. Stephan, *Angew. Chem. Int. Ed.*, 2012, **51**, 8272–8275.
- 113 G. Ménard and D. W. Stephan, *Angew. Chem. Int. Ed.*, 2012, **51**, 4409–4412.
- 114 G. Ménard, J. A. Hatnean, H. J. Cowley, A. J. Lough, J. M. Rawson and D. W. Stephan, *J. Am. Chem. Soc.*, 2013, **135**, 6446–6449.
- 115 G. Ménard, T. M. Gilbert, J. A. Hatnean, A. Kraft, I. Krossing and D. W. Stephan, *Organometallics*, 2013, **32**, 4416–4422.
- 116 Z. Yang, M. Zhong, X. Ma, S. De, C. Anusha, P. Parameswaran and H. W. Roesky, *Angew. Chem. Int. Ed.*, 2015, **54**, 10225–10229.
- 117 A. Caise, D. Jones, E. L. Kolychev, J. Hicks, J. M. Goicoechea and S. Aldridge, *Chem. Eur. J.*, 2018, **24**, 13624–13635.
- 118 Z. Yang, M. Zhong, X. Ma, K. Nijesh, S. De, P. Parameswaran and H. W. Roesky, *J. Am. Chem. Soc.*, 2016, **138**, 2548–2551.
- 119 A. Bismuto, S. P. Thomas and M. J. Cowley, *Angew. Chem. Int. Ed.*, 2016, **55**, 15356–15359.
- 120 D. Franz, L. Sirtl, A. Pöthig and S. Inoue, *Zeitschrift für Anorg. und Allg. Chemie*, 2016, **642**, 1245–1250.
- 121 V. K. Jakhar, M. K. Barman and S. Nembenna, *Org. Lett.*, 2016, **18**, 4710–4713.
- 122 V. A. Pollard, S. A. Orr, R. McLellan, A. R. Kennedy, E. Hevia and R. E. Mulvey, *Chem. Commun.*, 2018, **54**, 1233–1236.
- 123 L. E. Lemmerz, R. McLellan, N. R. Judge, A. R. Kennedy, S. A. Orr, M. Uzelac, E. Hevia, S. D. Robertson, J. Okuda and R. E. Mulvey, *Chem. Eur. J.*, 2018, **24**, 9940–9948.
- 124 V. A. Pollard, M. Á. Fuentes, A. R. Kennedy, R. McLellan and R. E. Mulvey, *Angew. Chem. Int. Ed.*, 2018, **57**, 10651–10655.
- 125 A. Bismuto, M. J. Cowley and S. P. Thomas, *ACS Catal.*, 2018, **8**, 2001–

- 2005.
- 126 A. Harinath, J. Bhattacharjee and T. K. Panda, *Adv. Synth. Catal.*, 2019, **361**, 850–857.
- 127 A. Harinath, I. Banerjee, J. Bhattacharjee and T. K. Panda, *New J. Chem.*, 2019, **43**, 10531–10536.
- 128 T. E. Müller, K. C. Hultsch, M. Yus, F. Foubelo and M. Tada, *Chem. Rev.*, 2008, **108**, 3795–3892.
- 129 Y. Hoshimoto and S. Ogoshi, *ACS Catal.*, 2019, **9**, 5439–5444.
- 130 T. Mahdi and D. W. Stephan, *Angew. Chem. Int. Ed.*, 2013, **52**, 12418–12421.
- 131 T. Mahdi and D. W. Stephan, *Chem. Eur. J.*, 2015, **21**, 11134–11142.
- 132 S. Tussing, M. Ohland, G. Wicker, U. Flörke and J. Paradies, *Dalton Trans.*, 2017, **46**, 1539–1545.
- 133 M. Shibuya, S. Kawano, S. Fujita and Y. Yamamoto, *Asian J. Org. Chem.*, 2019, **8**, 1075–1079.
- 134 T. F. Bresnahan and M. Trajtenberg, *J. Econom.*, 1995, **65**, 83–108.
- 135 M. R. Hartings and Z. Ahmed, *Nat. Rev. Chem.*, 2019, **3**, 305–314.
- 136 S. S. Zaleskiy, P. J. Kitson, P. Frei, A. Bubliauskas and L. Cronin, *Nat. Commun.*, 2019, **10**, 6–13.
- 137 M. Crosland, *Ann. Sci.*, 2005, **62**, 233–253.
- 138 T. T. Tidwell, *Angew. Chem. Int. Ed.*, 2001, **40**, 331–337.
- 139 M. Rentetzi, *Endeavour*, 2017, **41**, 39–50.
- 140 C. O. Kappe, *Angew. Chem. Int. Ed.*, 2004, **43**, 6250–6284.
- 141 N. Kuhnert, *Angew. Chem. Int. Ed.*, 2002, **41**, 1863–1866.
- 142 A. De La Hoz, Á. Díaz-Ortiz and A. Moreno, *Chem. Soc. Rev.*, 2005, **34**, 164–178.
- 143 C. O. Kappe, *Chem. Rec.*, 2019, **19**, 15–39.
- 144 C. O. Kappe, B. Pieber and D. Dallinger, *Angew. Chem. Int. Ed.*, 2013, **52**, 1088–1094.
- 145 L. Perreux and A. Loupy, *Tetrahedron*, 2001, **57**, 9199–9223.
- 146 D. Obermayer, B. Gutmann and C. O. Kappe, *Angew. Chem. Int. Ed.*, 2009, **48**, 8321–8324.
- 147 J. M. Kremsner and C. O. Kappe, *J. Org. Chem.*, 2006, **71**, 4651–4658.
- 148 C. O. Kappe, *Acc. Chem. Res.*, 2013, **46**, 1579–1587.
- 149 M. Larhed, C. Moberg and A. Hallberg, *Acc. Chem. Res.*, 2002, **35**, 717–727.
- 150 R. J. Giguere, T. L. Bray, S. M. Duncan and G. Majetich, *Tetrahedron Lett.*, 1986, **27**, 4945–4948.
- 151 R. Gedye, F. Smith, K. Westaway, H. Ali, L. Baldisera, L. Laberge and J. Rousell, *Tetrahedron Lett.*, 1986, **27**, 279–282.
- 152 V. P. Mehta and E. V. Van Der Eycken, *Chem. Soc. Rev.*, 2011, **40**, 4925–4936.

- 153 K. S. M. Salih and Y. Baqi, *Catalysts*, 2019, **10**, 4.
- 154 E. Calcio Gaudino, G. Cravotto, M. Manzoli and S. Tabasso, *Green Chem.*, 2019, **21**, 1202–1235.
- 155 P. Prieckel and J. A. Lopez-Sanchez, *ACS Sustain. Chem. Eng.*, 2019, **7**, 3–21.
- 156 C. O. Kappe and D. Dallinger, *Nat. Rev. Drug Discov.*, 2006, **5**, 51–63.
- 157 V. Polshettiwar and R. S. Varma, *Chem. Soc. Rev.*, 2008, **37**, 1546–1557.
- 158 N. Stock and S. Biswas, *Chem. Rev.*, 2012, **112**, 933–969.
- 159 I. Thomas-Hillman, A. Laybourn, C. Dodds and S. W. Kingman, *J. Mater. Chem. A*, 2018, **6**, 11564–11581.
- 160 V. Palma, D. Barba, M. Cortese, M. Martino, S. Renda and E. Meloni, *Catalysts*, 2020, **10**, 246.
- 161 S. Horikoshi and N. Serpone, *Catal. Sci. Technol.*, 2014, **4**, 1197–1210.
- 162 X. Huang, M. Wang, M. Wu, J. Wang, Y. Peng and G. Song, *ChemistrySelect*, 2017, **2**, 1381–1385.
- 163 S. W. Hadebe and R. S. Robinson, *Tetrahedron Lett.*, 2006, **47**, 1299–1302.
- 164 I. A. I. Mkhalid, R. B. Coapes, S. N. Edes, D. N. Coventry, F. E. S. Souza, R. L. Thomas, J. J. Hall, S. W. Bi, Z. Lin and T. B. Marder, *J. Chem. Soc., Dalton Trans.*, 2007, 1055–1064.
- 165 R. J. Burford, M. J. Geier, C. M. Vogels, A. Decken and S. A. Westcott, *J. Organomet. Chem.*, 2013, **731**, 1–9.
- 166 H. Prokopcová, J. Ramírez, E. Fernández and C. O. Kappe, *Tetrahedron Lett.*, 2008, **49**, 4831–4835.
- 167 B. D. Stevens, C. J. Bungard and S. G. Nelson, *J. Org. Chem.*, 2006, **71**, 6397–6402.
- 168 B. Gioia, A. Arnaud, S. Radix, N. Walchshofer, A. Doléans-Jordheim and L. Rocheblave, *Tetrahedron Lett.*, 2020, **61**, 151596.
- 169 S. Tussing and J. Paradies, *Dalton Trans.*, 2016, **45**, 6124–6128.
- 170 M. B. Plutschack, B. Pieber, K. Gilmore and P. H. Seeberger, *Chem. Rev.*, 2017, **117**, 11796–11893.
- 171 B. J. Deadman, D. L. Browne, I. R. Baxendale and S. V. Ley, *Chem. Eng. Technol.*, 2015, **38**, 259–264.
- 172 M. V. Gomez and A. De La Hoz, *Beilstein J. Org. Chem.*, 2017, **13**, 285–300.
- 173 C. G. Frost and L. Mutton, *Green Chem.*, 2010, **12**, 1687–1703.
- 174 R. Munirathinam, J. Huskens and W. Verboom, *Adv. Synth. Catal.*, 2015, **357**, 1093–1123.
- 175 V. Hessel, A. Renken, J. C. Schouten and J. Yoshida, *Micro Process Engineering: A Comprehensive Handbook*, Wiley-VCH Verlag, Weinheim, 2013, vol. 1.
- 176 M. D. Symes, P. J. Kitson, J. Yan, C. J. Richmond, G. J. T. Cooper, R. W. Bowman, T. Vilbrandt and L. Cronin, *Nat. Chem.*, 2012, **4**, 349–354.
- 177 J. M. Neumaier, A. Madani, T. Klein and T. Ziegler, *Beilstein J. Org. Chem.*, 2019, **15**, 558–566.

- 178 V. Dragone, V. Sans, M. H. Rosnes, P. J. Kitson and L. Cronin, *Beilstein J. Org. Chem*, 2013, **9**, 951–959.
- 179 K. S. Elvira, X. C. I Solvas, R. C. R. Wootton and A. J. Demello, *Nat. Chem.*, 2013, **5**, 905–915.
- 180 D. J. Lamberto, M. M. Alvarez and F. J. Muzzio, *Chem. Eng. Sci.*, 1999, **54**, 919–942.
- 181 J. I. Yoshida, Y. Takahashi and A. Nagaki, *Chem. Commun.*, 2013, **49**, 9896–9904.
- 182 R. L. Hartman, J. P. McMullen and K. F. Jensen, *Angew. Chem. Int. Ed.*, 2011, **50**, 7502–7519.
- 183 J. C. Pastre, D. L. Browne and S. V. Ley, *Chem. Soc. Rev.*, 2013, **42**, 8849–8869.
- 184 A. R. Bogdan and A. W. Dombrowski, *J. Med. Chem.*, 2019, **62**, 6422–6468.
- 185 A. Nagaki, D. Yamada, S. Yamada, M. Doi, D. Ichinari, Y. Tomida, N. Takabayashi and J. I. Yoshida, *Aust. J. Chem.*, 2013, **66**, 199–207.
- 186 J. A. Newby, D. W. Blaylock, P. M. Witt, R. M. Turner, P. L. Heider, B. H. Harji, D. L. Browne and S. V. Ley, *Org. Process Res. Dev.*, 2014, **18**, 1221–1228.
- 187 J. A. Newby, D. W. Blaylock, P. M. Witt, J. C. Pastre, M. K. Zacharova, S. V. Ley and D. L. Browne, *Org. Process Res. Dev.*, 2014, **18**, 1211–1220.
- 188 P. Ji, X. Feng, P. Oliveres, Z. Li, A. Murakami, C. Wang and W. Lin, *J. Am. Chem. Soc.*, 2019, **141**, 14878–14888.
- 189 A. Ciemiega, K. Maresz, J. J. Malinowski and J. Mrowiec-Białon, *Chem. Process Eng. - Inz. Chem. i Proces.*, 2018, **39**, 33–38.
- 190 K. Omoregbee, K. N. H. Luc, A. H. Dinh and T. V. Nguyen, *J. Flow Chem.*, 2020, **10**, 161–166.
- 191 M. K. Jackl, L. Legnani, B. Morandi and J. W. Bode, *Org. Lett.*, 2017, **19**, 4696–4699.
- 192 L. C. Wilkins, J. L. Howard, S. Burger, L. Frenzel-Beyme, D. L. Browne and R. L. Melen, *Adv. Synth. Catal.*, 2017, **359**, 2580–2584.
- 193 D. Voicu, M. Abolhasani, R. Choueiri, G. Lestari, C. Seiler, G. Menard, J. Greener, A. Guenther, D. W. Stephan and E. Kumacheva, *J. Am. Chem. Soc.*, 2014, **136**, 3875–3880.
- 194 J. J. Chi, T. C. Johnstone, D. Voicu, P. Mehlmann, F. Dielmann, E. Kumacheva and D. W. Stephan, *Chem. Sci.*, 2017, **8**, 3270–3275.
- 195 D. Voicu, D. W. Stephan and E. Kumacheva, *ChemSusChem*, 2015, **8**, 4202–4208.
- 196 R. J. Blagg, T. R. Simmons, G. R. Hatton, J. M. Courtney, E. L. Bennett, E. J. Lawrence and G. G. Wildgoose, *Dalton Trans.*, 2016, **45**, 6032–6043.
- 197 R. J. Blagg and G. G. Wildgoose, *RSC Adv.*, 2016, **6**, 42421–42427.
- 198 A. C. Massey, A. J. Park and F. G. A. Stone, *Proc. Chem. Soc.*, 1963, **127**, 212–212.
- 199 A. G. Massey and A. J. Park, *J. Organomet. Chem.*, 1964, **2**, 245–250.
- 200 J. L. W. Pohlmann and F. E. Brinckmann, *Z Naturforschdig*, 1965, **20 b**, 5–11.

- 201 S. Lancaster, *Chem Spider Synth. Pages*, 2003, 215.
- 202 T. A. Gazis, B. A. J. Mohajeri Thaker, D. Willcox, D. M. C. Ould, J. Wenz, J. M. Rawson, M. S. Hill, T. Wirth and R. L. Melen, *Chem. Commun.*, 2020, **56**, 3345–3348.
- 203 D. Chakraborty, A. Rodriguez and E. Y.-X. Chen, *Macromolecules*, 2003, **36**, 5470–5481.
- 204 T. Belgardt, J. Storre, H. W. Roesky, M. Noltemeyer and H.-G. Schmidt, *Inorg. Chem.*, 1995, **34**, 3821–3822.
- 205 J. Chen and E. Y.-X. Chen, *Dalton Trans.*, 2016, **45**, 6105–6110.
- 206 N. A. Sitte, M. Bursch, S. Grimme and J. Paradies, *J. Am. Chem. Soc.*, 2019, **141**, 159–162.
- 207 T. A. Gazis, A. Dasgupta, M. S. Hill, J. M. Rawson, T. Wirth and R. L. Melen, *Dalton Trans.*, 2019, **48**, 12391–12395.
- 208 Y. Soltani, S. J. Adams, J. Börger, L. C. Wilkins, P. D. Newman, S. J. A. Pope and R. L. Melen, *Dalton Trans.*, 2018, **47**, 12656–12660.
- 209 S. Tussing, L. Greb, S. Tamke, B. Schirmer, C. Muhle-Goll, B. Luy and J. Paradies, *Chem. Eur. J.*, 2015, **21**, 8056–8059.
- 210 H.-G. Stammer, S. Blomeyer, R. J. F. Berger and N. W. Mitzel, *Angew. Chem. Int. Ed.*, 2015, **54**, 13816–13820.
- 211 M. Schnürch, M. Spina, A. F. Khan, M. D. Mihovilovic and P. Stanetty, *Chem. Soc. Rev.*, 2007, **36**, 1046–1057.
- 212 M. Schlosser, *Angew. Chem. Int. Ed.*, 2005, **44**, 376–393.
- 213 M. Santi, D. M. C. Ould, J. Wenz, Y. Soltani, R. L. Melen and T. Wirth, *Angew. Chem. Int. Ed.*, 2019, **58**, 7861–7865.
- 214 E. L. Myers, C. P. Butts and V. K. Aggarwal, *Chem. Commun.*, 2006, 4434–4436.
- 215 T. J. Herrington, A. J. W. Thom, A. J. P. White and A. E. Ashley, *Dalton Trans.*, 2012, **41**, 9019–9022.
- 216 J. F. Kögel, A. Y. Timoshkin, A. Schröder, E. Lork and J. Beckmann, *Chem. Sci.*, 2018, **9**, 8178–8183.
- 217 D. L. Browne, M. Baumann, B. H. Harji, I. R. Baxendale and S. V. Ley, *Org. Lett.*, 2011, **13**, 3312–3315.
- 218 D. Sleveland and H. R. Bjørsvik, *Org. Process Res. Dev.*, 2012, **16**, 1121–1130.
- 219 A. Hafner, M. Meisenbach and J. Sedelmeier, *Org. Lett.*, 2016, **18**, 3630–3633.
- 220 Y. Soltani, L. C. Wilkins and R. L. Melen, *Angew. Chem. Int. Ed.*, 2017, **56**, 11995–11999.
- 221 K. L. Bamford, S. S. Chitnis, Z.-W. Qu and D. W. Stephan, *Chem. Eur. J.*, 2018, **24**, 16014–16018.
- 222 J. Bauer, H. Braunschweig, R. D. Dewhurst and K. Radacki, *Chem. Eur. J.*, 2013, **19**, 8797–8805.
- 223 T. D. Coyle, S. L. Stafford and F. G. A. Stone, *J. Chem. Soc.*, 1961, 3103–3108.

- 224 M. Kuprat, M. Lehmann, A. Schulz and A. Villinger, *Organometallics*, 2010, **29**, 1421–1427.
- 225 A. Zheng, S. Bin Liu and F. Deng, *J. Phys. Chem. C*, 2009, **113**, 15018–15023.
- 226 V. V Bardin, S. A. Prikhod'ko, M. M. Shmakov, A. Y. Shabalin and N. Y. Adonin, *Russ. J. Gen. Chem.*, 2020, **90**, 50–61.
- 227 L. Weber, D. Eickhoff, A. Chrostowska, A. Dargelos, C. Darrigan, H. G. Stammeler and B. Neumann, *Dalton Trans.*, 2019, **48**, 16911–16921.
- 228 E. A. Jacobs, R. Chandrasekar, D. A. Smith, C. M. White, M. Bochmann and S. J. Lancaster, *J. Organomet. Chem.*, 2013, **730**, 44–48.
- 229 K. Schlüter and A. Berndt, *Angew. Chemie*, 1980, **92**, 64–65.
- 230 H. Nöth and H. Pommerening, *Chem. Ber.*, 1981, **114**, 3044–3055.
- 231 I. P. Query, P. A. Squier, E. M. Larson, N. A. Isley and T. B. Clark, *J. Org. Chem.*, 2011, **76**, 6452–6456.
- 232 J. A. Newby, L. Huck, D. W. Blaylock, P. M. Witt, S. V Ley and D. L. Browne, *Chem. Eur. J.*, 2014, **20**, 263–271.
- 233 Y. M. Tian, X. N. Guo, M. W. Kuntze-Fechner, I. Krummenacher, H. Braunschweig, U. Radius, A. Steffen and T. B. Marder, *J. Am. Chem. Soc.*, 2018, **140**, 17612–17623.
- 234 P. A. Chase and D. W. Stephan, *Angew. Chem. Int. Ed.*, 2008, **47**, 7433–7437.
- 235 Y. Zhao and D. G. Truhlar, *Theor. Chem. Acc.*, 2008, **120**, 215–241.
- 236 T. H. Dunning, *J. Chem. Phys.*, 1989, **90**, 1007–1023.
- 237 J. M. Slattery and S. Hussein, *Dalton Trans.*, 2012, **41**, 1808–1815.
- 238 J. A. Nicasio, S. Steinberg, B. Inés and M. Alcarazo, *Chem. Eur. J.*, 2013, **19**, 11016–11020.
- 239 C. Wang, K. Huang, J. Wang, H. Wang, L. Liu, W. Chang and J. Li, *Adv. Synth. Catal.*, 2015, **357**, 2795–2802.
- 240 R. Brišar, F. Unglaube, D. Hollmann, H. Jiao and E. Mejía, *J. Org. Chem.*, 2018, **83**, 13481–13490.
- 241 J. McIntyre, I. Mayoral-Soler, P. Salvador, A. Poater and D. J. Nelson, *Catal. Sci. Technol.*, 2018, **8**, 3174–3182.
- 242 M. K. Barman, A. Baishya and S. Nembenna, *Dalton Trans.*, 2017, **46**, 4152–4156.
- 243 I. R. Cabrita, P. R. Florindo and A. C. Fernandes, *Tetrahedron*, 2017, **73**, 1511–1516.
- 244 J. L. N. Fernandes, M. C. De Souza, E. C. S. Brenelli and J. A. Brenelli, *Synthesis (Stuttg.)*, 2009, 4058–4062.
- 245 Z. Zhu, P. Dai, Z. Wu, M. Xue, Y. Yao, Q. Shen and X. Bao, *Catal. Commun.*, 2018, **112**, 26–30.
- 246 B. Sreedhar, P. Surendra Reddy and D. Keerthi Devi, *J. Org. Chem.*, 2009, **74**, 8806–8809.
- 247 Y. Hoshimoto, T. Kinoshita, S. Hazra, M. Ohashi and S. Ogoshi, *J. Am. Chem. Soc.*, 2018, **140**, 7292–7300.

-
- 248 O. Saidi, A. J. Blacker, M. M. Farah, S. P. Marsden and J. M. J. Williams, *Angew. Chem. Int. Ed.*, 2009, **48**, 7375–7378.
- 249 W. Zhang, X. Dong and W. Zhao, *Org. Lett.*, 2011, **13**, 5386–5389.
- 250 Y. C. Lin, E. Hatzakis, S. M. McCarthy, K. D. Reichl, T. Y. Lai, H. P. Yennawar and A. T. Radosevich, *J. Am. Chem. Soc.*, 2017, **139**, 6008–6016.
- 251 S. Kisan, V. Krishnakumar and C. Gunanathan, *ACS Catal.*, 2017, **7**, 5950–5954.
- 252 C. J. Lata and C. M. Crudden, *J. Am. Chem. Soc.*, 2010, **132**, 131–137.
- 253 R. Cano, D. J. Ramón and M. Yus, *J. Org. Chem.*, 2010, **75**, 3458–3460.
- 254 C. M. Crudden, Y. B. Hleba and A. C. Chen, *J. Am. Chem. Soc.*, 2004, **126**, 9200–9201.
- 255 A. Kaithal, B. Chatterjee and C. Gunanathan, *Org. Lett.*, 2015, **17**, 4790–4793.
- 256 Z. Zuo, L. Zhang, X. Leng and Z. Huang, *Chem. Commun.*, 2015, **51**, 5073–5076.
- 257 Z. Huang, S. Wang, X. Zhu, Q. Yuan, Y. Wei, S. Zhou and X. Mu, *Inorg. Chem.*, 2018, **57**, 15069–15078.
- 258 H. E. Ho, N. Asao, Y. Yamamoto and T. Jin, *Org. Lett.*, 2014, **16**, 4670–4673.
- 259 Y. Xiong and G. Zhang, *Org. Lett.*, 2019, **21**, 7873–7877.